PATTERNS AND DRIVERS OF LARGE WILDFIRES WITHIN AND SURROUNDING THE WILDLAND-URBAN INTERFACE OF THE EASTERN UNITED STATES

By

NOAH WEIDIG

A THESIS PRESENTED TO THE GRADUATE SCHOOL
OF THE UNIVERSITY OF FLORIDA IN PARTIAL FULFILLMENT
OF THE REQUIREMENTS FOR THE DEGREE OF
MASTER OF SCIENCE

UNIVERSITY OF FLORIDA

2025

© 2025 Noah Weidig

To my parents

ACKNOWLEDGMENTS

I wish to thank my parents for their unwavering support, encouragement, and belief in me throughout this journey. I am deeply grateful to my advisor, Dr. Victoria Donovan, for her invaluable assistance, expertise, and mentorship throughout my master's program. I also sincerely thank my thesis committee members, Dr. Carissa Wonkka and Dr. Daniel Johnson, for their guidance, insight, and encouragement.

TABLE OF CONTENTS

page

ACKNOWLEDGMENTS 4

LIST OF TABLES 7

LIST OF FIGURES 10

LIST OF ABBREVIATIONS 17

ABSTRACT 18

CHAPTER

1 LARGE WILDFIRES IN THE WILDLAND-URBAN INTERFACE OF THE EASTERN UNITED STATES 20

2 CHANGING LARGE WILDFIRE DYNAMICS IN THE WILDLAND-URBAN INTERFACE OF THE EASTERN UNITED STATES 25

Materials and Methods 27
Data 27
Temporal Patterns in the WUI 29
Spatial Patterns in WUI Large Wildfires 29
Temporal Patterns in WUI Large Wildfires 30
Results 31
Temporal Patterns in the WUI 31
Spatial Patterns in WUI Large Wildfires 31
Temporal Patterns in WUI Large Wildfires 32
Discussion 35

3 FIRE AT THE FRINGE: DRIVERS OF LARGE WILDFIRES IN AND NEAR THE WILDLAND-URBAN INTERFACE OF THE EASTERN UNITED STATES 49

Methods 52
Data 52
Wildfire Patterns within and near the WUI 56
Socio-environmental Factors Influencing Wildfires within and near the WUI 57
Results 59
Wildfire Patterns within and near the WUI 59
Socio-environmental Factors Influencing Wildfires in and near the WUI 60
Level 1 ecoregion scale 60
Level II ecoregion scale 61
Discussion 63

4 CONCLUSION 80

APPENDIX

A CHANGING LARGE WILDFIRE DYNAMICS IN THE WILDLAND-URBAN INTERFACE OF THE EASTERN UNITED STATES 82

B FIRE AT THE FRINGE: DRIVERS OF LARGE WILDFIRES IN AND NEAR THE WILDLAND-URBAN INTERFACE OF THE EASTERN UNITED STATES 99

LIST OF REFERENCES 170

BIOGRAPHICAL SKETCH 190

LIST OF TABLES

Table		page
2-1	Characteristics of large (>200 hectares) wildfires inside and outside the wildland-urban interface (WUI) across Level III ecoregions	44
2-2	Changes in regime characteristics for large (>200 hectares) wildfires inside and outside the wildland-urban interface (WUI) across Level III ecoregions	47
3-1	Description of environmental and social factors used as predictors in modeling the relationship between large wildfires (≥200 ha) and the wildland-urban interface (WUI) across the eastern United States	74
3-2	A list of candidate models used to predict large wildfire (≥200 ha) occurrence within the wildland-urban interface (WUI)	77
3-3	Results showing the relationship between large (≥200 ha) wildfires and the wildland-urban interface (WUI) compared to the general landscape	78
3-4	Model selection results for the top five models using Akaike's Information Criterion (AIC) for whether large wildfires (≥200 ha) burn in the WUI	79
A-1	Changes in housing density classes across Level III ecoregions of the eastern United States from 1990 to 2020	82
B-1	Model selection results for wind speed using Akaike's Information Criteria (AIC)	99
B-2	Model selection results for wind speed using Akaike's Information Criteria (AIC)	99
B-3	Model selection results for wind speed using Akaike's Information Criteria (AIC)	100
B-4	Model selection results for precipitation using Akaike's Information Criteria (AIC)	100
B-5	Model selection results for precipitation using Akaike's Information Criteria (AIC)	101
B-6	Model selection results for precipitation using Akaike's Information Criteria (AIC)	101
B-7	Model selection results for fuel moisture using Akaike's Information Criteria (AIC)	102

B-8 Model selection results for fuel moisture using Akaike's Information Criteria (AIC) 102

B-9 Model selection results for fuel moisture using Akaike's Information Criteria (AIC) 103

B-10 Model selection results for fire and EMS station density (n/km²) using Akaike's Information Criteria (AIC) 103

B-11 Model selection results for fire and EMS station density (n/km²) using Akaike's Information Criteria (AIC) 104

B-12 Model selection results for fire and EMS station density (n/km²) using Akaike's Information Criteria (AIC) 104

B-13 Model selection results for road density (km/km²) using Akaike's Information Criteria (AIC) 104

B-14 Model selection results for road density (km/km²) using Akaike's Information Criteria (AIC) 105

B-15 Model selection results for road density (km/km²) using Akaike's Information Criteria (AIC) 105

B-16 Model selection results for preparedness level using Akaike's Information Criteria (AIC) 105

B-17 Model selection results for preparedness level using Akaike's Information Criteria (AIC) 106

B-18 Model selection results for preparedness level using Akaike's Information Criteria (AIC) 106

B-19 Model selection results for whether large wildfires (≥200 ha) burned in the wildland-urban interface (WUI) 107

B-20 Model selection results for the proportion of large wildfires' (≥200 ha) areas that burned in the wildland-urban interface (WUI) 108

B-21 Model selection results for the distance large wildfires (≥200 ha) burned from the wildland-urban interface (WUI) 109

B-22 Model parameter estimates for predictors of whether large wildfires (≥200 ha) burned in the wildland-urban interface (WUI) 110

B-23 Model parameter estimates for predictors of the proportion of a large wildfire’s (≥200 ha) area that burned in the wildland-urban interface (WUI) 111

B-24 Model parameter estimates for predictors of the distance large wildfires (≥200 ha) burned from the wildland-urban interface (WUI)..... 112

LIST OF FIGURES

Figure page

2-1 Maps showing the percentage area occupied by the wildland-urban interface (WUI) in 2020; and the relative percentage change from 1990 to 2020 40

2-2 Maps showing the total number, average size (in ha), and total area burned (in ha) by large wildfires (>200 ha) inside and outside the wildland-urban interface (WUI) across Level III ecoregions 41

2-3 Maps showing Mann-Kendall tau values for annual changes in the number, average size (in ha), and total area burned (in ha) by large wildfires (>200 ha) inside and outside the WUI 42

2-4 Gaussian kernel density estimates for large (>200 ha) wildfire seasonality inside and outside the wildland-urban interface (WUI) of the Level 1 Eastern Temperate Forests ecoregion (the eastern US) 43

3-1 The distribution of the proportion of the wildland-urban interface (WUI) burned by large wildfires (≥200 ha) for all wildfires that did burn in the WUI compared to a null distribution across Level I and Level II ecoregions 69

3-2 The distribution of large wildfire (≥200 ha) distance to the wildland-urban interface (WUI) for all wildfires that did not burn in the WUI compared to a null distribution across Level I and Level II ecoregions 70

3-3 Model predictions for seven independent variables and their relationship to whether a large wildfire (≥200 ha) burned in the wildland-urban interface (WUI) within the eastern United States 71

3-4 Model predictions for seven independent variables and their relationship to the proportion of a large wildfire's (≥200 ha) area that burned in the wildland-urban interface (WUI) within the eastern United States 72

3-5 Model predictions for three independent variables and their relationship to the distance large wildfires (≥200 ha) burned from the wildland-urban interface (WUI) within the eastern United States between 1991 and 2021 73

A-1 Level III ecoregions of the Eastern Temperate Forests ecoregion, as designated by the United States Environmental Protection Agency 89

A-2 Decadal percent change in intermix (light grey) and interface (dark grey) wildland-urban interface (WUI) from 1990 to 2020 across Level III ecoregions of the eastern United States. 90

A-3 Change in the number of large (>200 ha) wildfires inside the wildland-urban interface (WUI) from 1986 to 2021 across Level III ecoregions of the eastern United States 91

A-4 Change in the number of large (>200 ha) wildfires outside the wildland-urban interface (WUI) from 1986 to 2021 across Level III ecoregions of the eastern United States 92

A-5 Change in the total area burned (hectares) by large (>200 ha) wildfires inside the wildland-urban interface (WUI) from 1986 to 2021 across Level III ecoregions of the eastern United States 93

A-6 Change in the total area burned (hectares) by large (>200 ha) wildfires in the wildland-urban interface (WUI) from 1986 to 2021 across Level III ecoregions of the eastern United States 94

A-7 Change in the average size (hectares) (± standard error) of large (>200 ha) wildfires inside the wildland-urban interface (WUI) from 1986 to 2021 across Level III ecoregions of the eastern United States 95

A-8 Change in the average size (hectares) (± standard error) of large (>200 ha) wildfires outside the wildland-urban interface (WUI) from 1986 to 2021 across Level III ecoregions of the eastern United States 96

A-9 Ignition sources for large (>200 hectares) wildfires inside and outside the wildland-urban interface (WUI) from 1986 to 2021 in the eastern United States (n = 1,749) 97

A-10 The proportion of large (>200 hectares) wildfires inside the wildland-urban interface (WUI) across Level III (L3) ecoregions of the eastern United States between 1986 and 2021 98

B-1 Map showing Level II ecoregions of the Eastern Temperate Forests Level I ecoregion. Ecoregions colored with grey were not used in this analysis due to an insufficient number of large wildfires (≥200 ha) 113

B-2 Raincloud plot showing the distribution of large wildfire durations across the Eastern Temperate Forests Level I ecoregion 114

B-3 Daily National Preparedness Levels between 1991 and 2021 within the United States 115

B-4 Bar graphs showing the proportion of large wildfires (≥200 ha) that burned wildland-urban interface (WUI) in the Eastern Temperate Forests Level I ecoregion and across three Level III ecoregions 116

B-5 Correlation matrix showing the Pearson's correlation coefficient between predictor variables used to model whether large wildfires (≥200 ha) burned in the wildland-urban interface (WUI) 117

B-6 Correlation matrix showing the Pearson's correlation coefficient between predictor variables used to model whether large wildfires (≥200 ha) burned in the wildland-urban interface (WUI) 118

B-7 Correlation matrix showing the Pearson's correlation coefficient between predictor variables used to model whether large wildfires (≥200 ha) burned in the wildland-urban interface (WUI) 119

B-8 Correlation matrix showing the Pearson's correlation coefficient between predictor variables used to model whether large wildfires (≥200 ha) burned in the wildland-urban interface (WUI) 120

B-9 Correlation matrix showing the Pearson's correlation coefficient between predictor variables used to model the proportion of a large wildfire's (≥200 ha) area that burned in the wildland-urban interface (WUI) 121

B-10 Correlation matrix showing the Pearson's correlation coefficient between predictor variables used to model the proportion of a large wildfire's (≥200 ha) area that burned in the wildland-urban interface (WUI) 122

B-11 Correlation matrix showing the Pearson's correlation coefficient between predictor variables used to model the proportion of a large wildfire's (≥200 ha) area that burned in the wildland-urban interface (WUI) 123

B-12 Correlation matrix showing the Pearson's correlation coefficient between predictor variables used to model the proportion of a large wildfire's (≥200 ha) area that burned in the wildland-urban interface (WUI) 124

B-13 Correlation matrix showing the Pearson's correlation coefficient between predictor variables used to model the distance large wildfires (≥200 ha) burned from the wildland-urban interface (WUI) 125

B-14 Correlation matrix showing the Pearson's correlation coefficient between predictor variables used to model the distance large wildfires (≥200 ha) burned from the wildland-urban interface (WUI) 126

B-15 Correlation matrix showing the Pearson's correlation coefficient between predictor variables used to model the distance large wildfires (≥200 ha) burned from the wildland-urban interface (WUI) 127

B-16 Correlation matrix showing the Pearson's correlation coefficient between predictor variables used to model the distance large wildfires (≥200 ha) burned from the wildland-urban interface (WUI) 128

B-17 Raincloud plots for variables used to model whether large wildfires (≥200 ha) burned in the wildland-urban interface (WUI) within the Eastern Temerate Forests 129

B-18 Raincloud plots for variables used to model whether large wildfires (≥200 ha) burned in the wildland-urban interface (WUI) within the Mississippi Alluvial and Southeast USA Coastal Plains 130

B-19 Raincloud plots for variables used to model whether large wildfires (≥200 ha) burned in the wildland-urban interface (WUI) within the Ozark/Ouachita-Appalachian Forests 131

B-20 Raincloud plots for variables used to model whether large wildfires (≥200 ha) burned in the wildland-urban interface (WUI) within the Southeast USA Plains 132

B-21 Raincloud plots for variables used to model the proportion of a large wildfire's (≥200 ha) area that burned in the wildland-urban interface (WUI) within the Eastern Temerate Forests 133

B-22 Raincloud plots for variables used to model the proportion of a large wildfire's (≥200 ha) area that burned in the wildland-urban interface (WUI) within the Mississippi Alluvial and Southeast USA Coastal Plains 134

B-23 Raincloud plots for variables used to model the proportion of a large wildfire's (≥200 ha) area that burned in the wildland-urban interface (WUI) within the Ozark/Ouachita-Appalachian Forests 135

B-24 Raincloud plots for variables used to model the proportion of a large wildfire's (≥200 ha) area that burned in the wildland-urban interface (WUI) within the Southeastern USA Plains 136

B-25 Raincloud plots for variables used to model the distance large wildfires (≥200 ha) burned from the wildland-urban interface (WUI) within the Eastern Temperate Forests 137

B-26 Raincloud plots for variables used to model the distance large wildfires (≥200 ha) burned from the wildland-urban interface (WUI) within the Mississippi Alluvial and Southeast USA Coastal Plains 138

B-27 Raincloud plots for variables used to model the distance large wildfires (≥200 ha) burned from the wildland-urban interface (WUI) within the Ozark/Ouachita-Appalachian Forests 139

B-28 Raincloud plots for variables used to model the distance large wildfires (≥200 ha) burned from the wildland-urban interface (WUI) within the Southeastern USA Plains 140

B-29 A Cullen and Frey graph examining the distribution of the proportion of large wildfires' (≥200 ha) areas that burned in the wildland-urban interface (WUI) within the Eastern Temperate Forests 141

B-30 A Cullen and Frey graph examining the distribution of the proportion of large wildfires' (≥200 ha) areas that burned in the wildland-urban interface (WUI) within the Mississippi Alluvial and Southeast USA Coastal Plains 142

B-31 A Cullen and Frey graph examining the distribution of the proportion of large wildfires' (≥200 ha) areas that burned in the wildland-urban interface (WUI) within the Ozark/Ouachita-Appalachian Forests 143

B-32 A Cullen and Frey graph examining the distribution of the proportion of large wildfires' (≥200 ha) areas that burned in the wildland-urban interface (WUI) within the Southeastern USA Plains 144

B-33 A Cullen and Frey graph examining the distribution of the distance large wildfires (≥200 ha) burned from the wildland-urban interface (WUI) within the Eastern Temperate Forests 145

B-34 A Cullen and Frey graph examining the distribution of the distance large wildfires (≥200 ha) burned from the wildland-urban interface (WUI) within the Mississippi Alluvial and Southeast USA Coastal Plains 146

B-35 A Cullen and Frey graph examining the distribution of the distance large wildfires (≥200 ha) burned from the wildland-urban interface (WUI) within the Ozark/Ouachita-Appalachian Forests 147

B-36 A Cullen and Frey graph examining the distribution of the distance large wildfires (≥200 ha) burned from the wildland-urban interface (WUI) within the Southeastern USA Plains 148

B-37 Global model diagnostics for whether large wildfires (≥200 ha) burned in the wildland-urban interface (WUI) within the Eastern Temperate Forests 149

B-38 Global model diagnostics for whether large wildfires (≥200 ha) burned in the wildland-urban interface (WUI) within the Mississippi Alluvial and Southeast USA Coastal Plains 150

B-39 Global model diagnostics for whether large wildfires (≥200 ha) burned in the wildland-urban interface (WUI) within the Ozark/Ouachita-Appalachian Forests 151

B-40 Global model diagnostics for whether large wildfires (≥200 ha) burned in the wildland-urban interface (WUI) within the Southeastern USA Plains 152

B-41 Global model diagnostics for the proportion of a large wildfire's (≥200 ha) perimeter that burned in the wildland-urban interface (WUI) within the Eastern Temperate Forests 153

B-42 Global model diagnostics for the proportion of a large wildfire's (≥200 ha) perimeter that burned in the wildland-urban interface (WUI) within the Mississippi Alluvial and Southeast USA Coastal Plains 154

B-43 Global model diagnostics for the proportion of a large wildfire's (≥200 ha) perimeter that burned in the wildland-urban interface (WUI) within the Ozark/Ouachita-Appalachian Forests 155

B-44 Global model diagnostics for the proportion of a large wildfire's (≥200 ha) perimeter that burned in the wildland-urban interface (WUI) within the Southeastern USA Plains 156

B-45 Global model diagnostics for the distance large wildfires (≥200 ha) burned from the wildland-urban interface (WUI) within the Eastern Temperate Forests 157

B-46 Global model diagnostics for the distance large wildfires (≥200 ha) burned from the wildland-urban interface (WUI) within the Mississippi Alluvial and Southeast USA Coastal Plains 158

B-47 Global model diagnostics for the distance large wildfires (≥200 ha) burned from the wildland-urban interface (WUI) within the Ozark/Ouachita-Appalachian Forests 159

B-48 Global model diagnostics for the distance large wildfires (≥200 ha) burned from the wildland-urban interface (WUI) within the Southeastern USA Plains .. 160

B-49 Top model predictions for whether large wildfires (≥200 ha) burned in the wildland-urban interface (WUI) within the Mississippi Alluvial and Southeast USA Coastal Plains 161

B-50 Top model predictions for whether large wildfires (≥200 ha) burned in the wildland-urban interface (WUI) within the Ozark/Ouachita-Appalachian Forests 162

B-51 Top model predictions for whether large wildfires (≥200 ha) burned in the wildland-urban interface (WUI) within the Southeastern USA Plains 163

B-52 Top model predictions for the proportion of a large wildfire's (≥200 ha) perimeter that burned in the wildland-urban interface (WUI) within the Mississippi Alluvial and Southeast USA Coastal Plains 164

B-53 Top model predictions for the proportion of a large wildfire's (≥200 ha) perimeter that burned in the wildland-urban interface (WUI) within the Ozark/Ouachita-Appalachian Forests 165

B-54 Top model predictions for the proportion of a large wildfire's (≥200 ha) perimeter that burned in the wildland-urban interface (WUI) within the Southeastern USA Plains 166

B-55 Top model predictions for the distance large wildfires (≥200 ha) burned from the wildland-urban interface (WUI) within the Mississippi Alluvial and Southeast USA Coastal Plains 167

B-56 Top model predictions for the distance large wildfires (≥200 ha) burned from the wildland-urban interface (WUI) within the Ozark/Ouachita-Appalachian Forests 168

B-57 Top model predictions for the distance large wildfires (≥200 ha) burned from the wildland-urban interface (WUI) within the Southeastern USA Plains 169

LIST OF ABBREVIATIONS

AIC	Akaike Information Criterion
cm	Centimeter(s)
EMS	Emergency Medical Services
EPA	The United States Environmental Protection Agency
FEMA	Federal Emergency Management Agency
FPA-FOD	Fire Program Analysis - Fire Occurrence Database
GLM	Generalized linear model
GridMET	Gridded Surface Meteorological Data
ha	Hectare(s)
km	Kilometer(s)
L1	The United States Environmental Protection Agency Level I ecoregion
L3	The United States Environmental Protection Agency Level III ecoregion
MTBS	The Monitoring Trends in Burn Severity Project
NIFC	National Interagency Fire Center
p	P-value
s.e.	Standard error
T	Mann-Kendall tau statistic
TIGER	Topologically Integrated Geographic Encoding and Referencing
US	The United States of America
USDA	The United States Department of Agriculture
USDI	The United States Department of the Interior
USFS	The United States Forest Service
WUI	Wildland-urban interface

Abstract of Thesis Presented to the Graduate School
of the University of Florida in Partial Fulfillment of the
Requirements for the Degree of Master of Science

PATTERNS AND DRIVERS OF LARGE WILDFIRES WITHIN AND SURROUNDING THE WILDLAND-URBAN INTERFACE OF THE EASTERN UNITED STATES

By

Noah Weidig

August 2025

Chair: Victoria Donovan
Major: Forest Resources and Conservation

The recent increase in large wildfires in the eastern United States makes it crucial to examine the subsequent risk to human life and property. In the East, the wildland-urban interface (WUI), where wildfire risk is greatest, has expanded tremendously over the last three decades. In this thesis, we aimed to understand how increasing large wildfires in the East are manifesting in the WUI. Using large (≥200 ha) wildfire perimeters, we (1) assessed WUI growth and its relationship with large wildfire regime characteristics and (2) determined the spatial WUI-wildfire relationships and the social and environmental factors driving these patterns over the last three decades in the eastern US at multiple spatial scales. While the WUI only makes up 22% of the East, WUI wildfires comprised 45% of all large wildfires and 55% of the area burned, were on average 46% larger than non-WUI wildfires, and are becoming more frequent in spring. Most increases in wildfire activity occurred outside of the WUI. Additionally, large wildfires burn less often in the WUI and less of the WUI than expected at random; however, wildfires that burn outside of the WUI burn closer to the WUI than expected. Environmental factors and, to a lesser extent, social variables are important for predicting these WUI-wildfire relationships. Higher levels of woody cover, drier

conditions, and strained federal suppression resources drove wildfire occurrence in and near the WUI. Our findings highlight important interactions between human development and large wildfire occurrence and the need for proactive fuels management in the East.

CHAPTER 1
LARGE WILDFIRES IN THE WILDLAND-URBAN INTERFACE OF THE EASTERN UNITED STATES

Fire dynamics are shifting drastically across the globe, posing an increased risk to human life and property (Bowman et al., 2017; Schug et al., 2023). While fire provides numerous ecological benefits, such as enhanced biodiversity, improved hydrology, and increased nutrient cycling (Carbone et al., 2025; Doherty et al., 2022; González et al., 2022; He et al., 2019), wildfires can cause immeasurable destruction when they occur in and near human settlements (Chen et al., 2024; Guo et al., 2024; Schug et al., 2023; Tang et al., 2024). Catastrophic wildfires are often the result of long-term fire exclusion combined with changing climatic conditions (Calkin et al., 2015; Kreider et al., 2024). Many of the world's ecosystems are in a fire deficit (i.e., when fire occurs less frequently than historically or ecologically expected) due to rapid land-use change, shifting perspectives on wildfire, and past wildland fire policy (Bowman et al., 2020; Ingalsbee, 2015; Parks et al., 2025). Ecological patterns and processes have been disrupted because lack of fire has altered the fuel load, plant communities, and vegetation structures of these systems (Knuckey et al., 2016). The change in plant communities reshape fire regimes, altering their frequency, intensity, seasonality, and spatial extent across numerous regions around the globe (Rogers et al., 2020).

In twentieth century, fire regimes have experienced changes across nearly every continent, altering landscapes and shifting ecosystems (Rogers et al., 2020). Changes in wildfire frequency, severity, and area burned have been documented in Europe (Marques et al., 2011; Schelhaas et al., 2003), Asia (Vadrevu et al., 2019), Australia (Cunningham et al., 2024; Fairman et al., 2015; Murphy et al., 2013), Africa (M. W. Jones et al., 2022), and South America (Feron et al., 2024). North America, in

particular, has experienced a surge in wildfires (Rogers et al., 2020). Several regions of Canada have experienced a dramatic increase in the number and the total area burned by wildfires over the last half-century (Hanes et al., 2019). The United States (US) has experienced drastic changes in wildfire activity in recent decades (Balch et al., 2017; Iglesias et al., 2022), with large wildfires increasing across many regions of the country (Dennison et al., 2014; Donovan, Crandall, et al., 2023; Donovan et al., 2017).

Changes in wildfire regimes within the US have been driven by both environmental and anthropogenic factors (Pausas & Keeley, 2021). Climate change has altered wildfire severity, frequency, and seasonality across the US by creating drier and hotter conditions conducive to fire (Abatzoglou et al., 2019; Ellis et al., 2022; M. W. Jones et al., 2022). Shifts in climatic conditions, coupled with policy change and declining public perspectives on fire, have also limited the ability of land managers to conduct prescribed fires, which, in turn, allows greater fuel accumulation (Kupfer et al., 2020). Throughout the 20th century, wildland fire policy promoted systematic fire suppression, resulting in greater fuel accumulation including wide-spread forest densification, and larger, more severe wildfires (Kreider et al., 2024).(Nowacki & Abrams, 2008) Increases in woody cover have been linked to a higher probability of large wildfire occurrence (Ivey et al., 2024). Woody fuels are also associated with increased fire severity, as they can create ladder fuels that result in a higher probability of crown fire (Donovan et al., 2022). The presence of invasive species can alter both the frequency and severity of fires (M. L. Brooks et al., 2004). For example, cheatgrass (*Bromus tectorum*) invasion in grassland biomes has increased fire frequency, giving this species a competitive advantage over native grasses (Bradley et al., 2018). In the

southeastern US, cogongrass (*Imperata cylindrica*) has negatively impacted native plant communities by increasing fire intensity (Brewer, 2008; Tomat-Kelly et al., 2021). Changes in land use have also altered fire regimes in many regions of the country (Butsic et al., 2015). For example, exurban growth has resulted in more potential human-caused ignition sources, thereby increasing fire frequency (Balch et al., 2017; Radeloff et al., 2018). Changes in wildfire regimes directly affect the well-being of millions of people, especially those living in the wildland-urban interface (WUI), where human settlement intermingles with wildland vegetation (Radeloff et al., 2005; Schug et al., 2023).

Coincident with increasing wildfire occurrence, the WUI has expanded in the last several decades, resulting in greater wildfire risk to human life and property (Chen et al., 2024; Schug et al., 2023; Tang et al., 2024). Since 1985, the WUI has grown by 12.56% and now covers roughly 6.62 million km^2 of the world's land area (Chen et al., 2024). Approximately 1.2 billion people live in the WUI (Guo et al., 2024). Much of the WUI is concentrated in the US, covering approximately 1.2 million km^2 (16.2%) (Carlson et al., 2022). In the US, the total WUI area has increased by 31% (179,000 km2) since 1990, while the number of houses in the WUI rose by 14 million (Chen et al., 2024; Radeloff, Mockrin, et al., 2023). Global expansion of the WUI has resulted in greater wildfire risk to human life and settlement (Guo et al., 2024; Schug et al., 2023; Tang et al., 2024). Worldwide, wildfires were the direct cause (excluding smoke inhalation) of 1,890 fatalities and 14,360 injuries between 2000 and 2023 (Mani et al., 2024). Johnston et al. (2012) estimated that wildfire smoke inhalation causes over 339,000 premature deaths annually. In the US alone, wildfires cause anywhere from US$63.5 billion to US$285.0

billion in annual losses (Thomas et al., 2017), destroying over 100,000 buildings in the last 30 years (Barrett, 2020). Losses from wildfire underscore the importance of understanding the causes of wildfires in and near the WUI.

Wildfire risk is heightened in the WUI due to several factors, predominantly due to increased human activity (Chen et al., 2024). Accidental ignitions from power lines, campfires, equipment/vehicle use, and intentional ignitions via arson/incendiarism can increase the potential for wildfires in the WUI (Ganteaume & Syphard, 2018; Short, 2014). Human structures in the WUI are often built from highly flammable materials and surrounded by dense vegetation (Committee on the Chemistry of Urban Wildfires et al., 2022). Fragmentation of forested landscapes within the WUI can create an “edge effect,” which can create drier microclimates, thereby increasing wildfire risk (Narayanaraj & Wimberly, 2012, 2013). In addition, fracturing of continuous vegetation can increase the potential for invasion from exotic plant species, which can be more flammable than native species (Fuentes-Ramirez et al., 2016).

In recent years, the US has experienced a surge in highly destructive wildfires burning in the WUI across numers regions of the US (Balch et al., 2024; Iglesias et al., 2022; Radeloff, Mockrin, et al., 2023). For example, in California, the 2018 Camp Fire claimed 85 lives, destroyed 18,806 structures, and caused US$16.5 billion in damages (Committee on the Chemistry of Urban Wildfires et al., 2022; Modaresi Rad et al., 2023). However, increases in destructive wildfires are not limited to the western US (Balch et al., 2024; Donovan, Crandall, et al., 2023; Donovan et al., 2017). Texas has experienced several catastrophic wildfires since the early 2000s. For example, the 2006 East Amarillo Fort Complex Fire killed 12 people and burned over 907,000 acres (Balch

et al., 2024). In 2011, the Bastrop County Complex fire destroyed 1,696 structures (Lee & Chow, 2015). Tennessee also experienced the Chimney Top fires in 2016, which destroyed over 2,000 structures, killed 14 people, and injured an additional 139 (United States Fire Administration, 2021). While fire management and policy have focused on the western US, these recent, highly destructive wildfires in other parts of the US highlight the need to address increasing wildfire risk to human life and property, particularly in regions containing extensive WUI areas.

The eastern US, which contains the most WUI area in the country, is experiencing increases in large wildfires (Donovan, Crandall, et al., 2023; Radeloff, Mockrin, et al., 2023). In the last two decades, wildfires threatened 106,650 people, 105,335 km of roads, and 10,605 km of power lines across the East (Modaresi Rad et al., 2023). Wildfires in the eastern US have destroyed thousands of structures since the early 2000s, underscoring the need to identify key factors driving wildfire patterns in and near the WUI (St. Denis et al., 2023). This thesis aims to deepen our understanding of large wildfire patterns inside and outside the WUI across the eastern US to inform wildfire risk management and better prepare those living in the East. The second chapter assesses large wildfire regimes inside and outside the WUI across the eastern US and quantifies spatial and temporal wildfire patterns between 1985 and 2021. The third chapter examines the spatial relationship between large wildfires and the WUI and investigates which social and environmental factors may be driving these patterns between 1991 and 2022. The fourth chapter summarizes the major findings of the thesis and suggests ways to mitigate wildfire risk in the East.

CHAPTER 2
CHANGING LARGE WILDFIRE DYNAMICS IN THE WILDLAND-URBAN INTERFACE OF THE EASTERN UNITED STATES

The wildland-urban interface (WUI), which occurs at the intersection between human development and wildland vegetative fuels (Radeloff et al., 2005), remains a core focus for predicting and mitigating wildfire risk. Since the 1990s, the United States has experienced substantial growth in the total area of WUI (Radeloff et al., 2018; Radeloff, Mockrin, et al., 2023). The recent historical shift from an industrial economy to an informational one has allowed humans to live in more rural areas with easy access to outdoor recreation (Krannich et al., 2011; Matilainen et al., 2017). However, living in and building structures near wildland vegetation poses several economic and ecological problems (Radeloff et al., 2005), predominantly stemming from the 'edge effect' (Murcia, 1995; Ranney, 1977). The issues created by the WUI include habitat fragmentation, shifts in microclimates, and the spread of exotic invasive species (Alston & Richardson, 2006; Gehlhausen et al., 2000; Sanczuk et al., 2023). However, increased wildfire risk is arguably the most consequential problem posed by the WUI (Radeloff et al., 2005, 2018; Radeloff, Mockrin, et al., 2023). Increased wildfire risk in the WUI results from the interactions of multiple factors, including the WUI's proximity to human-caused ignition sources, the flammability of exotic invasive species, and increased fuel loading (Mandle et al., 2011; Mietkiewicz et al., 2020; Toman et al., 2011).

Wildfires in the WUI require more suppression resources, destroy more homes, and pose a greater threat to human life than wildfires elsewhere in the landscape

Reprinted with permission from Weidig, N. (2023). Changing large wildfire dynamics in the wildland–urban interface of the eastern United States. *International Journal of Wildland Fire 33,* WF24110 https://doi.org/10.1071/WF24110

(Modaresi Rad et al., 2023; Radeloff et al., 2018; Swimley, 2021). Previous studies have shown that 32% of all wildfires in the conterminous US are started in the WUI, even though the WUI only makes up one-tenth of the country by area (Mietkiewicz et al., 2020). WUI wildfires result in greater property damage and pose logistical difficulties for firefighters because a large majority of the WUI (89%) is private property, thereby limiting access (Haynes et al., 2020; L. Johnston et al., 2019; Theobald & Romme, 2007). In a 2021 report, the US Fire Administration determined that wildfires in the WUI result in 14% more firefighter injuries and 20% more civilian casualties than urban structure fires (FEMA, 2021). This increased wildfire risk in the WUI highlights the need to characterize wildfire regimes at finer scales in regions that contain high proportions of WUI area.

Large wildfire numbers are increasing in the eastern US (Donovan, Crandall, et al., 2023). It is crucial to understand how these increases in large wildfire interact with the WUI to better assess the risk of these changes to human life and infrastructure (Donovan, Crandall, et al., 2023; Iglesias et al., 2022). The eastern US contains a disproportionately large area of WUI relative to the rest of the country (Radeloff et al., 2018; Theobald & Romme, 2007). Although wildfires in the eastern US currently result in fewer casualties and less property damage than in the West, the eastern US experiences frequent human-caused (~88%) wildfires that burn seven times more area of the WUI than western ones (Balch et al., 2017; Mietkiewicz et al., 2020; Nagy et al., 2018). On average, eastern wildfires in the WUI cost US$18,300/km^2 to suppress (Mietkiewicz et al., 2020), and as the number of these fires continues to rise, suppression capacity will become strained. Additionally, as climate and land use alter

wildfire regimes, the eastern US will continue to experience more human-caused wildfires originating in the WUI (Abatzoglou & Williams, 2016; Butsic et al., 2015). Yet differences between WUI and non-WUI large wildfire regimes in this region of the country remain unclear, and as the WUI continues to expand, it becomes imperative to quantify changing wildfire risk to human life and structures.

We examined how changes in large wildfire regimes across the eastern US are manifesting in the WUI. Specifically, we aimed to (1) assess temporal changes in the WUI; (2) contrast characteristics of WUI versus non-WUI large (>200 ha) wildfire regimes; and (3) assess temporal trends in WUI versus non-WUI large wildfire regime characteristics across the eastern US at multiple spatial scales. As the eastern US is a large area that contains regions with vastly different ecological properties, a multiscale assessment is needed to understand changes in fire regimes. we combine spatio-temporal large wildfire perimeter data and decadal WUI maps across the Eastern Temperate Forests Level I Environmental Protection Agency (EPA) ecoregion and within 31 Level III ecoregions that subdivide the eastern US. We characterize spatial and temporal characteristics of wildfire regimes inside and outside the WUI using six fundamental components of fire regimes: average wildfire size, number, total area burned within an ecoregion, annual probability of occurrence, seasonality, and ignition source.

Materials and Methods

Data

We used the US EPA ecoregions to designate and subdivide our study region. We used the Level I (L1) Eastern Temperate Forests ecoregion (hereafter referred to as the ‘eastern US’) to characterize the eastern US (Figure B-1). This area is characterised

by high population and housing density compared with the rest of the US (Radeloff et al., 2018; Theobald, 2005). The eastern US is ecologically distinct from the rest of the country because of its high humidity, high precipitation (100-150 cm annually), and gradient of mild to cold winters (Gilliam, 2016). Forests of the eastern US are mostly hardwoods in the north and mixed pines and hardwoods in the south (Woodbridge et al., 2022). We further subdivided the eastern US using Level III (L3) ecoregions (n = 31) (EPA, 2013; Omernik & Griffith, 2014). The EPA has created Level I through IV ecoregions as a framework for spatially subdividing the United States hierarchically, with Level I ecoregions being the largest scale and Level IV ecoregions being the finest scale. Ecoregions are areas with fairly homogeneous landscapes and similar environmental resources (Bryce et al., 1999; EPA, 2013).

We used the USDA's decadal WUI maps from 1990 to 2020 (Radeloff, Helmers, et al., 2023). Census block polygons in this dataset are classified as intermix WUI, interface WUI or non-WUI according to the Federal Register definition (FMB, 2019; USDA & USDI, 2001). Intermix WUI is any area containing at least 6.17 housing units km^2 and 50% vegetation. Interface WUI is any area containing more than 6.17 housing units km^2 and less than 50% vegetation but is within 2.4 km of a highly vegetated area larger than 5 km^2 (Radeloff et al., 2005; USDA & USDI, 2001).

Wildfire data were collected from the 'Burned Areas Boundary Dataset' from the Monitoring Trends in Burn Severity (MTBS) database (Eidenshink et al., 2007; MTBS, 2023). Among the categories of fires (Prescribed Fire, Unknown, Wildfire, and Wildland Fire Use), we only included fires greater than 200 ha classified as 'Wildfires' between 1986 and 2021 for our assessment (n = 2388) (Nagy et al., 2018). MTBS defines a

wildfire as any fire initiated from an unplanned ignition, whether a human cause, a natural cause, or an uncontrolled prescribed burn (FMB, 2019). we joined ignition source data from the USDA's Fire Program Analysis Fire Occurrence database with wildfire perimeters where corresponding MTBS identifiers existed (n = 1749) (Short, 2022). For analysing ignition patterns, we only used fires with known ignition causes (n = 1652). This dataset only contains wildfires between the years 1992 and 2020.

Temporal Patterns in the WUI

To assess temporal changes in the WUI across the eastern US, we summarised the proportion of area for interface and intermix WUI within each L3 ecoregion for the years 1990, 2000, 2010 and 2020. we also summarised the proportion of vegetated and non-vegetated or agricultural areas within each ecoregion for each of the 4 years. we calculated the relative change in intermix WUI, interface WUI, vegetated, and unvegetated/agricultural areas from 1990 to 2020 across L3 ecoregions (Figure 2-1, Table A-1).

Spatial Patterns in WUI Large Wildfires

To contrast characteristics of WUI versus non-WUI large wildfire regimes across the eastern US, we combined large wildfire perimeters from the MTBS dataset with the WUI geodatabase. we defined a 'WUI wildfire' as one that burns any area of the WUI (interface or intermix). A limitation of this method is the fact that our definition of a WUI large wildfire may favour larger wildfires because larger wildfires could spread into and burn a small portion of the WUI. However, as the WUI is often a source of wildfire ignitions (Syphard and Keeley 2015; Mietkiewicz et al. 2020), many of these large wildfires may have begun within the WUI and spread outwards. WUI maps are decadal. Wildfires were categorised as WUI or non-WUI using the WUI map from the year

closest to their ignition date. we used the 1990 WUI map for categorising all large wildfires between 1986 and 1995, the 2000 WUI map for all large wildfires between 1996 and 2005, the 2010 WUI map for all large wildfires between 2006 and 2015, and the 2020 WUI map for all large wildfires between 2016 and 2021. we characterised large wildfire regimes within WUI and non-WUI areas by calculating the total number, average size, total area burned, and ignition sources of large wildfires inside and outside the WUI for each L3 ecoregion. The average large wildfire size is the mean area burned by a single wildfire within a given ecoregion, measured in hectares. In contrast, the total area burned is the sum of the area burned by all large wildfires within a given ecoregion, measured in hectares (Figure 2-2, Table 2-1).

Temporal Patterns in WUI Large Wildfires

To assess temporal trends in WUI versus non-WUI large wildfire regime characteristics across the eastern US, we examined changes in total number, average size, total area burned within an ecoregion and ignition source of large wildfires inside and outside the WUI for each L3 ecoregion from 1986 to 2021 using the Mann-Kendall Trend Test ($\alpha = 0.05$), which determines the presence, strength and direction of monotonic trends. we only included ecoregions that contained 10 or more WUI ($n = 16$) or 10 or more non-WUI ($n = 15$) large wildfires from 1986 to 2021 because a smaller sample size would be insufficient for statistical analysis (Donovan, Crandall, et al., 2023). We used a logistic model ($\alpha = 0.05$) to assess temporal trends in the presence and absence of wildfires inside and outside the WUI. We also examined temporal trends in the probability of human-ignited wildfires inside and outside the WUI using a logistic model ($\alpha = 0.05$). We visualised changes in wildfire seasonality across L3 ecoregions using Gaussian kernel density estimates of fire density for the first and last decades of

our study period (H. Wickham, 2016). We only included ecoregions that contained five or more WUI and non-WUI large wildfires per decade, as we deemed that a smaller sample size would be insufficient for visualisation purposes (Donovan, Crandall, et al., 2023). Bandwidth was calculated using 'Silverman's rule of thumb' (Silverman, 1986).

We used ArcGIS Pro (version 3.1.2) to merge spatial datasets. We used the R statistical environment (R Core Team, 2023) in RStudio (RStudio Team, 2023) for data visualisation and statistical analysis.

Results

Temporal Patterns in the WUI

In 2020, the WUI covered 548,361 km^2, constituting 22% of the eastern US (Table A-1, Figure 2-1). Intermix WUI covered 17% of the area, and interface WUI covered 5% (Table A-1). In 2020, WUI area in the eastern US had expanded 29% relative to 1990. Intermix WUI grew 28%, while interface WUI grew 34% (Table A-1, Figure 2-1).

We observed unique patterns in the WUI's geographic distribution and growth across the eastern US. Central and northeastern ecoregions contained the highest proportion of WUI area (Table A-1, Figure 2-1). In 2020, southwestern ecoregions had experienced the greatest increase in intermix WUI area relative to 1990 (Table A-1, Figure 2-1). Ecoregions in the central and western parts of the eastern US experienced the greatest increase in interface WUI (Table A-1, Figure 2-1).

Spatial Patterns in WUI Large Wildfires

Forty-five percent of the 2388 wildfires that burned in the eastern US burned in the WUI, more than would be expected based on WUI land area (Table 2-1). WUI large wildfires made up the majority of the area burned in the eastern US, accounting for 55%

of the area burned (1.6 million ha) (Table 2-1). Large wildfires that burned in the WUI were, on average, also 46% larger than those outside the WUI (Table 2-1). WUI large wildfires were 1468 ± 167 s.e. ha, whereas non-WUI large wildfires were 1003 ± 97 s.e. ha (Table 2-1).

WUI large wildfires were more often ignited by humans than non-WUI large wildfires. Human ignitions were responsible for 91% of WUI large wildfires, compared with 80% of non-WUI large wildfires (Table 2-1). 'Arson and incendiarism' was the most common cause of WUI large wildfires (52%), and 'debris and open burning' was the next most common cause (18%) (Figure A-9).

The Central Appalachians ecoregion contained the greatest number of large wildfires inside the WUI. In contrast, the Southern Coastal Plain ecoregion had the greatest number of large wildfires outside the WUI (Table 2-1, Figure 2-2). WUI and non-WUI large wildfires burned the greatest total area within the Southern Coastal Plain (569,212 and 594,588 ha, respectively) (Table 2-1, Figure 2-2). All WUI and non-WUI large wildfires in the Central Appalachians were human-caused, whereas in the Southern Coastal Plain, only 59% of non-WUI large wildfires and 76% of WUI large wildfires were human-caused (Table 2-1, Figure 2-2). Southwestern and southeastern ecoregions had the greatest average size for WUI large wildfires, ranging from 2206 to 2741 ha (Arkansas Valley and Southern Coastal Plain, respectively) (Table 2-1).

Temporal Patterns in WUI Large Wildfires

At the L1 ecoregion scale, both the number and the total area burned by large wildfires outside the WUI increased, though only trends in large wildfire number were statistically significant (Table 2-2). In contrast, there was a slight, non-significant negative trend in WUI large wildfire number and total area burned (Table 2-2). At the L3

ecoregion scale, increasing trends in large wildfires in the WUI were generally weaker than those occurring outside the WUI (Table 2-2). For example, 75% (12 of 16) of ecoregions analysed showed increasing trends in the number and total area burned by large wildfires inside the WUI; however, these trends were fairly weak, with only 13% (2 of 16) of ecoregions showing statistical significance in large wildfire number and 6% (1 of 16) in total area burned (Table 2-2, Figure 2-3). However, 87% (13 of 15) of ecoregions analysed showed increasing trends in the number of large wildfires outside the WUI, with 33% (5 of 15) being statistically significant (Table 2-2, Figure 2-3). Additionally, 73% (11 of 15) showed increases in total area burned by large wildfires outside the WUI, with 27% (4 of 15) showing statistical significance (Table 2-2, Figure 2-3). Southwestern ecoregions such as the Ouachita Mountains and Arkansas Valley had very consistent increasing trends in the number and total area burned by both WUI and non-WUI large wildfires (Table 2-2, Figure 2-3).

The eastern US as a whole did not experience any substantial changes in the average size of large wildfires inside the WUI. At the L3 ecoregion scale, 50% of ecoregions showed slight declining trends in the average size of large wildfires inside the WUI, with only 6% (1 of 16; Southwestern Appalachians) being statistically significant (Table 2-2, Figure 2-3). Large wildfires outside the WUI also showed weak declining trends; 60% of ecoregions showed slight declining trends in the average size of large wildfires outside the WUI, with 7% being statistically significant (1 of 15; Table 2-2, Figure 2-3). The Ozark Highlands showed a strong increasing trend in the average size of large wildfires outside the WUI, whereas central ecoregions, such as the Central

Appalachians and Piedmont as well as the Atlantic Coastal Pine Barrens, showed strong decreasing trends in the average size of large wildfires (Table 2-2, Figure 2-3).

Across the eastern US, WUI and non-WUI large wildfires occurred every year between 1986 and 2021. At the L3 ecoregion scale, most ecoregions showed signals of increases in the annual probability of occurrence for both WUI and non-WUI large wildfires (Table 2-2). Southwestern ecoregions, such as the Arkansas Valley and Ouachita Mountains, showed some of the greatest increases in the annual probability of a WUI and non-WUI large wildfire occurring over time (Table 2-2). Not all ecoregions experienced increases in the annual probability of large wildfire occurrence. For instance, the North Central Hardwood Forests ecoregion showed a significant decline in the annual probability of occurrence of large wildfires outside the WUI. The Southern Coastal Plain experienced non-WUI large wildfires every year of our study period.

The eastern US also experienced changes in the seasonality of WUI and non-WUI large wildfires. During the first decade of our assessment (1986-1995), WUI large wildfires occurred predominantly during the fall (autumn). By the last decade of our assessment, WUI large wildfires were more equally distributed between spring and fall (2012-2021) (Figure 2-4a). This pattern contrasts with non-WUI large wildfire seasonality, which remained fairly consistent across the first and last decades of our assessment. At the L3 ecoregion scale, WUI and non-WUI large wildfires became more common during the spring in the Ridge and Valley ecoregion (Figure 2-4b). In the Southeastern Plains ecoregion, large wildfires outside the WUI became less common during the fall, whereas WUI large wildfires became less common during the summer (Figure 2-4b). In the Southern Coastal Plain, WUI large wildfires became slightly more

common during early fall, whereas in the Central Appalachian ecoregion, WUI large wildfires became slightly more common during spring (Figure 2-4b).

Across the eastern US, the odds of a large wildfire being human-ignited increased both inside and outside the WUI; however, neither was statistically significant (Table 2-2). At the L3 ecoregion scale, the odds of a large wildfire being human-ignited increased through time in the Ouachita Mountains ecoregion inside the WUI, whereas the Middle Atlantic Coastal Plain showed an increasing trend in the odds of human-ignited large wildfires outside the WUI. That said, neither ecoregion trend was statistically significant (Table 2-2).

Discussion

Large wildfire regime characteristics in the eastern US displayed unique dynamics in the WUI compared with non-WUI wildfires. Although the WUI covers 22% of the area in the eastern US, 45% of large wildfires burned there, indicating that the WUI disproportionately affects wildfire risk in the eastern US. Southwestern ecoregions of the eastern US experienced rapid WUI growth, which coincided with the strongest signals of increasing wildfire both inside and outside the WUI. WUI wildfires are increasing in certain ecoregions; however, increasing trends were more substantial and abundant outside the WUI, suggesting that non-WUI wildfires are likely the primary driver of increasing large wildfire trends documented across the eastern US (Donovan, Crandall, et al., 2023). Furthermore, we found that northern ecoregions experienced very few large wildfires, despite having a high proportion of WUI. These findings suggest that increasing large wildfire trends in the eastern US are primarily driven by large wildfires outside the WUI.

The disparity in shifting wildfire regime characteristics within and outside the WUI is likely linked to a host of social-ecological factors. Numerous studies have demonstrated links between increasing wildfire and shifting climate and vegetation dynamics (Brown et al., 2021; Donovan et al., 2020; Weltzin & McPherson, 2003). The southeast is experiencing increasingly drier and warmer climatic conditions, which likely plays an important role in increasing large wildfire occurrence across the region (Fill et al., 2019; Kupfer et al., 2020). However, factors that function at smaller scales, such as fuel dynamics, ignitions, and suppression potential are more likely to be influencing differences in wildfire regime characteristics inside and outside the WUI. For example, the WUI is more likely to have higher-density forests (Sonti et al., 2022), more invasive species (Gavier-Pizarro et al., 2010), and a greater number of ignition sources (Calviño-Cancela et al., 2016; Syphard et al., 2017), all of which have the potential to increase wildfire risk. We correspondingly found that wildfires occur disproportionately more in the WUI. Interestingly, however, increases in large wildfires are largely occurring outside the WUI. Although decades of fire suppression are likely leading to more large wildfires outside the WUI owing to increased fuel loads (Kreider et al. 2024) combined with changing climate (Brown et al., 2021), within the WUI, these same drivers may be largely mitigated by timely and effective firefighting (e.g., Calkin et al., 2014; Daniels et al., 2024; Kreider et al., 2024; Swimley, 2021). Suppression resources are often directed toward larger wildfires that burn in areas with higher housing density, thereby minimising economic loss (Swimley, 2021). However, this may leave areas of low housing density without firefighting resources, allowing fires to grow larger and burn for longer. Furthermore, higher levels of fragmentation in the WUI, particularly as it

becomes more densely populated (Radeloff et al., 2018), may inherently drive smaller wildfires, meaning that increases in their occurrence were not captured in this study (Kreider et al., 2024). Although our findings may suggest that suppression efforts have been fairly effective at preventing increases in large wildfire risk to people and structures in many areas in the eastern US, the slight increases in WUI large wildfires in the majority of ecoregions analysed may be a potential early warning for future increases in WUI wildfires if current socio-ecological trajectories continue.

Although the northeastern US has a high proportion of WUI area, it experienced relatively few large wildfires compared with southern ecoregions. This difference in the occurrence of large wildfires may be due, in part, to a high degree of fragmentation in the north (e.g., Carlson et al., 2021; Hanberry, 2020; Riitters et al., 2012; J. D. Wickham et al., 2008). Although these regions contain a high proportion of WUI area, they also contain dense urban areas and croplands, which have been shown to limit the occurrence of large wildfires owing to insufficient fuel and fuel connectivity (Hanberry, 2020) to generate wildfires greater than 200 ha (the threshold for inclusion in our analysis). Prior research has suggested that fragmented landscapes in the northeastern US hamper wildfire spread, driving numerous small wildfires not captured in our study (Carlson et al., 2021). Further research could examine the overall trends of small wildfires to determine if shifts in large wildfire occurrence are happening in smaller wildfires in northern regions. Northern regions of our study area have also experienced wetter conditions that may be increasing fuel moisture and thereby reducing wildfire risk (Thibeault & Seth, 2014; Vaittinada Ayar & Mailhot, 2021). Furthermore, the north has experienced substantial ‘mesophication’, in which tree species experience a

compositional change toward shade tolerance following fire exclusion, creating conditions that further preclude fire from the system (Donovan, Crandall, et al., 2023; Nowacki & Abrams, 2008). Nonetheless, climate change is predicted to increase the risk of wildfires across the eastern US (Bedel et al., 2013; Fill et al., 2019; Swanston et al., 2018), making preemptive and adaptive management imperative.

Increased wildfire risk in ecoregions that experienced significant increases in large wildfire within the WUI may be driven by changing land use and WUI expansion. We observed the greatest increases in WUI area in southwestern ecoregions, which also experienced the most consistent increases in wildfire activity. This may be due to heightened ignition potential, the spread of exotic and woody species, and an increase in the presence of flammable materials associated with WUI growth (Donovan et al., 2020; Fernandez-Pello, 2017; Hanberry, 2020; Mietkiewicz et al., 2020). For instance, the Ouachita Mountains of Arkansas experienced an increase in the odds of human-ignited large wildfires in the WUI, suggesting that additional ignition sources associated with WUI expansion may be a driving factor for increased WUI wildfire activity. Although WUI growth may be heightening wildfire risk in southwestern ecoregions, this area also experienced changing land use associated with timber harvesting (Drummond et al., 2020). Timber operation can increase wildfire activity through ignition from machinery and increased dry fuels from slash piles (Sjöström et al., 2019; Stone et al., 2004). Timber harvesting has been shown to promote the invasion of exotic species such as cogongrass (*Imperata cylindrica*), thereby substantially altering the fuelbed (Burrell et al., 2015; McGranahan & Wonkka, 2022). This alteration can heighten fire intensity by increasing fuel loading and continuity and promote more rapid and expansive fire

spread in logged areas (Tomat-Kelly et al., 2021). With the number of large wildfires projected to continue to increase under future climate (Senande-Rivera et al., 2022) and the continuing expansion of the WUI, suppression capacity is likely to be spread increasingly thinly in the eastern US. Proactive fuels management, especially in and around communities in the WUI, will be important, particularly in regions showing signals of increasing large wildfire activity in the WUI. Our study highlights the importance of the WUI in influencing large wildfire regimes and provides a starting point for more region-specific analyses of drivers of changing large wildfire dynamics inside and outside the WUI.

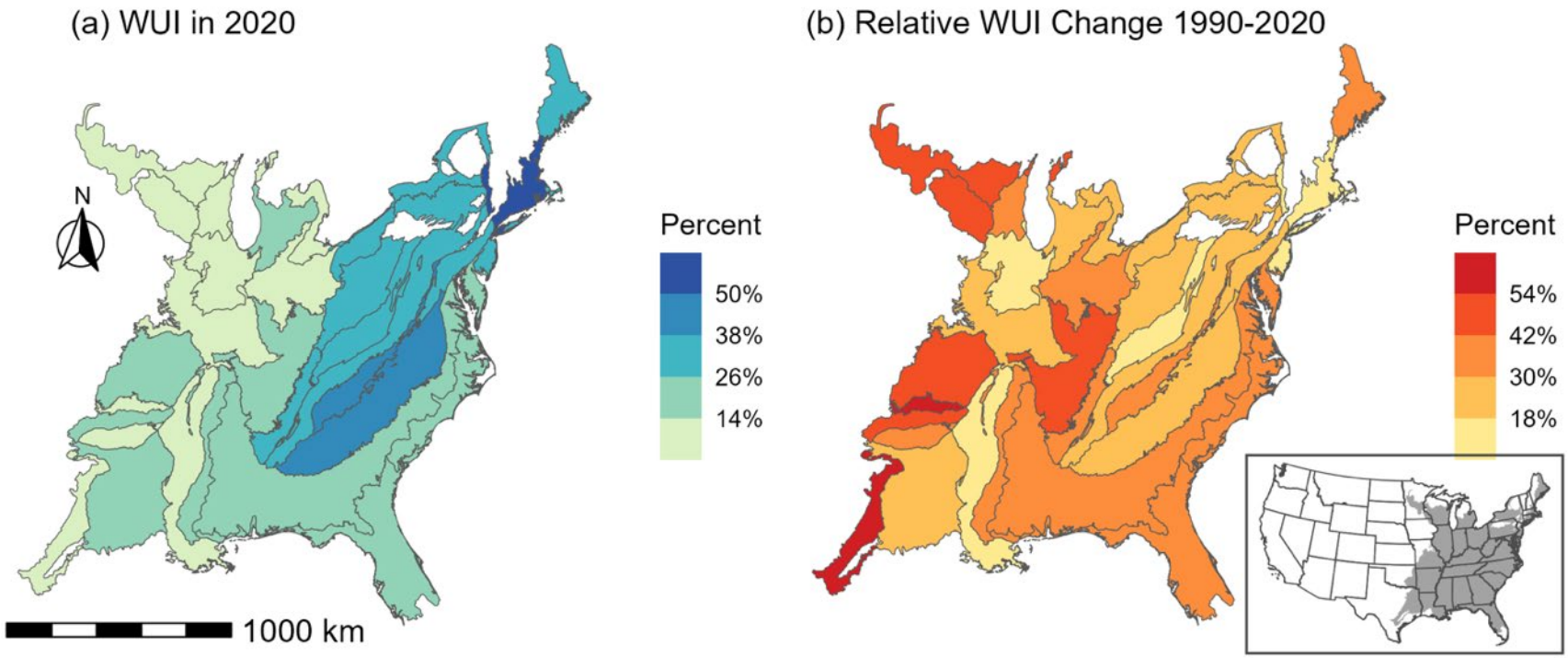


Figure 2-1. Maps showing the percentage area occupied by the wildland-urban interface (WUI) in 2020; and the relative percentage change from 1990 to 2020 ((area 2020 − area 1990) ÷ area 1990) for Level III ecoregions of the eastern United States.

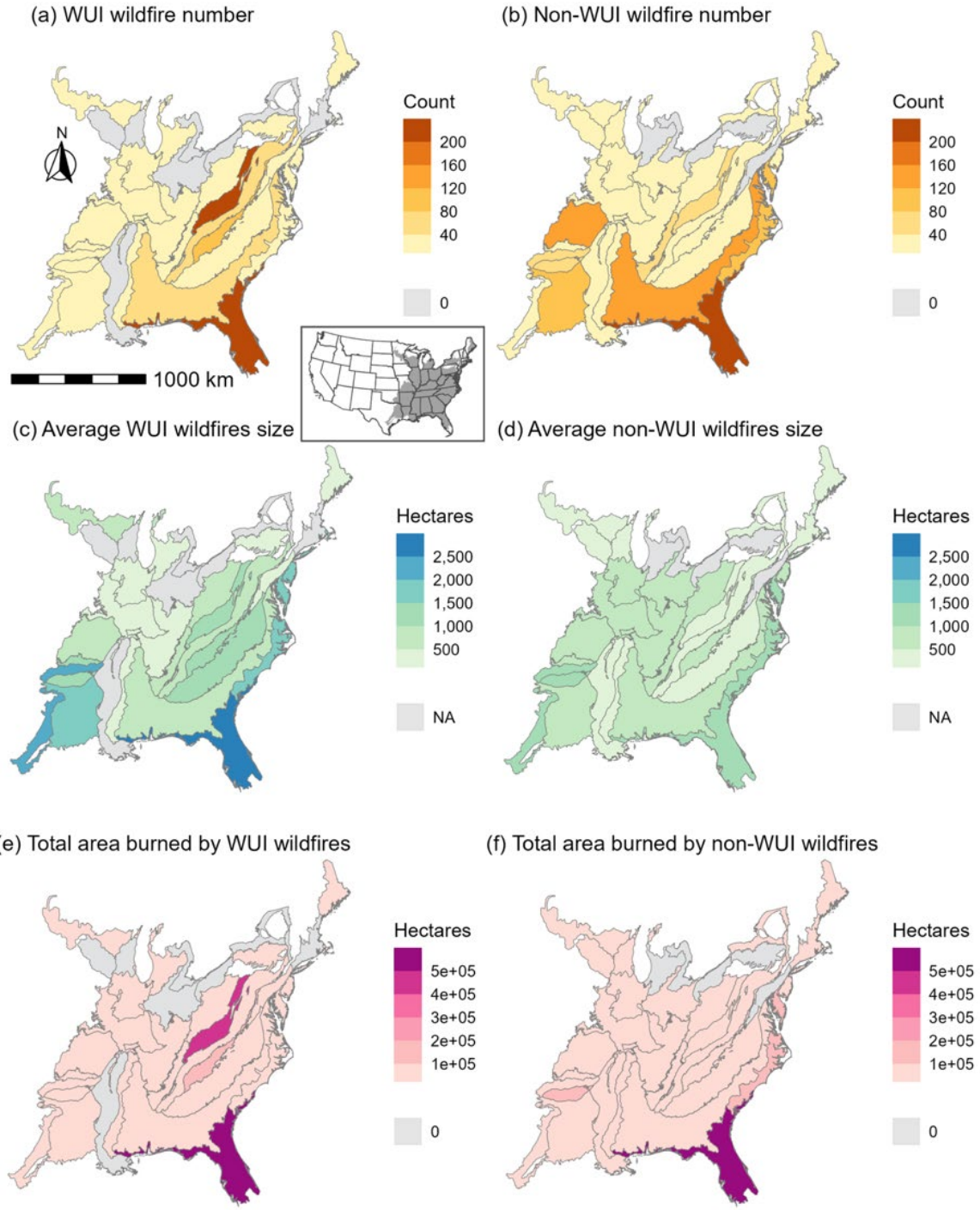


Figure 2-2. Maps showing the total number, average size (in ha), and total area burned (in ha) by large wildfires (>200 ha) inside and outside the wildland-urban interface (WUI) across Level III ecoregions of the eastern United States between 1986 and 2021. Darker colours indicate larger values, while lighter colours indicate smaller values. Ecoregions in grey contained no WUI or non-WUI large wildfires during the study period.

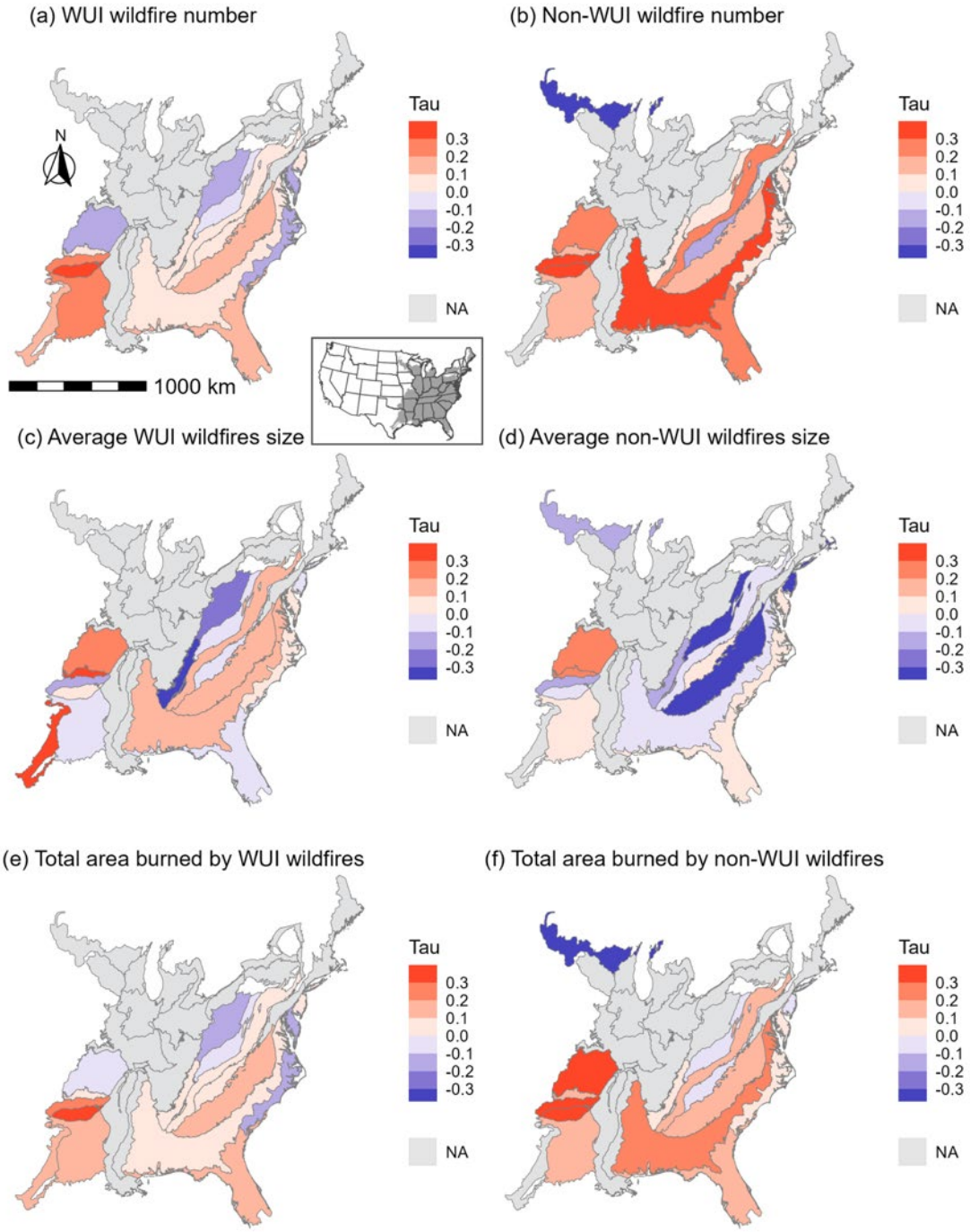


Figure 2-3. Maps showing Mann-Kendall tau values for annual changes in the number, average size (in ha), and total area burned (in ha) by large wildfires (>200 ha) inside and outside the WUI. Darker red colours represent ecoregions with more consistent positive trends over time, whereas darker blue colours represent ecoregions with more consistent negative trends over time. Grey represents ecoregions excluded from analysis owing to insufficient wildfire numbers over the study period.

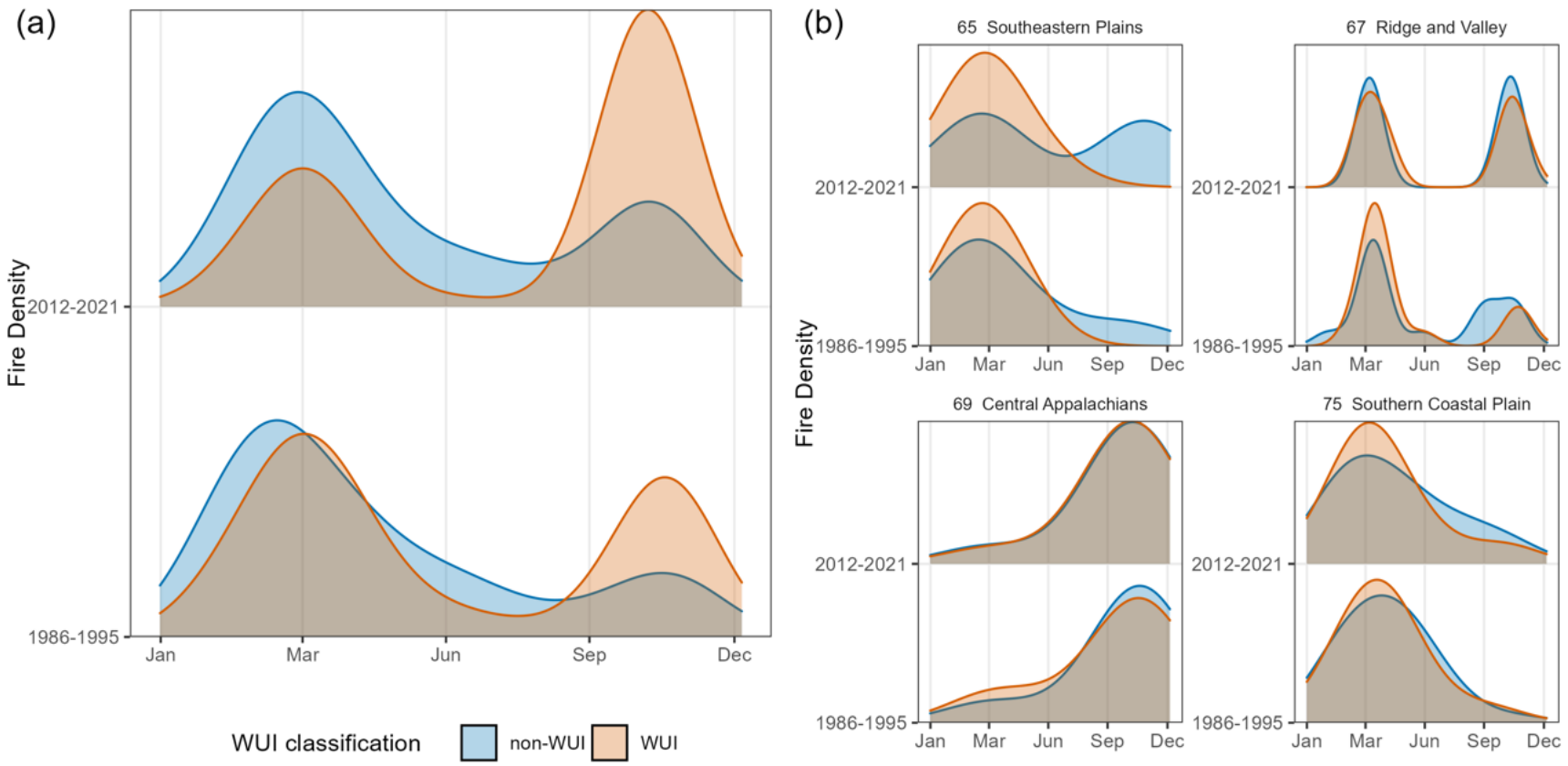


Figure 2-4. Gaussian kernel density estimates for large (>200 ha) wildfire seasonality inside and outside the wildland-urban interface (WUI) of the Level 1 Eastern Temperate Forests ecoregion (the eastern US), and Level III ecoregions. Only ecoregions that contained five or more WUI and non-WUI large wildfires within the first and last decades of our assessment were used to create density estimates because a smaller sample size would be insufficient for proper visualisation. Bandwidth was determined using 'Silverman's Rule of Thumb' (Silverman 1986).

Table 2-1. Characteristics of large (>200 hectares) wildfires inside and outside the wildland-urban interface (WUI) across Level III ecoregions of the eastern United States between 1986 and 2021, including total number, average size (± standard error) (in hectares), total area burned (in hectares) (n = 2,388), and proportion of wildfires ignited by humans (n = 1,749). Dashes (–) represent the absence of a large wildfire for a given ecoregion.

Ecoregion	Number of non-WUI wildfires	Number of WUI wildfires	Average non-WUI wildfire size ± SE (ha)	Average WUI wildfire size ± SE (ha)	Area burned by non-WUI wildfires (ha)	Area burned by WUI wildfires (ha)	Proportion non-WUI wildfires ignited by humans	Proportion WUI wildfires ignited by humans
L1 Eastern Temperate Forests (eastern US)	1,308	1,080	1,003 ± 97	1,468 ± 167	1,311,490	1,585,195	0.80	0.91
Acadian Plains and Hills	1	1	285	254	285	254	1.00	1.00
Arkansas Valley	51	23	1,500 ± 228	2,206 ± 593	76,506	50,737	0.93	1.00
Atlantic Coastal Pine Barrens	24	20	588 ± 101	1,685 ± 518	14,124	33,698	0.79	1.00
Blue Ridge	40	89	691 ± 271	1,155 ± 169	27,621	102,777	0.62	0.86
Boston Mountains	34	13	878 ± 96	1,417 ± 388	29,846	18,420	0.96	1.00
Central Appalachians	69	406	480 ± 40	1,202 ± 98	33,134	488,140	1.00	1.00
Central Corn Belt Plains	1	1	648	349	648	349	–	–
Driftless Area	1	0	223	–	223	0	–	–
East Central Texas Plains	4	10	1,309 ± 359	2,272 ± 1190	5,237	22,722	1.00	1.00
Eastern Corn Belt Plains	3	0	637 ± 134	–	1,912	0	1.00	–
Eastern Great Lakes Lowlands	1	0	412	–	412	0	–	–
Interior Plateau	7	5	577 ± 222	347 ± 69	4,039	1,736	0.60	1.00

Table 2-1. Continued

Ecoregion	Number of non-WUI wildfires	Number of WUI wildfires	Average non-WUI wildfire size ± SE (ha)	Average WUI wildfire size ± SE (ha)	Area burned by non-WUI wildfires (ha)	Area burned by WUI wildfires (ha)	Proportion non-WUI wildfires ignited by humans	Proportion WUI wildfires ignited by humans
Interior River Valleys and Hills	2	2	525 ± 105	433 ± 174	1,050	866	1.00	1.00
Middle Atlantic Coastal Plain	88	40	1,338 ± 308	1,554 ± 788	117,709	62,180	0.85	0.84
Mississippi Alluvial Plain	3	0	396 ± 69	–	1,187	0	0.00	–
Mississippi Valley Loess Plains	7	7	335 ± 48	333 ± 40	2,343	2,329	1.00	1.00
North Central Hardwood Forests	18	6	380 ± 45	774 ± 188	6,837	4,642	1.00	1.00
Northeastern Coastal Zone	1	0	308	–	308	0	1.00	–
Northern Allegheny Plateau	0	1	–	382	0	382	–	1.00
Northern Piedmont	0	2	–	292 ± 37	0	584	–	1.00
Ouachita Mountains	72	17	1,475 ± 169	1,177 ± 218	106,188	20,005	0.86	0.79
Ozark Highlands	126	39	631 ± 67	707 ± 122	79,508	27,561	0.97	1.00
Piedmont	23	20	385 ± 50	1,080 ± 315	8,866	21,590	0.93	0.80
Ridge and Valley	38	57	434 ± 34	917 ± 145	16,474	52,268	0.88	0.93
South Central Plains	83	40	751 ± 99	1,787 ± 465	62,357	71,495	0.82	0.79

Table 2-1. Continued

Ecoregion	Number of non-WUI wildfires	Number of WUI wildfires	Average non-WUI wildfire size ± SE (ha)	Average WUI wildfire size ± SE (ha)	Area burned by non-WUI wildfires (ha)	Area burned by WUI wildfires (ha)	Proportion non-WUI wildfires ignited by humans	Proportion WUI wildfires ignited by humans
Southeastern Plains	160	65	617 ± 47	534 ± 46	98,776	34,711	0.94	0.95
Southeastern Wisconsin Till Plains	2	0	354 ± 26	–	709	0	1.00	–
Southern Coastal Plain	442	214	1,413 ± 271	2,741 ± 788	624,362	586,560	0.59	0.76
Southern Michigan/Northern Indiana Drift Plains	0	2	–	392 ± 44	0	785	–	–
Southwestern Appalachians	49	38	541 ± 51	694 ± 100	26,519	26,365	1.00	1.00
Western Allegheny Plateau	4	22	559 ± 195	944 ± 207	2,237	20,769	1.00	1.00

Table 2-2. Changes in regime characteristics for large (>200 hectares) wildfires inside and outside the wildland-urban interface (WUI) across Level III ecoregions of the eastern United States from 1986 to 2021. The number, average size (in hectares), and total area burned (in hectares) were assessed using the Mann-Kendall Trend Test. The annual probability of large wildfire occurrence and the probability of human ignition were also evaluated using a binomial generalized linear model. We only included ecoregions containing ten or more WUI or non-WUI large wildfires during the study period for these assessments. Dashes (–) indicate insufficient data for analysis.

Ecoregion	WUI status	Number (#)		Avg. size (ha)		Area burned (ha)		Annual probability of occurrence				Probability of human ignition			
		τ	p	τ	p	τ	p	odds ratio	2.5%	97.5%	p	odds ratio	2.5%	97.5%	p
L1 Eastern Temperate Forests (eastern US)	WUI	-0.04	0.75	0.00	1.00	-0.05	0.65	–	–	–	–	1.02	0.98	1.07	0.25
	non-WUI	0.29	0.01	0.03	0.80	0.21	0.08	–	–	–	–	1.00	0.98	1.03	0.89
Arkansas Valley	WUI	0.27	0.05	-0.15	0.50	0.23	0.08	1.08	1.01	1.18	0.04	–	–	–	–
	non-WUI	0.42	<0.01	-0.11	0.54	0.33	<0.01	1.12	1.04	1.23	<0.01	–	–	–	–
Atlantic Coastal Pine Barrens	WUI	0.08	0.58	-0.07	0.77	0.07	0.57	1.02	0.96	1.09	0.49	–	–	–	–
	non-WUI	0.02	0.88	-0.34	0.10	-0.03	0.83	1.01	0.94	1.07	0.84	–	–	–	–
Blue Ridge	WUI	0.08	0.54	-0.03	0.87	0.07	0.59	1.02	0.96	1.09	0.52	1.04	0.93	1.15	0.49
	non-WUI	-0.14	0.30	0.04	0.81	-0.05	0.68	0.98	0.92	1.05	0.57	0.94	0.82	1.07	0.37
Boston Mountains	WUI	0.04	0.79	0.36	0.27	0.04	0.78	1.00	0.93	1.08	0.97	–	–	–	–
	non-WUI	0.18	0.18	0.25	0.17	0.17	0.18	1.02	0.96	1.09	0.45	–	–	–	–
Central Appalachians	WUI	-0.08	0.53	-0.10	0.49	-0.08	0.53	1.03	0.96	1.11	0.46	–	–	–	–
	non-WUI	0.01	0.92	-0.39	0.02	-0.04	0.76	1.03	0.97	1.10	0.37	–	–	–	–
East Central Texas Plains	WUI	0.16	0.25	0.40	0.46	0.17	0.22	1.06	0.96	1.18	0.27	–	–	–	–
	non-WUI	–	–	–	–	–	–	–	–	–	–	–	–	–	–
Middle Atlantic Coastal Plain	WUI	-0.18	0.17	0.01	1.00	-0.15	0.24	0.96	0.89	1.02	0.18	0.90	0.68	1.15	0.38
	non-WUI	0.07	0.61	0.03	0.82	0.04	0.76	0.98	0.87	1.11	0.79	1.08	0.99	1.20	0.08

Table 2-2. Continued

Ecoregion	WUI status	Number (#)		Avg. size (ha)		Area burned (ha)		Annual probability of occurrence				Probability of human ignition			
		τ	p	τ	p	τ	p	odds ratio	2.5%	97.5%	p	odds ratio	2.5%	97.5%	p
North Central Hardwood Forests	WUI	–	–	–	–	–	–	–	–	–	–	–	–	–	–
	non-WUI	-0.33	0.02	-0.13	0.64	-0.31	0.02	0.92	0.84	0.99	0.04	–	–	–	–
Ouachita Mountains	WUI	0.40	<0.01	0.07	0.86	0.38	<0.01	1.14	1.05	1.29	0.01	1.98	1.10	6.16	0.08
	non-WUI	0.39	<0.01	-0.03	0.88	0.37	<0.01	1.12	1.04	1.24	<0.01	1.05	0.92	1.21	0.44
Ozark Highlands	WUI	-0.14	0.30	0.21	0.18	-0.06	0.62	0.96	0.90	1.02	0.23	–	–	–	–
	non-WUI	0.24	0.05	0.28	0.03	0.31	<0.01	1.15	1.02	1.36	0.05	–	–	–	–
Piedmont	WUI	0.20	0.15	0.13	0.58	0.19	0.14	1.04	0.98	1.12	0.21	–	–	–	–
	non-WUI	0.17	0.20	-0.36	0.10	0.12	0.36	1.03	0.97	1.11	0.36	–	–	–	–
Ridge and Valley	WUI	0.09	0.48	0.16	0.29	0.10	0.43	1.02	0.95	1.09	0.59	–	–	–	–
	non-WUI	0.22	0.10	-0.05	0.77	0.18	0.14	1.06	0.99	1.14	0.10	–	–	–	–
South Central Plains	WUI	0.20	0.14	-0.07	0.77	0.18	0.16	1.05	0.99	1.14	0.12	1.07	0.92	1.26	0.35
	non-WUI	0.18	0.15	0.01	0.96	0.16	0.19	1.06	0.99	1.15	0.11	0.99	0.89	1.08	0.78
Southeastern Plains	WUI	0.07	0.61	0.11	0.47	0.07	0.56	1.00	0.93	1.07	0.99	–	–	–	–
	non-WUI	0.36	<0.01	-0.07	0.59	0.25	0.04	1.26	1.04	1.83	0.09	–	–	–	–
Southern Coastal Plain	WUI	0.13	0.28	-0.00	0.99	0.11	0.37	1.18	0.98	1.68	0.18	1.01	0.95	1.06	0.83
	non-WUI	0.26	0.03	0.05	0.67	0.16	0.19	–	–	–	–	1.00	0.96	1.03	0.84
Southwestern Appalachians	WUI	0.04	0.79	-0.52	0.02	0.01	0.94	1.01	0.95	1.08	0.71	–	–	–	–
	non-WUI	0.07	0.61	-0.18	0.29	0.06	0.65	1.02	0.96	1.09	0.47	–	–	–	–
Western Allegheny Plateau	WUI	-0.18	0.19	-0.20	0.47	-0.17	0.20	0.96	0.89	1.04	0.34	–	–	–	–
	non-WUI	–	–	–	–	–	–	–	–	–	–	–	–	–	–

CHAPTER 3
FIRE AT THE FRINGE: DRIVERS OF LARGE WILDFIRES IN AND NEAR THE WILDLAND-URBAN INTERFACE OF THE EASTERN UNITED STATES

The wildland-urban interface (WUI), where wildland and urban environments intermingle, is a complex socio-environmental system (Pulver et al., 2018) that creates conditions for heightened wildfire risk (Calviño-Cancela et al., 2016; Radeloff et al., 2018). Houses in the WUI are more likely to be exposed to wildfire due to various social and environmental factors, such as increased ignition potential from human activity, the presence of highly flammable materials, and the invasion of exotic species (Radeloff, Mockrin, et al., 2023). WUI wildfires have resulted in a substantial number of fatalities of both civilians and firefighting personnel (Haynes et al., 2020). For example, the 2018 Camp Fire that burned through the WUI of Paradise, California, United States (US), destroyed more than 18,000 structures and took 85 lives (Maranghides et al., 2021). In addition to structural damage, wildfires that burn in the WUI can expose individuals living nearby to unhealthy levels of smoke, leading to adverse health outcomes (D'Evelyn et al., 2022; Stefanidou et al., 2008). As wildfire risk continues to increase (Schug et al., 2023; Tang et al., 2024), it is imperative to understand what drivers increase wildfire risk within and surrounding the WUI.

Wildfire dynamics are controlled by several biophysical factors, including fuels, climate, and weather (Ellis et al., 2022; Ganteaume, Camia, et al., 2013; Moritz et al., 2005; Rao et al., 2023). Vegetation types and patterns can alter fire occurrence, severity, and intensity. For instance, increasing woody cover has been linked to increasing wildfire risk (Donovan et al., 2020; Ivey et al., 2024). Changes in vegetation structure can also alter wildfire risk. For example, increased "ladder fuels" (Forbes et al., 2022) can facilitate fire spreading from the ground layer to the canopy, thereby

increasing firebrands and spotting (Donovan, Fogarty, et al., 2023; Wadhwani et al., 2022). Firebrands can then travel onto roofs, a leading cause of property damage and loss during wildfire (Manzello et al., 2010, 2011). The spread of wildfire via firebrands is exacerbated by increased wind gusts (Wei et al., 2023). High wind speeds also increase wildfire spread, leading to larger, more destructive wildfires (Balch et al., 2024). (Zhai et al., 2023) Changes in local weather patterns, including lower relative humidity, lower precipitation, and higher average temperature, can dry out fuels and make them more susceptible to burning (P. Jain et al., 2022). Global changes in climate have also been linked to longer fire seasons and larger, more destructive wildfires (Pausas et al., 2017). Social-ecological interactions can further alter these dynamics through variability in vegetation management, human-caused ignition sources, suppression resource allocation and prioritization, and invasive plant facilitation, among others.

Anthropogenic activity greatly alters wildfire risk within and near the WUI (Liu et al., 2015; Tepley et al., 2018). For example, human development in the WUI can change the structure and flammability of surrounding vegetation by increasing woody encroachment and invasive species (Carlson et al., 2023; Ganteaume, Jappiot, et al., 2013). WUI areas are often more invaded than non-WUI areas and have higher tree density (Potter et al., 2024; Sonti et al., 2022). Wildfire ignitions are also twice as likely to occur in the WUI as outside the WUI (Chas-Amil et al., 2013), where the vast majority of WUI wildfire ignitions (97%) are caused by humans (Mietkiewicz et al., 2020). Wildfire ignitions from human sources are more likely to occur closer to roads and developed areas (Calviño-Cancela et al., 2017; Jaafari et al., 2022). However, the WUI also has a higher suppression potential (Stasiewicz & Paveglio, 2022). While roads have been

shown to increase the probability of wildfire ignitions (Syphard & Keeley, 2015), they can also act as a fuel break that prevents wildfire spread while simultaneously facilitating firefighter access (Povak et al., 2018). Highly toxic smoke produced by WUI wildfires can impede firefighting efforts (Tang et al., 2025). Because social and environmental factors can often interact in complex ways, the drivers of wildfire risk within and surrounding the WUI likely vary among regions. Since wildfire risk is highest in the WUI, wildfire-WUI interactions are often used as a proxy for assessing risk to human life and settlement (Pierce et al., 2022). Understanding the factors that drive wildfires in and near the WUI is essential for recognizing and preventing wildfire risk to human development and lives, particularly in areas experiencing increasing wildfire activity.

Large wildfires are increasing in the eastern US (Donovan, Crandall, et al., 2023), posing a potentially substantial risk to human life and settlement due to the extensive WUI (Gaither et al., 2011; Mietkiewicz et al., 2020; Radeloff et al., 2005, 2018; Radeloff, Mockrin, et al., 2023; Theobald & Romme, 2007). The East contains the highest proportion of WUI area in the US (Radeloff et al., 2018). Just under half of all large wildfires in the eastern US intersect the WUI (Chapter 2). WUI wildfires make up the majority of the area burned by large wildfires. However, only certain regions of the East, particularly southwestern ones, are experiencing increases in large wildfire activity within the WUI, suggesting complex socio-economic dynamics that vary from region to region (Chapter 2). Understanding which social-ecological factors most influence large wildfire risk within and surrounding the WUI is imperative to support preemptive wildfire management to get ahead of the growing wildfire problem in the East.

We assessed spatial patterns and factors influencing large wildfire occurrence within and surrounding the WUI in the eastern US using large wildfire (≥200 ha) data over a 31-year period at multiple spatial scales. Specifically, we aimed to (1) determine large wildfire patterns within and around the WUI and (2) identify which social and environmental factors are most associated with large wildfire occurrence within and surrounding the WUI. We focused specifically on factors linked to ignitions, suppression potential, fuels, and weather. We assess large wildfires relative to three categories of wildfire-WUI interaction. First, we assess whether wildfires were more likely to occur within the WUI than expected at random. Second, for the wildfires that did intersect the WUI, we determine if the proportion of their perimeter that falls within the WUI is greater than expected at random. Lastly, of the wildfires that did not fall within the WUI, we assess whether these wildfires are closer to the WUI than expected at random. For each category, we then assess what socio-environmental factors were best at predicting this relationship.

Methods

Data

We delineated the eastern United States using the Environmental Protection Agency's Eastern Temperate Forest Level I (L1) ecoregion (hereafter referred to as the “eastern US”) (EPA, 2013). Ecoregions are hierarchical spatial subdivisions of the landscape based on comparable ecological characteristics (Omernik & Griffith, 2014). This region also has a high degree of variability in vegetative and climatic conditions, necessitating a multiscale assessment (Gilliam et al., 2011). Therefore, we further subdivided the study area using three Level II (L2) ecoregions (Figure B-1). Only three L2 ecoregions had a sufficient number of large wildfires for statistical modeling (>100

large wildfires). The Mississippi Alluvial and Southeast USA Coastal Plains ecoregion is characterized by diverse forests, from longleaf pine to bottomland hardwood forests, and a humid, subtropical climate (Zhu, 2014). The Ozark/Ouachita-Appalachian Forests ecoregion is heavily forested with mainly mixed oak-hickory forests and is characterized by a humid continental climate (Zhu, 2014). The Southeastern USA Plains ecoregion has a mix of oak-hickory and southern pine forests and a moist, subtropical climate (Zhu, 2014).

We used spatial WUI data from the United States Department of Agriculture's (USDA) wildland-urban interface database, containing census block-level WUI classification for 1990, 2000, 2010, and 2020 (Radeloff, Helmers, et al., 2023). We used the decade closest to a wildfire's ignition date to assess its spatial relationship to the WUI. We used the 1990 WUI classification for wildfires between 1991 and 1995, the 2000 classification for wildfires between 1996 and 2005, the 2010 classification for wildfires between 2006 and 2015, and the 2020 classification for wildfires between 2016 and 2021 (Chapter 2).

Wildfire perimeter data were taken from the "Burned Area Boundary Dataset" from the Monitoring Trends in Burn Severity (MTBS) project, a collaboration between federal agencies for recording and publicizing large (≥400 ha in the western US and ≥200 ha in the eastern US) fire data across the US (Eidenshink et al., 2007; MTBS, 2023). We only included large (≥200 ha) fires classified as "wildfires" from 1991 to 2021 (n = 2,184) (Nagy et al., 2018). Wildfire perimeters from MTBS are digitized polygons derived from Landsat imagery using differenced Normalized Burn Ratio (Eidenshink et

al., 2007). We also used the USDA's Fire Occurrence Database (Short, 2022) to roughly assess the duration of large wildfires in the eastern US (Figure B-2).

Weather conditions can greatly affect fire behavior and spread, thereby impacting whether a wildfire burns in the WUI (Wei et al., 2023) (Table 3-1). Weather data were acquired from the Gridded Surface Meteorological (gridMET) dataset using Google Earth Engine (Google Earth Engine, 2024; Gorelick et al., 2017). GridMET data are derived from local weather stations and PRISM climate data (Kittel et al., 1997) to produce a 4-km resolution daily weather dataset from 1979 to the current date (Abatzoglou, 2013). We calculated average windspeed, 100-hour fuel moisture, and precipitation across various temporal windows before and after each wildfire's ignition date. We used Akaike's Information Criterion (AIC) to compare variables to determine the window that best explained the data (*MuMIn* package; Table B-1 to B-9) (Akaike, 1973).

The amount of existing suppression resources in a given area can also affect where wildfires burn relative to human settlements (Renkas et al., 2022). We used the "Forest Service Office Locations" (USDA Forest Service, 2021) and the Homeland Infrastructure Foundation-Level "Fire and Emergency Medical Service (EMS) Stations" (HIFLD, 2024) datasets to calculate existing suppression resources around large wildfires. We created multiple buffer sizes around each wildfire to calculate fire and EMS station density (n/km^2) (Pourmohamad et al., 2024). We used AIC to compare the different buffer sizes and selected fire and EMS station density within a 1 km buffer around each wildfire perimeter as our final variable (Tables B-10 to B-12).

Woody cover has been linked to increasing wildfire risk in multiple regions (Donovan et al., 2020; Hessburg et al., 2005), including the eastern US (Ivey et al., 2024) (Table 3-1). Woody cover data were collected from the Rangeland Analysis Platform (RAP, version 3.0), which provides 30-meter annual fractional cover estimates for six plant functional groups (trees, shrubs, perennial forbs/grasses, annual forbs/grasses, litter, and bare ground) across the conterminous US (M. O. Jones et al., 2018). The RAP's ability to distinguish between trees and shrubs in the eastern US may be limited since the product was originally developed for the western US (Ivey et al., 2024). I, therefore, combined the tree and shrub bands to calculate a mean woody cover value across each wildfire perimeter using data from the year before each wildfire's ignition date. We excluded wildfires before 1991 due to high interannual variability in the RAP dataset (Ivey et al., 2024).

Roads can alter wildfire activity in and near the WUI in several ways (Table 3-1). We obtained historical road data from the US Census Bureau's Topologically Integrated Geographic Encoding and Referencing (TIGER) database (Carbaugh & Marx, 1990; U.S. Census Bureau, 1992 - 2021). We chose to use the TIGER dataset over other datasets due to TIGER's relative completeness and temporal span (Zielstra et al., 2013); however, since TIGER's road classifications (primary, secondary, tertiary, etc.) were temporally inconsistent, we used all roads, regardless of classification (Trainor, 2005). We calculated road density (km/km^2) within each wildfire perimeter and multiple buffers around the perimeter. We then compared these variables using AIC and selected the road density within each wildfire perimeter for use in our models (Tables B-13 to B-15).

The availability of wildfire suppression resources can also affect whether a wildfire burns in the WUI (Swimley, 2021). We used daily national preparedness level data from the National Interagency Fire Center (NIFC, 2024). Preparedness levels are on a discrete scale ranging from one to five, where a value of one represents high suppression resource availability, low fire activity, and/or mild weather conditions, and a value of five represents severely limited suppression resource availability, high fire activity, and/or extreme weather conditions (Figure B-3). We calculated the mean and median preparedness levels across various temporal windows before each wildfire's ignition date. Using AIC, we selected the preparedness level for the day prior to a large wildfire's ignition date (Tables B-16 to B-18).

Wildfire Patterns within and near the WUI

To assess the probability of a wildfire burning within the WUI, we compared the proportion of verified wildfires that burned in the WUI to a null distribution of fires randomly sampled across the general landscape at the L1 and L2 scales. To do this, we categorized wildfires as WUI or non-WUI fires based on whether a wildfire intersected the WUI (hereafter referred to as "WUI status") (n = 2,181). We then created a null distribution of buffered points equal in number and average size of large wildfires within each ecoregion. We omitted any buffered points that contained more than 30% water within their perimeters, as wildfire occurrence would be highly unlikely ("Open Water" classification used from the United States Geological Survey's 2005 National Land Cover Database (NLCD) Land Use and Land Cover product). Using a proportion test ($\alpha = 0.05$), we compared the distribution of verified wildfires to our null distribution (Fisher, 1992; Newcombe, 1998). We also visualized the difference in these distributions using

bar graphs. We used WUI status as a binary proxy for whether or not a wildfire impacts human settlement (Mietkiewicz et al., 2020).

We also separately assessed WUI and non-WUI wildfires by looking at the proportion of WUI area burned for WUI wildfires and wildfire distance to the WUI for non-WUI wildfires. To assess the probability of a wildfire burning a large proportion of the WUI, we compared the proportion of area of verified wildfires and randomly distributed buffered points that overlapped the WUI (hereafter referred to as “Proportion WUI Area”) (n = 967). For wildfires that did not intersect the WUI (n = 1,217), we assessed whether wildfires occurred closer to the WUI than expected by comparing the Euclidean distances (hereafter referred to as “distance to WUI”) of verified wildfires and random buffered points to the nearest WUI edge. We compared the distribution of verified wildfires to our null distribution generated from random points using kernel density estimation, boxplots, and a Mann-Whitney U non-parametric test ($\alpha = 0.05$) (Mann & Whitney, 1947; H. Wickham, 2016). The Mann-Whitney U test can be used to detect a difference between two non-normal distributions. Bandwidth for density estimates was calculated using Silverman’s Rule of Thumb (Silverman, 1986). We used the proportion of WUI area burned and distance to the WUI as quantitative proxies for the relative impact of large wildfires on human settlement (Kramer et al., 2019; Syphard et al., 2022).

Socio-environmental Factors Influencing Wildfires within and near the WUI

To determine socio-environmental factors that have the greatest influence on wildfires within and surrounding the WUI, we modeled our three separate dependent variables representing various spatial relationships between large wildfires and the WUI in the eastern US between 1991 and 2021 at the L1 and L2 scales. To determine which

predictors are most associated with whether a wildfire burned in the WUI, we modeled WUI status using a logit binomial generalized linear model in the R statistical environment (n = 2,184) (Nelder & Wedderburn, 1972; R Core Team, 2023; RStudio Team, 2023). For wildfires that occurred within the WUI, we further modeled the proportion of WUI area burned relative to our various predictors using a beta regression (n = 967) (M. E. Brooks et al., 2017; Zeileis et al., 2024). For wildfires that occurred outside the WUI (n = 1,217), we modeled wildfire distance to WUI relative to our various predictor variables using a generalized linear model with a log gamma family (Nelder & Wedderburn, 1972). We generated 11 candidate models containing various predictors related to ignition potential, fuel, weather, climate, and suppression potential (Table 3-2, Figures B-17 through B-36) (Burnham & Anderson, 2002; Moritz et al., 2005).

We tested model assumptions on the global model using the *performance* package (Figures B-37 to B-48) (Hartig et al., 2024; Lüdecke, Makowski, et al., 2024). Using Pearson's correlation coefficient, we assessed collinearity among predictor variables (Figures B-5 to B-16). If two variables showed a strong correlation ($r > |0.60|$), we removed one variable from the model (all variables showed low correlation values of $< |0.30|$). We also tested for multicollinearity within the global models containing two or more predictor variables using the variance inflation factor (all variables showed low VIF values of < 1.5). We used AIC to select the most parsimonious model for each dependent variable by balancing complexity and goodness of fit using the *MuMIn* package (Akaike, 1973; Bartoń, 2024). If multiple models fell within two delta AIC of the top model, we classified these models as our confidence set and employed model averaging (Symonds & Moussalli, 2011). We extracted model coefficients using

parameters (Lüdecke et al., 2025) and visualized predictions using *ggeffects* (Lüdecke, Aust, et al., 2024).

Results

Wildfire Patterns within and near the WUI

We found that large wildfires burned significantly less within the WUI and burned a significantly smaller proportion of the WUI than expected at random at the L1 ecoregion scale (Figure 3-1, Figure B-4; Table 3-3). At the L2 scale, the Southeastern USA Plains ecoregion showed the greatest difference (30.5%) between the proportion of wildfires in the WUI compared to the null distribution (Figure B-5d, Table 3-3); large wildfires that burned in the WUI in this ecoregion also burned the smallest proportion of WUI area and showed the greatest difference (20.7%) compared to the null distribution (Figure 3-1d, Table 3-3). The Ozark/Ouachita-Appalachian Forests ecoregion had the highest proportion of wildfires burning in the WUI (Figure B-5c) and wildfires that burned the highest proportion of the WUI of the L2 ecoregions (Figure 3-1c, Table 3-3).

Wildfires that burned outside the WUI burned significantly closer to the WUI than expected at random at the L1 scale (Figure 3-2a, Table 3-3). This pattern was consistent in the Ozark/Ouachita-Appalachian Forests and the Mississippi Alluvial and Southeast USA Coastal Plains L2 ecoregions (Table 3-3). In the Ozark/Ouachita-Appalachian Forests ecoregion, wildfires burned closer to the WUI than in any other ecoregion (Table 3-3). Although large wildfires in the Mississippi Alluvial and Southeast USA Coastal Plains ecoregion burned farther from the WUI than other L2 ecoregions, they burned substantially closer to the WUI than expected at random, more so than other L2 ecoregions (Figure 3-2b, Table 3-3). The Southeastern USA Plains ecoregion

did not show a statistically significant difference in distance to WUI between wildfires and our null distribution (Figure 3-2d, Table 3-3).

Socio-environmental Factors Influencing Wildfires in and near the WUI

Level 1 ecoregion scale

At the L1 scale, the global model containing social and environmental factors consistently fell within two delta AIC for all variables measured (Table 3-4). The global model was the most parsimonious model for predicting the probability of a large wildfire burning within the WUI and how much of the WUI was burned by WUI wildfires (Table 3-4). There were two models within two delta AIC for best predicting wildfire distance to the WUI: the global model and model 4, which contained woody cover, fuel moisture levels, and road density (Table 3-4).

Both environmental and social variables were important for predicting whether large wildfires burned within the WUI at the L1 scale. Woody cover was positively associated with and precipitation was negatively associated with a higher probability of wildfires occurring within the WUI, a greater proportion of WUI wildfires burning in the WUI, and non-WUI wildfires burning closer to the WUI (Figures 3-3 through 3-5, Tables B-22 through B-25). While fuel moisture was included in all top model sets, it was negatively associated with wildfire distance to WUI, where wildfires occurred closer to the WUI under drier fuel moisture conditions (Figures 3-3 to 3-5, Tables B-22 through B-25). Wind speed similarly occurred in all top models; however, higher wind speeds were most strongly associated with smaller proportions of wildfires burning within the WUI (Figure 3-4). As anticipated, road density and fire and EMS stations were consistently positively associated with wildfires in and near the WUI. Preparedness levels (i.e., strain

on federal suppression resources) were not a significant predictor in any model (Figures 3-3 through 3-5, Tables B-22 to B-25).

Level II ecoregion scale

Patterns influencing the probability of the wildfire occurring within the WUI at the L2 scale were similar to those observed at the L1 scale. The global model best predicted the probability of large wildfires burning in the WUI in the Southeastern USA Plains and the Ozark/Ouachita-Appalachian Forests (Table B-19). In the Mississippi Alluvial and Southeast USA Coastal Plains, model 3, which contained preparedness level, nearby fire and EMS stations, and road density, best predicted whether large wildfires burned in the WUI. In the Southeastern USA Plains and the Ozark/Ouachita-Appalachian Forests, woody cover and precipitation were moderately associated with increasing wildfire risk in the WUI. Higher levels of woody cover and lower levels of precipitation were associated with a higher probability of a wildfire occurring in the WUI, mirroring the L1 pattern (Table B-22). In the Southeastern USA Plains, wildfires were more likely to occur in the WUI at lower fuel moisture levels and higher wind speed (Table B-22). In contrast, in the Ozark/Ouachita-Appalachian Forests, large wildfires were more likely to occur in the WUI under higher fuel moisture levels and lower wind speeds (Table B-22). Consistent with the L1 ecoregion scale, road density and fire and EMS stations were positively associated with wildfires in the WUI across all three L2 ecoregions (Table B-22). Preparedness levels consistently showed weak relationships across ecoregions (Table B-22).

The global model best predicted the proportion of large wildfires that burned in the WUI in the Ozark/Ouachita-Appalachian Forests (Table B-20). In the Mississippi Alluvial and Southeast USA Coastal Plains, two models containing social variables were

within two delta AIC: model 10, which contained nearby fire and EMS stations, and model 3, which contained preparedness level, nearby fire and EMS stations, and road density (Table B-20). In the Southeastern USA Plains, two models were within two delta AIC: model 11, which contained road density, model 4, which contained woody cover, fuel moisture levels, and road density, and model 3, which contained preparedness level, nearby fire and EMS stations, and road density (Table B-20).

There was high variability in predictors of the proportion of WUI burned by large wildfires at the L2 scale. In the Southeastern USA Plains and the Ozark/Ouachita-Appalachian Forests, higher fuel moisture conditions were also associated with wildfires burning greater proportions of the WUI, although the trend was strongest in the Ozark/Ouachita-Appalachian Forests (Table B-23). The Ozark/Ouachita-Appalachian Forests was the only L2 ecoregion to contain wind speed within its top model predictor set. Contrary to expectations, wildfires that burned more of the WUI occurred at lower wind speeds in this region (Table B-23). Consistent with the L1 ecoregion scale, road density and fire and EMS stations were positively associated with the proportion of large wildfires burning in the WUI across all three L2 ecoregions, while preparedness levels consistently showed weak relationships across ecoregions (Table B-23). In the Southeastern USA Plains and the Ozark/Ouachita-Appalachian Forests, lower levels of woody cover were weakly associated with wildfires burning a greater proportion of the WUI (Table B-23).

Drivers of large wildfire distance to WUI were consistently predicted by the same three variables; Model 4, which contained woody cover, road density, and fuel moisture, best predicted how close large non-WUI wildfires burned to the WUI across all three L2

ecoregions (Table B-21). However, in the Ozark/Ouachita-Appalachian Forests, model 11, which contained road density, fell within 2 delta AIC of our top model (Table B-21).

Trends in predictors of large wildfire distance to WUI were consistent across L2 ecoregions. Large wildfires burned closer to the WUI at higher levels of woody cover across all three L2 ecoregions (Table B-24). Wildfires also burned closer to the WUI under lower fuel moisture conditions within all L2 ecoregions; however, the trend was weak in the Ozark/Ouachita-Appalachian Forests (Table B-24). As expected, higher road density was associated with wildfires closer to the WUI, although this trend was strongest in the Ozark/Ouachita-Appalachian Forests and the Southeastern USA Plains (Table B-24).

Discussion

Regional variation in the drivers of large wildfires in the WUI highlights the complex social-ecological dynamics that shape the WUI in the eastern US. Drivers of WUI wildfire occurrence and proportion of the WUI burned varied across ecoregions, which may be due to the differing patterns in weather, climate conditions, topographic features, and fuel dynamics that shape each region (Parisien & Moritz, 2009). However, we found relatively consistent predictors for non-WUI wildfire distance to the WUI among ecoregions, suggesting that variable social interactions among regions likely play an important role in shaping regional variation in WUI wildfires. For instance, the probability of WUI wildfire occurrence and the proportion of WUI area burned were consistently predicted by only social variables in the Mississippi Alluvial and Southeast USA Plains, while a combination of social, weather, and fuel variables shaped their dynamics in the Southeastern USA Plains. Strong regional variability in wildfire interactions with the WUI has been found in other regions. For instance, Gong et al.

(2024) found that the drivers of WUI wildfires differed across regions of China, where climatic conditions were important for predicting WUI wildfire occurrence in some regions, while suppression resource availability was important in others. At finer scales, variability in housing arrangement and its interactions with vegetation have been shown to help shape wildfire dynamics in the WUI (Syphard et al., 2014, 2022). Our findings highlight the complex interactions between human activity and environmental conditions that alter wildfire risk in the WUI and the need for further fine-scale, region-specific assessment of the drivers of WUI large wildfires. Further and more in-depth investigation of additional social variables may be required to unravel WUI wildfire dynamics in the eastern US.

Wildfires associated with the WUI burn under conditions that promote more extreme fire behavior, which can make large wildfires more difficult to suppress. In Chapter 2, we found that increases in large wildfire activity are largely occurring outside of the WUI; however, when wildfires do burn in the WUI, they are typically larger than those outside of the WUI. We hypothesized that this trend may be due to differences in suppression potential and resource allocation within versus outside of the WUI, where suppression resources tend to be directed toward the WUI to protect human life and property (Daniels et al., 2024; Kreider et al., 2024). Thus, wildfires are likely only to reach the size of ≥200 ha when they occur under conditions that promote fire behavior that is more difficult to control and suppress. Our findings in Chapter 3 support this hypothesis. We found that drier conditions coupled with higher levels of woody cover were associated with WUI wildfires and wildfires occurring closer to the WUI. Drier conditions can lead to more extreme fire behavior that can impede firefighting efforts

(Kreider et al., 2024). More woody cover can promote extreme wildfire behaviors by increasing spot fires, flame lengths, and convective plumes (Andreu et al., 2012; Donovan et al., 2020; Donovan, Fogarty, et al., 2023; Palmero-Iniesta et al., 2017; Resco de Dios, 2020). Woody ladder fuels can carry fire from the ground to the canopy (Ottmar, 2020) and create lofted embers that can ignite the roofs of homes (Manzello et al., 2010, 2011). Although the WUI has more potential fuel breaks, such as roads, denser fuels combined with more fire-conducive weather may negate this barrier to fire spread once a wildfire has become adequately large or intense (Narayanaraj & Wimberly, 2013). Fuels along these road edges may also be more susceptible to drying and can thereby create conditions more conducive to fire in and near the WUI (Narayanaraj & Wimberly, 2013). At a regional level, the Southeastern USA Plains showed the strongest trend of WUI large wildfires burning under dry conditions, high wind speeds, and high levels of woody cover. However, contrary to our hypotheses, wildfires that burned more of the WUI occurred at lower wind speeds, highlighting complex regional dynamics within the WUI.

Contrary to expectations, lower wind speed was associated with large wildfires in the WUI at the L1 scale and regionally within the Ozark/Ouachita-Appalachian Forests. Consistent trends in wind speed between the L1 Eastern Temperate Forests and the L2 Ozark/Ouachita-Appalachian Forests are likely due to the vast majority of WUI wildfires in the East being concentrated within this L2 ecoregion (Chapter 2). This finding is at odds with previous research showing that high winds are a major driver of highly destructive wildfires (Balch et al., 2024) and increase the likelihood of a wildfire reaching the WUI (Wei et al, 2023), highlighting the unique wildfire-WUI dynamics occurring in

the eastern US. WUI wildfires in the Ozark/Ouachita-Appalachian Forests are often caused by humans, particularly arson, and ignition pressure in the WUI may outweigh the role of weather in WUI wildfire occurrence, thereby allowing wildfires to burn during lighter wind conditions (Chapter 2). Alternatively, a higher probability of large wildfire occurrence within the WUI during lower wind speeds may be caused by rugged topography in wildland areas of this region (Dobis et al., 2023). The steep slopes, chimneys, and chutes in wildland areas outside the WUI can channel air and thereby increase local wind speeds and drive wildfire spread (Clements, 2011). Because wind speed was measured at large scales (4 km^2) in our study, our variable for wind speed may not have captured these more local wind dynamics created by topographic features. Further research investigating the role of topography in shaping wildfire activity in and near the WUI is needed to help unravel these relationships.

Fuel played a primary role in shaping wildfire proximity to the WUI, regardless of region. Fuel moisture, woody cover, and roads were consistently important for predicting wildfire distance to the WUI, with wildfires closer to the WUI occurring at higher levels of woody cover, lower levels of fuel moisture, and higher road densities. While wildfire dynamics inside the WUI are quite complex due to anthropogenic activity, the drivers of wildfires outside the WUI may be more predictable. These findings suggest that utilizing fuel management will be an important factor in controlling wildfires and their impacts near the WUI. While targeted grazing and mechanical thinning are commonly recommended management methods around the WUI (Donovan et al., 2022), applying them over large scales is logistically challenging and costly (Rummer, 2008). Future expansion of the WUI may necessitate greater use of prescribed fire, an

effective fuel reduction technique at large scales (T. B. Jain et al., 2021). However, several legal and social barriers limit the use of prescribed burning (Wonkka et al., 2015), in addition to other major obstacles to prescribed burning, including lack of funding, personnel, and limited burning windows (Kupfer et al., 2020; Schultz et al., 2019). Efforts to facilitate the use of prescribed burning will be paramount in managing wildfire risk near the WUI.

Continued WUI expansion combined with increasing woody cover (Ivey et al., 2024) and predicted shifts in climatic conditions could further exacerbate wildfire risk in the WUI of the eastern US. The WUI is the fastest-growing land-use type in the US (Radeloff et al., 2018) and is predicted to continue to expand in the future (Tang et al., 2024). As the WUI grows, higher ignition potential from human activity and an increasingly complex built environment may hinder firefighting efforts in the future, further driving up already-increasing suppression costs, particularly in the WUI (Burke et al., 2021; Mietkiewicz et al., 2020). Moreover, numerous small wildfires within the expanding WUI may continue to strain suppression resources, making preemptive suppression planning and coordination imperative (Carlson et al., 2021; Mietkiewicz et al., 2020). If unchecked, increasing woody cover across the eastern US will further heighten wildfire risk, leading to larger, more destructive wildfires (Ivey et al., 2024). In addition, the southeast is predicted to become considerably warmer and drier due to climate change, which will create conditions favorable to more extreme wildfires (Bedel et al., 2013; Fill et al., 2019). WUI growth, coupled with greater fuel loads and drier weather conducive to fire, makes preparing for wildfires imperative, especially in and near human settlements. Despite the need for further investigation into social factors

influencing WUI wildfire dynamics in the East, our findings demonstrate that fuels management will be imperative to reduce wildfire risk near the WUI in the future.

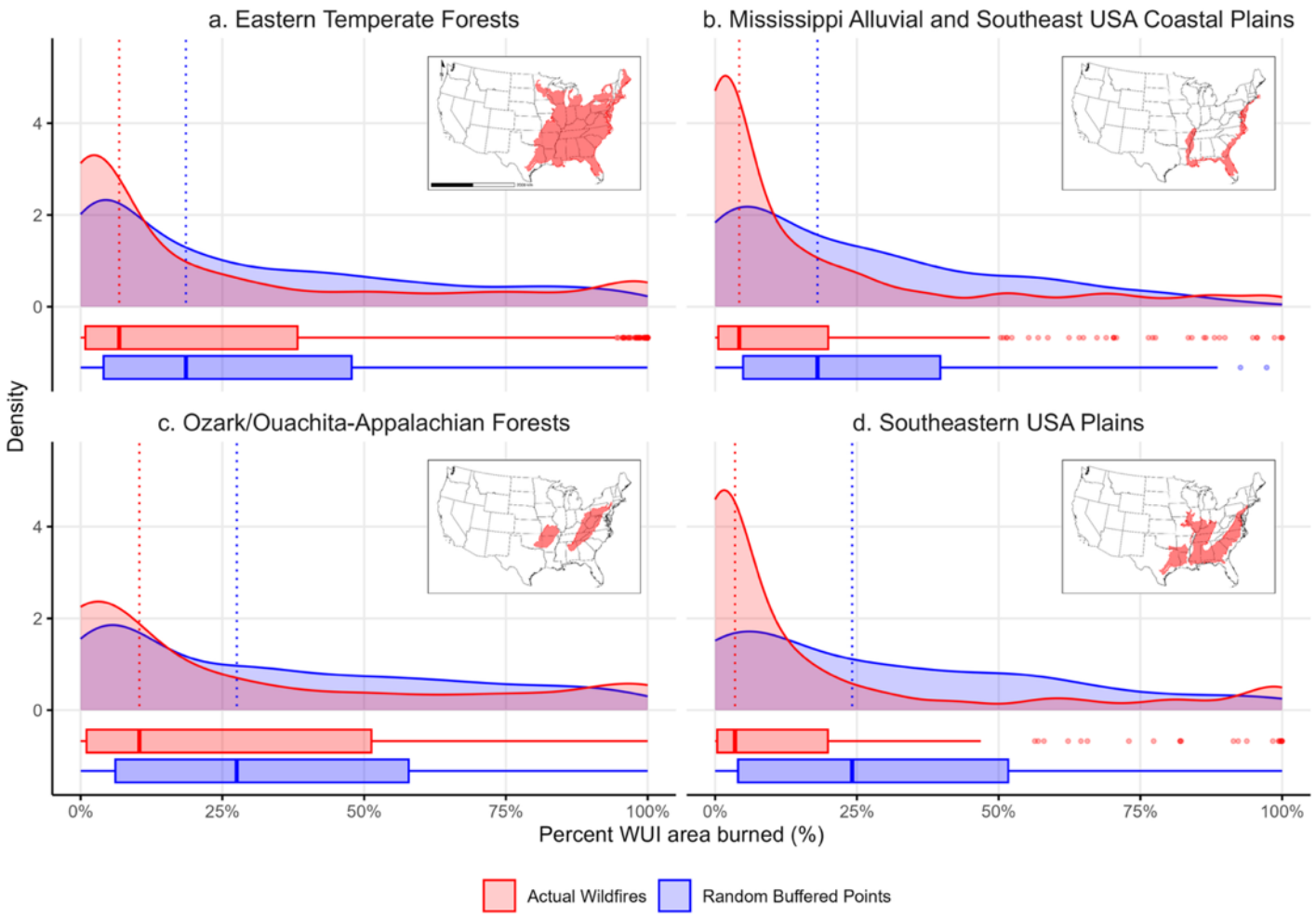


Figure 3-1. The distribution of the proportion of the wildland-urban interface (WUI) burned by large wildfires (≥200 ha) for all wildfires that did burn in the WUI compared to a null distribution across Level I and Level II ecoregions of the eastern United States. Randomly distributed points were buffered to the average size of large wildfires within a given ecoregion. The vertical dotted line represents the median distance to WUI for each distribution.

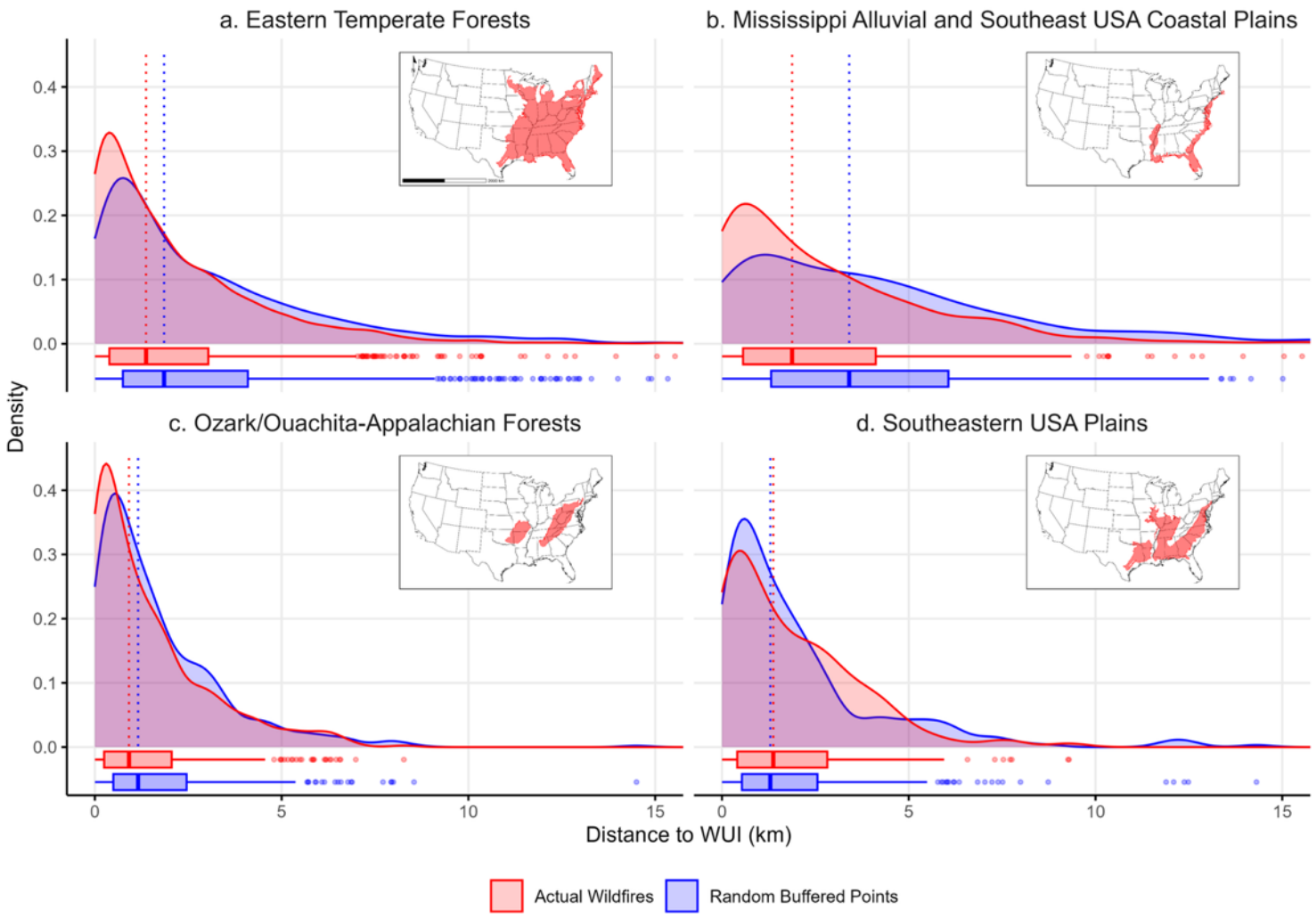


Figure 3-2. The distribution of large wildfire (≥200 ha) distance to the wildland-urban interface (WUI) for all wildfires that did not burn in the WUI compared to a null distribution across Level I and Level II ecoregions of the eastern United States. Randomly distributed points were buffered to the average size of large wildfires within a given ecoregion. The vertical dotted line represents the median distance to WUI.

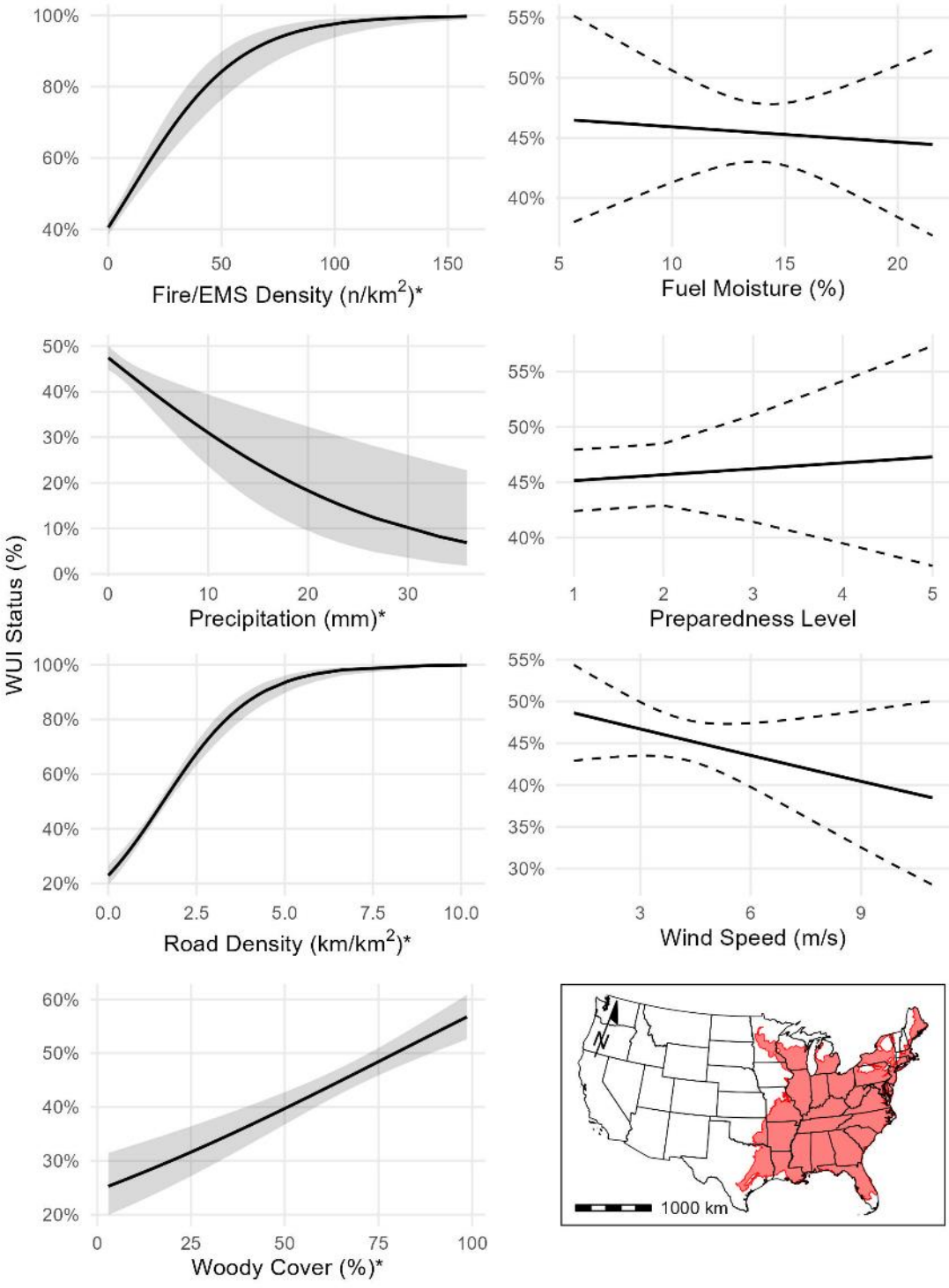


Figure 3-3. Model predictions for seven independent variables and their relationship to whether a large wildfire (≥200 ha) burned in the wildland-urban interface (WUI) within the eastern United States between 1991 and 2021. The asterisk (*) and shaded confidence intervals denote statistical significance.

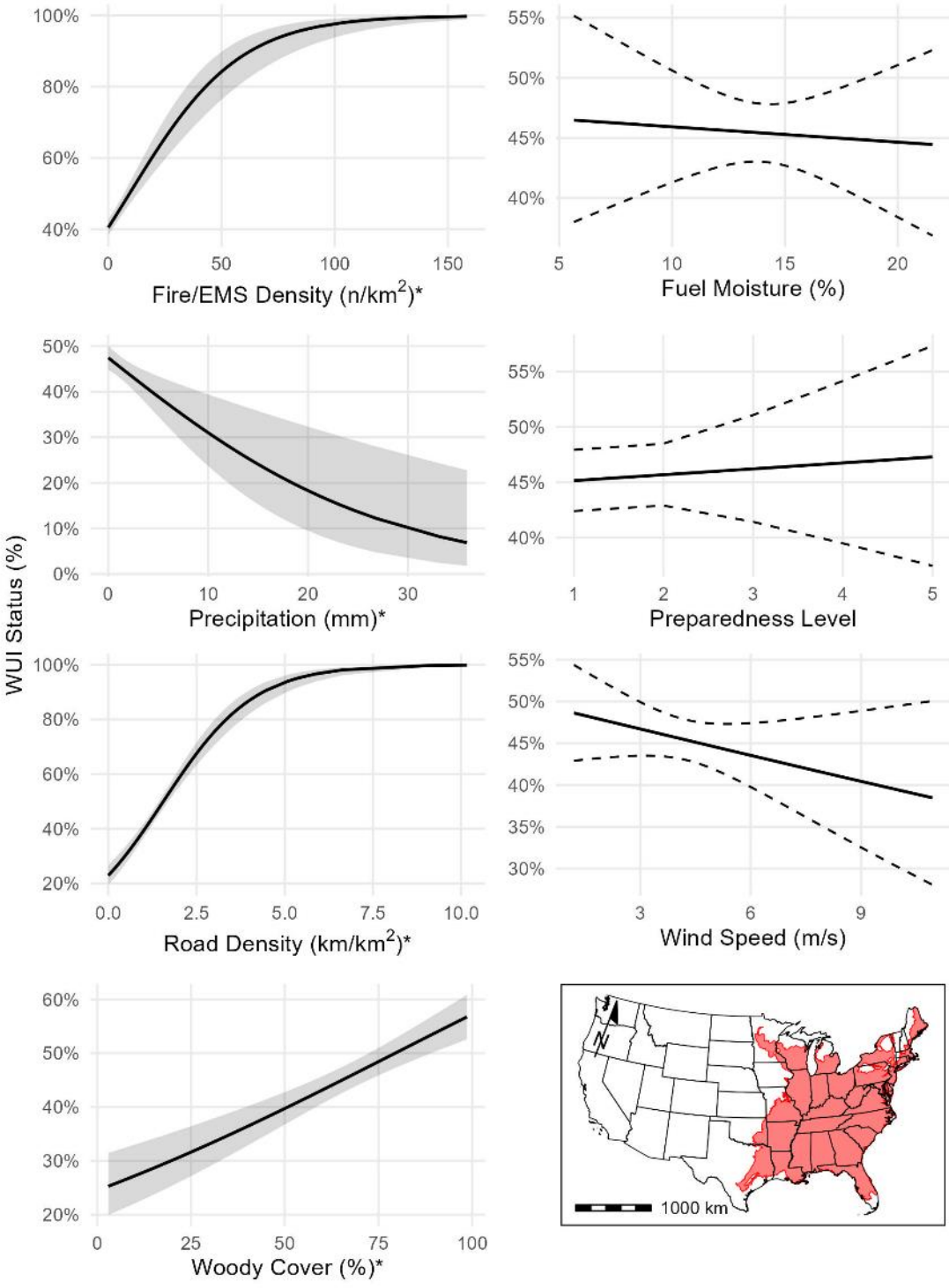


Figure 3-4. Model predictions for seven independent variables and their relationship to the proportion of a large wildfire's (≥200 ha) area that burned in the wildland-urban interface (WUI) within the eastern United States between 1991 and 2021. The asterisk (*) and shaded confidence intervals denote statistical significance.

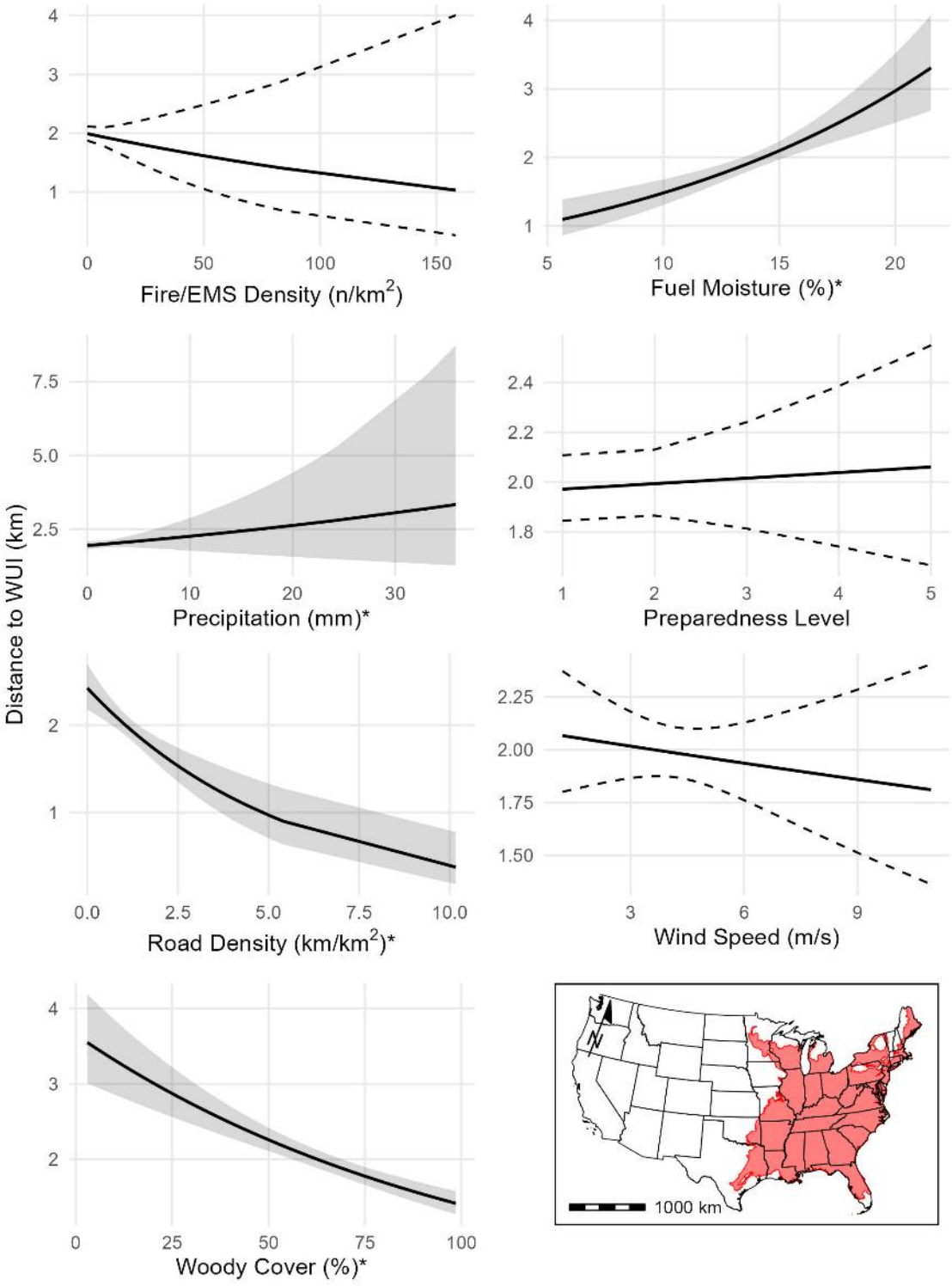


Figure 3-5. Model predictions for three independent variables and their relationship to the distance large wildfires (≥200 ha) burned from the wildland-urban interface (WUI) within the eastern United States between 1991 and 2021. The asterisk (*) and shaded confidence intervals denote statistical significance.

Table 3-1. Description of environmental and social factors used as predictors in modeling the relationship between large wildfires (≥200 ha) and the wildland-urban interface (WUI) across the eastern United States between 1991 and 2021.

Variable	Description	Data source	Mean WUI	Mean non-WUI	Units	Temporal Resolution	Spatial Resolution	Predictions on Wildfires in and near the WUI
Precipitation	Mean precipitation one day before and after a wildfire's ignition date	Gridded Meteorological Data (gridMET)	0.84	1.44	mm/day	Daily from 1991-2021	4 km	Lower precipitation will increase the flammability of living and dead vegetation by decreasing fuel moisture, thereby increasing wildfire activity and spread (Coen et al., 2013; Ellis et al., 2022; Hysa, 2021).
Wind Speed	Mean wind velocity at 10 meters one day before and after a wildfire's ignition date	Gridded Meteorological Data (gridMET)	4.20	4.27	m/s	Daily from 1991-2021	4 km	Increased wind speed will carry firebrands into the WUI (Fernandez-Pello, 2017) and increase the probability of a wildfire reaching the WUI (Wei et al., 2023).
Fuel Moisture	Mean fuel moisture one day before and after a wildfire's ignition date	Gridded Meteorological Data (gridMET)	13.84	14.19	%	Daily from 1991-2021	4 km	Lower fuel moisture will lead to drier fuels and increase wildfire behavior and spread into the WUI (Ellis et al., 2022).
Woody Cover	Percent woody cover within a wildfire's perimeter from the year prior	Rangeland Analysis Platform (RAP)	70.12	63.54	%	Annual from 1991-2021	30 m	Higher woody cover, which may be higher in the WUI (Sonti et al., 2022), will increase risk of wildfire occurrence (Ivey et al., 2024).

Table 3-1. Continued

Variable	Description	Data source	Mean WUI	Mean non-WUI	Units	Temporal Resolution	Spatial Resolution	Predictions on Wildfires in and near the WUI
Road Density	Road density within a wildfire's perimeter	Topologically Integrated Geographic Encoding and Referencing (TIGER)	1.16	1.00	km/km^2	1992, 2000, 2010-2021	Lines	Roads will increase wildfire ignition potential (Syphard & Keeley, 2015), facilitate firefighter accessibility (Thompson et al., 2021), and decrease fuel continuity (Narayanaraj & Wimberly, 2012; Povak et al., 2018).
Preparedness Level	National preparedness level for the day prior to a wildfire's ignition date	National Interagency Fire Center (NIFC)	1.47	1.48	-	Daily from 1990-2021	National	Suppression resources will be strained at higher preparedness levels, increasing wildfire activity and limiting fire suppression (Swimley, 2021). While a given area near a wildfire may have sufficient wildfire suppression personnel and equipment, these resources may be occupied by wildfire activity in other regions of the country (Cullen et al., 2020).

Table 3-1. Continued

Variable	Description	Data source	Mean WUI	Mean non-WUI	Units	Temporal Resolution	Spatial Resolution	Predictions on Wildfires in and near the WUI
Fire/EMS Density	Fire/EMS station density within 1 km	United States Forest Service (FS)/ Homeland Infrastructure Foundation Level data (HIFL)	9.82	1.00	n/km^2	2024	Points	More fire and EMS stations near the WUI will facilitate faster firefighting response times and prevent wildfires from burning the WUI (Vacca et al., 2023). Local fire stations play an important role in wildfire suppression efforts, particularly in the southeastern US (Ahrens, 2013).

Table 3-2. A list of candidate models used to predict (1) large wildfire (≥200 ha) occurrence within the wildland-urban interface (WUI), (2) the proportion of large wildfire area burned within the WUI, and (3) large wildfire distance to the WUI in the eastern United States and across three Level II ecoregions between 1991 and 2021.

#	formula
1	~ Woody Cover + Road Density + Wind Speed + Precipitation + Fuel Moisture + Preparedness Level + Fire & EMS Stations
2	~ Wind Speed + Fuel Moisture + Precipitation
3	~ Preparedness Level + Fire & EMS Stations + Road Density
4	~ Woody Cover + Fuel Moisture + Road Density
5	~ Wind Speed
6	~ Precipitation
7	~ Fuel Moisture
8	~ Wood Cover
9	~ Preparedness Level
10	~ Fire & EMS Stations
11	~ Road Density
12	~ 1

Table 3-3. Relations between large (≥200 ha) wildfires and the wildland-urban interface (WUI) compared to the general landscape using a distribution of random points equal in number to and buffered to the average size of wildfires within a given ecoregion across the Eastern Temperate Forests Level I ecoregion and three Level II ecoregions. The proportion of all wildfires ("WUI Status") (n = 2,184) within the WUI was calculated and compared to a null distribution of an equal sample size using a Chi-squared (χ^2) test. The median proportion WUI area burned by each large wildfire in the WUI (n = 967) was calculated and compared to a null distribution of equal sample size using a two-sample Mann-Whitney U test (W = The Wilcoxon rank-sum statistic). The median distance to WUI for all large wildfires that did not burn in the WUI (n = 1,217) was calculated and compared to a null distribution of equal sample size using a two-sample Mann-Whitney U test.

Ecoregion	WUI Status				Median Proportion WUI Area burned				Median Distance to WUI			
	Wildfire (%)	Random (%)	χ^2	p	Wildfire (%)	Random (%)	W	p	Wildfire (km)	Random (km)	W	p
Level I Eastern Temperate Forests	44.3	68.2	154.3	<0.001	6.8	18.6	378,693	<0.001	1.37	1.85	610,143	<0.001
Mississippi Alluvial and Southeast USA Coastal Plains	33.7	61.4	82.1	<0.001	4.2	18.0	21,908	<0.001	1.88	3.41	98,797	<0.001
Ozark/Ouachita-Appalachian Forests	57.4	77.0	46.0	<0.001	10.4	27.5	149,986	<0.001	0.91	1.16	90,129	0.0015
Southeastern USA Plains	35.1	65.6	52.8	<0.001	3.5	24.2	7,012	<0.001	1.37	1.29	37,207	0.6384

Table 3-4. Model selection results for the top five models using Akaike's Information Criterion (AIC) for whether large wildfires (≥200 ha) burn in the WUI (WUI Status), how much of the WUI they burn (Proportion WUI Area), and how far they burn from the WUI (Distance to WUI) across the eastern United States (df = degrees of freedom, logLik = natural logarithm of the maximum likelihood, ΔAIC = change in AIC, weight = Akaike's weight).

model	df	logLik	AIC	ΔAIC	weight
WUI Status					
1	8	-1,304.49	2,624.98	0.00	1.000
3	4	-1,333.86	2,675.72	50.74	<0.001
4	4	-1,368.39	2,744.78	119.80	<0.001
11	2	-1,388.74	2,781.49	156.51	<0.001
10	2	-1,411.12	2,826.24	201.26	<0.001
Proportion WUI Area					
1	9	1,067.39	-2,116.79	0.00	0.981
3	5	1,059.46	-2,108.92	7.87	0.019
10	3	1,048.36	-2,090.71	26.08	<0.001
11	3	1,044.97	-2,083.95	32.84	<0.001
4	5	1,046.56	-2,083.12	33.67	<0.001
Distance to WUI					
1	9	-2,026.92	4,071.83	0.00	0.618
4	5	-2,031.40	4,072.79	0.96	0.382
8	3	-2,058.43	4,122.85	51.02	<0.01
7	3	-2,064.60	4,135.21	63.38	<0.01
2	5	-2,062.89	4,135.78	63.95	<0.01

CHAPTER 4
CONCLUSION

Large wildfire regimes are changing across the eastern US, concurrent with rapid WUI expansion. We found that 45% of all large wildfires burned some portion of the WUI and account for 55% of the total area burned by large wildfires, even though the WUI only constitutes roughly 22% of the eastern US area. Increases in the number and total area burned by large wildfires are mostly occurring outside the WUI; however, certain southwest regions of the eastern US are experiencing an increase in WUI wildfire activity. These southwestern regions also showed the most dramatic WUI growth, suggesting that human activity may be driving more large wildfires. WUI wildfires are experiencing a shift in their seasonality across the eastern US, becoming more frequent in the earlier part of the year. These findings highlight the importance of considering human settlement in assessing wildfire risk and the need for proactive risk management in order to protect human life and property.

Large wildfire patterns in and near the WUI are driven by both social and environmental factors that vary regionally. We found that wildfires occurred disproportionately less in the WUI and burned less of the WUI than expected at random. Wildfires outside the WUI burned significantly closer to the WUI than expected at random. Drivers of large wildfires in and near the WUI were related to both social and environmental factors and varied across regions. Higher woody cover greatly increased the likelihood that large wildfires would burn in the WUI and more of the WUI, and, for those outside the WUI, closer to the WUI. Dry conditions, such as lower precipitation and lower fuel moisture, also drove large wildfires burning in and close to the WUI; however, in the Ozark/Ouachita-Appalachian Forests, large wildfires actually burned

more of the WUI at higher fuel moisture levels. Surprisingly, increased wind speed actually decreased the likelihood that a large wildfire would burn in the WUI or more of the WUI; however, in the Southeastern USA Plains, large wildfires burned more of the WUI at higher wind speeds than those that burned less of the WUI. Large wildfires were more likely to burn in the WUI, more of it, or, if they burned outside the WUI, closer to it when federal wildfire suppression resources were slightly more strained, although the trend was weak. The unequivocal role of woody cover in WUI large wildfire occurrence underscores the need for proactive fuels management. Additionally, regional differences in what drives wildfires in and near the WUI highlight the complex socio-environmental dynamics within and near the WUI.

Further WUI growth, concurrent with increasing woody cover and changing climatic conditions across the East, makes it crucial to prepare for heightened wildfire risk in and near the WUI. Our findings underscore the importance of managing woody fuels to reduce the risk of large wildfires in and near the WUI. Property owners can create defensible spaces around their homes and utilize fire-resistant building materials. Forest managers can reduce woody fuels through prescribed burning, mechanical thinning, and targeted grazing. Additionally, policymakers can enact laws that promote the use of prescribed burning to reduce fuels. Given the uncertainty of future climatic conditions, mitigating large wildfire risk will be imperative in order to protect human life and property across the eastern US.

APPENDIX A
CHANGING LARGE WILDFIRE DYNAMICS IN THE WILDLAND-URBAN INTERFACE OF THE EASTERN UNITED STATES

Table A-1. Changes in housing density classes across Level III ecoregions of the eastern United States from 1990 to 2020, including interface wildland-urban interface (WUI), intermix WUI, and varying vegetation and housing density combinations. Water was omitted due to negligible changes.

Ecoregion	Area (km^2)	Class	1990	2000	2010	2020	% Δ	rel. Δ
Acadian Plains and Hills	45,244	Interface WUI	1.5%	1.8%	1.9%	1.9%	0.4%	26.7%
		Intermix WUI	18.5%	22.0%	24.9%	24.9%	6.4%	34.6%
		Non-vegetated low & very low housing density	46.9%	45.2%	42.4%	40.6%	-6.3%	-13.4%
		Non-vegetated medium & high housing density	0.2%	0.2%	0.2%	0.2%	0.0%	0.0%
		Vegetated very low housing density	1.7%	1.7%	1.7%	1.7%	0.0%	0.0%
		Vegetated/no housing	25.6%	23.5%	23.4%	25.1%	-0.5%	-2.0%
Arkansas Valley	28,422	Interface WUI	3.0%	4.4%	5.0%	4.8%	1.7%	60.0%
		Intermix WUI	6.4%	7.8%	9.6%	9.5%	3.0%	48.4%
		Non-vegetated low & very low housing density	53.4%	50.8%	50.2%	50.5%	-2.9%	-5.4%
		Non-vegetated medium & high housing density	1.1%	1.4%	1.6%	1.6%	0.5%	45.5%
		Vegetated very low housing density	20.0%	20.2%	18.4%	18.5%	-1.4%	-7.5%
		Vegetated/no housing	12.4%	11.7%	11.4%	11.3%	-1.0%	-8.9%
Atlantic Coastal Pine Barrens	14,308	Interface WUI	9.7%	10.5%	11.4%	11.6%	1.9%	19.6%
		Intermix WUI	21.8%	21.9%	21.6%	21.7%	-0.2%	-0.5%
		Non-vegetated low & very low housing density	21.7%	19.7%	18.3%	17.3%	-4.4%	-20.3%
		Non-vegetated medium & high housing density	17.0%	18.5%	20.2%	20.7%	3.7%	21.8%
		Vegetated very low housing density	4.6%	3.7%	3.2%	3.5%	-1.0%	-23.9%
		Vegetated/no housing	22.3%	22.7%	22.3%	22.3%	0.0%	0.0%
Blue Ridge	46,595	Interface WUI	4.2%	5.2%	5.6%	5.7%	1.5%	35.7%
		Intermix WUI	26.2%	31.5%	36.6%	37.2%	11.0%	42.0%
		Non-vegetated low & very low housing density	36.2%	30.0%	25.5%	24.9%	-11.3%	-31.2%
		Non-vegetated medium & high housing density	0.4%	0.5%	0.6%	0.6%	0.2%	50.0%
		Vegetated very low housing density	2.2%	1.8%	1.2%	1.2%	-1.0%	-45.5%
		Vegetated/no housing	29.9%	30.1%	29.5%	29.5%	-0.3%	-1.3%

Table A-1. Continued

Ecoregion	Area (km2)	Class	1990	2000	2010	2020	% Δ	rel. Δ
Boston Mountains	14,178	Interface WUI	1.8%	2.2%	2.4%	2.2%	0.4%	22.2%
		Intermix WUI	5.5%	7.9%	10.4%	9.9%	4.4%	80.0%
		Non-vegetated low & very low housing density	58.9%	56.9%	55.0%	55.3%	-3.6%	-6.1%
		Non-vegetated medium & high housing density	0.2%	0.3%	0.4%	0.4%	0.2%	100.0%
		Vegetated very low housing density	5.2%	4.8%	4.4%	4.5%	-0.8%	-13.5%
		Vegetated/no housing	27.4%	26.8%	26.4%	26.8%	-0.6%	-2.2%
Central Appalachians	62,050	Interface WUI	3.6%	3.9%	3.9%	3.9%	0.3%	8.3%
		Intermix WUI	24.4%	26.9%	27.7%	26.1%	1.7%	7.0%
		Non-vegetated low & very low housing density	51.3%	48.9%	47.6%	49.2%	-2.2%	-4.1%
		Non-vegetated medium & high housing density	0.1%	0.1%	0.1%	0.1%	0.0%	0.0%
		Vegetated very low housing density	2.8%	2.7%	2.6%	2.5%	-0.2%	-10.7%
		Vegetated/no housing	17.2%	17.0%	17.5%	17.6%	0.4%	2.3%
Central Corn Belt Plains	76,510	Interface WUI	0.7%	0.8%	0.9%	0.9%	0.1%	28.6%
		Intermix WUI	1.1%	1.2%	1.2%	1.2%	0.0%	9.1%
		Non-vegetated low & very low housing density	19.7%	20.3%	20.6%	21.0%	1.3%	6.6%
		Non-vegetated medium & high housing density	5.4%	6.1%	6.8%	7.0%	1.6%	29.6%
		Vegetated very low housing density	70.9%	69.3%	68.4%	67.7%	-3.2%	-4.5%
		Vegetated/no housing	1.5%	1.6%	1.6%	1.6%	0.1%	6.7%
Driftless Area	47,386	Interface WUI	1.0%	1.1%	1.3%	1.3%	0.4%	30.0%
		Intermix WUI	2.1%	2.6%	3.2%	3.4%	1.3%	61.9%
		Non-vegetated low & very low housing density	31.1%	30.8%	31.1%	31.0%	-0.2%	-0.3%
		Non-vegetated medium & high housing density	1.0%	1.1%	1.3%	1.4%	0.5%	40.0%
		Vegetated very low housing density	57.3%	56.8%	55.8%	55.6%	-1.7%	-3.0%
		Vegetated/no housing	5.4%	5.4%	5.2%	5.1%	-0.3%	-5.6%
East Central Texas Plains	55,753	Interface WUI	0.7%	1.2%	1.4%	1.5%	0.8%	114.3%
		Intermix WUI	3.6%	3.8%	4.9%	5.4%	1.8%	50.0%
		Non-vegetated low & very low housing density	50.1%	38.7%	40.7%	42.6%	-7.5%	-15.0%
		Non-vegetated medium & high housing density	0.9%	1.1%	1.2%	1.3%	0.4%	44.4%
		Vegetated very low housing density	37.2%	48.8%	45.9%	42.8%	5.6%	15.1%
		Vegetated/no housing	5.2%	4.2%	3.6%	4.1%	-1.1%	-21.2%

Table A-1. Continued

Ecoregion	Area (km^2)	Class	1990	2000	2010	2020	% Δ	rel. Δ
Eastern Corn Belt Plains	86,858	Interface WUI	1.3%	1.6%	1.8%	1.8%	0.5%	38.5%
		Intermix WUI	2.8%	3.3%	3.7%	3.7%	0.9%	32.1%
		Non-vegetated low & very low housing density	29.3%	31.8%	33.5%	33.5%	4.2%	14.3%
		Non-vegetated medium & high housing density	6.3%	7.3%	8.3%	8.7%	2.4%	38.1%
		Vegetated very low housing density	58.1%	53.6%	50.3%	50.0%	-8.1%	-13.9%
		Vegetated/no housing	1.5%	1.5%	1.5%	1.5%	0.0%	0.0%
Eastern Great Lakes Lowlands	40,301	Interface WUI	5.8%	6.4%	6.7%	6.9%	1.1%	19.0%
		Intermix WUI	18.0%	19.7%	21.3%	21.6%	3.7%	20.0%
		Non-vegetated low & very low housing density	39.9%	38.4%	37.9%	37.4%	-2.5%	-6.3%
		Non-vegetated medium & high housing density	6.5%	7.0%	7.6%	7.9%	1.4%	21.5%
		Vegetated very low housing density	18.6%	17.3%	15.6%	15.4%	-3.1%	-17.2%
		Vegetated/no housing	5.9%	5.6%	5.4%	5.3%	-0.5%	-10.2%
Erie Drift Plain	30,960	Interface WUI	5.4%	5.6%	6.0%	6.0%	0.6%	11.1%
		Intermix WUI	20.4%	22.8%	24.7%	24.5%	4.1%	20.1%
		Non-vegetated low & very low housing density	41.6%	41.7%	41.7%	42.0%	0.4%	1.0%
		Non-vegetated medium & high housing density	7.9%	8.9%	9.7%	9.9%	2.0%	25.3%
		Vegetated very low housing density	19.2%	15.3%	12.5%	12.1%	-7.0%	-37.0%
		Vegetated/no housing	4.1%	4.2%	4.0%	4.0%	-0.1%	-2.4%
Huron/Erie Lake Plains	31,595	Interface WUI	3.0%	3.1%	3.3%	3.2%	0.3%	6.7%
		Intermix WUI	6.3%	7.5%	7.8%	7.8%	1.5%	23.8%
		Non-vegetated low & very low housing density	28.6%	30.0%	31.6%	31.3%	2.6%	9.4%
		Non-vegetated medium & high housing density	9.0%	9.7%	10.4%	10.5%	1.5%	16.7%
		Vegetated very low housing density	49.5%	46.0%	43.2%	43.5%	-6.0%	-12.1%
		Vegetated/no housing	2.6%	2.8%	2.7%	2.7%	0.1%	3.8%
Interior Plateau	123,527	Interface WUI	4.0%	5.4%	5.8%	5.9%	1.9%	47.5%
		Intermix WUI	12.1%	14.9%	17.3%	17.6%	5.5%	45.5%
		Non-vegetated low & very low housing density	47.7%	44.7%	43.9%	43.8%	-3.9%	-8.2%
		Non-vegetated medium & high housing density	2.6%	3.5%	4.1%	4.5%	1.9%	73.1%
		Vegetated very low housing density	24.5%	22.6%	20.1%	19.5%	-4.9%	-20.4%
		Vegetated/no housing	6.8%	6.5%	6.4%	6.3%	-0.5%	-7.4%

Table A-1. Continued

Ecoregion	Area (km^2)	Class	1990	2000	2010	2020	% Δ	rel. Δ
Interior River Valleys and Hills	120,448	Interface WUI	1.3%	1.5%	1.6%	1.6%	0.3%	23.1%
		Intermix WUI	4.2%	4.8%	5.5%	5.5%	1.3%	31.0%
		Non-vegetated low & very low housing density	31.6%	31.1%	31.5%	32.0%	0.4%	1.3%
		Non-vegetated medium & high housing density	2.6%	2.9%	3.1%	3.2%	0.6%	23.1%
		Vegetated very low housing density	53.5%	52.8%	51.5%	50.8%	-2.7%	-5.0%
		Vegetated/no housing	4.4%	4.5%	4.3%	4.5%	0.0%	2.3%
Middle Atlantic Coastal Plain	78,476	Interface WUI	4.6%	5.4%	6.0%	6.0%	1.4%	30.4%
		Intermix WUI	14.1%	17.0%	18.7%	18.5%	4.4%	31.2%
		Non-vegetated low & very low housing density	44.6%	42.2%	41.1%	40.9%	-3.7%	-8.3%
		Non-vegetated medium & high housing density	2.7%	3.3%	3.8%	4.1%	1.3%	51.9%
		Vegetated very low housing density	11.0%	9.7%	8.7%	8.7%	-2.3%	-20.9%
		Vegetated/no housing	20.0%	19.4%	18.8%	18.9%	-1.1%	-5.5%
Mississippi Alluvial Plain	116,119	Interface WUI	1.6%	1.8%	1.8%	1.8%	0.2%	12.5%
		Intermix WUI	1.5%	1.6%	1.6%	1.5%	0.1%	0.0%
		Non-vegetated low & very low housing density	28.1%	29.6%	30.1%	31.5%	3.5%	12.1%
		Non-vegetated medium & high housing density	1.1%	1.2%	1.3%	1.3%	0.2%	18.2%
		Vegetated very low housing density	44.4%	42.8%	40.7%	38.9%	-5.5%	-12.4%
		Vegetated/no housing	15.2%	14.9%	16.4%	16.8%	1.7%	10.5%
Mississippi Valley Loess Plains	51,810	Interface WUI	2.8%	3.7%	3.7%	3.8%	1.0%	35.7%
		Intermix WUI	10.8%	12.0%	14.0%	14.8%	3.9%	37.0%
		Non-vegetated low & very low housing density	50.4%	49.2%	49.4%	48.4%	-2.0%	-4.0%
		Non-vegetated medium & high housing density	2.9%	3.6%	4.1%	4.4%	1.5%	51.7%
		Vegetated very low housing density	24.9%	23.8%	20.9%	20.7%	-4.2%	-16.9%
		Vegetated/no housing	7.3%	6.9%	7.1%	7.1%	-0.2%	-2.7%
North Central Hardwood Forests	88,910	Interface WUI	2.1%	2.4%	2.8%	2.9%	0.8%	38.1%
		Intermix WUI	6.4%	7.7%	9.1%	9.3%	2.9%	45.3%
		Non-vegetated low & very low housing density	33.3%	33.6%	33.6%	33.5%	0.2%	0.6%
		Non-vegetated medium & high housing density	2.6%	3.1%	3.6%	3.8%	1.3%	46.2%
		Vegetated very low housing density	43.2%	40.5%	38.5%	38.0%	-5.2%	-12.0%
		Vegetated/no housing	7.8%	8.0%	7.6%	7.8%	0.0%	0.0%

Table A-1. Continued

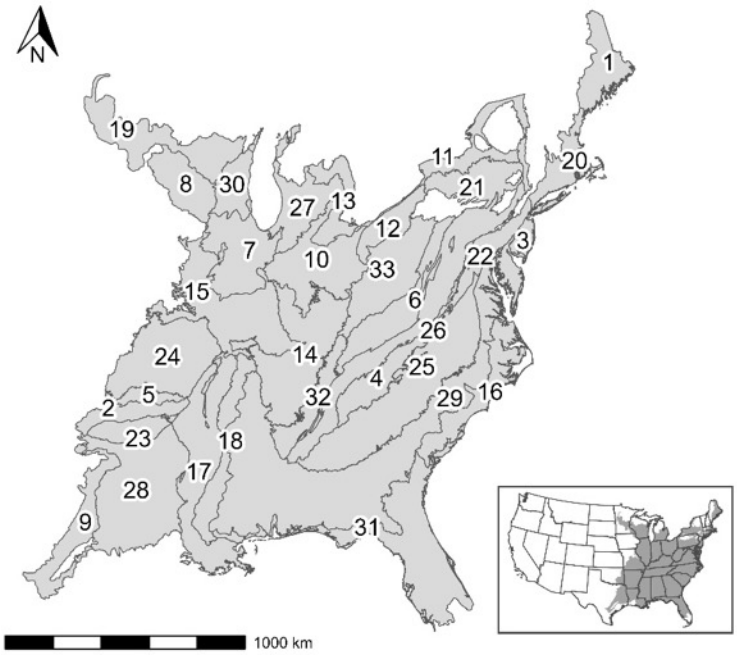
Ecoregion	Area (km^2)	Class	1990	2000	2010	2020	% Δ	rel. Δ
Northeastern Coastal Zone	42,067	Interface WUI	10.8%	10.6%	11.8%	12.1%	1.3%	12.0%
		Intermix WUI	47.0%	49.7%	49.9%	50.1%	3.0%	6.6%
		Non-vegetated low & very low housing density	14.8%	12.4%	10.6%	9.8%	-4.9%	-33.8%
		Non-vegetated medium & high housing density	12.1%	12.5%	13.4%	13.7%	1.6%	13.2%
		Vegetated very low housing density	1.9%	1.6%	1.5%	1.4%	-0.5%	-26.3%
		Vegetated/no housing	9.6%	9.6%	9.2%	9.2%	-0.4%	-4.2%
Northern Allegheny Plateau	46,510	Interface WUI	6.6%	7.3%	7.7%	7.6%	0.9%	15.2%
		Intermix WUI	22.5%	26.4%	30.1%	28.8%	6.3%	28.0%
		Non-vegetated low & very low housing density	49.2%	45.7%	43.2%	44.3%	-5.0%	-10.0%
		Non-vegetated medium & high housing density	0.5%	0.6%	0.6%	0.6%	0.1%	20.0%
		Vegetated very low housing density	12.4%	11.7%	10.4%	10.4%	-1.9%	-16.1%
		Vegetated/no housing	7.3%	6.9%	6.6%	6.8%	-0.5%	-6.8%
Northern Piedmont	31,365	Interface WUI	10.5%	9.9%	10.6%	10.7%	0.2%	1.9%
		Intermix WUI	14.4%	18.2%	18.8%	18.7%	4.3%	29.9%
		Non-vegetated low & very low housing density	38.3%	35.4%	34.1%	33.3%	-5.0%	-13.1%
		Non-vegetated medium & high housing density	17.0%	19.2%	21.3%	22.5%	5.5%	32.4%
		Vegetated very low housing density	13.8%	11.0%	9.2%	8.8%	-5.0%	-36.2%
		Vegetated/no housing	4.2%	4.4%	4.3%	4.1%	-0.1%	-2.4%
Ouachita Mountains	26,895	Interface WUI	1.7%	2.5%	2.7%	2.7%	1.0%	58.8%
		Intermix WUI	6.6%	8.0%	9.0%	9.0%	2.4%	36.4%
		Non-vegetated low & very low housing density	41.6%	40.9%	39.8%	39.0%	-2.6%	-6.3%
		Non-vegetated medium & high housing density	0.4%	0.5%	0.6%	0.6%	0.2%	50.0%
		Vegetated very low housing density	3.8%	3.8%	3.8%	3.8%	-0.1%	0.0%
		Vegetated/no housing	43.6%	42.0%	41.9%	42.7%	-0.9%	-2.1%
Ozark Highlands	106,391	Interface WUI	1.9%	2.7%	3.0%	3.0%	1.1%	57.9%
		Intermix WUI	8.0%	10.0%	11.9%	11.5%	3.6%	43.8%
		Non-vegetated low & very low housing density	53.7%	49.6%	49.0%	49.1%	-4.6%	-8.6%
		Non-vegetated medium & high housing density	0.9%	1.2%	1.4%	1.5%	0.6%	66.7%
		Vegetated very low housing density	21.3%	22.8%	21.3%	21.1%	-0.2%	-0.9%
		Vegetated/no housing	12.7%	12.0%	11.8%	12.3%	-0.4%	-3.1%

Table A-1. Continued

Ecoregion	Area (km^2)	Class	1990	2000	2010	2020	% Δ	rel. Δ
Piedmont	166,117	Interface WUI	4.4%	6.0%	6.5%	6.7%	2.2%	52.3%
		Intermix WUI	29.3%	33.3%	36.9%	36.9%	7.5%	25.9%
		Non-vegetated low & very low housing density	46.2%	40.6%	37.0%	36.7%	-9.6%	-20.6%
		Non-vegetated medium & high housing density	3.8%	5.1%	6.1%	6.5%	2.7%	71.1%
		Vegetated very low housing density	3.9%	3.6%	2.9%	2.9%	-1.1%	-25.6%
		Vegetated/no housing	10.0%	9.0%	8.3%	8.1%	-1.8%	-19.0%
Ridge and Valley	116,716	Interface WUI	9.8%	11.5%	12.2%	12.2%	2.4%	24.5%
		Intermix WUI	19.5%	21.9%	24.2%	24.0%	4.4%	23.1%
		Non-vegetated low & very low housing density	41.8%	39.0%	36.8%	36.7%	-5.2%	-12.2%
		Non-vegetated medium & high housing density	3.0%	3.7%	4.3%	4.5%	1.5%	50.0%
		Vegetated very low housing density	9.8%	8.2%	7.0%	6.9%	-2.9%	-29.6%
		Vegetated/no housing	14.3%	13.9%	13.7%	14.0%	-0.3%	-2.1%
South Central Plains	152,132	Interface WUI	2.1%	3.2%	3.2%	3.3%	1.2%	57.1%
		Intermix WUI	11.1%	12.0%	13.5%	13.6%	2.6%	22.5%
		Non-vegetated low & very low housing density	57.9%	55.7%	55.0%	54.5%	-3.4%	-5.9%
		Non-vegetated medium & high housing density	0.7%	0.8%	1.0%	1.1%	0.4%	57.1%
		Vegetated very low housing density	7.7%	8.8%	7.9%	7.8%	0.1%	1.3%
		Vegetated/no housing	17.8%	16.7%	16.6%	16.9%	-0.8%	-5.1%
Southeastern Plains	328,885	Interface WUI	3.1%	4.5%	4.7%	4.7%	1.6%	51.6%
		Intermix WUI	13.4%	16.1%	18.3%	18.2%	4.9%	35.8%
		Non-vegetated low & very low housing density	57.1%	53.0%	51.8%	51.8%	-5.2%	-9.3%
		Non-vegetated medium & high housing density	1.1%	1.4%	1.6%	1.7%	0.6%	54.5%
		Vegetated very low housing density	10.5%	10.8%	9.6%	9.6%	-0.9%	-8.6%
		Vegetated/no housing	13.4%	12.7%	12.4%	12.4%	-1.0%	-7.5%
Southeastern Wisconsin Till Plains	31,350	Interface WUI	2.7%	3.1%	3.5%	3.7%	0.9%	37.0%
		Intermix WUI	2.8%	3.6%	3.8%	3.8%	1.0%	35.7%
		Non-vegetated low & very low housing density	27.1%	29.6%	30.5%	30.8%	3.7%	13.7%
		Non-vegetated medium & high housing density	7.6%	9.1%	10.6%	11.2%	3.6%	47.4%
		Vegetated very low housing density	51.5%	45.7%	42.8%	41.7%	-9.7%	-19.0%
		Vegetated/no housing	3.6%	4.2%	4.1%	4.2%	0.6%	16.7%

Table A-1. Continued

Ecoregion	Area (km^2)	Class	1990	2000	2010	2020	% Δ	rel. Δ
Southern Coastal Plain	141,414	Interface WUI	3.4%	4.8%	5.5%	5.8%	2.4%	70.6%
		Intermix WUI	10.6%	11.2%	12.8%	13.2%	2.6%	24.5%
		Non-vegetated low & very low housing density	34.0%	31.2%	29.9%	28.8%	-5.3%	-15.3%
		Non-vegetated medium & high housing density	4.2%	5.2%	6.2%	6.6%	2.4%	57.1%
		Vegetated very low housing density	8.4%	9.3%	8.6%	8.6%	0.2%	2.4%
		Vegetated/no housing	34.4%	33.3%	32.0%	31.9%	-2.4%	-7.3%
Southern Michigan/Northern Indiana Drift Plains	53,035	Interface WUI	5.3%	5.4%	5.8%	5.8%	0.5%	9.4%
		Intermix WUI	11.4%	14.6%	15.4%	15.5%	4.1%	36.0%
		Non-vegetated low & very low housing density	32.8%	33.8%	34.8%	34.5%	1.7%	5.2%
		Non-vegetated medium & high housing density	6.4%	7.3%	8.2%	8.5%	2.2%	32.8%
		Vegetated very low housing density	38.3%	32.9%	29.8%	29.7%	-8.6%	-22.5%
		Vegetated/no housing	3.6%	3.6%	3.6%	3.6%	0.1%	0.0%
Southwestern Appalachians	37,995	Interface WUI	4.3%	6.0%	6.1%	6.1%	1.9%	41.9%
		Intermix WUI	18.5%	21.8%	24.4%	24.9%	6.4%	34.6%
		Non-vegetated low & very low housing density	53.8%	49.9%	48.2%	48.0%	-5.8%	-10.8%
		Non-vegetated medium & high housing density	0.7%	0.9%	1.1%	1.1%	0.5%	57.1%
		Vegetated very low housing density	4.4%	4.3%	3.6%	3.6%	-0.8%	-18.2%
		Vegetated/no housing	16.8%	15.5%	14.9%	14.7%	-2.2%	-12.5%
Western Allegheny Plateau	81,440	Interface WUI	6.8%	7.4%	7.8%	7.7%	0.9%	13.2%
		Intermix WUI	24.5%	28.2%	30.9%	29.6%	5.1%	20.8%
		Non-vegetated low & very low housing density	51.8%	47.9%	45.4%	46.6%	-5.2%	-10.0%
		Non-vegetated medium & high housing density	1.6%	1.7%	1.9%	2.0%	0.4%	25.0%
		Vegetated very low housing density	6.3%	6.0%	5.5%	5.4%	-0.9%	-14.3%
		Vegetated/no housing	8.0%	7.6%	7.5%	7.7%	-0.3%	-3.7%



1 Acadian Plains and Hills
2 Arkansas Valley
3 Atlantic Coastal Pine Barrens
4 Blue Ridge
5 Boston Mountains
6 Central Appalachians
7 Central Corn Belt Plains
8 Driftless Area
9 East Central Texas Plains
10 Eastern Corn Belt Plains
11 Eastern Great Lakes Lowlands
12 Erie Drift Plain
13 Huron/Erie Lake Plains
14 Interior Plateau
15 Interior River Valleys and Hills
16 Middle Atlantic Coastal Plain
17 Mississippi Alluvial Plain
18 Mississippi Valley Loess Plains
19 North Central Hardwood Forests
20 Northeastern Coastal Zone
21 Northern Allegheny Plateau
22 Northern Piedmont
23 Ouachita Mountains
24 Ozark Highlands
25 Piedmont
26 Ridge and Valley
27 S Michigan/N Indiana Drift Plains
28 South Central Plains
29 Southeastern Plains
30 Southeastern Wisconsin Till Plains
31 Southern Coastal Plain
32 Southwestern Appalachians
33 Western Allegheny Plateau

Figure A-1. Level III ecoregions of the Eastern Temperate Forests ecoregion, as designated by the United States Environmental Protection Agency. The inset map shows the location of the Eastern Temperate Forests ecoregion in relation to the United States of America.

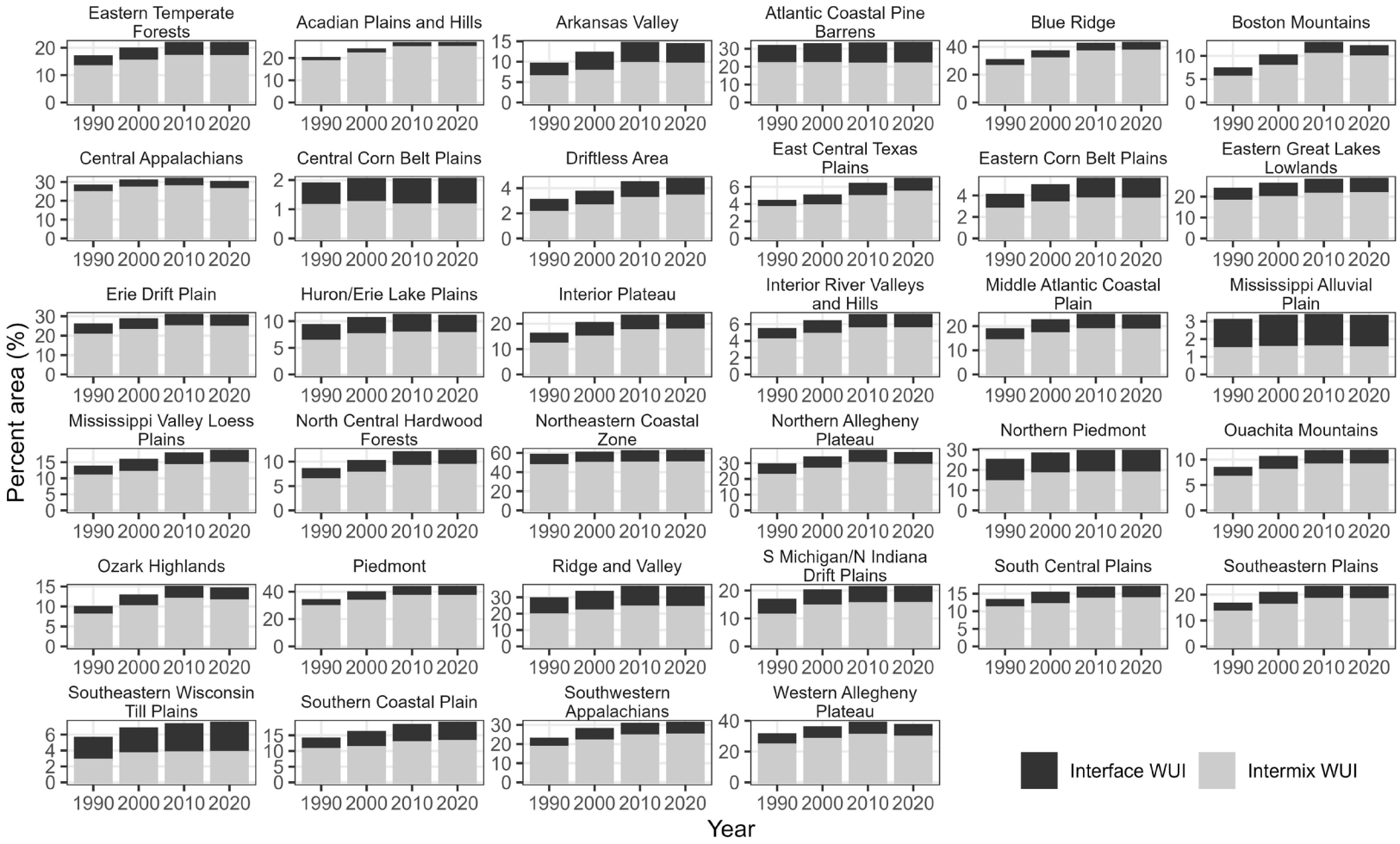


Figure A-2. Decadal percent change in intermix (light grey) and interface (dark grey) wildland-urban interface (WUI) from 1990 to 2020 across Level III ecoregions of the eastern United States.

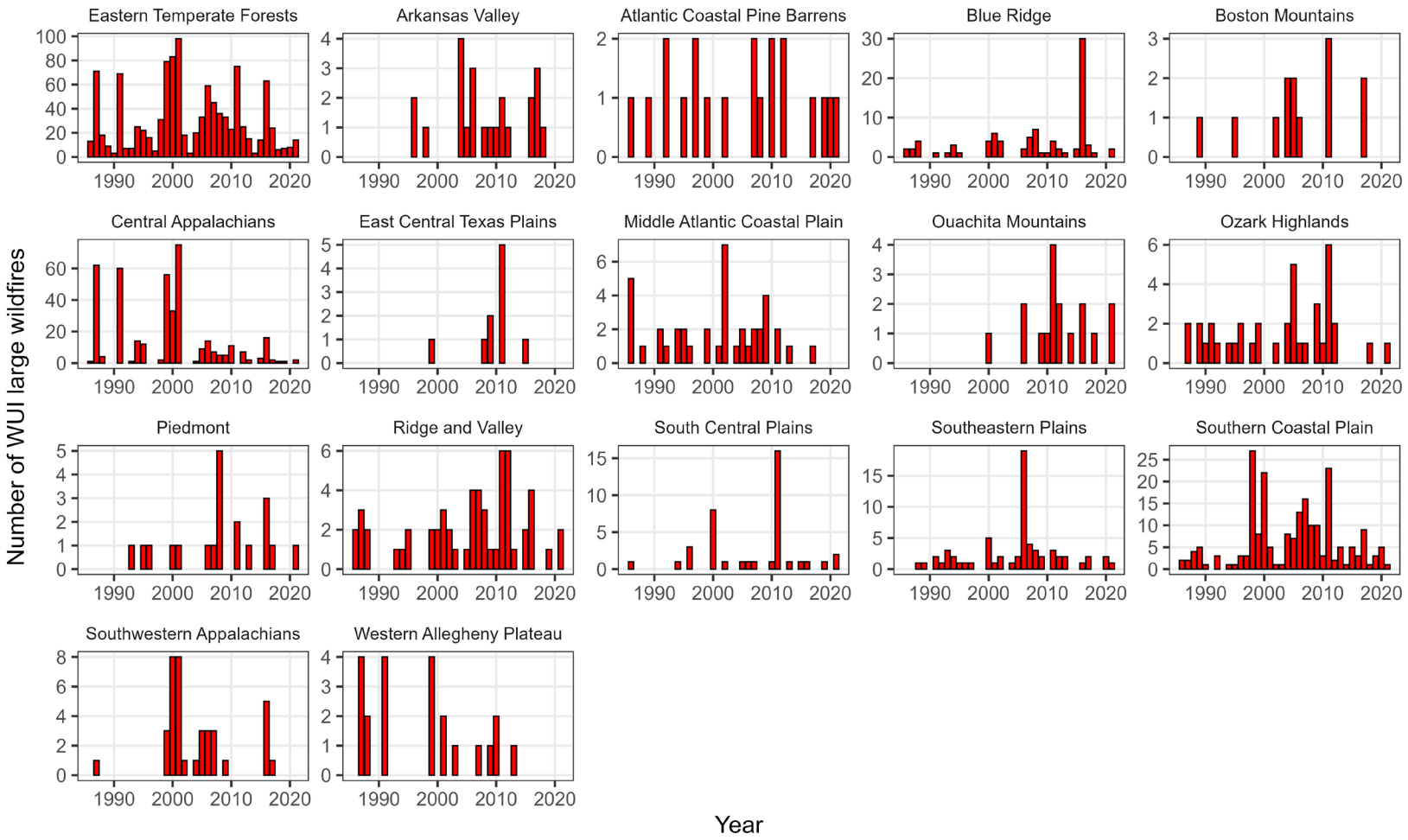


Figure A-3. Change in the number of large (>200 ha) wildfires inside the wildland-urban interface (WUI) from 1986 to 2021 across Level III ecoregions of the eastern United States.

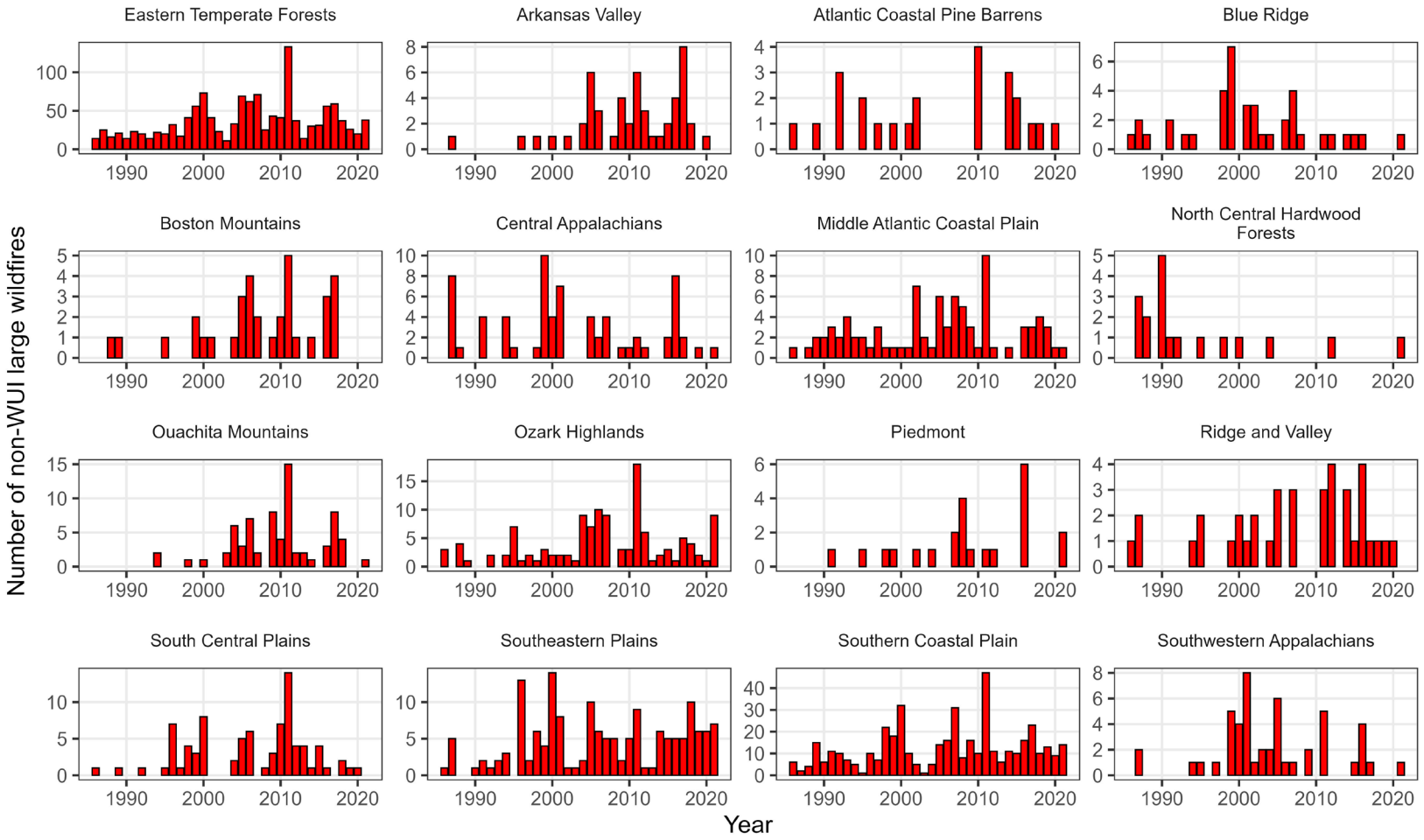


Figure A-4. Change in the number of large (>200 ha) wildfires outside the wildland-urban interface (WUI) from 1986 to 2021 across Level III ecoregions of the eastern United States.

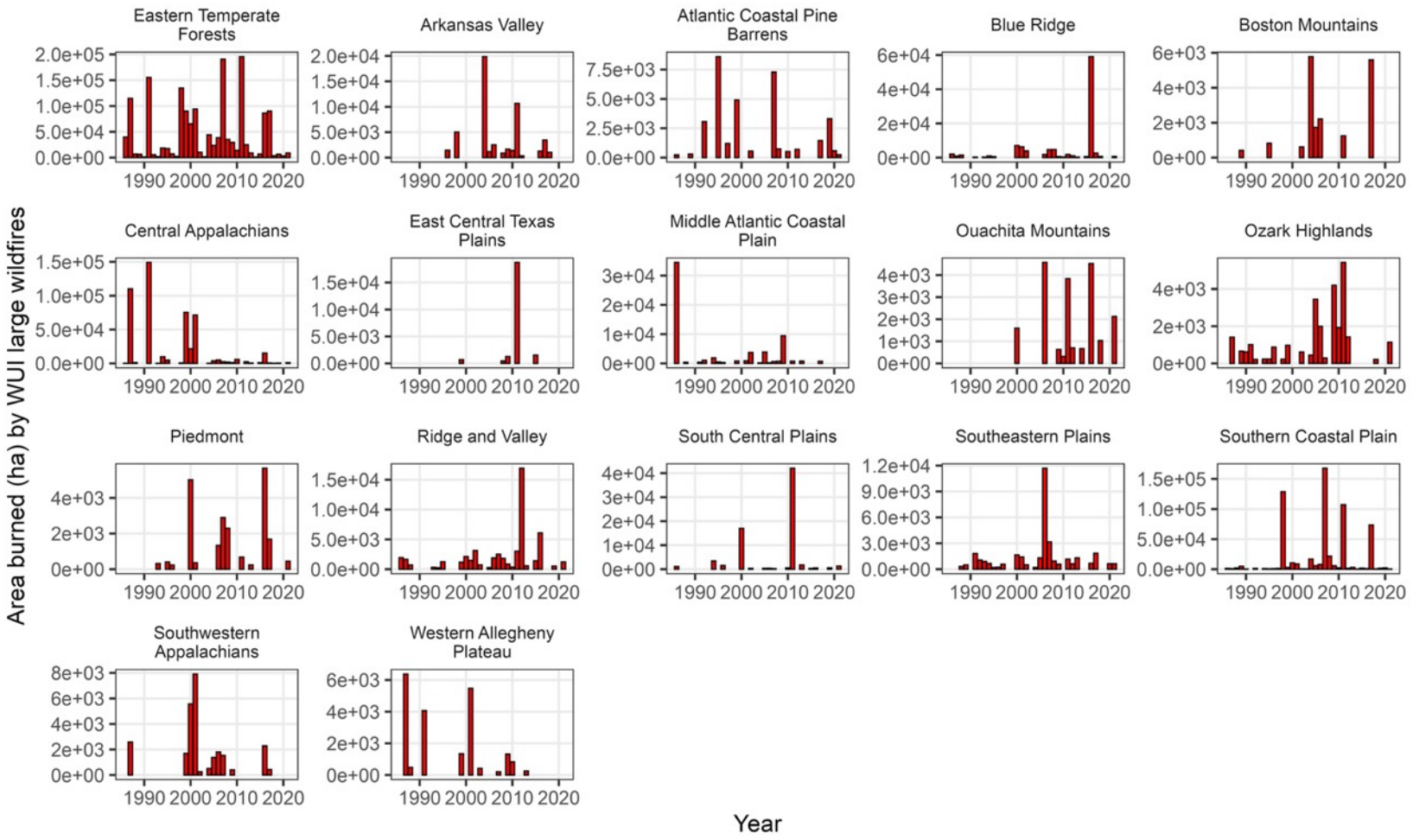


Figure A-5. Change in the total area burned (hectares) by large (>200 ha) wildfires inside the wildland-urban interface (WUI) from 1986 to 2021 across Level III ecoregions of the eastern United States.

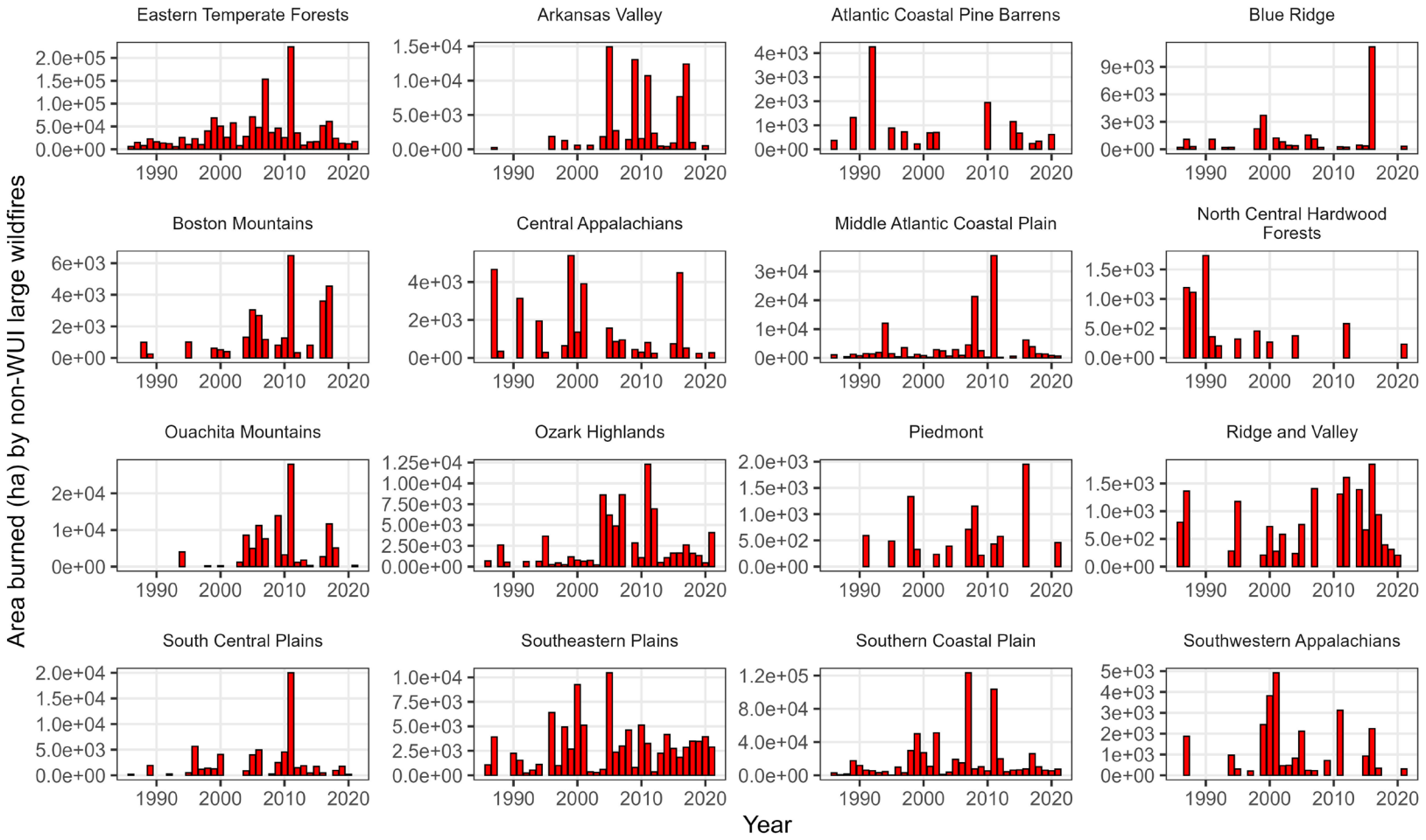


Figure A-6. Change in the total area burned (hectares) by large (>200 ha) wildfires in the wildland-urban interface (WUI) from 1986 to 2021 across Level III ecoregions of the eastern United States.

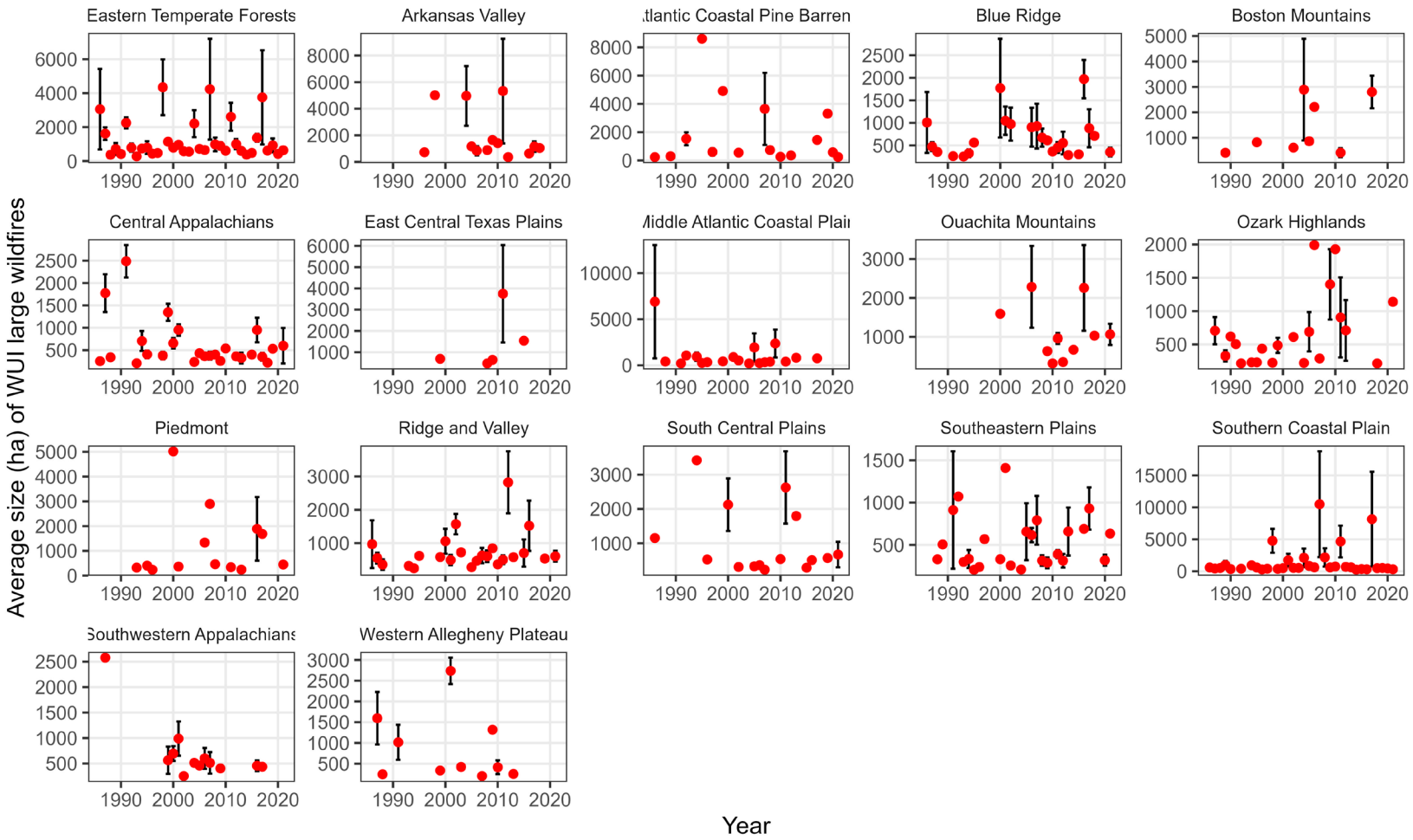


Figure A-7. Change in the average size (hectares) (± standard error) of large (>200 ha) wildfires inside the wildland-urban interface (WUI) from 1986 to 2021 across Level III ecoregions of the eastern United States.

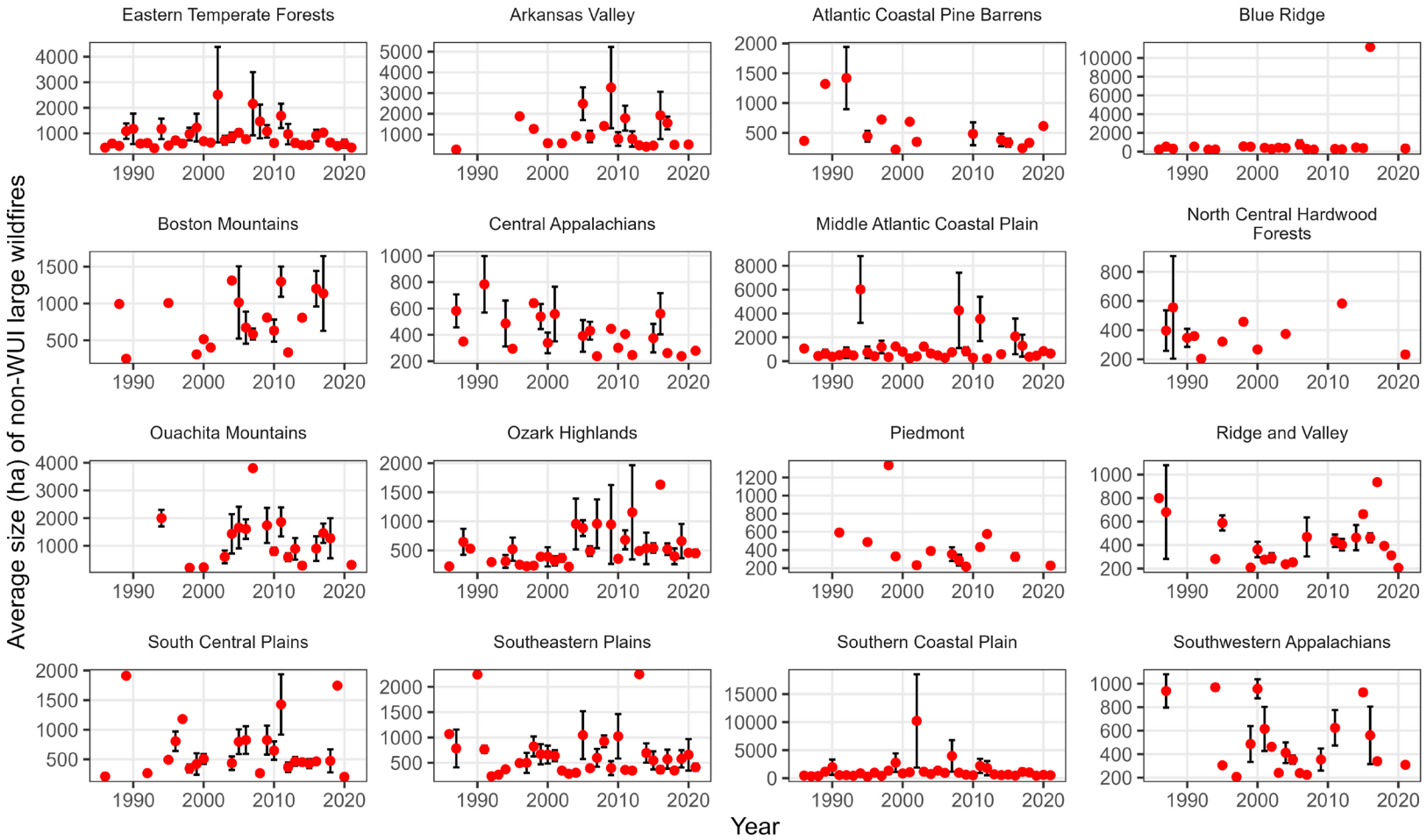


Figure A-8. Change in the average size (hectares) (± standard error) of large (>200 ha) wildfires outside the wildland-urban interface (WUI) from 1986 to 2021 across Level III ecoregions of the eastern United States.

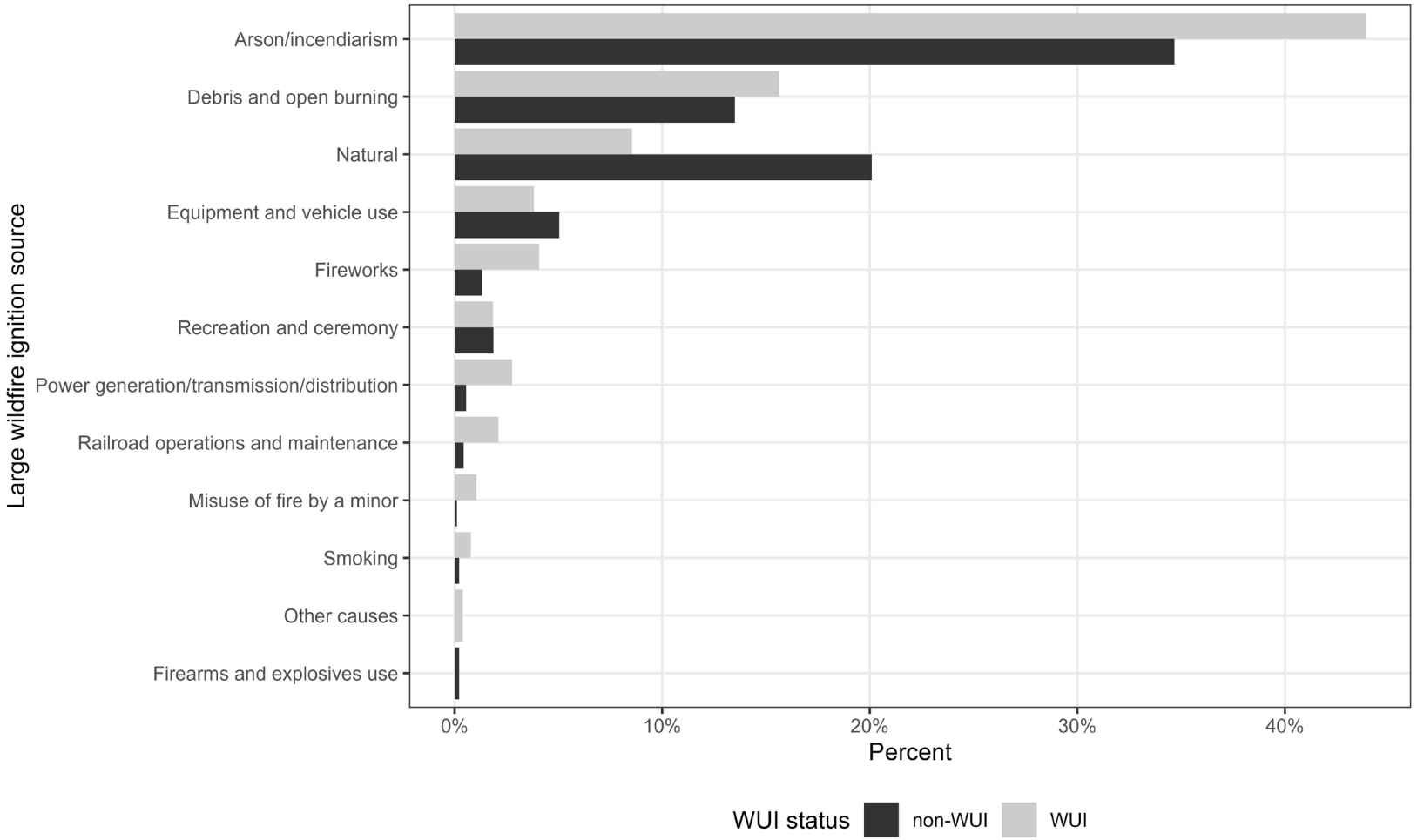


Figure A-9. Ignition sources for large (>200 hectares) wildfires inside and outside the wildland-urban interface (WUI) from 1986 to 2021 in the eastern United States (n = 1,749).

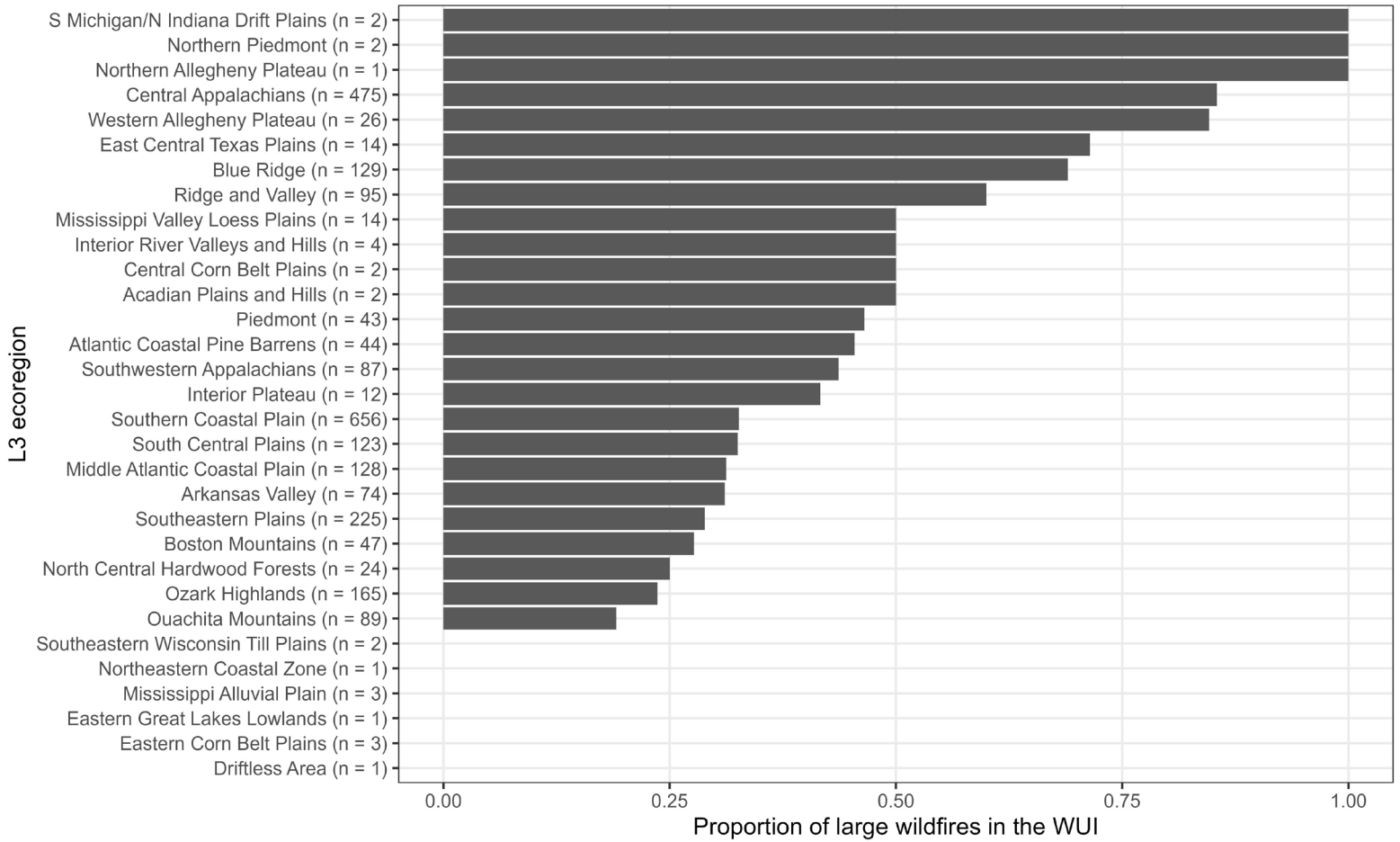


Figure A-10. The proportion of large (>200 hectares) wildfires inside the wildland-urban interface (WUI) across Level III (L3) ecoregions of the eastern United States between 1986 and 2021. The total number of large wildfires both inside and outside the WUI in each ecoregion is shown on the y-axis.

APPENDIX B
FIRE AT THE FRINGE: DRIVERS OF LARGE WILDFIRES IN AND NEAR THE WILDLAND-URBAN INTERFACE OF THE EASTERN UNITED STATES

Table B-1. Model selection results for wind speed using Akaike's Information Criteria (AIC). Large wildfire (≥200 ha) occurrence in the wildland-urban interface (WUI) was modelled using a binomial generalized linear model and wild speed as a predictor with various temporal windows around each wildfire's ignition date (df = degrees of freedom, logLik = natural logarithm of the maximum likelihood, delta = change in AIC, weight = Akaike's weight).

variable	df	logLik	AIC	delta	weight
Wind Speed 1b-1a	2	-1,493.472	2,990.943	0.000	0.24547
Wind Speed 1b-2a	2	-1,493.472	2,990.943	0.000	0.24547
Wind Speed 1b-3a	2	-1,493.717	2,991.434	0.491	0.19201
Wind Speed 1b-5a	2	-1,494.298	2,992.597	1.654	0.10738
Wind Speed 1b-10a	2	-1,494.298	2,992.597	1.654	0.10738
Wind Speed 1b-15a	2	-1,494.606	2,993.211	2.268	0.07897
Wind Speed 2b-1a	2	-1,496.754	2,997.508	6.565	0.00921
Wind Speed 2b-2a	2	-1,497.437	2,998.874	7.931	0.00465
Wind Speed 2b-3a	2	-1,497.748	2,999.497	8.554	0.00341
Wind Speed 2b-5a	2	-1,497.781	2,999.562	8.619	0.00330
Wind Speed 2b-10a	2	-1,498.470	3,000.940	9.997	0.00166
Wind Speed 2b-15a	2	-1,498.896	3,001.792	10.849	0.00108

Table B-2. Model selection results for wind speed using Akaike's Information Criteria (AIC). The proportion of a large wildfire's (≥200 ha) area that burned the wildland-urban interface (WUI) was modelled using a beta regression and wild speed as a predictor with various temporal windows around each wildfire's ignition date (df = degrees of freedom, logLik = natural logarithm of the maximum likelihood, delta = change in AIC, weight = Akaike's weight).

variable	df	logLik	AIC	delta	weight
Wind Speed 1b-1a	3	1,030.232	-2,054.464	0.000	0.1241
Wind Speed 1b-2a	3	1,030.232	-2,054.464	0.000	0.1241
Wind Speed 1b-3a	3	1,030.168	-2,054.336	0.128	0.1164
Wind Speed 1b-5a	3	1,030.043	-2,054.087	0.377	0.1028
Wind Speed 1b-10a	3	1,030.043	-2,054.087	0.377	0.1028
Wind Speed 1b-15a	3	1,029.959	-2,053.918	0.545	0.0945
Wind Speed 2b-1a	3	1,029.747	-2,053.494	0.970	0.0764
Wind Speed 2b-2a	3	1,029.696	-2,053.392	1.072	0.0726
Wind Speed 2b-3a	3	1,029.495	-2,052.991	1.473	0.0594
Wind Speed 2b-5a	3	1,029.486	-2,052.972	1.491	0.0589
Wind Speed 2b-10a	3	1,029.030	-2,052.060	2.404	0.0373
Wind Speed 2b-15a	3	1,028.825	-2,051.651	2.813	0.0304

Table B-3. Model selection results for wind speed using Akaike's Information Criteria (AIC). Large wildfire (≥200 ha) distance to the wildland-urban interface (WUI) was modelled using a generalized linear model with a gamma family and wild speed as a predictor with various temporal windows around each wildfire's ignition date (df = degrees of freedom, logLik = natural logarithm of the maximum likelihood, delta = change in AIC, weight = Akaike's weight).

variable	df	logLik	AIC	delta	weight
Wind Speed 1b-1a	3	-2,081.513	4,169.026	0.000	0.1614
Wind Speed 1b-2a	3	-2,081.513	4,169.026	0.000	0.1614
Wind Speed 1b-3a	3	-2,081.760	4,169.519	0.493	0.1261
Wind Speed 1b-5a	3	-2,081.760	4,169.519	0.493	0.1261
Wind Speed 1b-10a	3	-2,081.914	4,169.828	0.802	0.1081
Wind Speed 1b-15a	3	-2,082.160	4,170.321	1.295	0.0845
Wind Speed 2b-1a	3	-2,082.533	4,171.067	2.041	0.0582
Wind Speed 2b-2a	3	-2,082.755	4,171.510	2.484	0.0466
Wind Speed 2b-3a	3	-2,082.925	4,171.850	2.824	0.0393
Wind Speed 2b-5a	3	-2,083.159	4,172.317	3.291	0.0311
Wind Speed 2b-10a	3	-2,083.175	4,172.350	3.324	0.0306
Wind Speed 2b-15a	3	-2,083.313	4,172.626	3.600	0.0267

Table B-4. Model selection results for precipitation using Akaike's Information Criteria (AIC). Large wildfire (≥200 ha) occurrence in the wildland-urban interface (WUI) was modelled using a binomial generalized linear model and precipitation as a predictor with various temporal windows around each wildfire's ignition date (df = degrees of freedom, logLik = natural logarithm of the maximum likelihood, delta = change in AIC, weight = Akaike's weight).

variable	df	logLik	AIC	delta	weight
Precip. 1b-1a	2	-1,483.166	2,970.333	0.000	0.346675
Precip. 1b-2a	2	-1,483.166	2,970.333	0.000	0.346675
Precip. 1b-3a	2	-1,484.793	2,973.585	3.253	0.068179
Precip. 1b-5a	2	-1,484.793	2,973.585	3.253	0.068179
Precip. 1b-10a	2	-1,484.896	2,973.793	3.460	0.061463
Precip. 1b-15a	2	-1,485.333	2,974.667	4.334	0.039702
Precip. 2b-1a	2	-1,485.386	2,974.772	4.439	0.037669
Precip. 2b-2a	2	-1,486.618	2,977.236	6.903	0.010990
Precip. 2b-3a	2	-1,486.926	2,977.852	7.519	0.008077
Precip. 2b-5a	2	-1,487.116	2,978.232	7.899	0.006679
Precip. 2b-10a	2	-1,487.421	2,978.841	8.508	0.004925
Precip. 2b-15a	2	-1,489.252	2,982.504	12.171	7.89e-04

Table B-5. Model selection results for precipitation using Akaike's Information Criteria (AIC). The proportion of a large wildfire's (≥200 ha) area that burned the wildland-urban interface (WUI) was modelled using a beta regression and precipitation as a predictor with various temporal windows around each wildfire's ignition date (df = degrees of freedom, logLik = natural logarithm of the maximum likelihood, delta = change in AIC, weight = Akaike's weight).

variable	df	logLik	AIC	delta	weight
Precip. 1b-1a	3	1,030.529	-2,055.057	0.000	0.38192
Precip. 1b-2a	3	1,030.497	-2,054.993	0.064	0.36986
Precip. 1b-3a	3	1,028.616	-2,051.233	3.825	0.05643
Precip. 1b-5a	3	1,028.553	-2,051.107	3.951	0.05298
Precip. 1b-10a	3	1,028.525	-2,051.051	4.007	0.05152
Precip. 1b-15a	3	1,028.430	-2,050.860	4.197	0.04683
Precip. 2b-1a	3	1,026.569	-2,047.138	7.919	0.00728
Precip. 2b-2a	3	1,026.569	-2,047.138	7.919	0.00728
Precip. 2b-3a	3	1,026.533	-2,047.066	7.992	0.00702
Precip. 2b-5a	3	1,026.440	-2,046.879	8.178	0.00640
Precip. 2b-10a	3	1,026.440	-2,046.879	8.178	0.00640
Precip. 2b-15a	3	1,026.386	-2,046.773	8.285	0.00607

Table B-6. Model selection results for precipitation using Akaike's Information Criteria (AIC). Large wildfire (≥200 ha) distance to the wildland-urban interface (WUI) was modelled using a generalized linear model with a gamma family and precipitation as a predictor with various temporal windows around each wildfire's ignition date (df = degrees of freedom, logLik = natural logarithm of the maximum likelihood, delta = change in AIC, weight = Akaike's weight).

variable	df	logLik	AIC	delta	weight
Precip. 1b-1a	3	-2,078.534	4,163.068	0.000	0.69811
Precip. 1b-2a	3	-2,080.023	4,166.045	2.977	0.15756
Precip. 1b-3a	3	-2,080.566	4,167.131	4.063	0.09155
Precip. 1b-5a	3	-2,081.958	4,169.915	6.847	0.02276
Precip. 1b-10a	3	-2,082.877	4,171.754	8.686	0.00908
Precip. 1b-15a	3	-2,083.250	4,172.500	9.432	0.00625
Precip. 2b-1a	3	-2,083.945	4,173.890	10.822	0.00312
Precip. 2b-2a	3	-2,083.945	4,173.890	10.822	0.00312
Precip. 2b-3a	3	-2,084.007	4,174.013	10.945	0.00293
Precip. 2b-5a	3	-2,084.165	4,174.330	11.261	0.00250
Precip. 2b-10a	3	-2,084.672	4,175.343	12.275	0.00151
Precip. 2b-15a	3	-2,084.672	4,175.343	12.275	0.00151

Table B-7. Model selection results for fuel moisture using Akaike's Information Criteria (AIC). Large wildfire (≥200 ha) occurrence in the wildland-urban interface (WUI) was modelled using a binomial generalized linear model and fuel moisture as a predictor with various temporal windows around each wildfire's ignition date (df = degrees of freedom, logLik = natural logarithm of the maximum likelihood, delta = change in AIC, weight = Akaike's weight).

variable	df	logLik	AIC	delta	weight
Fuel Moist. 1b-1a	2	-1,485.451	2,974.902	0.000	3.39e-01
Fuel Moist. 1b-2a	2	-1,485.451	2,974.902	0.000	3.39e-01
Fuel Moist. 1b-3a	2	-1,486.383	2,976.766	1.865	1.34e-01
Fuel Moist. 1b-5a	2	-1,486.938	2,977.876	2.975	7.67e-02
Fuel Moist. 1b-10a	2	-1,486.938	2,977.876	2.975	7.67e-02
Fuel Moist. 1b-15a	2	-1,487.971	2,979.942	5.040	2.73e-02
Fuel Moist. 2b-1a	2	-1,489.683	2,983.366	8.464	4.93e-03
Fuel Moist. 2b-2a	2	-1,491.241	2,986.482	11.581	1.04e-03
Fuel Moist. 2b-3a	2	-1,491.592	2,987.184	12.282	7.31e-04
Fuel Moist. 2b-5a	2	-1,493.048	2,990.097	15.195	1.70e-04
Fuel Moist. 2b-10a	2	-1,494.057	2,992.114	17.212	6.21e-05
Fuel Moist. 2b-15a	2	-1,495.166	2,994.331	19.430	2.05e-05

Table B-8. Model selection results for fuel moisture using Akaike's Information Criteria (AIC). The proportion of a large wildfire's (≥200 ha) area that burned the wildland-urban interface (WUI) was modelled using a beta regression and fuel moisture as a predictor with various temporal windows around each wildfire's ignition date (df = degrees of freedom, logLik = natural logarithm of the maximum likelihood, delta = change in AIC, weight = Akaike's weight).

variable	df	logLik	AIC	delta	weight
Fuel Moist. 1b-1a	3	1,026.218	-2,046.436	0.000	0.1081
Fuel Moist. 1b-2a	3	1,026.218	-2,046.436	0.000	0.1081
Fuel Moist. 1b-3a	3	1,026.194	-2,046.388	0.048	0.1055
Fuel Moist. 1b-5a	3	1,026.194	-2,046.388	0.048	0.1055
Fuel Moist. 1b-10a	3	1,026.068	-2,046.135	0.301	0.0930
Fuel Moist. 1b-15a	3	1,026.054	-2,046.108	0.328	0.0918
Fuel Moist. 2b-1a	3	1,025.747	-2,045.493	0.943	0.0675
Fuel Moist. 2b-2a	3	1,025.726	-2,045.452	0.984	0.0661
Fuel Moist. 2b-3a	3	1,025.720	-2,045.439	0.997	0.0657
Fuel Moist. 2b-5a	3	1,025.697	-2,045.395	1.041	0.0642
Fuel Moist. 2b-10a	3	1,025.680	-2,045.359	1.077	0.0631
Fuel Moist. 2b-15a	3	1,025.652	-2,045.303	1.133	0.0613

Table B-9. Model selection results for fuel moisture using Akaike's Information Criteria (AIC). Large wildfire (≥200 ha) distance to the wildland-urban interface (WUI) was modelled using a generalized linear model with a gamma family and fuel moisture as a predictor with various temporal windows around each wildfire's ignition date (df = degrees of freedom, logLik = natural logarithm of the maximum likelihood, delta = change in AIC, weight = Akaike's weight).

variable	df	logLik	AIC	delta	weight
Fuel Moist. 1b-1a	3	-2,063.474	4,132.947	0.000	0.4505
Fuel Moist. 1b-2a	3	-2,064.548	4,135.096	2.148	0.1539
Fuel Moist. 1b-3a	3	-2,064.603	4,135.206	2.258	0.1456
Fuel Moist. 1b-5a	3	-2,065.217	4,136.434	3.487	0.0788
Fuel Moist. 1b-10a	3	-2,065.609	4,137.217	4.270	0.0533
Fuel Moist. 1b-15a	3	-2,066.269	4,138.537	5.590	0.0275
Fuel Moist. 2b-1a	3	-2,066.625	4,139.251	6.304	0.0193
Fuel Moist. 2b-2a	3	-2,066.801	4,139.603	6.656	0.0162
Fuel Moist. 2b-3a	3	-2,066.884	4,139.767	6.820	0.0149
Fuel Moist. 2b-5a	3	-2,066.884	4,139.767	6.820	0.0149
Fuel Moist. 2b-10a	3	-2,067.053	4,140.106	7.158	0.0126
Fuel Moist. 2b-15a	3	-2,067.053	4,140.106	7.158	0.0126

Table B-10. Model selection results for fire and EMS station density (n/km²) using Akaike's Information Criteria (AIC). Large wildfire (≥200 ha) occurrence in the wildland-urban interface (WUI) was modelled using a binomial generalized linear model and fire and EMS station density as a predictor with various buffer sizes windows around each wildfire's perimeter (df = degrees of freedom, logLik = natural logarithm of the maximum likelihood, delta = change in AIC, weight = Akaike's weight).

variable	df	logLik	AIC	delta	weight
Fire/EMS Dens. 1km	2	-1,304.740	2,613.481	0.000	1.00e+00
Fire/EMS Dens. 5km	2	-1,357.503	2,719.006	105.525	1.22e-23
Fire/EMS Dens. 10km	2	-1,405.991	2,815.982	202.501	1.07e-44
Fire/EMS Dens. 20km	2	-1,411.120	2,826.239	212.758	6.31e-47

Table B-11. Model selection results for fire and EMS station density (n/km²) using Akaike's Information Criteria (AIC). The proportion of a large wildfire's (≥200 ha) area that burned the wildland-urban interface (WUI) was modelled using a beta regression and fire and EMS station density as a predictor with various buffer sizes windows around each wildfire's perimeter (df = degrees of freedom, logLik = natural logarithm of the maximum likelihood, delta = change in AIC, weight = Akaike's weight).

variable	df	logLik	AIC	delta	weight
Fire/EMS Dens. 1km	3	1,049.072	-2,092.145	0.000	6.47e-01
Fire/EMS Dens. 5km	3	1,048.355	-2,090.711	1.434	3.16e-01
Fire/EMS Dens. 10km	3	1,046.222	-2,086.445	5.700	3.74e-02
Fire/EMS Dens. 20km	3	1,036.276	-2,066.551	25.594	1.79e-06

Table B-12. Model selection results for fire and EMS station density (n/km²) using Akaike's Information Criteria (AIC). Large wildfire (≥200 ha) distance to the wildland-urban interface (WUI) was modelled using a generalized linear model with a gamma family and fire and EMS station density as a predictor with various buffer sizes windows around each wildfire's perimeter (df = degrees of freedom, logLik = natural logarithm of the maximum likelihood, delta = change in AIC, weight = Akaike's weight).

variable	df	logLik	AIC	delta	weight
Fire/EMS Dens. 1km	3	-1,999.507	4,005.015	0.000	1.00e+00
Fire/EMS Dens. 5km	3	-2,013.291	4,032.582	27.567	1.03e-06
Fire/EMS Dens. 10km	3	-2,019.692	4,045.385	40.370	1.71e-09
Fire/EMS Dens. 20km	3	-2,085.341	4,176.682	171.667	5.28e-38

Table B-13. Model selection results for road density (km/km²) using Akaike's Information Criteria (AIC). Large wildfire (≥200 ha) occurrence in the wildland-urban interface (WUI) was modelled using a binomial generalized linear model and road density as a predictor with various buffer sizes windows around each wildfire's perimeter (df = degrees of freedom, logLik = natural logarithm of the maximum likelihood, delta = change in AIC, weight = Akaike's weight).

variable	df	logLik	AIC	delta	weight
Road Dens.	2	-1,388.744	2,781.488	0.000	1.00e+00
Road Dens. at 50m	2	-1,448.210	2,900.420	118.932	1.49e-26
Road Dens. at 100m	2	-1,471.106	2,946.211	164.724	1.70e-36
Road Dens. at 200m	2	-1,485.201	2,974.402	192.915	1.29e-42
Road Dens. at 1000m	2	-1,492.018	2,988.036	206.548	1.41e-45

Table B-14. Model selection results for road density (km/km²) using Akaike's Information Criteria (AIC). The proportion of a large wildfire's (≥200 ha) area that burned the wildland-urban interface (WUI) was modelled using a beta regression and road density as a predictor with various buffer sizes windows around each wildfire's perimeter (df = degrees of freedom, logLik = natural logarithm of the maximum likelihood, delta = change in AIC, weight = Akaike's weight).

variable	df	logLik	AIC	delta	weight
Road Dens. within	3	1,044.974	-2,083.948	0.000	9.79e-01
Road Dens. at 50m	3	1,041.154	-2,076.307	7.641	2.14e-02
Road Dens. at 100m	3	1,034.088	-2,062.176	21.772	1.83e-05
Road Dens. at 200m	3	1,030.144	-2,054.288	29.660	3.55e-07
Road Dens. at 1000m	3	1,028.184	-2,050.368	33.580	5.00e-08

Table B-15. Model selection results for road density (km/km²) using Akaike's Information Criteria (AIC). Large wildfire (≥200 ha) distance to the wildland-urban interface (WUI) was modelled using a generalized linear model with a gamma family and road density as a predictor with various buffer sizes windows around each wildfire's perimeter (df = degrees of freedom, logLik = natural logarithm of the maximum likelihood, delta = change in AIC, weight = Akaike's weight).

variable	df	logLik	AIC	delta	weight
Road Dens. within	3	-2,074.989	4,155.977	0.000	1.00e+00
Road Dens. at 50m	3	-2,084.475	4,174.950	18.973	7.59e-05
Road Dens. at 100m	3	-2,085.312	4,176.623	20.646	3.29e-05
Road Dens. at 200m	3	-2,085.547	4,177.094	21.116	2.60e-05
Road Dens. at 1000m	3	-2,085.644	4,177.288	21.311	2.36e-05

Table B-16. Model selection results for preparedness level using Akaike's Information Criteria (AIC). Large wildfire (≥200 ha) occurrence in the wildland-urban interface (WUI) was modelled using a binomial generalized linear model and preparedness level as a predictor with various temporal windows before each wildfire's ignition date (df = degrees of freedom, logLik = natural logarithm of the maximum likelihood, delta = change in AIC, weight = Akaike's weight).

variable	df	logLik	AIC	delta	weight
PL 1d	2	-1,494.326	2,992.651	0.000	0.95746
Mdn. PL 07d	2	-1,499.156	3,002.311	9.660	0.00765
Mdn. PL 14d	2	-1,499.346	3,002.691	10.040	0.00632
Mdn. PL 30d	2	-1,499.390	3,002.780	10.128	0.00605
Mn. PL 07d	2	-1,499.437	3,002.873	10.222	0.00577
Mn. PL 14d	2	-1,499.437	3,002.873	10.222	0.00577
Mn. PL 30d	2	-1,499.485	3,002.971	10.319	0.00550
% PL >3 30d	2	-1,499.492	3,002.983	10.332	0.00546

Table B-17. Model selection results for preparedness level using Akaike's Information Criteria (AIC). The proportion of a large wildfire's (≥200 ha) area that burned the wildland-urban interface (WUI) was modelled using a beta regression and preparedness level as a predictor with various temporal windows before each wildfire's ignition date (df = degrees of freedom, logLik = natural logarithm of the maximum likelihood, delta = change in AIC, weight = Akaike's weight).

variable	df	logLik	AIC	delta	weight
PL 1d	3	1,030.875	-2,055.750	0.000	0.94289
Mdn. PL 07d	3	1,026.811	-2,047.621	8.129	0.01619
Mdn. PL 14d	3	1,026.743	-2,047.485	8.264	0.01513
Mdn. PL 30d	3	1,025.873	-2,045.746	10.004	0.00634
Mn. PL 07d	3	1,025.647	-2,045.295	10.455	0.00506
Mn. PL 14d	3	1,025.610	-2,045.219	10.531	0.00487
Mn. PL 30d	3	1,025.585	-2,045.170	10.580	0.00476
% PL >3 30d	3	1,025.585	-2,045.170	10.580	0.00476

Table B-18. Model selection results for preparedness level using Akaike's Information Criteria (AIC). Large wildfire (≥200 ha) distance to the wildland-urban interface (WUI) was modelled using a generalized linear model with a gamma family and preparedness level as a predictor with various temporal windows before each wildfire's ignition date (df = degrees of freedom, logLik = natural logarithm of the maximum likelihood, delta = change in AIC, weight = Akaike's weight).

variable	df	logLik	AIC	delta	weight
PL 1d	3	-2,085.431	4,176.861	0.000	0.142
Mdn. PL 07d	3	-2,085.453	4,176.906	0.044	0.139
Mdn. PL 14d	3	-2,085.530	4,177.060	0.198	0.128
Mdn. PL 30d	3	-2,085.530	4,177.060	0.198	0.128
Mn. PL 07d	3	-2,085.570	4,177.140	0.279	0.123
Mn. PL 14d	3	-2,085.613	4,177.225	0.364	0.118
Mn. PL 30d	3	-2,085.666	4,177.332	0.471	0.112
% PL >3 30d	3	-2,085.688	4,177.376	0.515	0.110

Table B-19. Model selection results for whether large wildfires (≥200 ha) burned in the wildland-urban interface (WUI) of the Eastern Temperate Forests Level I ecoregion using Akaike's Information Criteria (AIC). WUI status was modelled using a binomial generalized linear model (df = degrees of freedom, logLik = natural logarithm of the maximum likelihood, delta = change in AIC, weight = Akaike's weight).

model	df	logLik	AIC	delta	weight
Mississippi Alluvial and Southeast USA Coastal Plains					
03	4	-415.3398	838.6795	0.0000	9.00e-01
01	8	-413.5370	843.0740	4.3945	1.00e-01
11	2	-425.7657	855.5313	16.8518	1.97e-04
04	4	-425.4654	858.9308	20.2512	3.60e-05
10	2	-464.4036	932.8072	94.1277	3.27e-21
Ozark/Ouachita-Appalachian Forests					
01	8	-594.1895	1,204.3790	0.0000	1.00e+00
03	4	-623.5708	1,255.1416	50.7626	9.49e-12
04	4	-641.1104	1,290.2208	85.8418	2.29e-19
11	2	-650.1403	1,304.2806	99.9016	2.03e-22
10	2	-675.9689	1,355.9378	151.5588	1.23e-33
Southeastern USA Plains					
01	8	-245.4991	506.9981	0.0000	1.00e+00
03	4	-259.1081	526.2162	19.2181	6.71e-05
04	4	-259.6611	527.3221	20.3240	3.86e-05
02	4	-260.5301	529.0603	22.0621	1.62e-05
10	2	-262.9213	529.8425	22.8444	1.09e-05

Table B-20. Model selection results for the proportion of large wildfires' (≥200 ha) areas that burned in the wildland-urban interface (WUI) of the Eastern Temperate Forests Level I ecoregion using Akaike's Information Criteria (AIC). The proportion WUI area burned was modelled using a beta regression (df = degrees of freedom, logLik = natural logarithm of the maximum likelihood, delta = change in AIC, weight = Akaike's weight).

model	df	logLik	AIC	delta	weight
Mississippi Alluvial and Southeast USA Coastal Plains					
10	3	333.0479	-660.0958	0.0000	4.68e-01
03	5	334.8006	-659.6013	0.4945	3.66e-01
11	3	331.1616	-656.3231	3.7727	7.10e-02
01	9	336.5897	-655.1793	4.9165	4.01e-02
04	5	332.3239	-654.6477	5.4481	3.07e-02
Ozark/Ouachita-Appalachian Forests					
01	9	605.5091	-1,193.0181	0.0000	9.97e-01
03	5	595.6446	-1,181.2892	11.7289	2.83e-03
04	5	587.8930	-1,165.7861	27.2320	1.22e-06
10	3	584.9490	-1,163.8980	29.1201	4.74e-07
11	3	584.4675	-1,162.9350	30.0831	2.93e-07
Southeastern USA Plains					
11	3	221.2834	-436.5668	0.0000	5.39e-01
04	5	222.4314	-434.8628	1.7040	2.30e-01
03	5	222.3691	-434.7383	1.8286	2.16e-01
01	9	223.6706	-429.3411	7.2257	1.45e-02
10	3	212.3033	-418.6066	17.9602	6.79e-05

Table B-21. Model selection results for the distance large wildfires (≥200 ha) burned from the wildland-urban interface (WUI) of the Eastern Temperate Forests Level I ecoregion using Akaike's Information Criteria (AIC). The Distance to WUI (km) was modelled using a gamma generalized linear model (df = degrees of freedom, logLik = natural logarithm of the maximum likelihood, delta = change in AIC, weight = Akaike's weight).

model	df	logLik	AIC	delta	weight
Mississippi Alluvial and Southeast USA Coastal Plains					
04	5	-1,016.4349	2,042.8698	0.0000	8.97e-01
01	9	-1,014.9459	2,047.8918	5.0220	7.29e-02
11	3	-1,022.0070	2,050.0139	7.1441	2.52e-02
03	5	-1,021.7909	2,053.5817	10.7119	4.24e-03
08	3	-1,027.1245	2,060.2490	17.3792	1.51e-04
Ozark/Ouachita-Appalachian Forests					
04	5	-593.7852	1,197.5703	0.0000	6.00e-01
11	3	-596.5441	1,199.0883	1.5180	2.81e-01
01	9	-591.9317	1,201.8633	4.2930	7.01e-02
03	5	-596.3064	1,202.6129	5.0425	4.82e-02
08	3	-603.1082	1,212.2164	14.6461	3.96e-04
Southeastern USA Plains					
04	5	-429.4408	868.8816	0.0000	6.99e-01
01	9	-426.5061	871.0122	2.1306	2.41e-01
08	3	-433.9699	873.9398	5.0582	5.58e-02
07	3	-436.9556	879.9112	11.0296	2.82e-03
02	5	-436.8908	883.7816	14.9000	4.07e-04

Table B-22. Model parameter estimates for predictors of whether large wildfires (≥200 ha) burned in the wildland-urban interface (WUI) within the Eastern Temperate Forests Level I ecoregion and three Level II ecoregions.

Parameter	Odds Ratio	SE	95% CI	z	p
L1 Eastern Temperate Forests					
(Intercept)	0.128	0.054	(0.056, 0.29)	-4.914	<.001
Woody Cover	1.014	0.002	(1.01, 1.019)	6.215	<.001
Road Density	2.176	0.151	(1.903, 2.498)	11.205	<.001
Wind Speed	0.958	0.034	(0.894, 1.027)	-1.211	0.226
Precipitation	0.933	0.019	(0.895, 0.969)	-3.449	0.001
Fuel Moisture	0.995	0.020	(0.956, 1.035)	-0.253	0.8
Prep. Level	1.022	0.058	(0.913, 1.142)	0.377	0.706
Fire/EMS Density	1.042	0.005	(1.032, 1.054)	7.878	<.001
Mississippi Alluvial and Southeast USA Coastal Plains					
(Intercept)	0.093	0.022	(0.058, 0.147)	-10.042	<.001
Prep. Level	1.177	0.112	(0.974, 1.417)	1.705	0.088
Fire/EMS Density	1.031	0.008	(1.016, 1.048)	3.817	<.001
Road Density	2.666	0.293	(2.161, 3.325)	8.927	<.001
Ozark/Ouachita-Appalachian Forests					
(Intercept)	0.150	0.093	(0.045, 0.501)	-3.070	0.002
Woody Cover	1.007	0.004	(0.998, 1.016)	1.538	0.124
Road Density	3.559	0.487	(2.739, 4.684)	9.280	<.001
Wind Speed	0.769	0.040	(0.694, 0.85)	-5.075	<.001
Precipitation	0.920	0.034	(0.853, 0.987)	-2.261	0.024
Fuel Moisture	1.115	0.032	(1.054, 1.18)	3.799	<.001
Prep. Level	0.828	0.085	(0.675, 1.013)	-1.829	0.067
Fire/EMS Density	1.047	0.010	(1.029, 1.069)	4.797	<.001
Southeastern USA Plains					
(Intercept)	0.274	0.285	(0.035, 2.096)	-1.244	0.213
Woody Cover	1.010	0.005	(0.999, 1.021)	1.756	0.079
Road Density	1.285	0.184	(0.97, 1.707)	1.748	0.08
Wind Speed	1.289	0.108	(1.096, 1.523)	3.035	0.002
Precipitation	0.993	0.035	(0.919, 1.062)	-0.193	0.847
Fuel Moisture	0.875	0.045	(0.79, 0.967)	-2.598	0.009
Prep. Level	1.150	0.118	(0.937, 1.403)	1.363	0.173
Fire/EMS Density	1.033	0.009	(1.017, 1.054)	3.617	<.001

Table B-23. Model parameter estimates for predictors of the proportion of a large wildfire's (≥200 ha) area that burned in the wildland-urban interface (WUI) within the Eastern Temperate Forests Level I ecoregion and three Level II ecoregions.

Parameter	Odds Ratio	SE	95% CI	z	p
L1 Eastern Temperate Forests					
(Intercept)	0.190	0.070	(0.092, 0.39)	-4.519	<.001
Woody Cover	1.003	0.002	(0.999, 1.007)	1.362	0.173
Road Density	1.304	0.068	(1.177, 1.445)	5.063	<.001
Wind Speed	0.936	0.027	(0.884, 0.991)	-2.265	0.023
Precipitation	0.952	0.019	(0.917, 0.989)	-2.518	0.012
Fuel Moisture	1.026	0.018	(0.992, 1.062)	1.487	0.137
Prep. Level	1.035	0.051	(0.941, 1.14)	0.712	0.476
Fire/EMS Density	1.010	0.002	(1.006, 1.014)	5.068	<.001
Mississippi Alluvial and Southeast USA Coastal Plains					
(Int)	0.201	0.046	(0.129, 0.315)	7.035	<.001
Fire/EMS Density	1.011	0.004	(1.003, 1.019)	2.784	0.005
Prep. Level	1.088	0.085	(0.935, 1.268)	1.091	0.275
Road Density	1.128	0.085	(0.972, 1.308)	1.587	0.113
Ozark/Ouachita-Appalachian Forests					
(Intercept)	0.267	0.129	(0.104, 0.686)	-2.743	0.006
Woody Cover	0.997	0.004	(0.99, 1.004)	-0.813	0.416
Road Density	1.466	0.111	(1.264, 1.701)	5.058	<.001
Wind Speed	0.894	0.034	(0.83, 0.963)	-2.971	0.003
Precipitation	0.946	0.030	(0.89, 1.007)	-1.754	0.079
Fuel Moisture	1.048	0.023	(1.004, 1.094)	2.149	0.032
Prep. Level	1.026	0.091	(0.862, 1.22)	0.286	0.775
Fire/EMS Density	1.010	0.002	(1.006, 1.015)	4.256	<.001
Southeastern USA Plains					
(Int)	0.122	0.057	(0.049, 0.306)	4.488	<.001
Road Density	1.840	0.241	(1.423, 2.378)	4.653	<.001
Woody Cover	0.993	0.005	(0.983, 1.002)	1.501	0.133
Fuel Moisture	1.007	0.043	(0.926, 1.095)	0.165	0.869
Prep. Level	1.103	0.091	(0.938, 1.297)	1.185	0.236
Fire/EMS Density	1.004	0.004	(0.996, 1.013)	1.037	0.3

Table B-24. Model parameter estimates for predictors of the distance large wildfires (≥200 ha) burned from the wildland-urban interface (WUI) within the Eastern Temperate Forests Level I ecoregion and three Level II ecoregions.

Parameter	Prevalence Ratio	SE	95% CI	z	p
L1 Eastern Temperate Forests					
(Intercept)	1.702	0.449	(1.014, 2.855)	2.014	0.044
Woody Cover	0.990	0.001	(0.988, 0.993)	7.353	<.001
Road Density	0.833	0.034	(0.769, 0.902)	4.500	<.001
Wind Speed	0.978	0.023	(0.935, 1.023)	0.970	0.332
Precipitation	1.025	0.010	(1.006, 1.045)	2.561	0.010
Fuel Moisture	1.072	0.015	(1.044, 1.101)	5.050	<.001
Prep. Level	1.018	0.037	(0.948, 1.094)	0.499	0.618
Fire/EMS Density	0.993	0.004	(0.986, 1)	1.887	0.059
Mississippi Alluvial and Southeast USA Coastal Plains					
(Intercept)	1.711	0.655	(0.796, 3.722)	1.403	0.161
Woody Cover	0.995	0.002	(0.991, 0.999)	-2.721	0.006
Fuel Moisture	1.067	0.025	(1.017, 1.12)	2.781	0.005
Road Density	0.779	0.044	(0.7, 0.874)	-4.469	<.001
Ozark/Ouachita-Appalachian Forests					
(Intercept)	2.867	0.984	(1.464, 5.616)	3.071	0.002
Woody Cover	0.992	0.003	(0.987, 0.998)	2.534	0.011
Fuel Moisture	1.012	0.020	(0.973, 1.051)	0.582	0.56
Road Density	0.657	0.059	(0.551, 0.783)	4.679	<.001
Southeastern USA Plains					
(Intercept)	0.885	0.373	(0.365, 2.168)	-0.290	0.772
Woody Cover	0.991	0.003	(0.985, 0.996)	-3.583	<.001
Fuel Moisture	1.080	0.026	(1.028, 1.135)	3.202	0.001
Road Density	1.139	0.087	(0.976, 1.335)	1.714	0.086

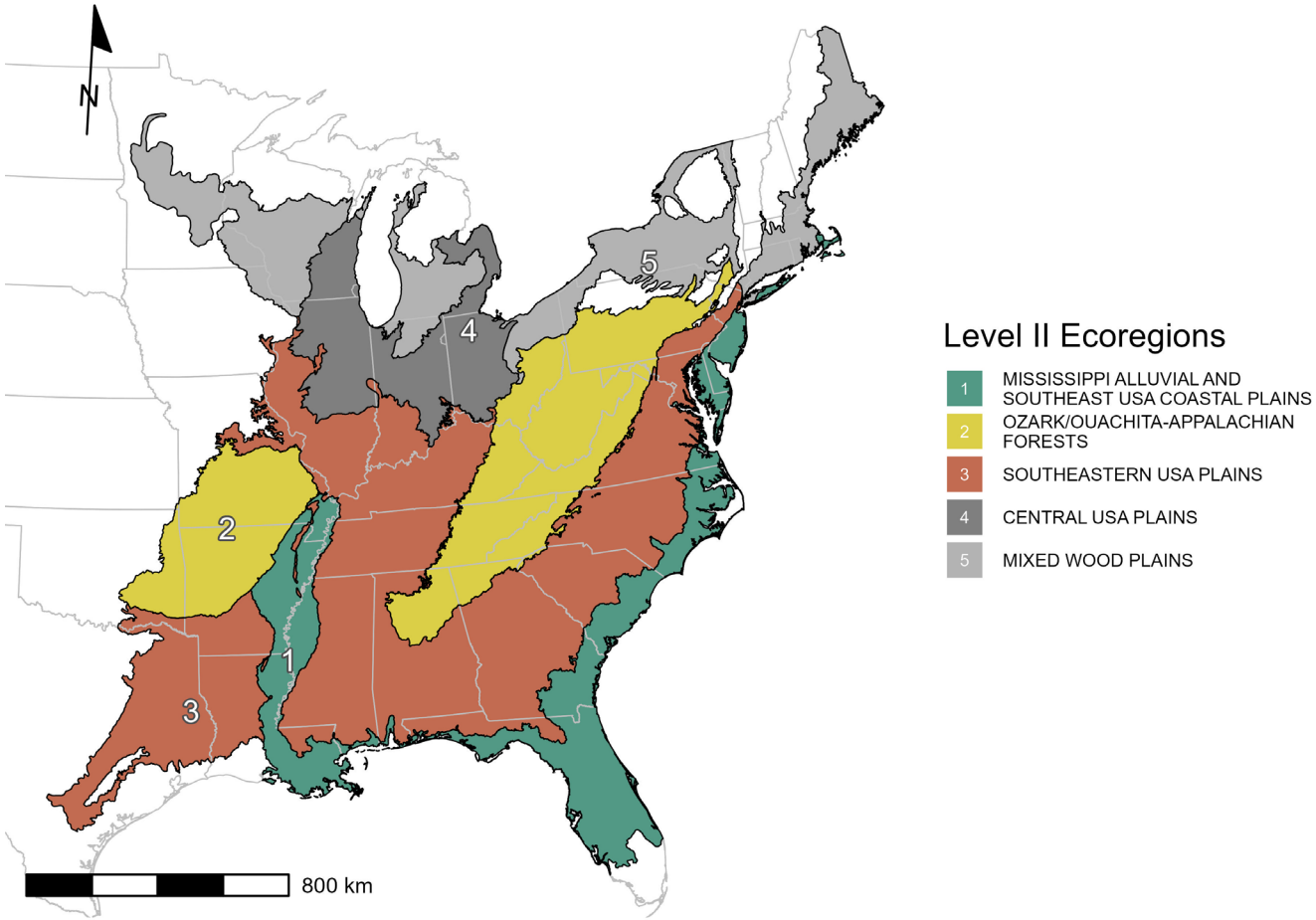


Figure B-1. Map showing Level II ecoregions of the Eastern Temperate Forests Level I ecoregion. Ecoregions colored with grey were not used in this analysis due to an insufficient number of large wildfires (≥200 ha).

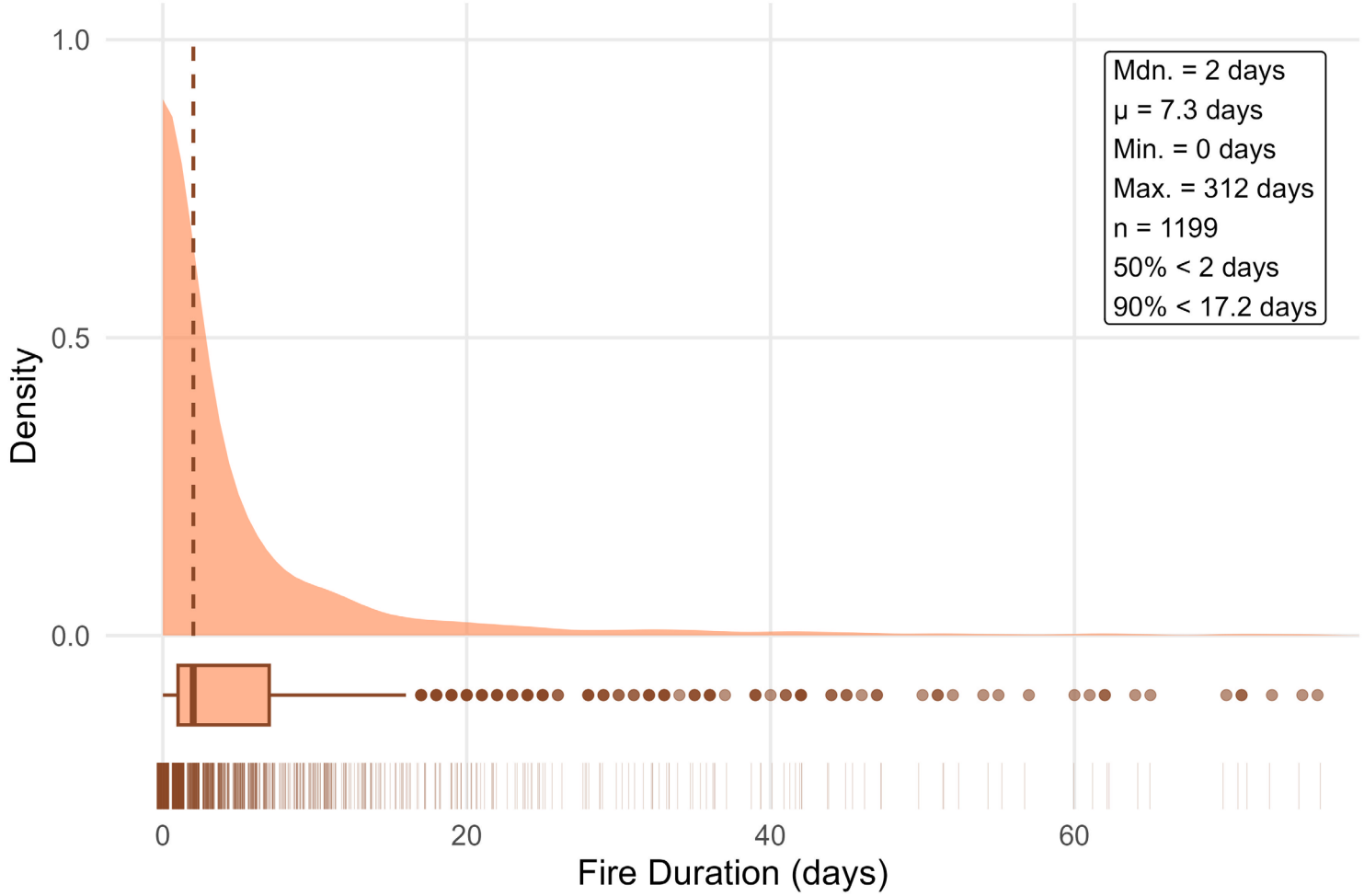


Figure B-2. Raincloud plot showing the distribution of large wildfire durations across the Eastern Temperate Forests Level I ecoregion. Data from the Monitoring Trends in Burn Severity Project and the USDA Fire-Occurrence Dataset were used to assess wildfire duration.

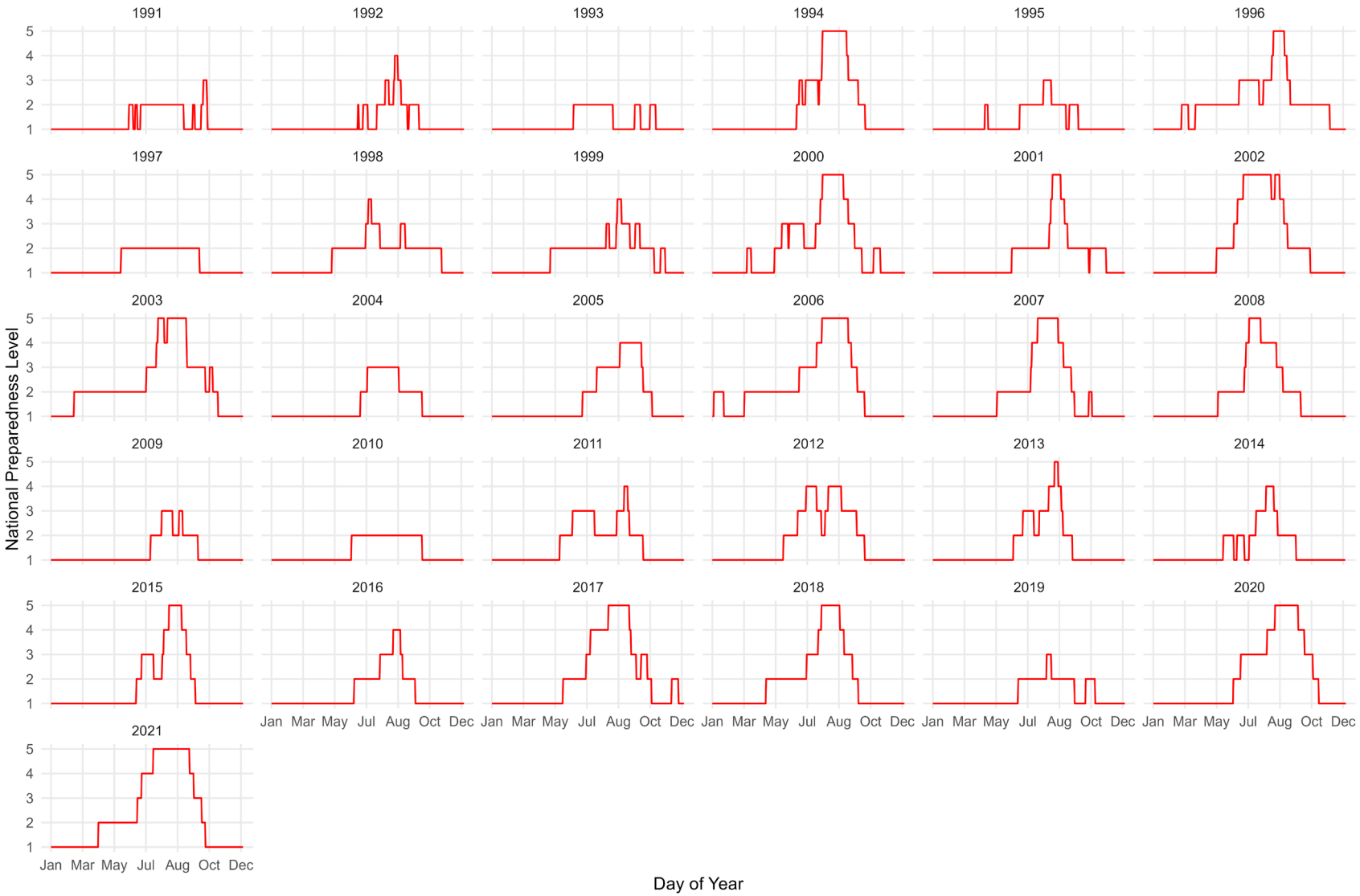


Figure B-3. Daily National Preparedness Levels between 1991 and 2021 within the United States.

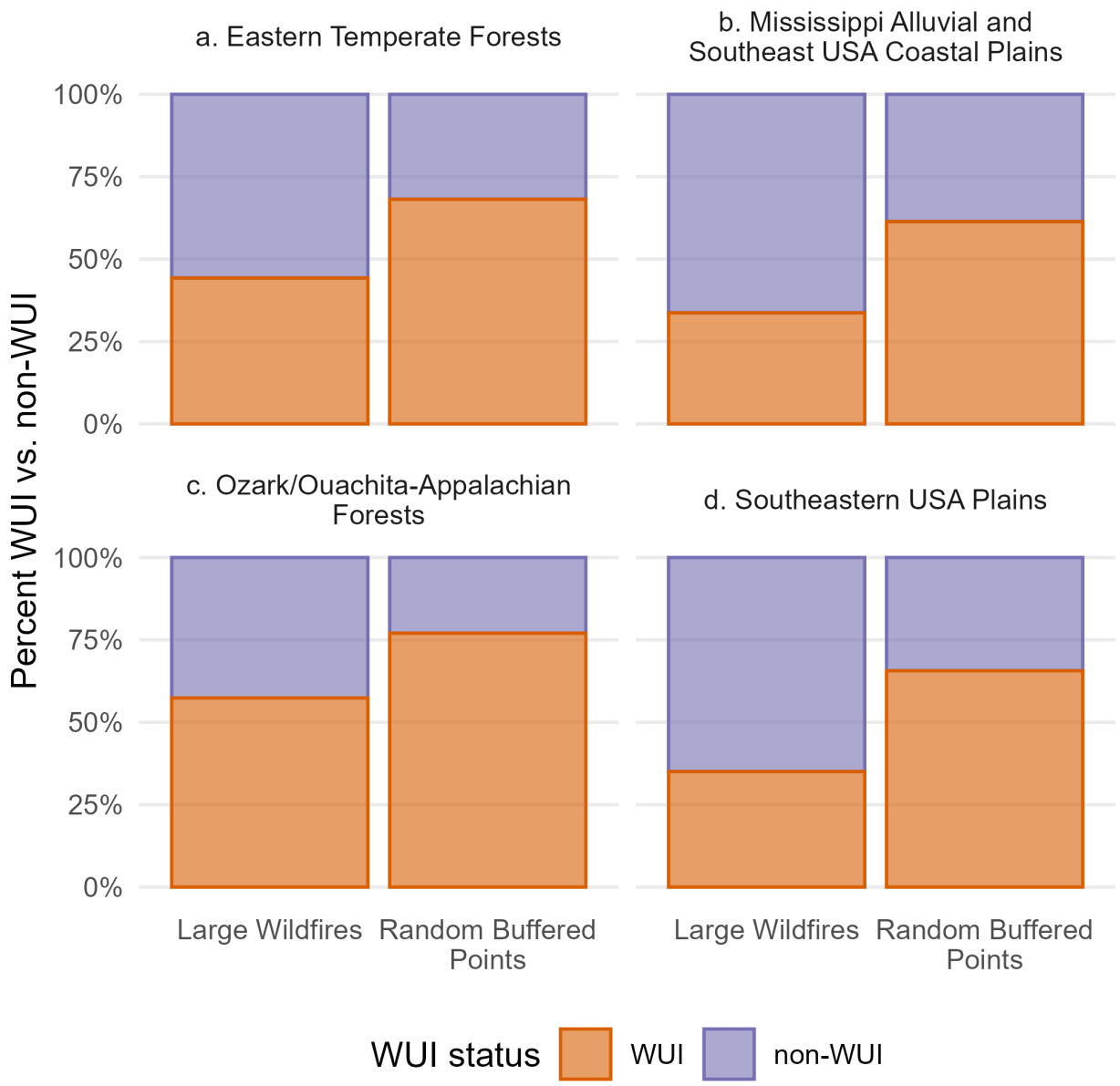


Figure B-4. Bar graphs showing the proportion of large wildfires (≥200 ha) that burned wildland-urban interface (WUI) in the Eastern Temperate Forests Level I ecoregion and across three Level III ecoregions.

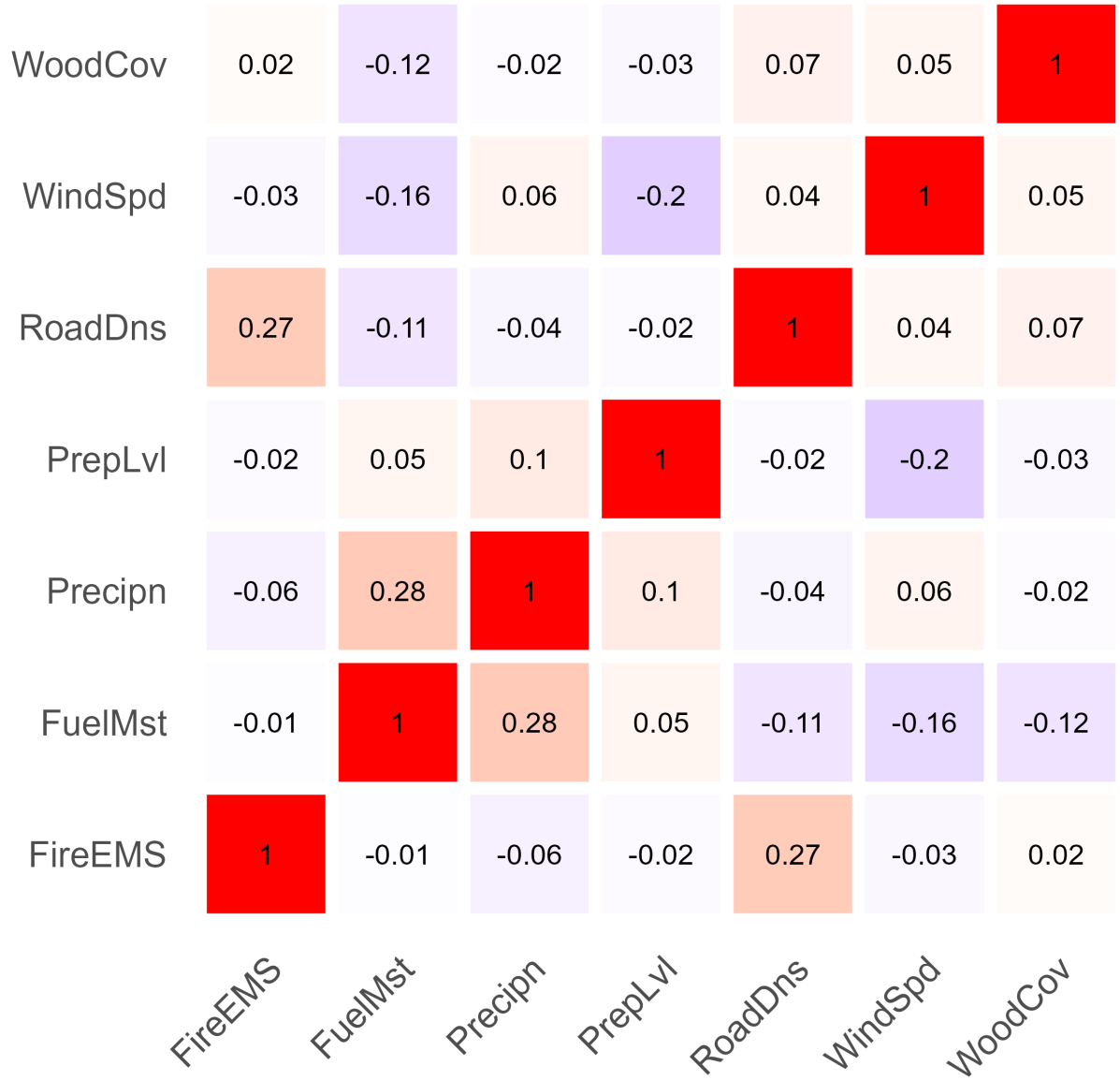


Figure B-5. Correlation matrix showing the Pearson's correlation coefficient between predictor variables used to model whether large wildfires (≥200 ha) burned in the wildland-urban interface (WUI) within the Eastern Temperate Forests Level I ecoregion.

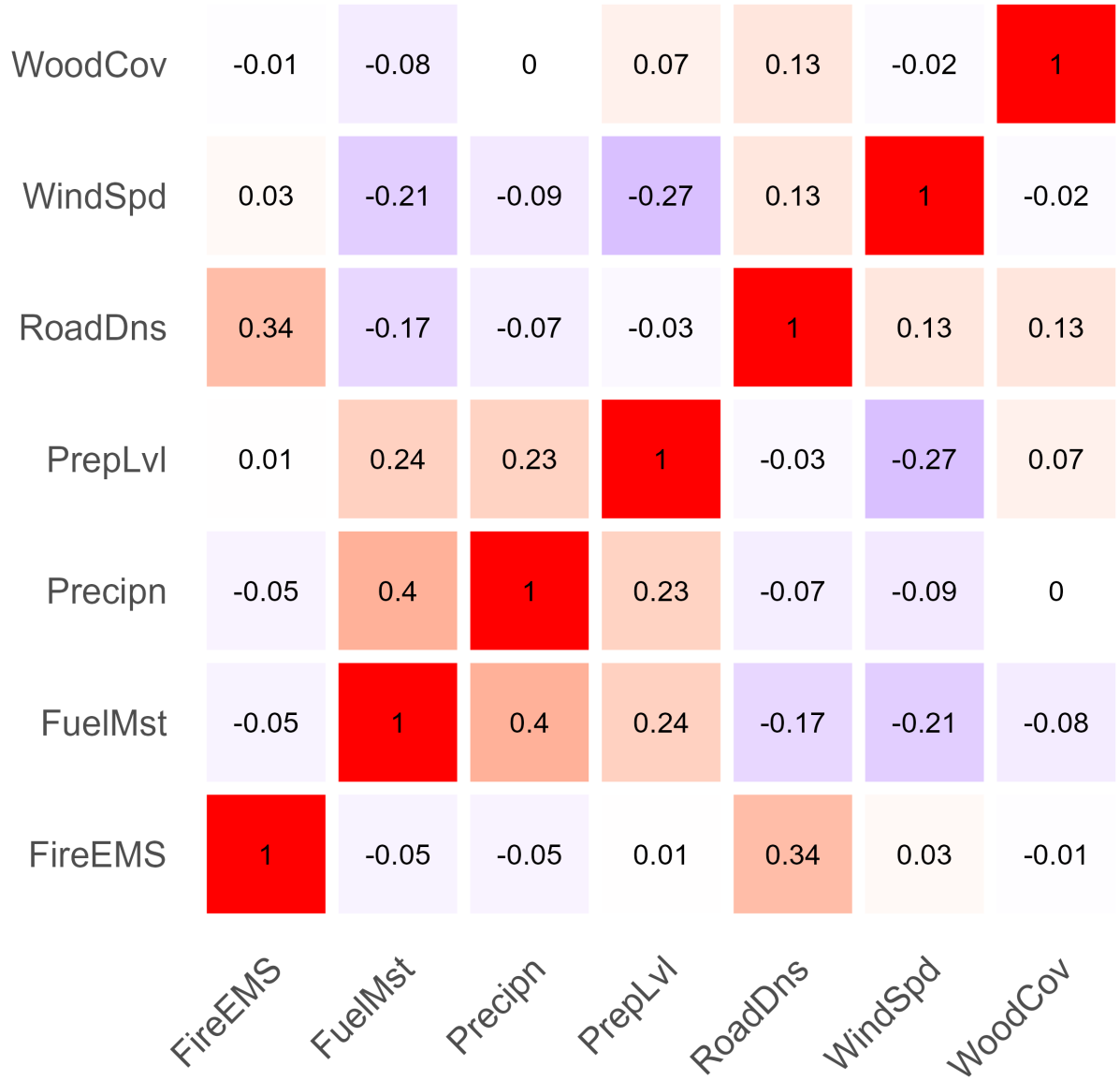


Figure B-6. Correlation matrix showing the Pearson's correlation coefficient between predictor variables used to model whether large wildfires (≥200 ha) burned in the wildland-urban interface (WUI) within the Mississippi Alluvial and Southeast USA Coastal Plains Level II ecoregion.

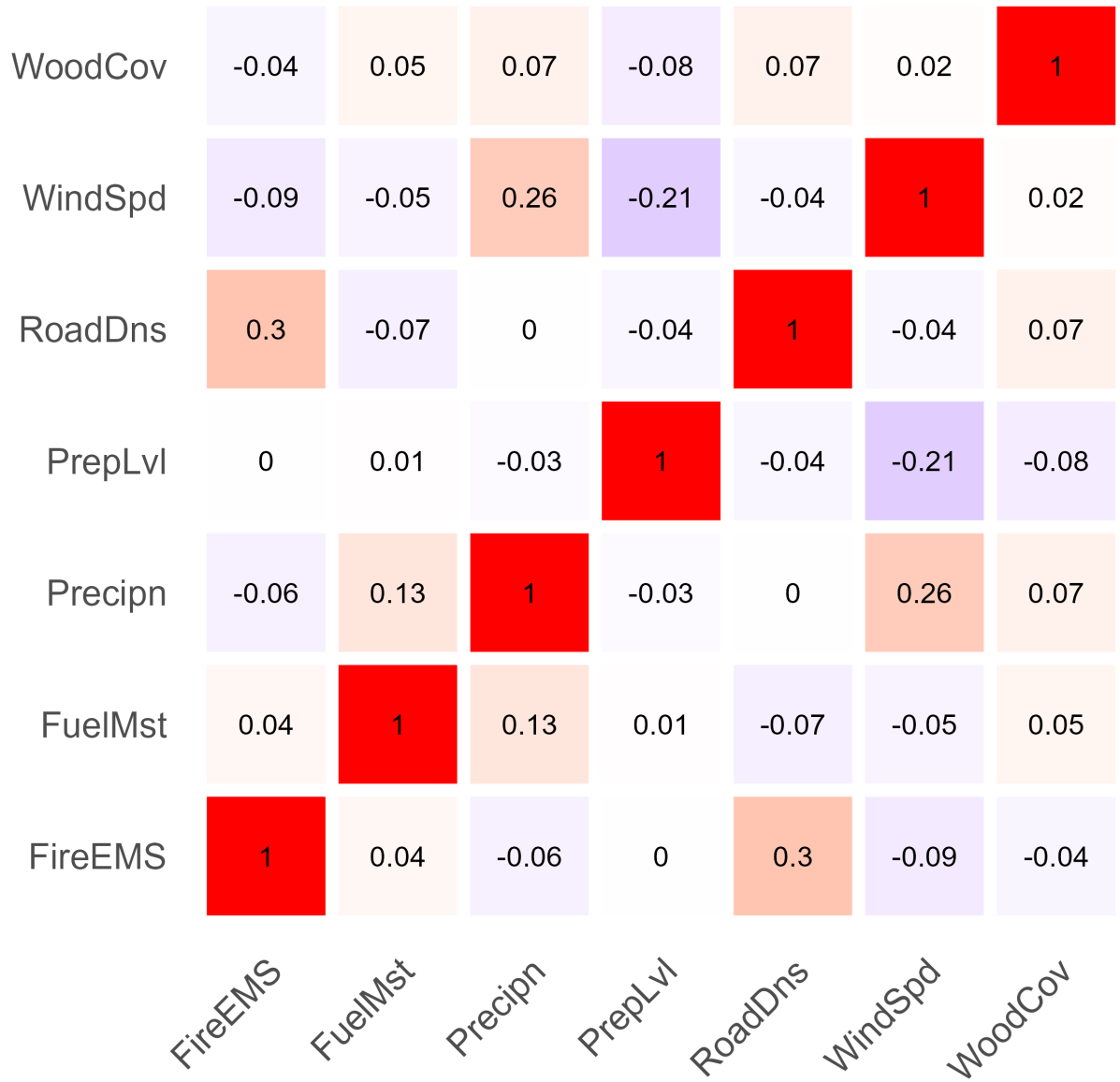


Figure B-7. Correlation matrix showing the Pearson's correlation coefficient between predictor variables used to model whether large wildfires (≥200 ha) burned in the wildland-urban interface (WUI) within the Ozark/Ouachita-Appalachian Forests Level II ecoregion.

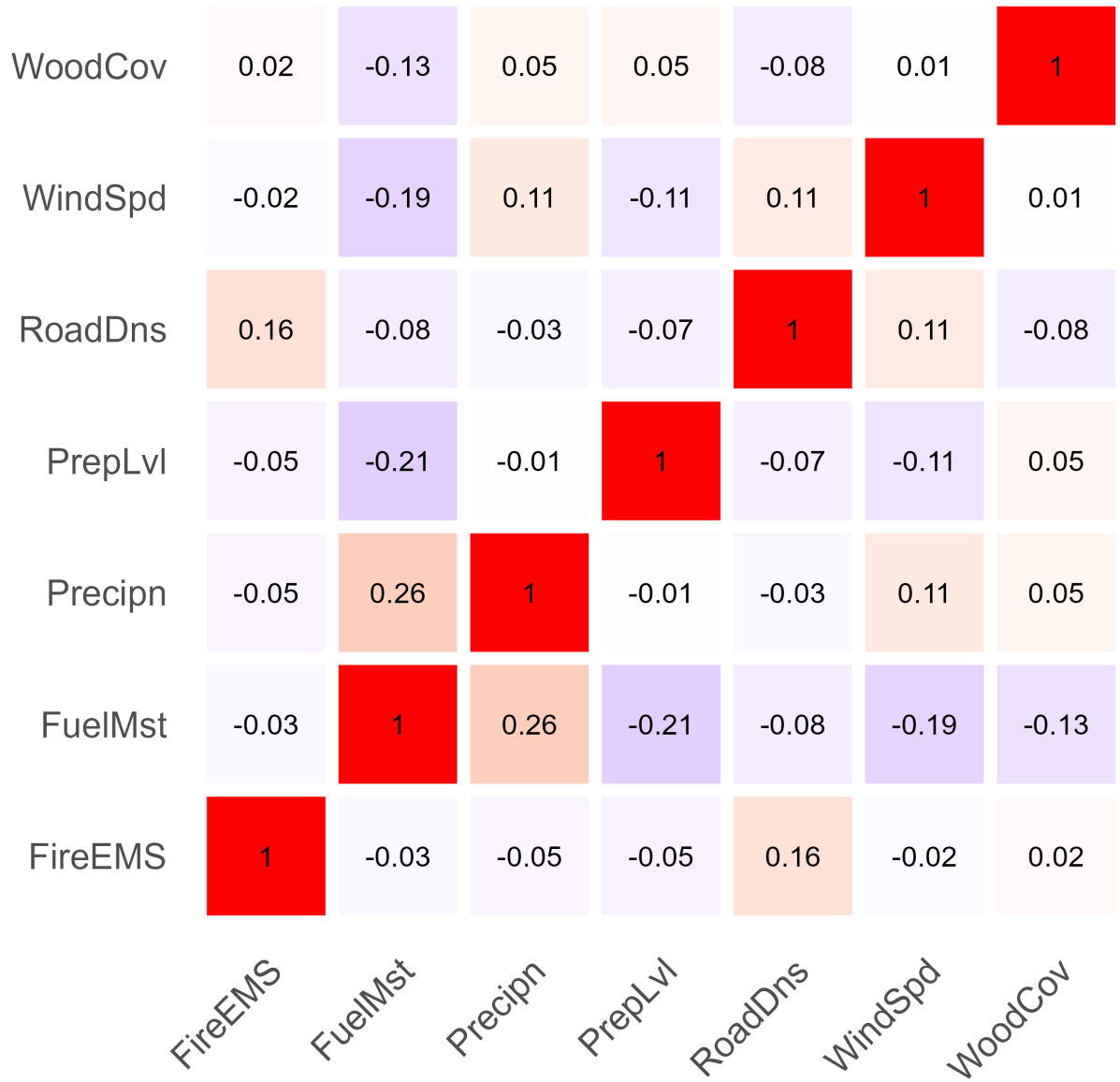


Figure B-8. Correlation matrix showing the Pearson's correlation coefficient between predictor variables used to model whether large wildfires (≥200 ha) burned in the wildland-urban interface (WUI) within the Southeastern USA Plains Level II ecoregion.

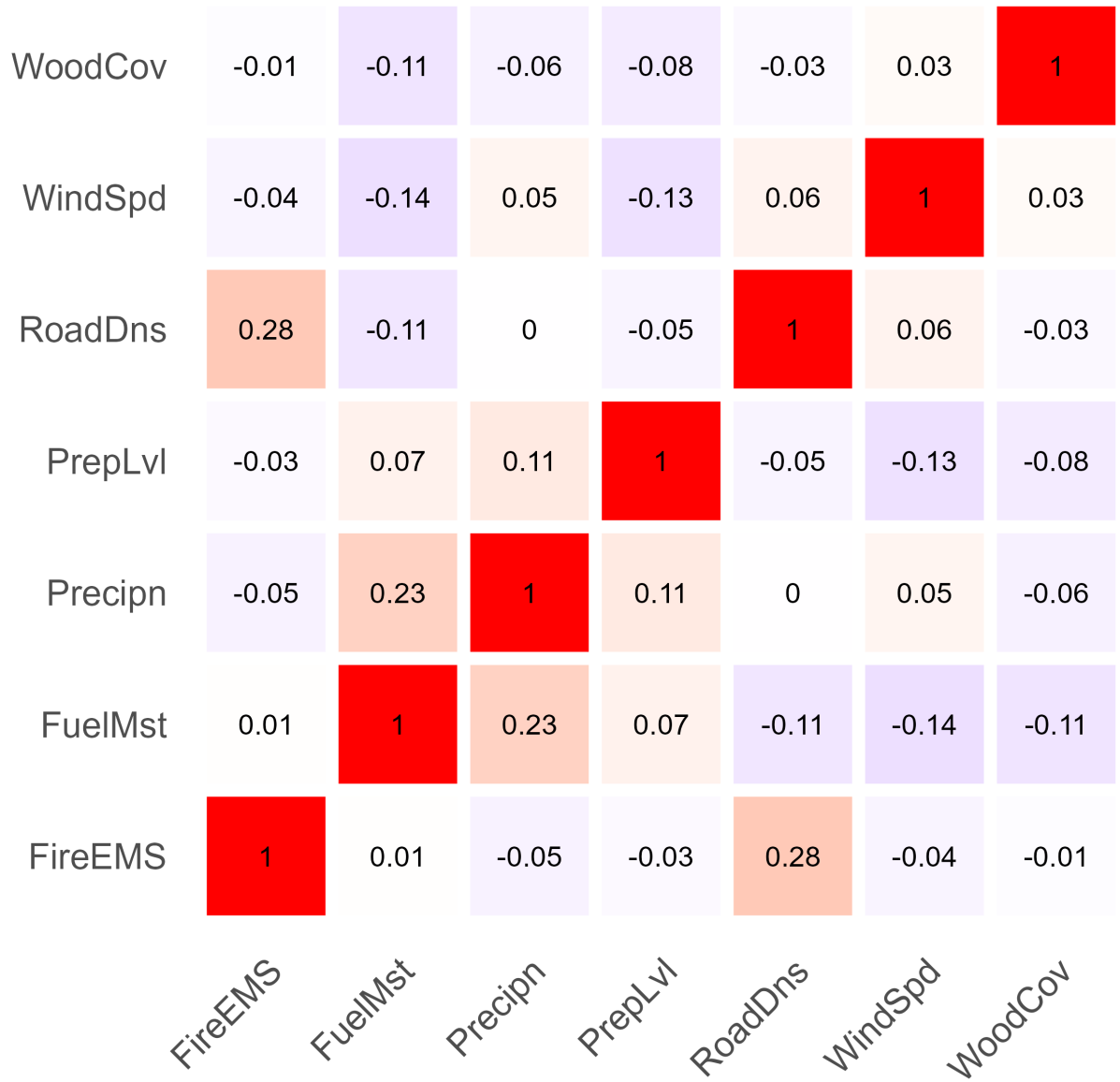


Figure B-9. Correlation matrix showing the Pearson's correlation coefficient between predictor variables used to model the proportion of a large wildfire's (≥200 ha) area that burned in the wildland-urban interface (WUI) within the Eastern Temperate Forests Level I ecoregion.

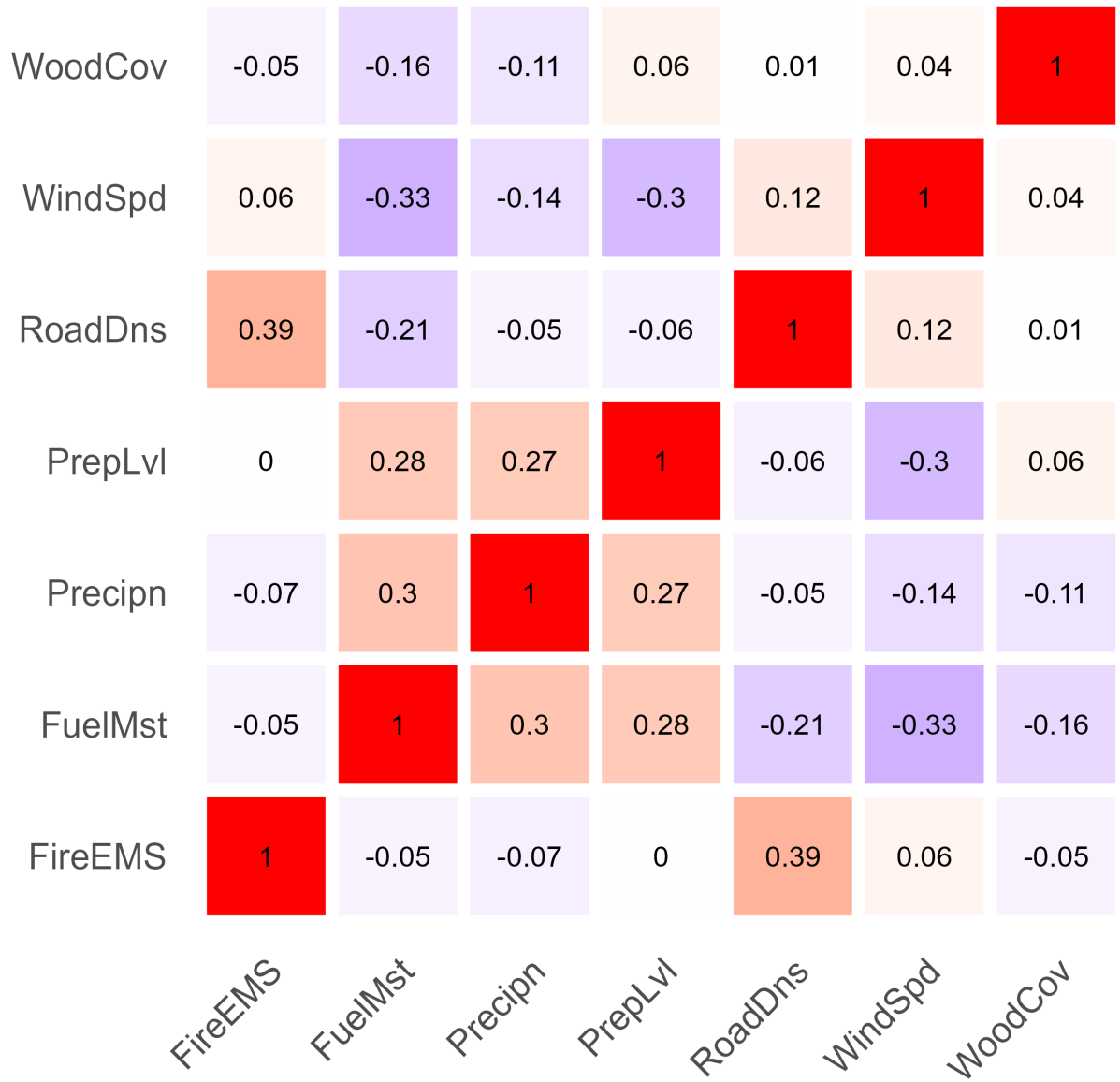


Figure B-10. Correlation matrix showing the Pearson's correlation coefficient between predictor variables used to model the proportion of a large wildfire's (≥200 ha) area that burned in the wildland-urban interface (WUI) within the Mississippi Alluvial and Southeast USA Coastal Plains Level II ecoregion.

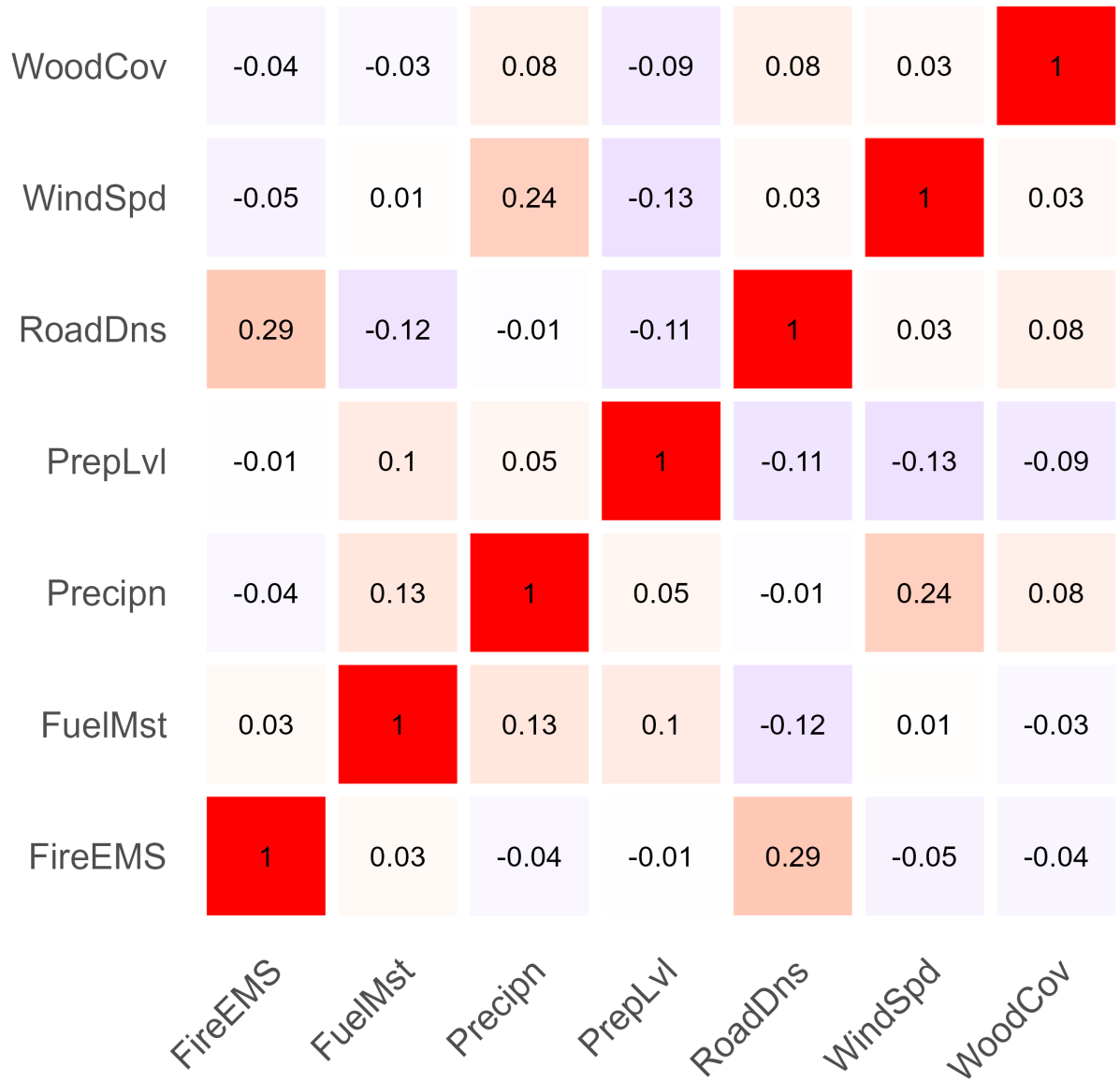


Figure B-11. Correlation matrix showing the Pearson's correlation coefficient between predictor variables used to model the proportion of a large wildfire's (≥200 ha) area that burned in the wildland-urban interface (WUI) within the Ozark/Ouachita-Appalachian Forests Level II ecoregion.

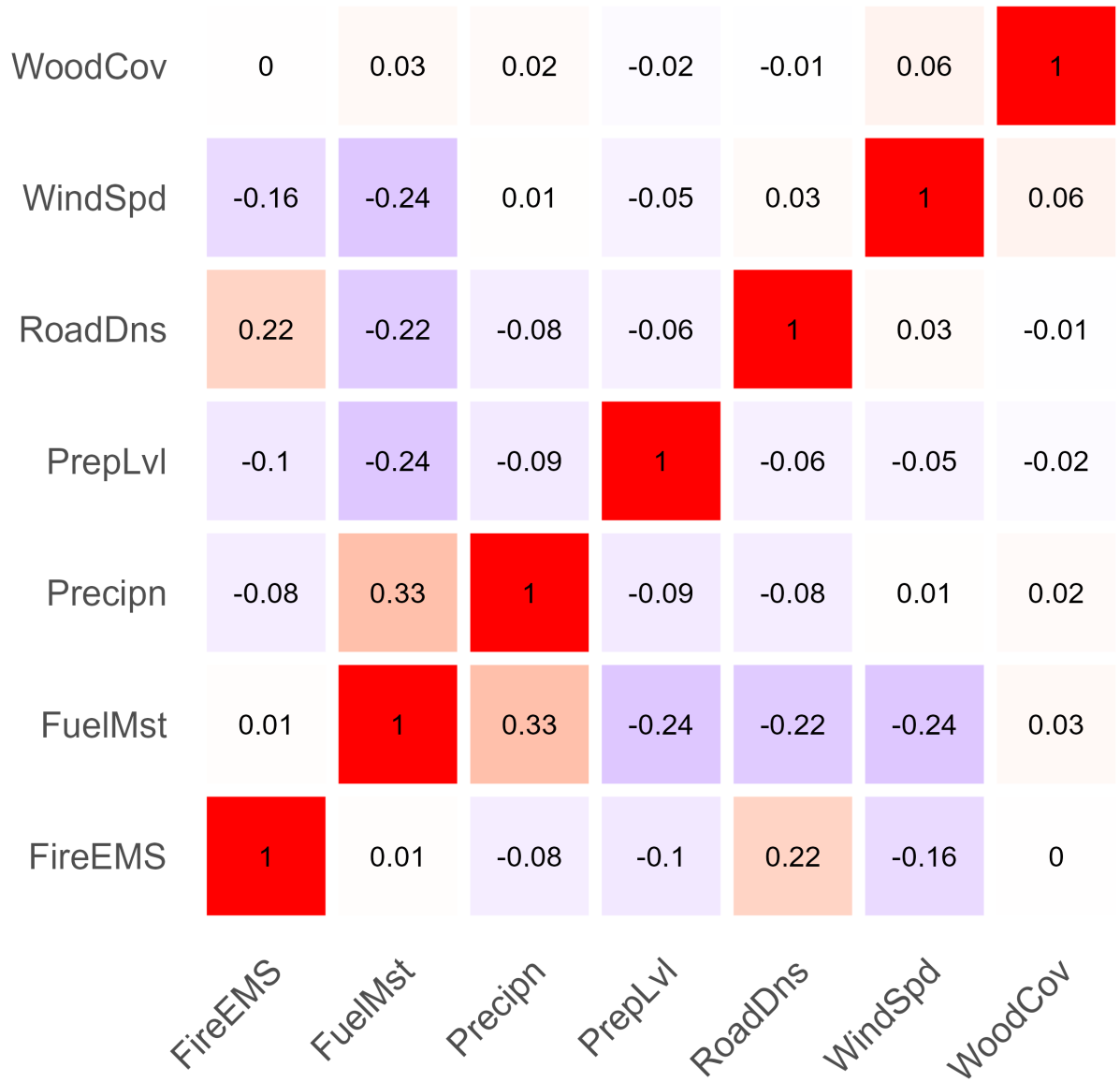


Figure B-12. Correlation matrix showing the Pearson's correlation coefficient between predictor variables used to model the proportion of a large wildfire's (≥200 ha) area that burned in the wildland-urban interface (WUI) within the Southeastern USA Plains Level II ecoregion.

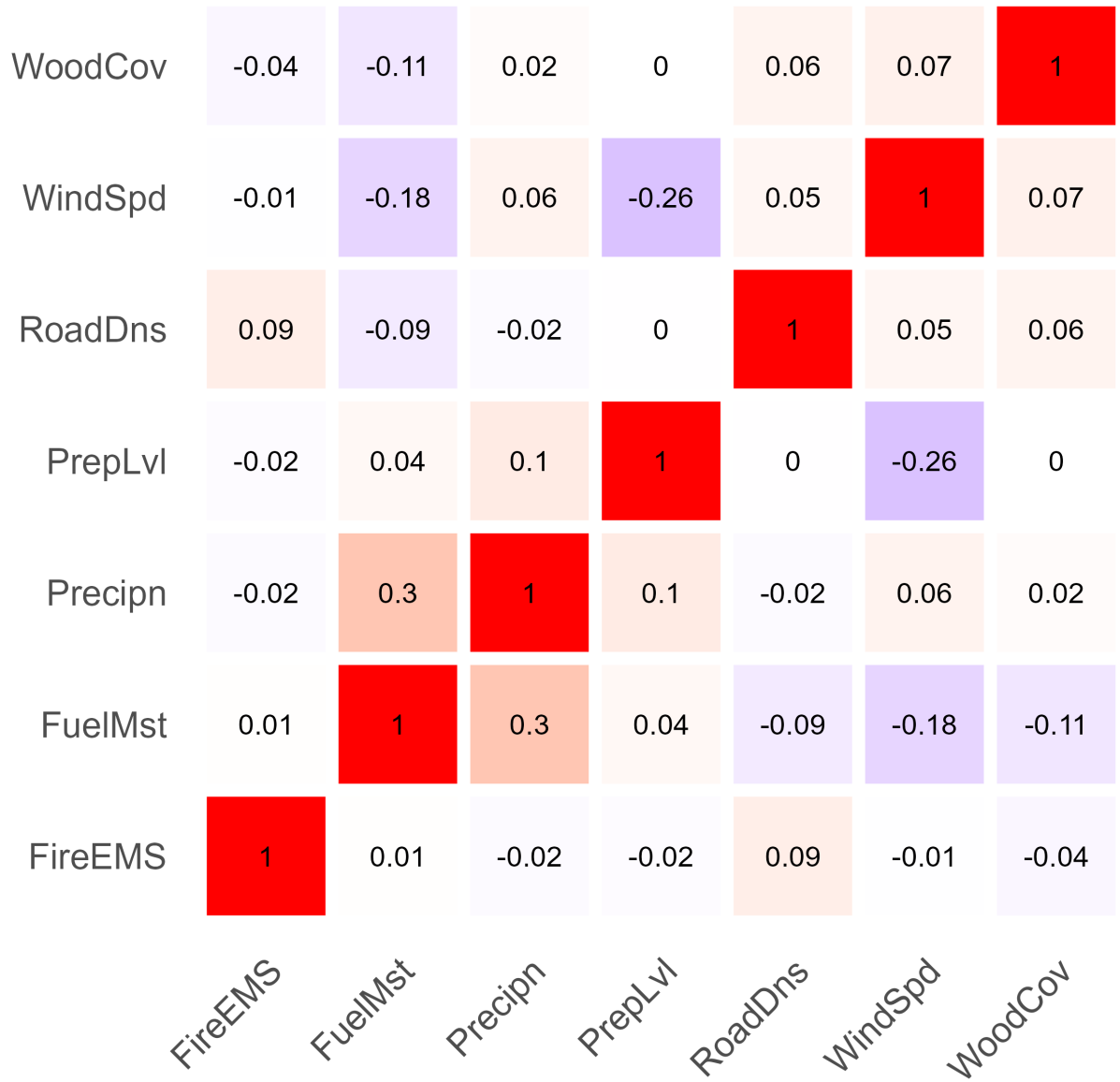


Figure B-13. Correlation matrix showing the Pearson's correlation coefficient between predictor variables used to model the distance large wildfires (≥200 ha) burned from the wildland-urban interface (WUI) within the Eastern Temperate Forests Level I ecoregion.

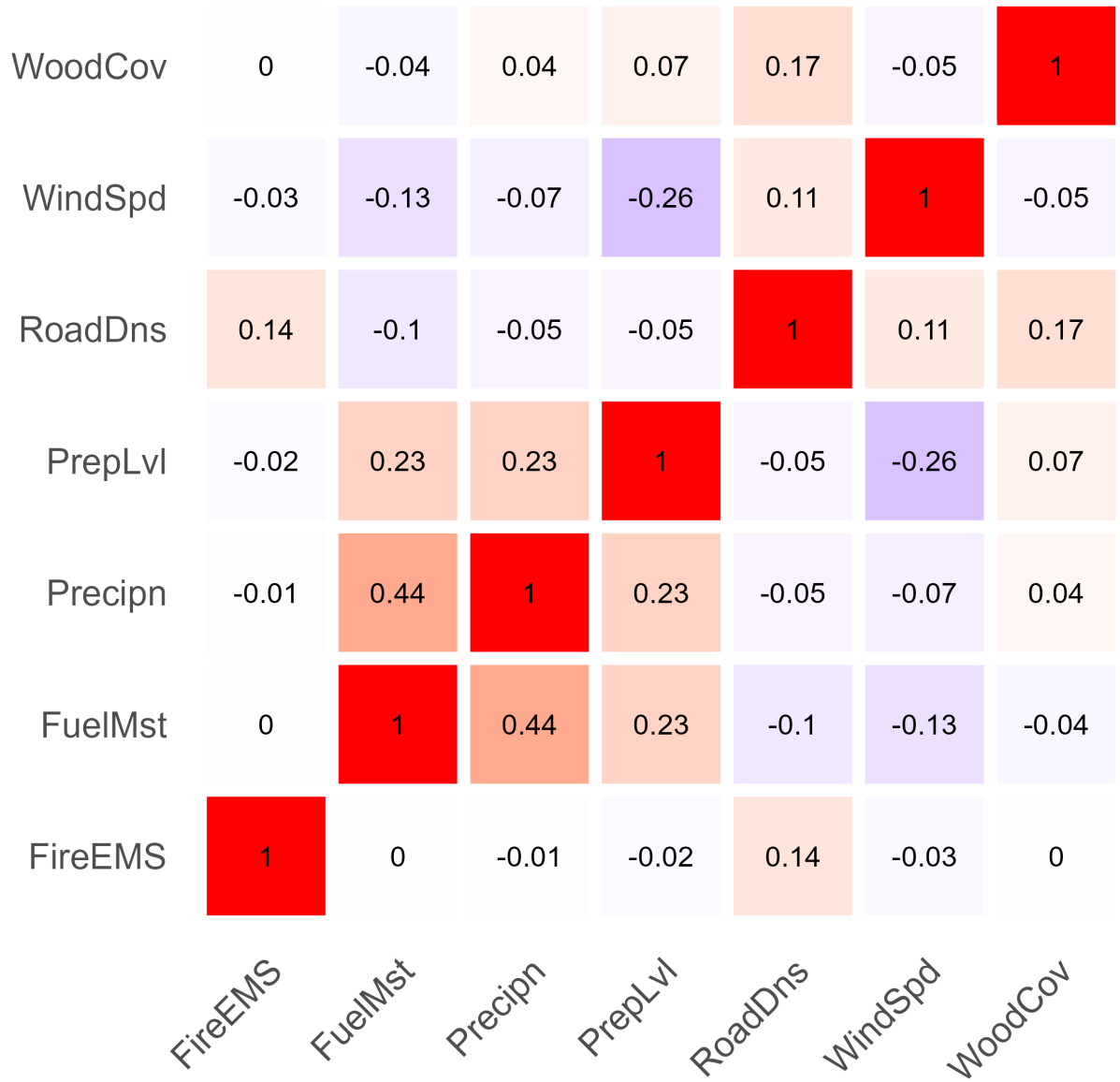


Figure B-14. Correlation matrix showing the Pearson's correlation coefficient between predictor variables used to model the distance large wildfires (≥200 ha) burned from the wildland-urban interface (WUI) within the Mississippi Alluvial and Southeast USA Coastal Plains Level II ecoregion.

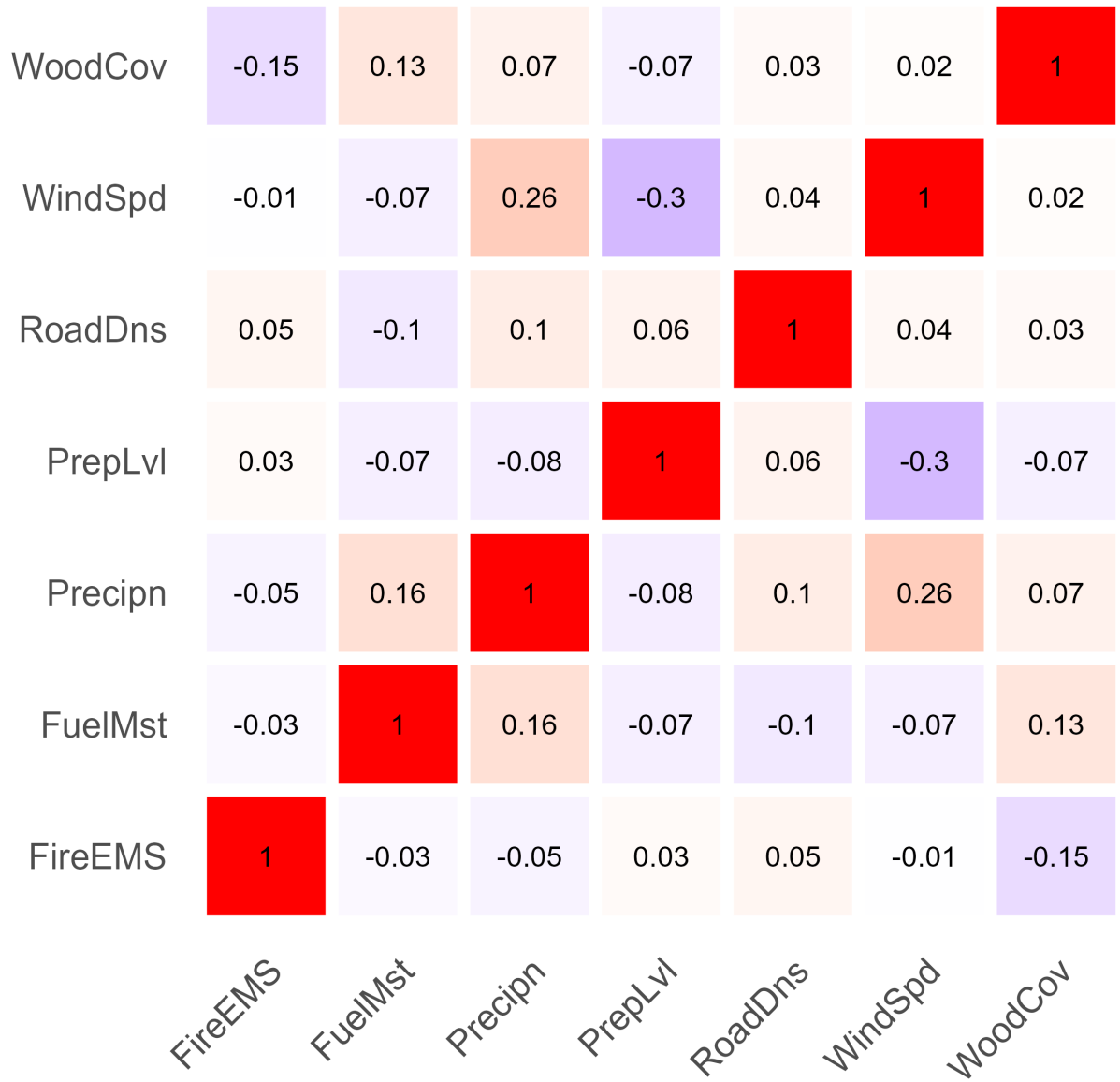


Figure B-15. Correlation matrix showing the Pearson's correlation coefficient between predictor variables used to model the distance large wildfires (≥200 ha) burned from the wildland-urban interface (WUI) within the Ozark/Ouachita-Appalachian Forests Level II ecoregion.

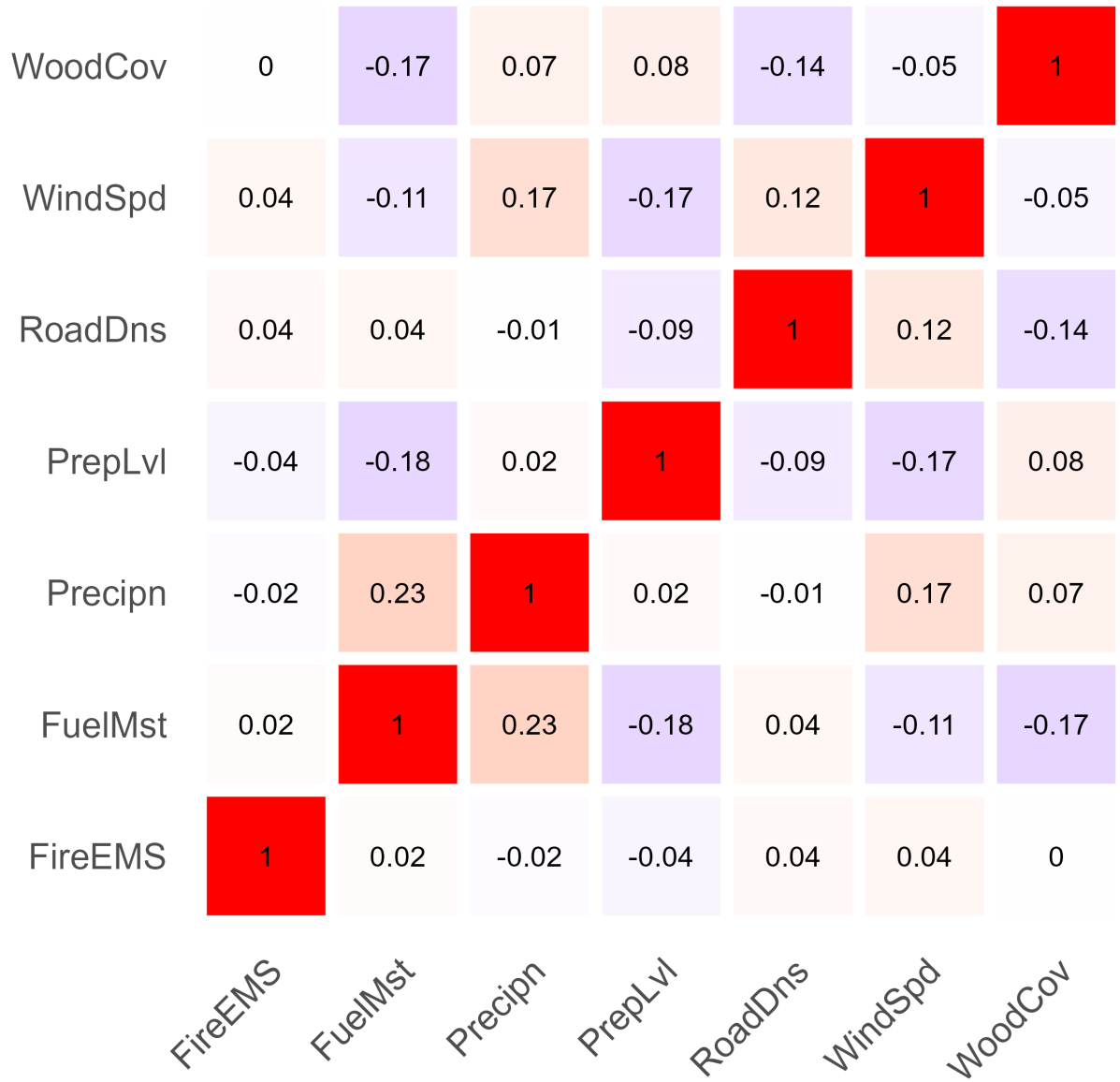


Figure B-16. Correlation matrix showing the Pearson's correlation coefficient between predictor variables used to model the distance large wildfires (≥200 ha) burned from the wildland-urban interface (WUI) within the Southeastern USA Plains Level II ecoregion.

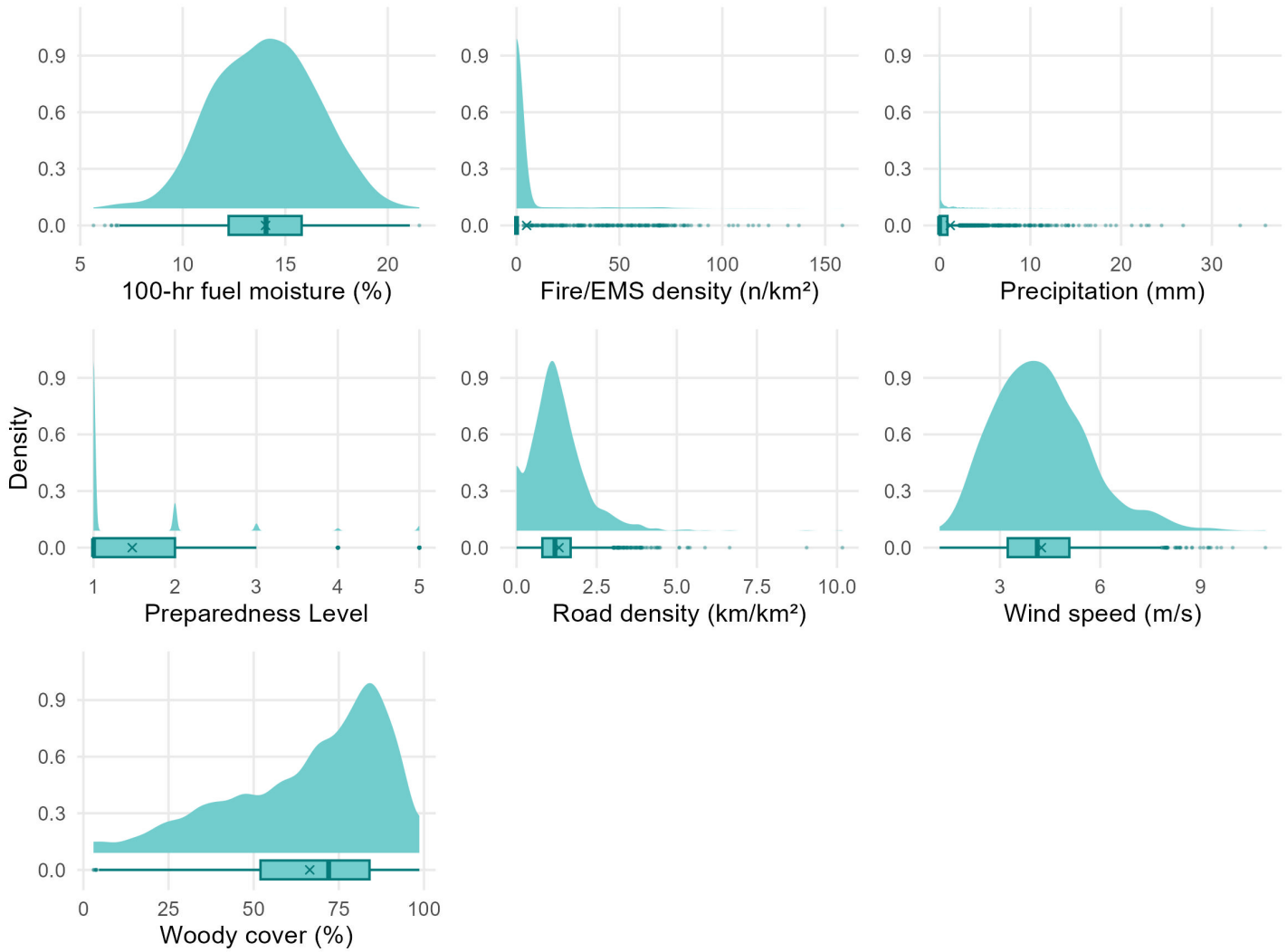


Figure B-17. Raincloud plots for variables used to model whether large wildfires (≥200 ha) burned in the wildland-urban interface (WUI) within the Eastern Temperate Forests Level I ecoregion.

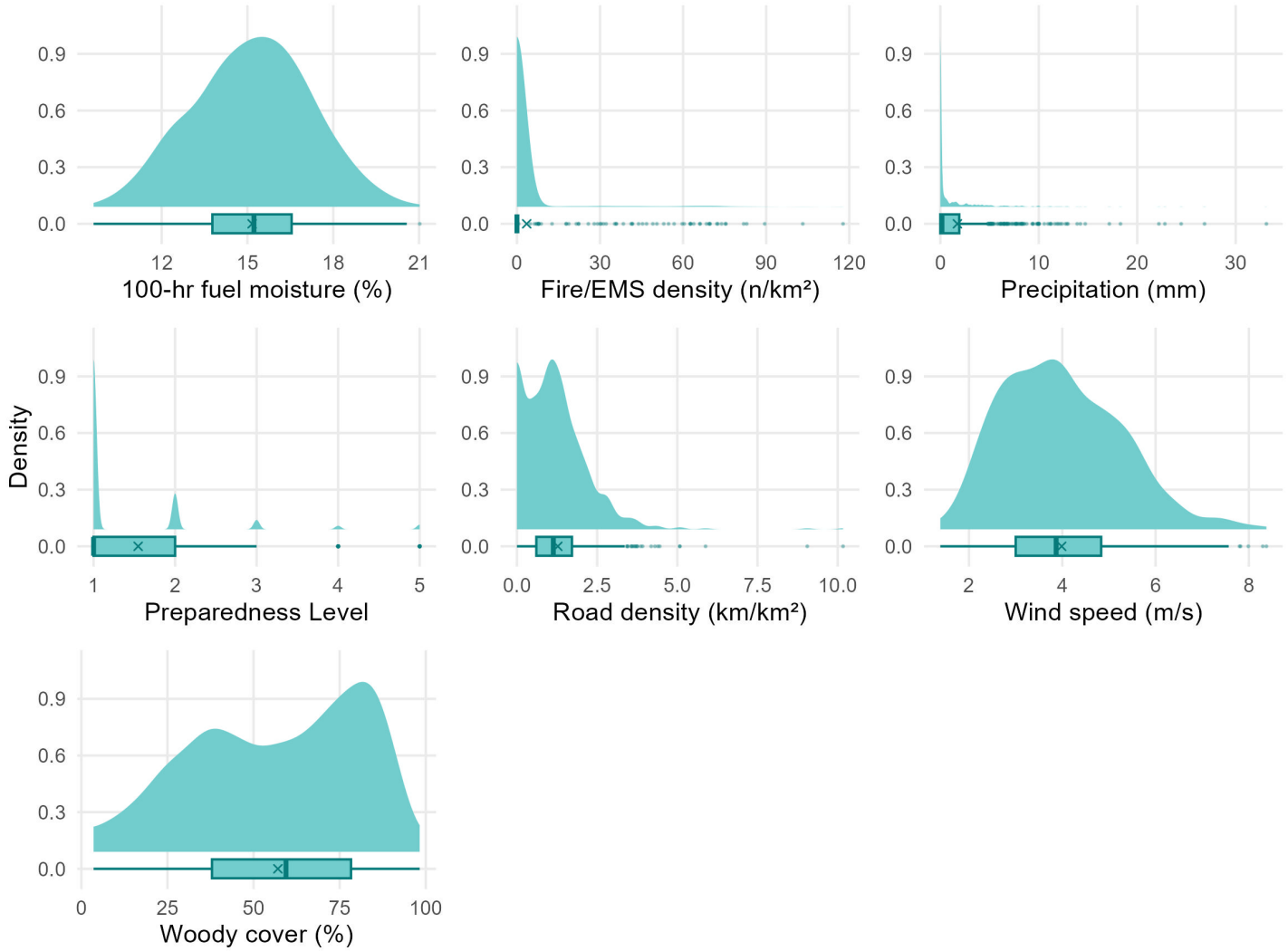


Figure B-18. Raincloud plots for variables used to model whether large wildfires (≥200 ha) burned in the wildland-urban interface (WUI) within the Mississippi Alluvial and Southeast USA Coastal Plains Level II ecoregion.

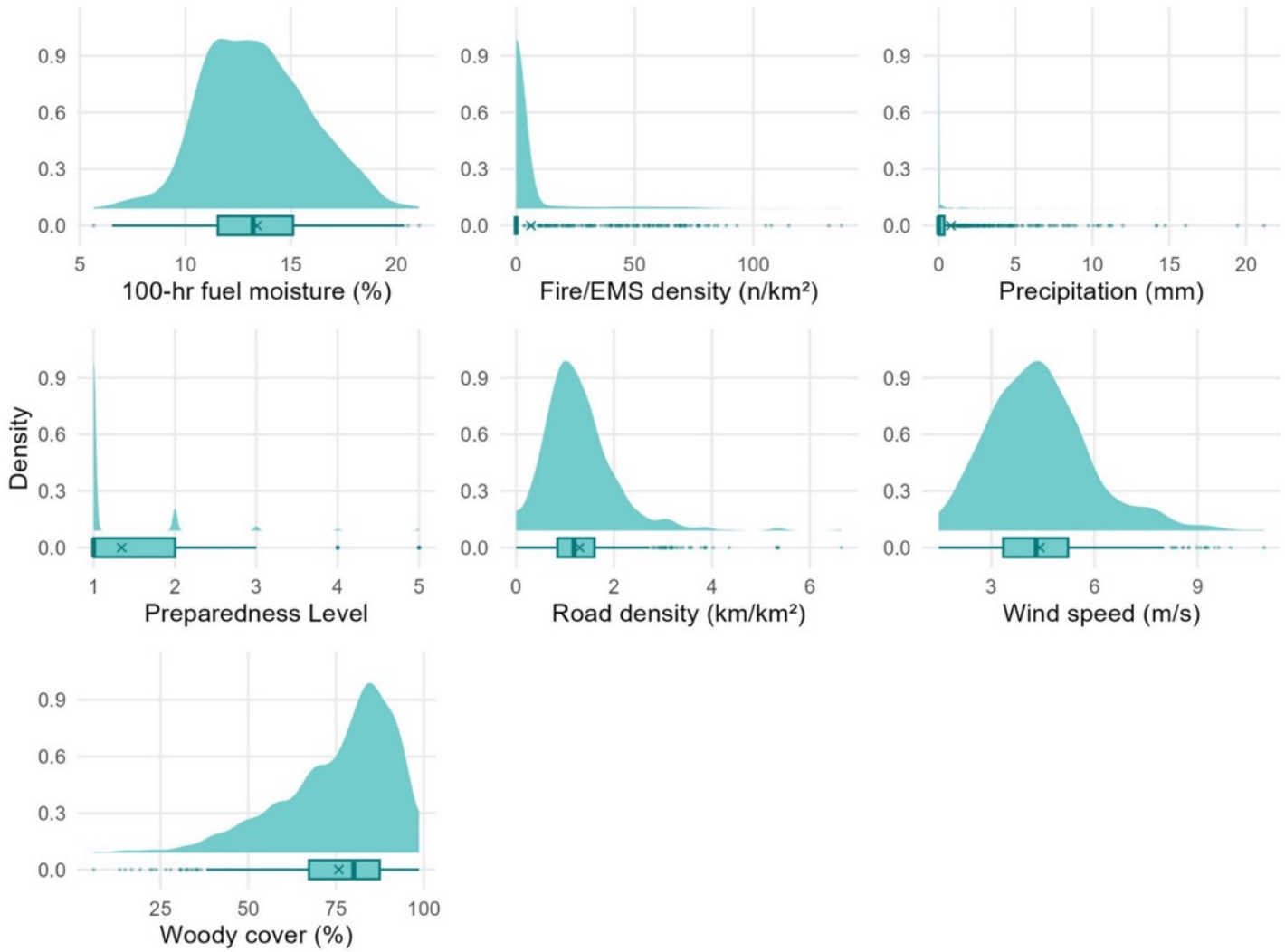


Figure B-19. Raincloud plots for variables used to model whether large wildfires (≥200 ha) burned in the wildland-urban interface (WUI) within the Ozark/Ouachita-Appalachian Forests Level II ecoregion.

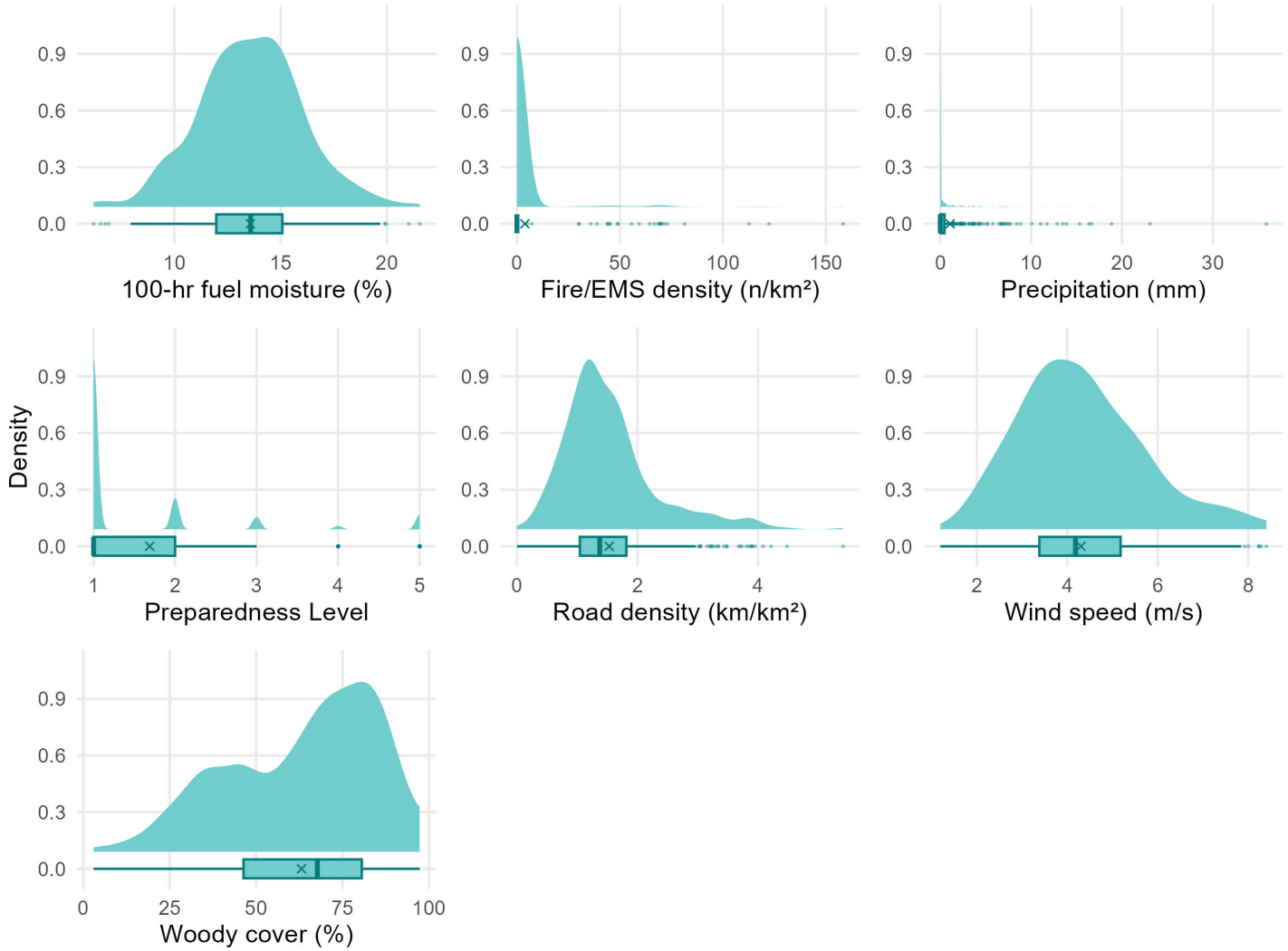


Figure B-20. Raincloud plots for variables used to model whether large wildfires (≥200 ha) burned in the wildland-urban interface (WUI) within the Southeastern USA Plains Level II ecoregion.

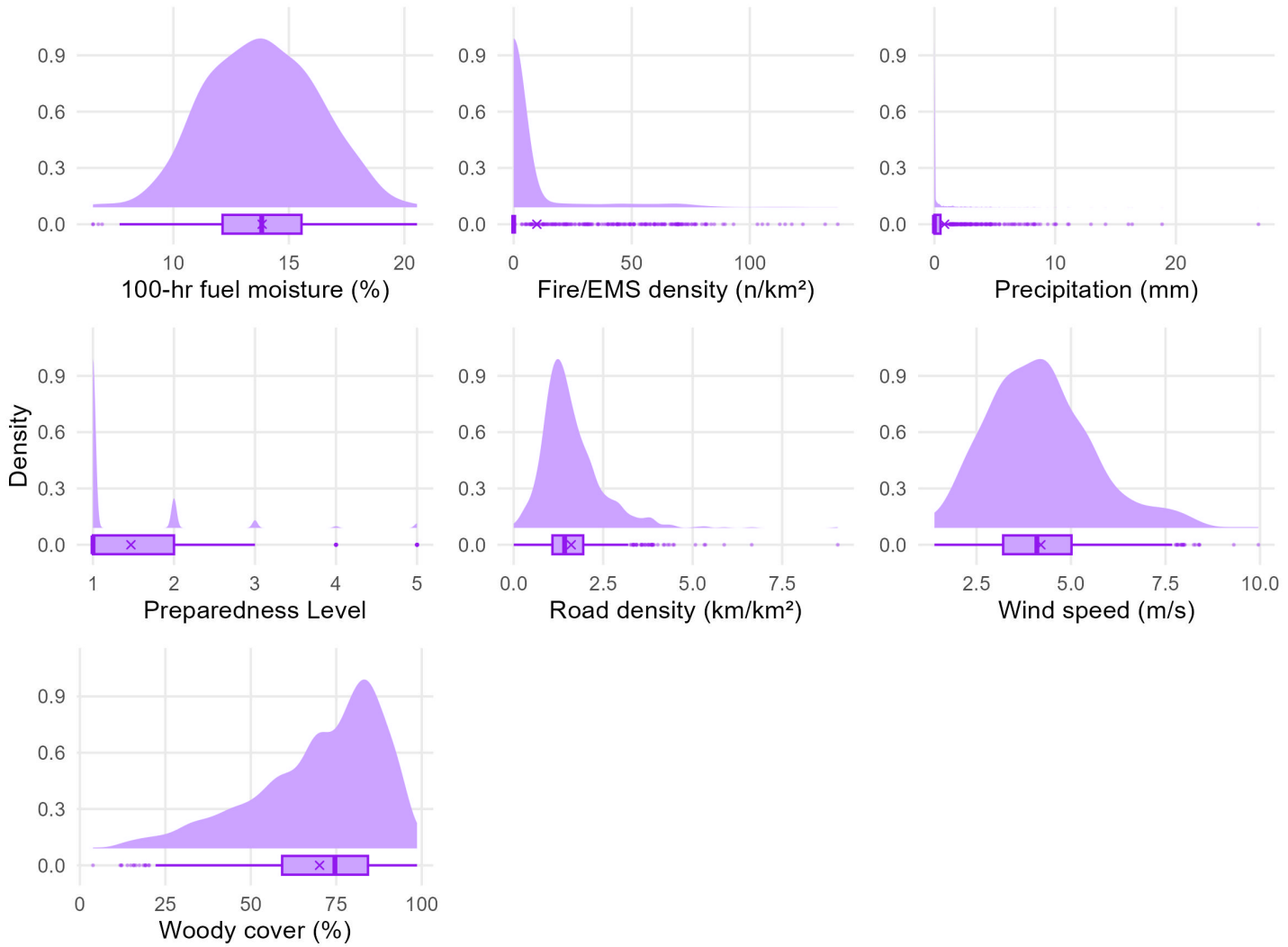


Figure B-21. Raincloud plots for variables used to model the proportion of a large wildfire's (≥200 ha) area that burned in the wildland-urban interface (WUI) within the Eastern Temperate Forests Level I ecoregion.

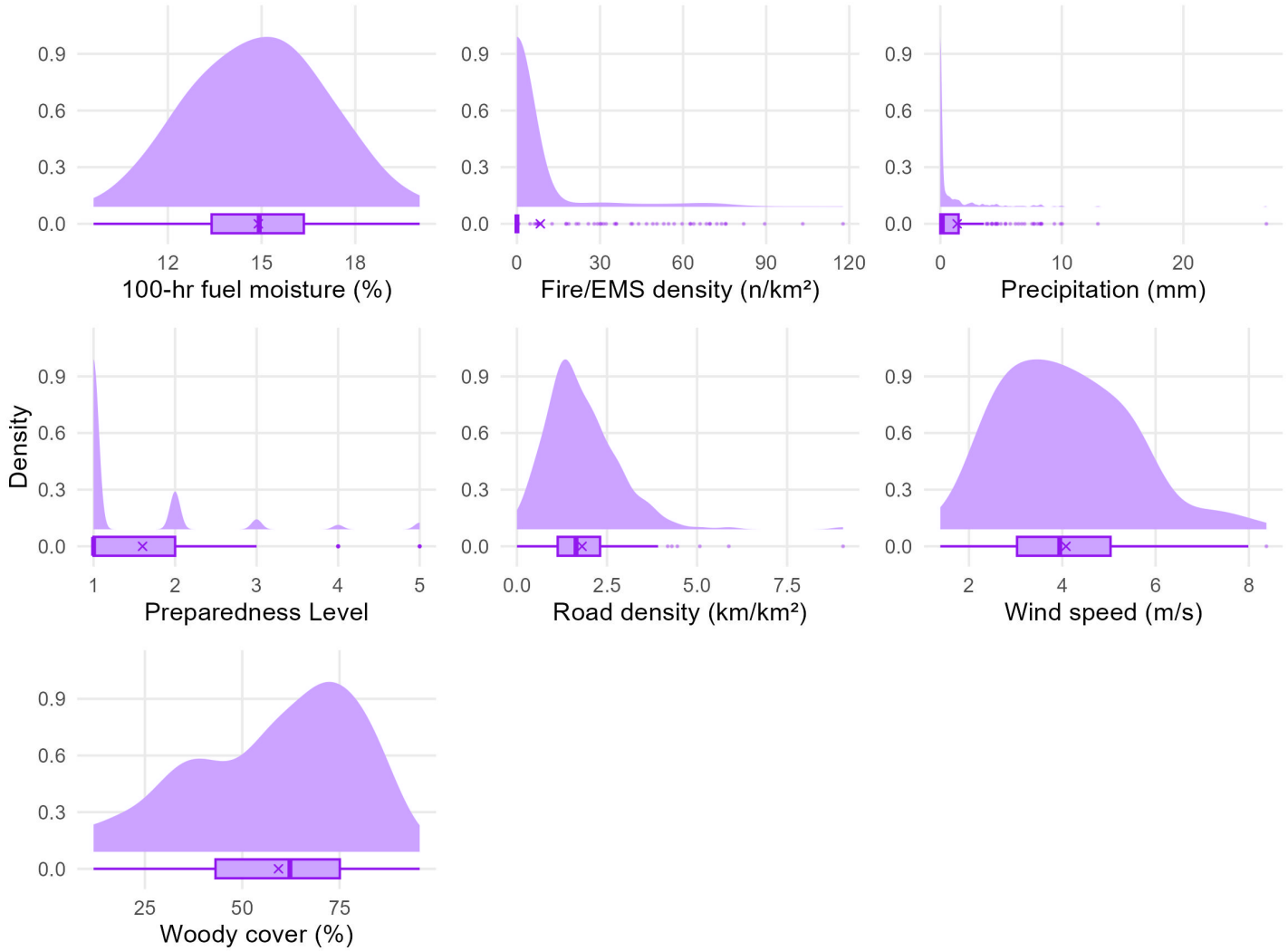


Figure B-22. Raincloud plots for variables used to model the proportion of a large wildfire's (≥200 ha) area that burned in the wildland-urban interface (WUI) within the Mississippi Alluvial and Southeast USA Coastal Plains Level II ecoregion.

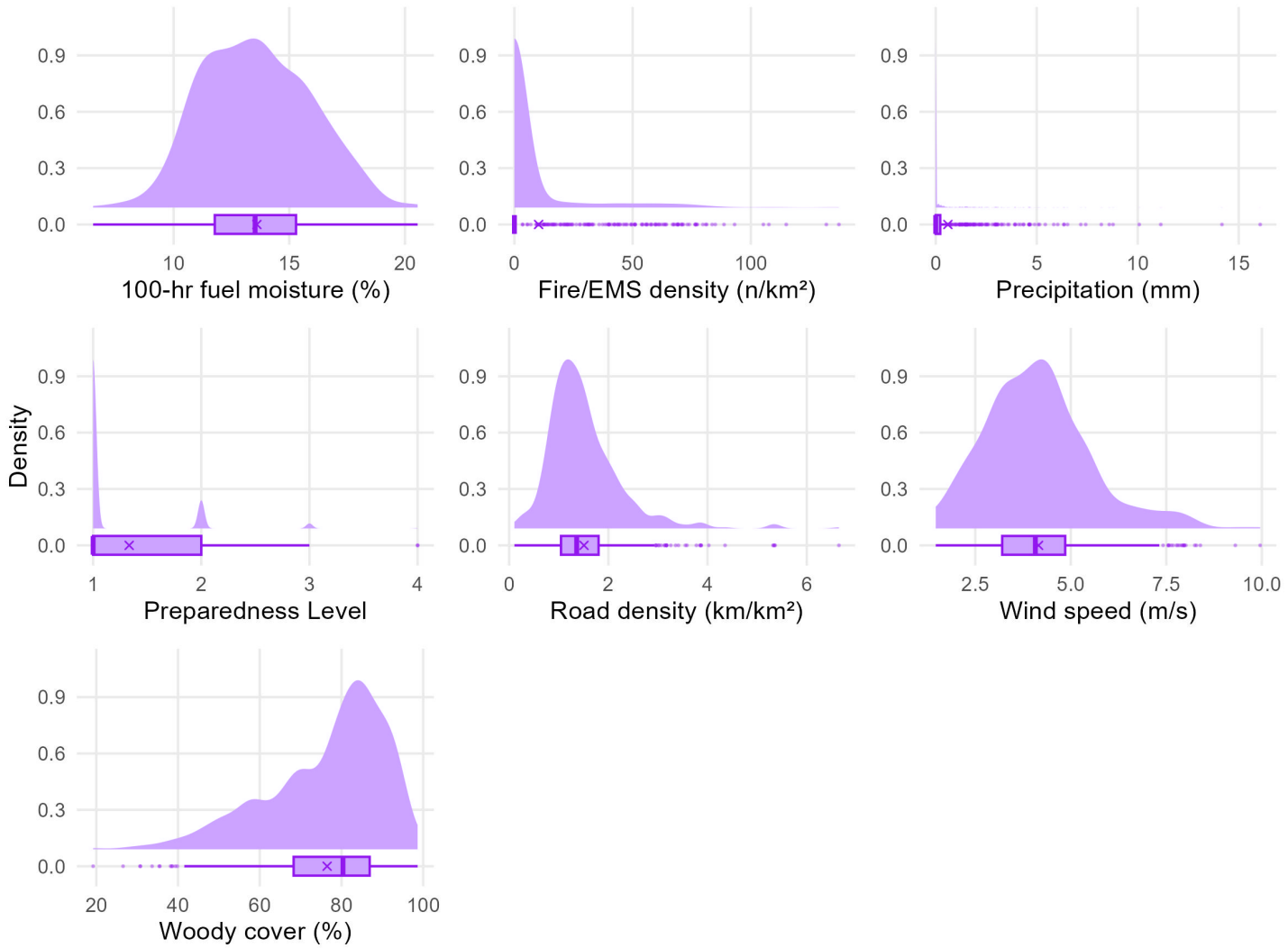


Figure B-23. Raincloud plots for variables used to model the proportion of a large wildfire's (≥200 ha) area that burned in the wildland-urban interface (WUI) within the Ozark/Ouachita-Appalachian Forests Level II ecoregion.

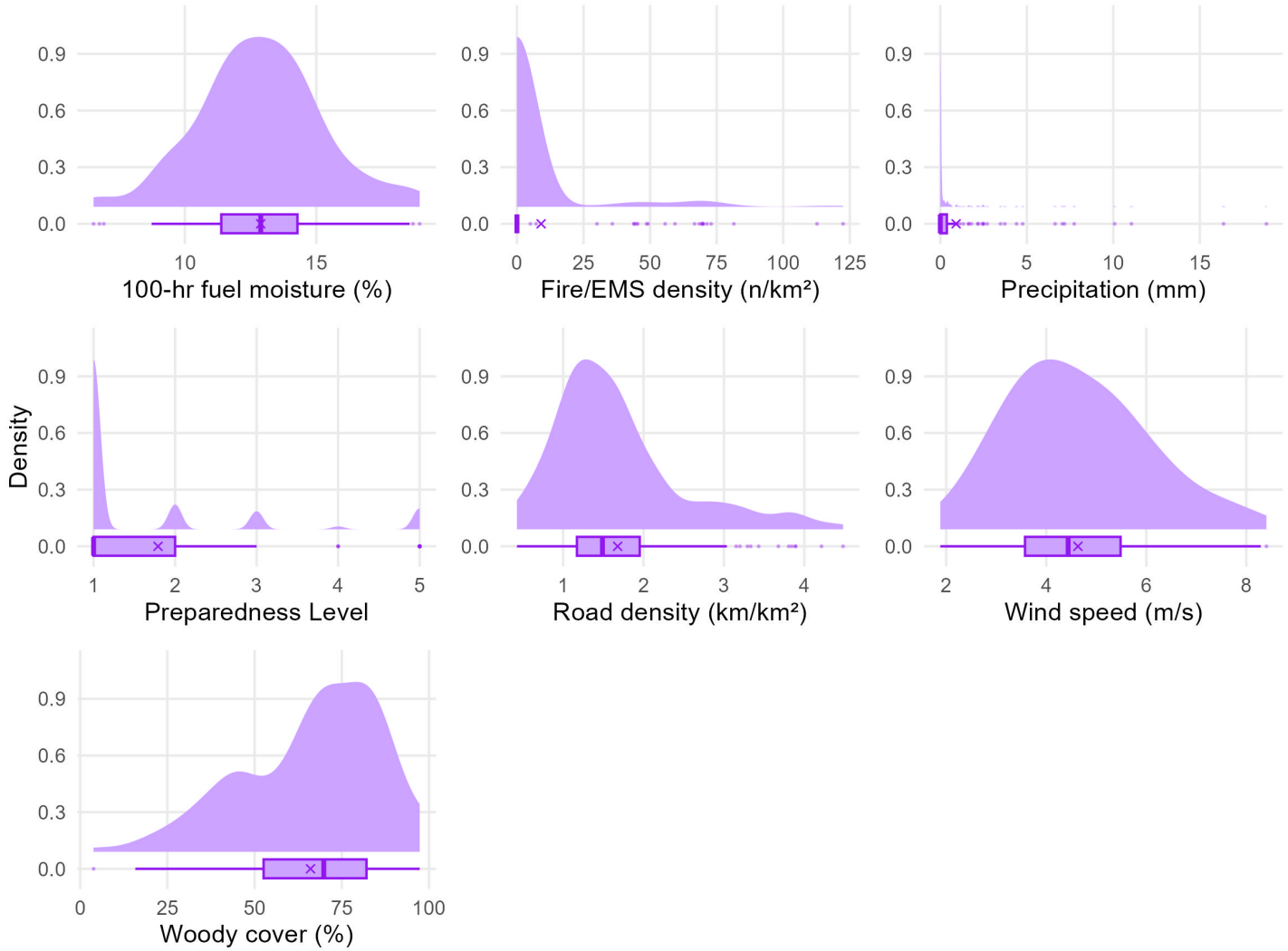


Figure B-24. Raincloud plots for variables used to model the proportion of a large wildfire's (≥200 ha) area that burned in the wildland-urban interface (WUI) within the Southeastern USA Plains Level II ecoregion.

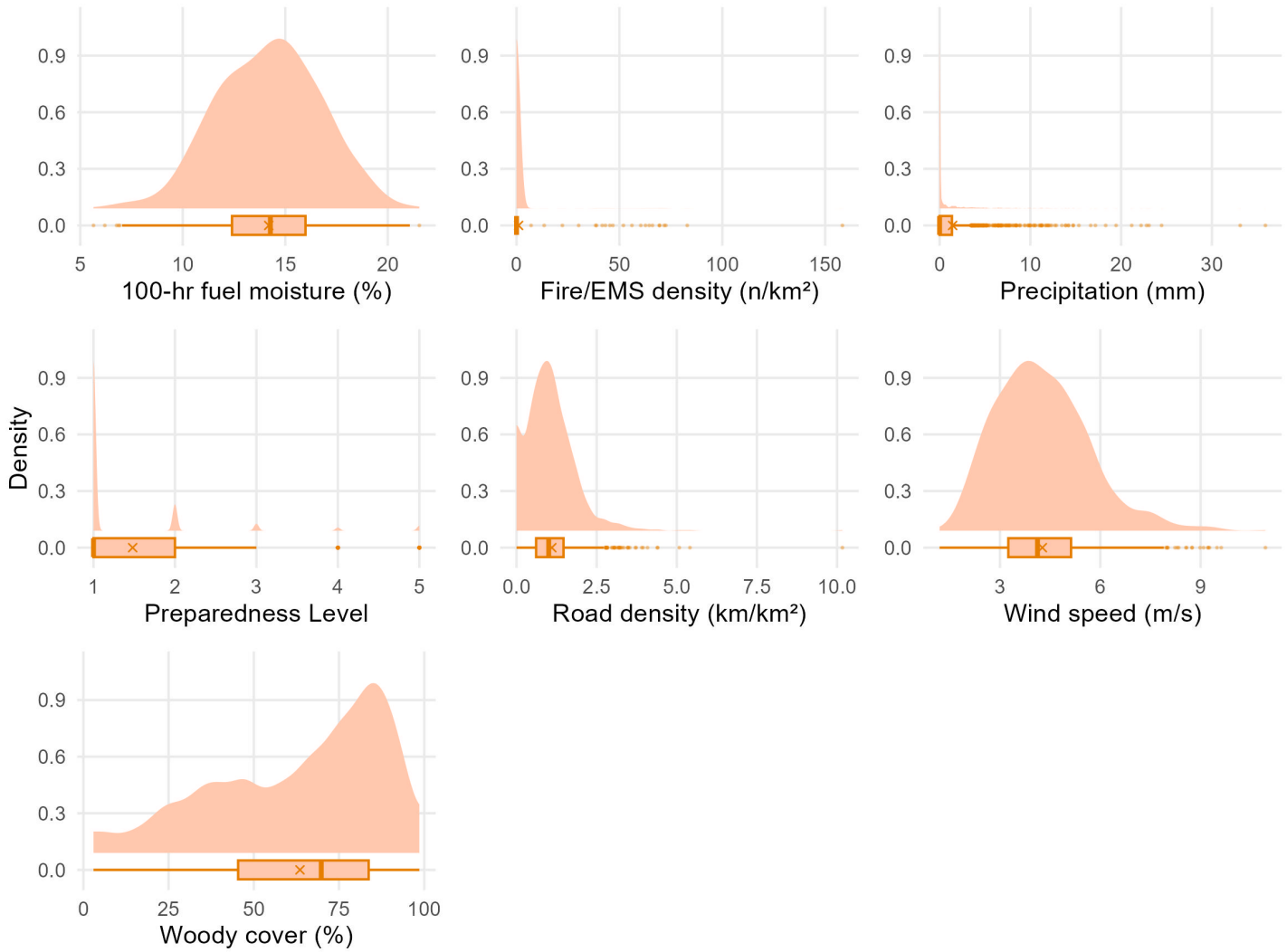


Figure B-25. Raincloud plots for variables used to model the distance large wildfires (≥200 ha) burned from the wildland-urban interface (WUI) within the Eastern Temperate Forests Level I ecoregion.

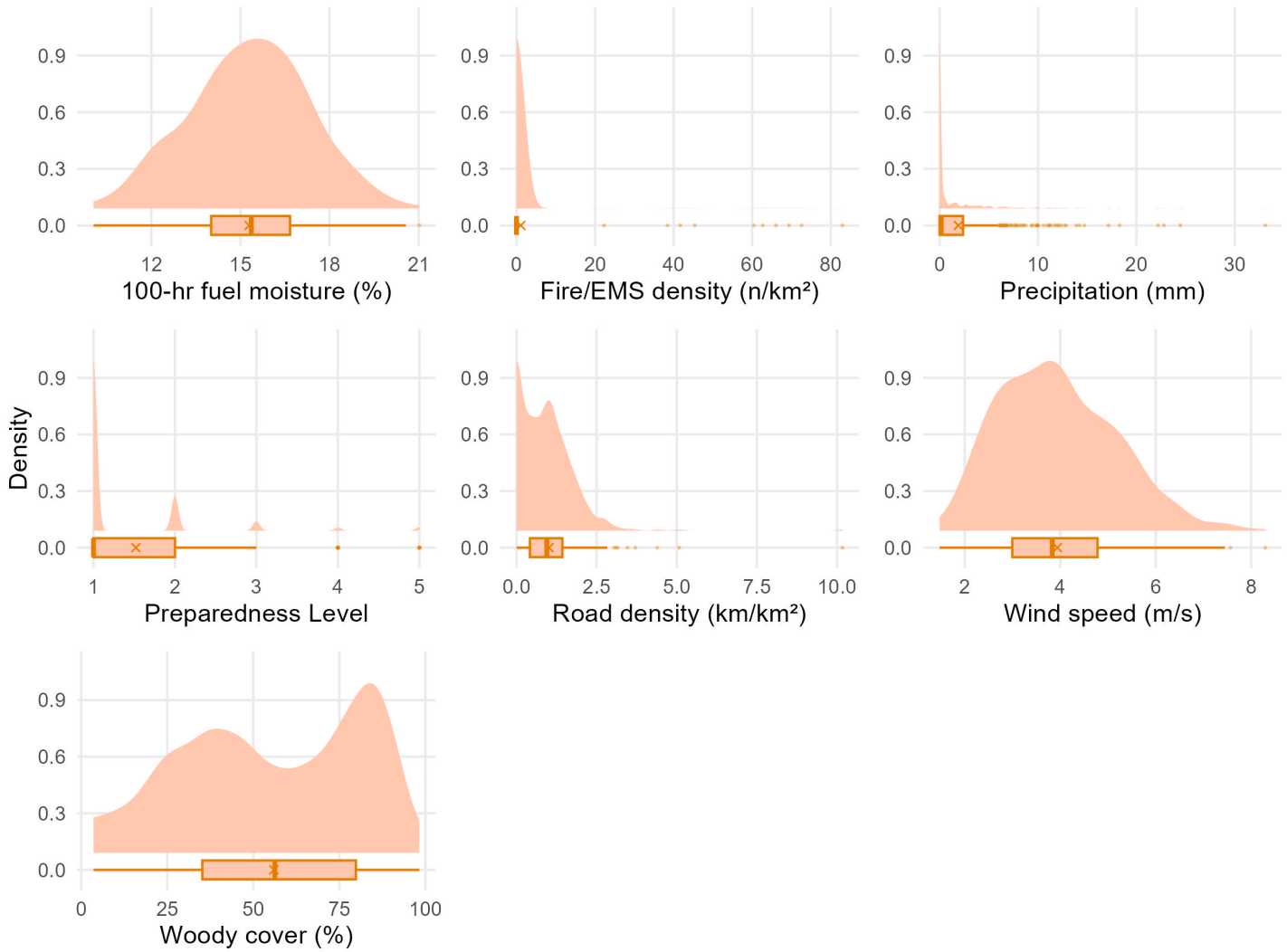


Figure B-26. Raincloud plots for variables used to model the distance large wildfires (≥200 ha) burned from the wildland-urban interface (WUI) within the Mississippi Alluvial and Southeast USA Coastal Plains Level II ecoregion.

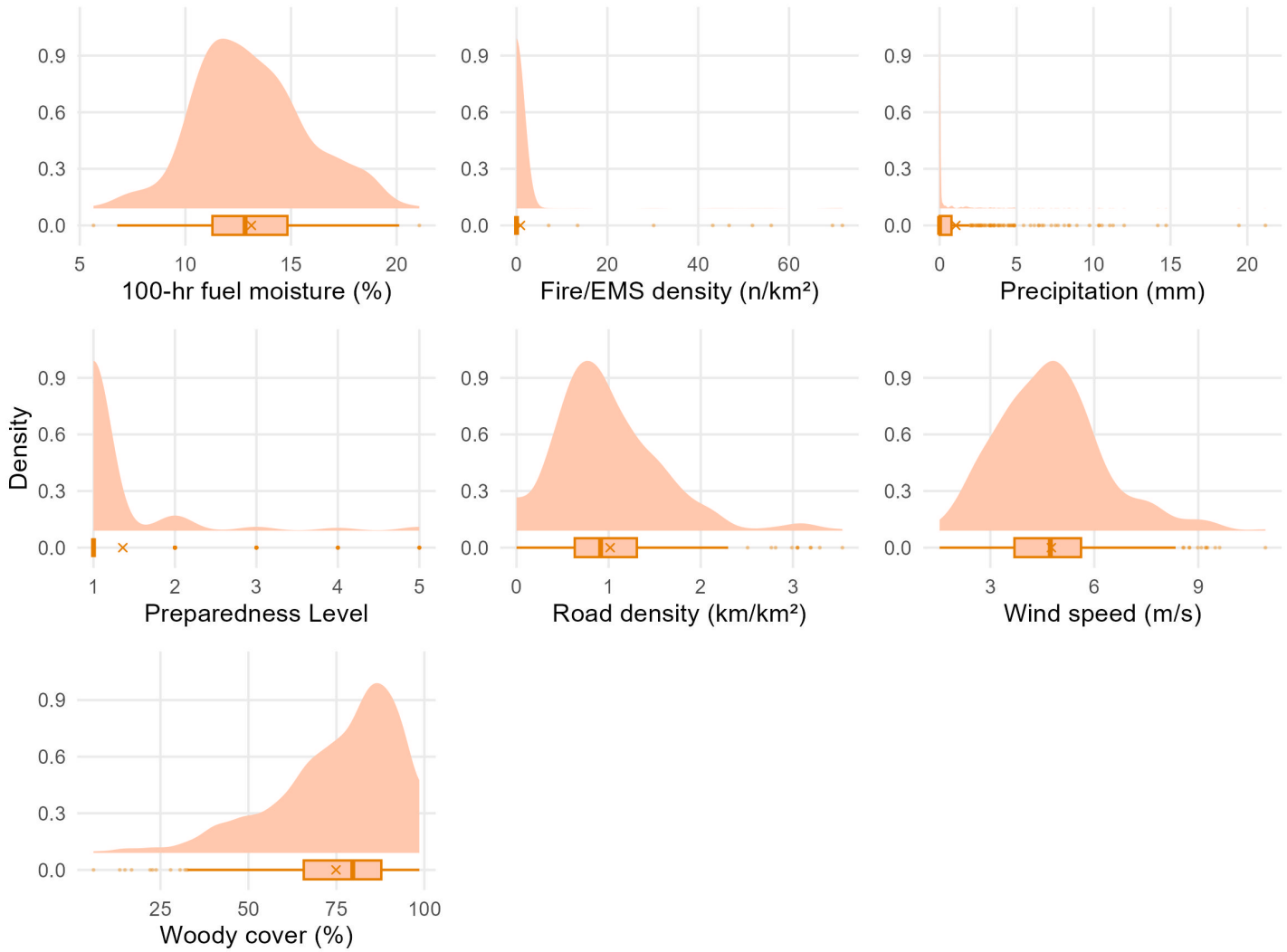


Figure B-27. Raincloud plots for variables used to model the distance large wildfires (≥200 ha) burned from the wildland-urban interface (WUI) within the Ozark/Ouachita-Appalachian Forests Level II ecoregion.

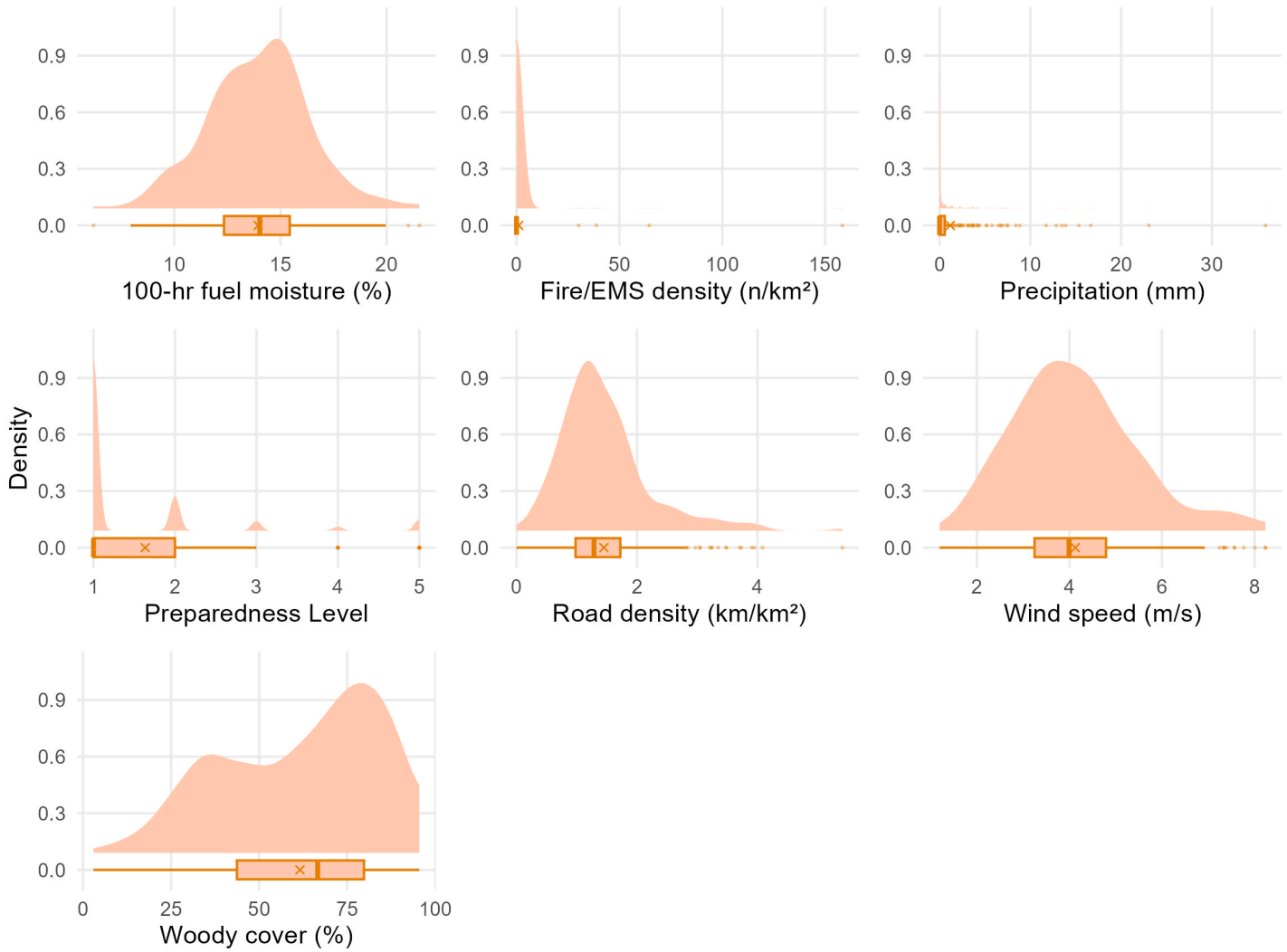


Figure B-28. Raincloud plots for variables used to model the distance large wildfires (≥200 ha) burned from the wildland-urban interface (WUI) within the Southeastern USA Plains Level II ecoregion.

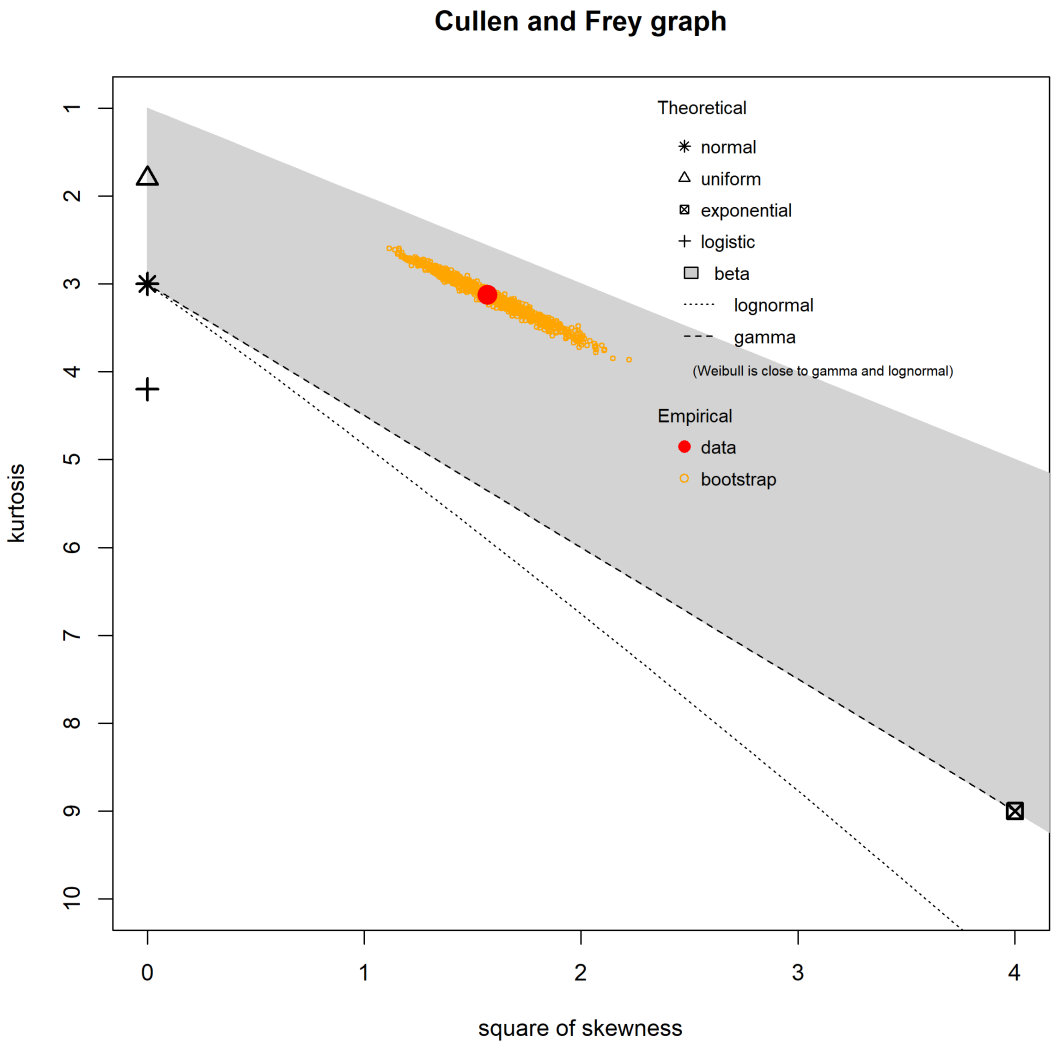


Figure B-29. A Cullen and Frey graph examining the distribution of the proportion of large wildfires' (≥200 ha) areas that burned in the wildland-urban interface (WUI) within the Eastern Temperate Forests Level I ecoregion.

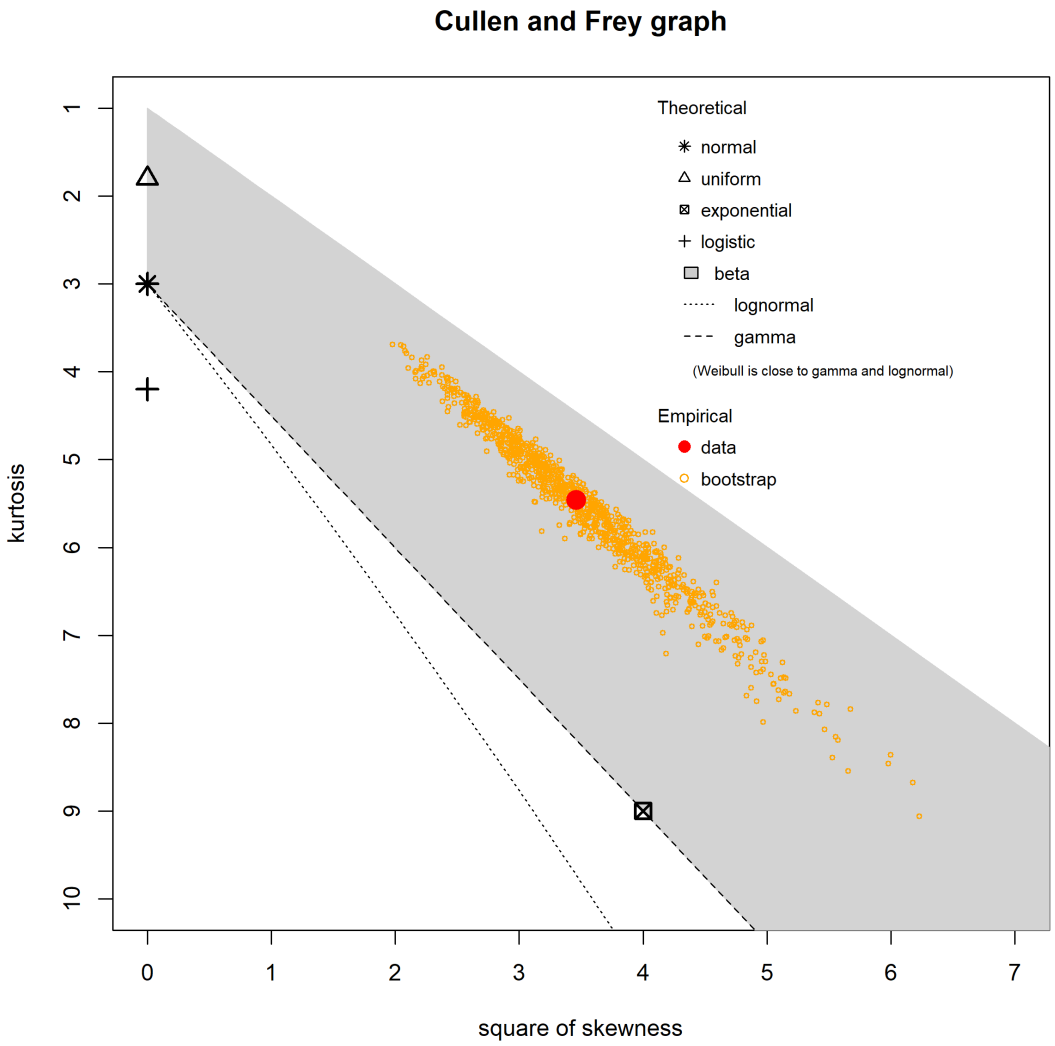


Figure B-30. A Cullen and Frey graph examining the distribution of the proportion of large wildfires' (≥200 ha) areas that burned in the wildland-urban interface (WUI) within the Mississippi Alluvial and Southeast USA Coastal Plains Level II ecoregion.

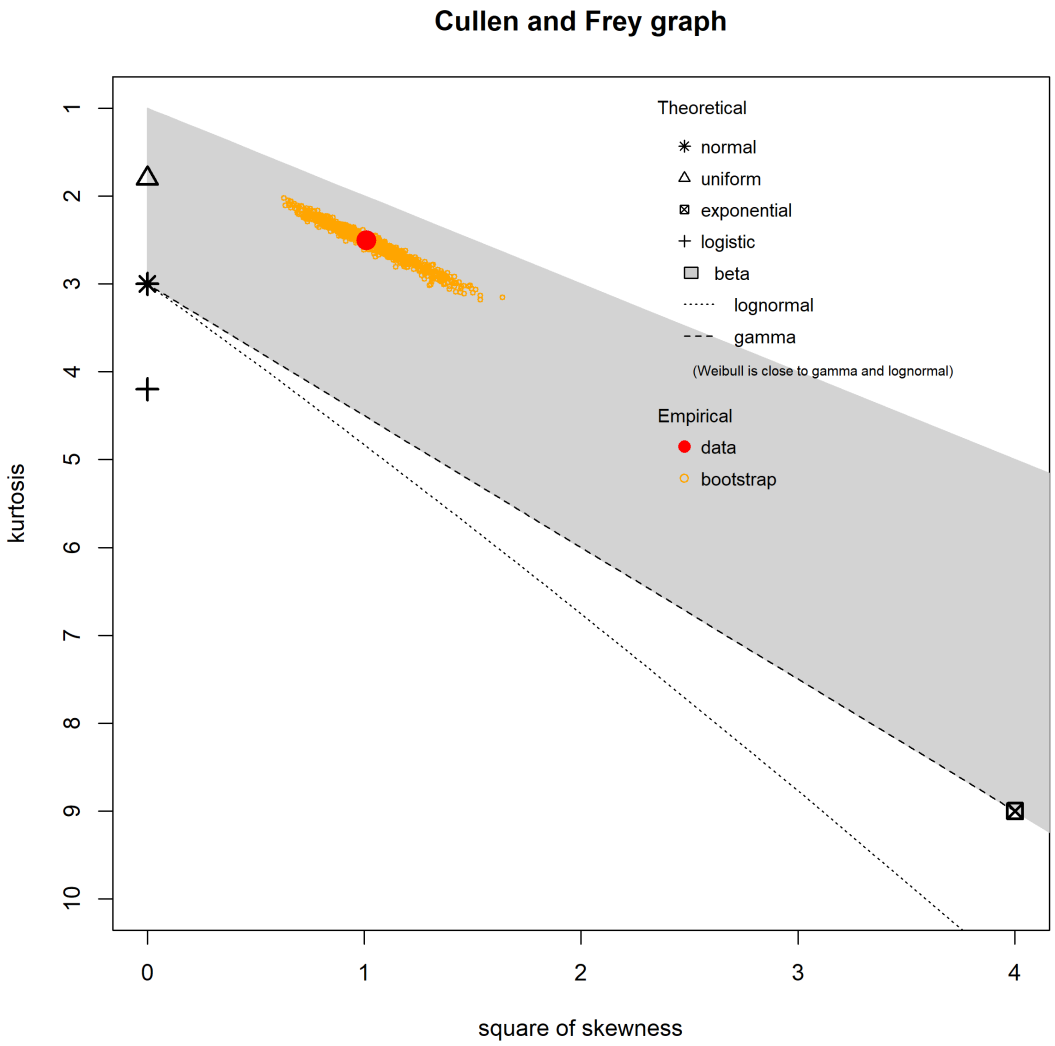


Figure B-31. A Cullen and Frey graph examining the distribution of the proportion of large wildfires' (≥200 ha) areas that burned in the wildland-urban interface (WUI) within the Ozark/Ouachita-Appalachian Forests Level II ecoregion.

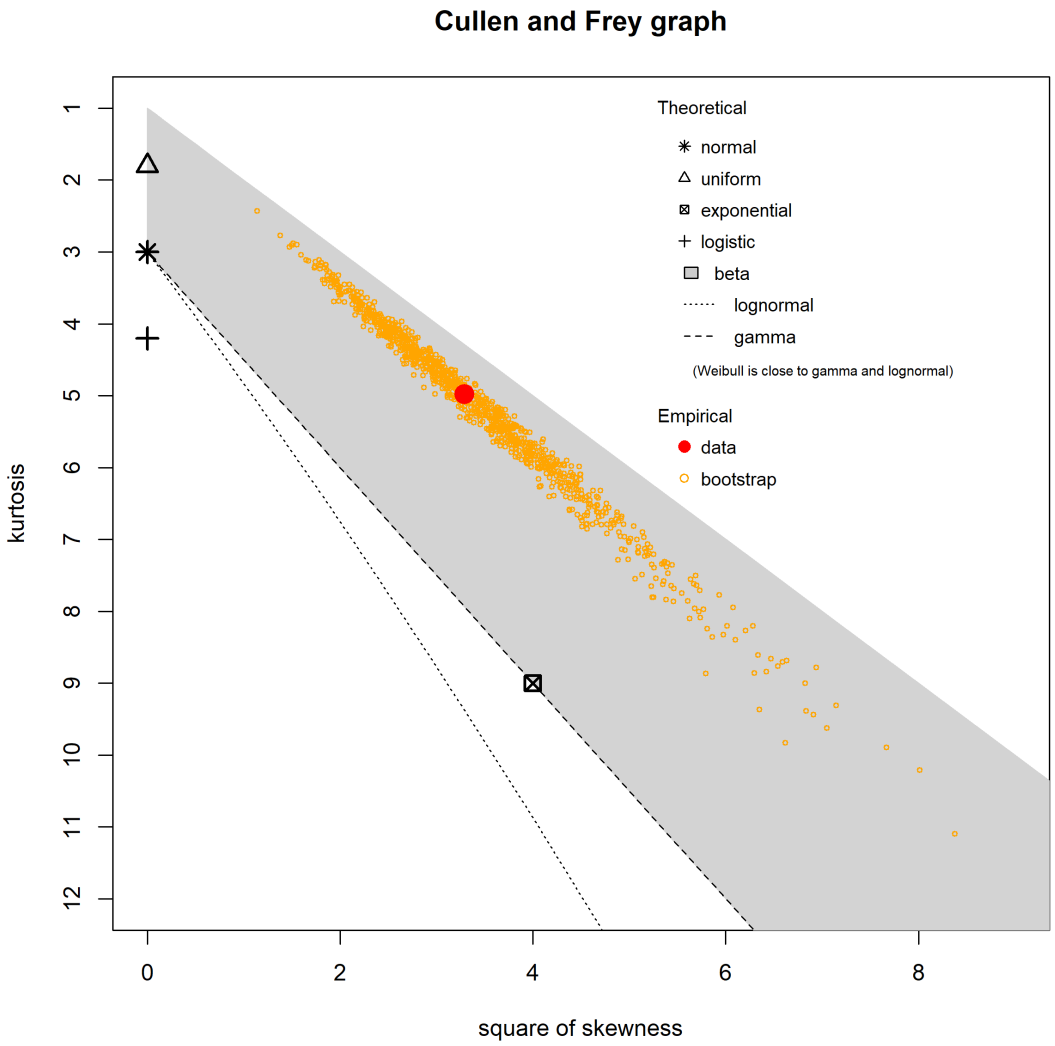


Figure B-32. A Cullen and Frey graph examining the distribution of the proportion of large wildfires' (≥200 ha) areas that burned in the wildland-urban interface (WUI) within the Southeastern USA Plains Level II ecoregion.

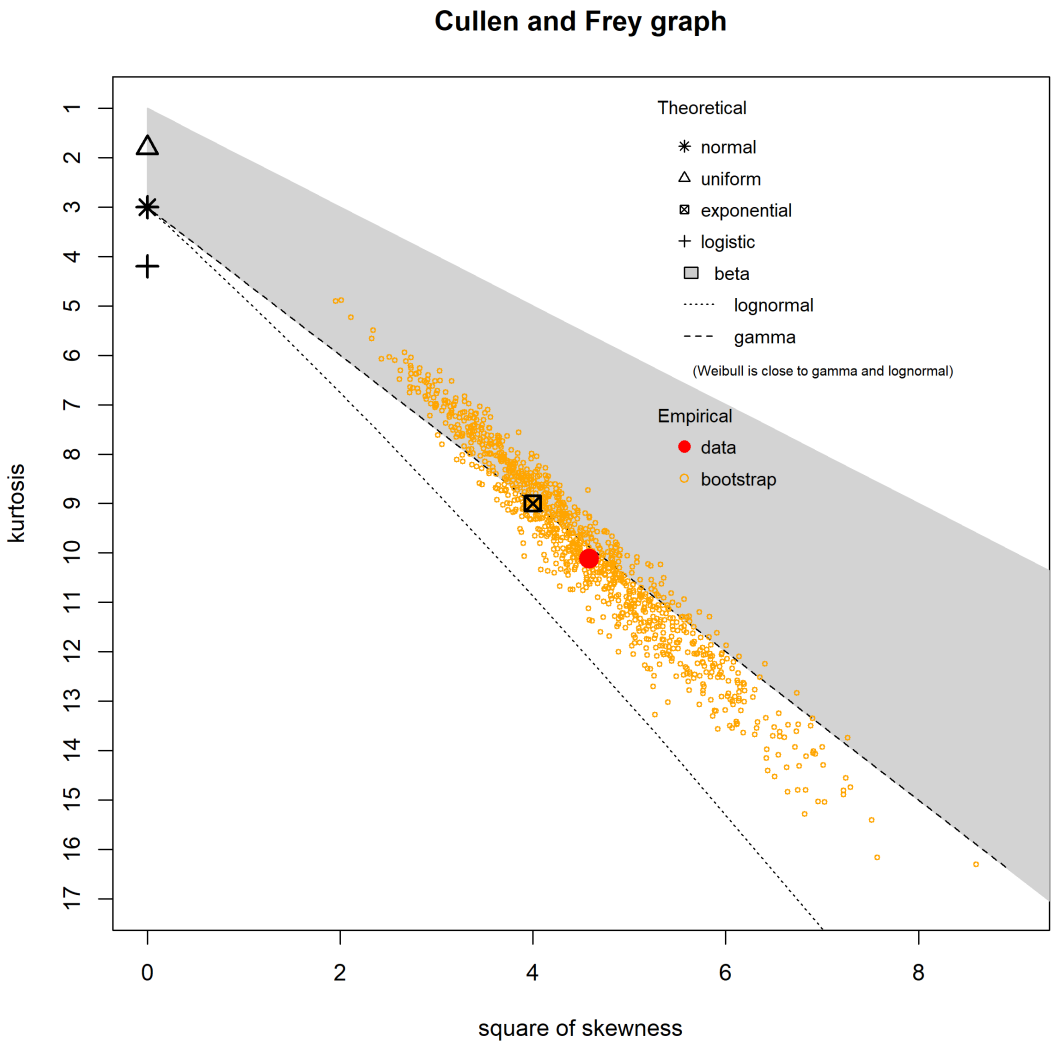


Figure B-33. A Cullen and Frey graph examining the distribution of the distance large wildfires (≥200 ha) burned from the wildland-urban interface (WUI) within the Eastern Temperate Forests Level I ecoregion.

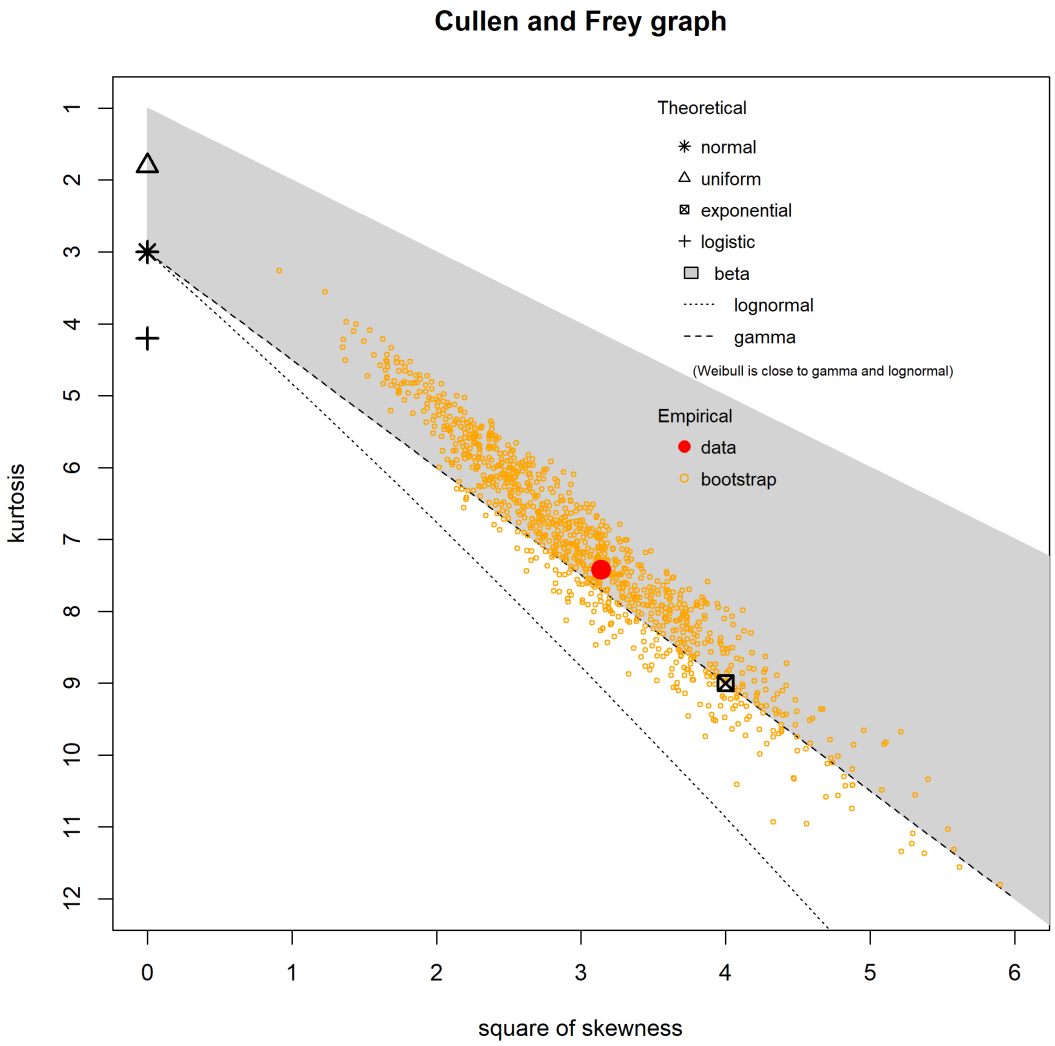


Figure B-34. A Cullen and Frey graph examining the distribution of the distance large wildfires (≥200 ha) burned from the wildland-urban interface (WUI) within the Mississippi Alluvial and Southeast USA Coastal Plains Level II ecoregion.

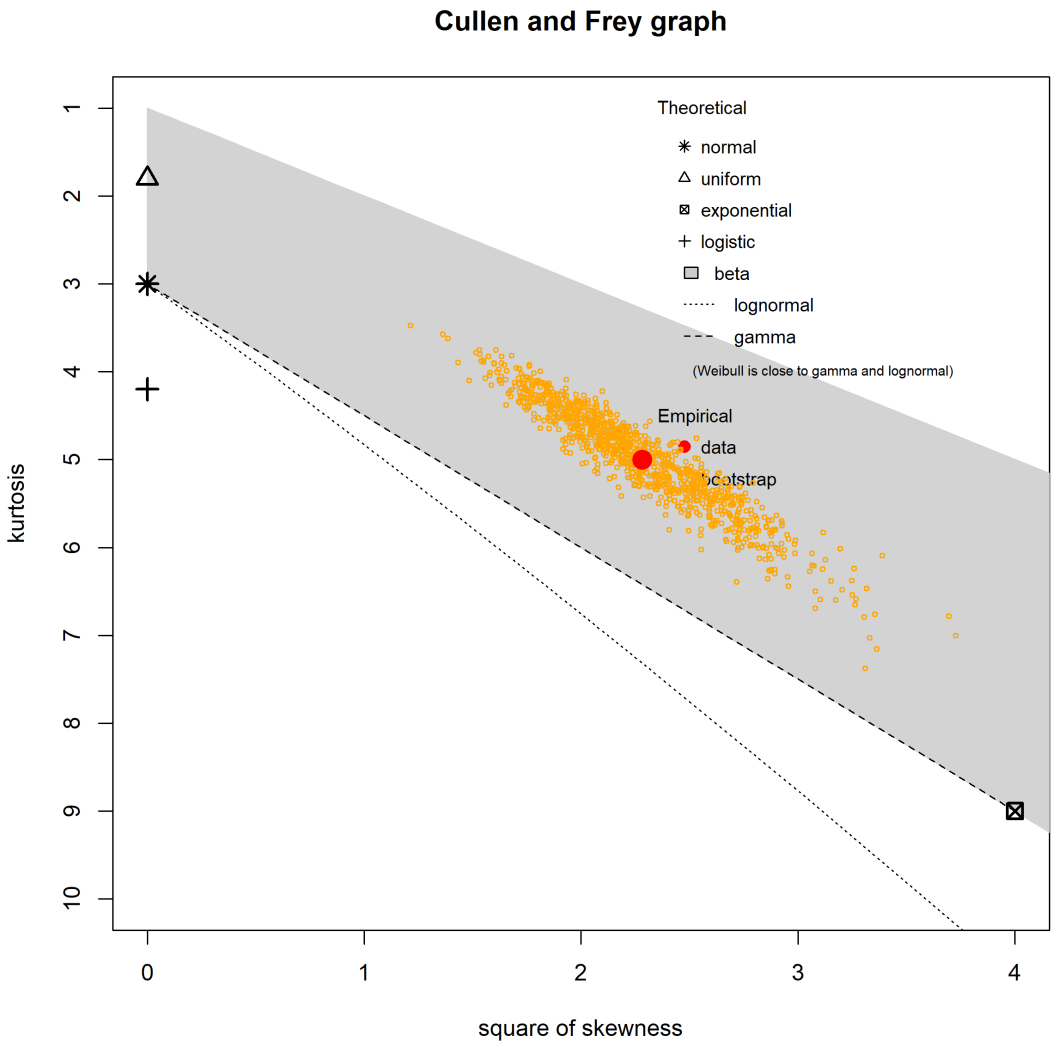


Figure B-35. A Cullen and Frey graph examining the distribution of the distance large wildfires (≥200 ha) burned from the wildland-urban interface (WUI) within the Ozark/Ouachita-Appalachian Forests Level II ecoregion.

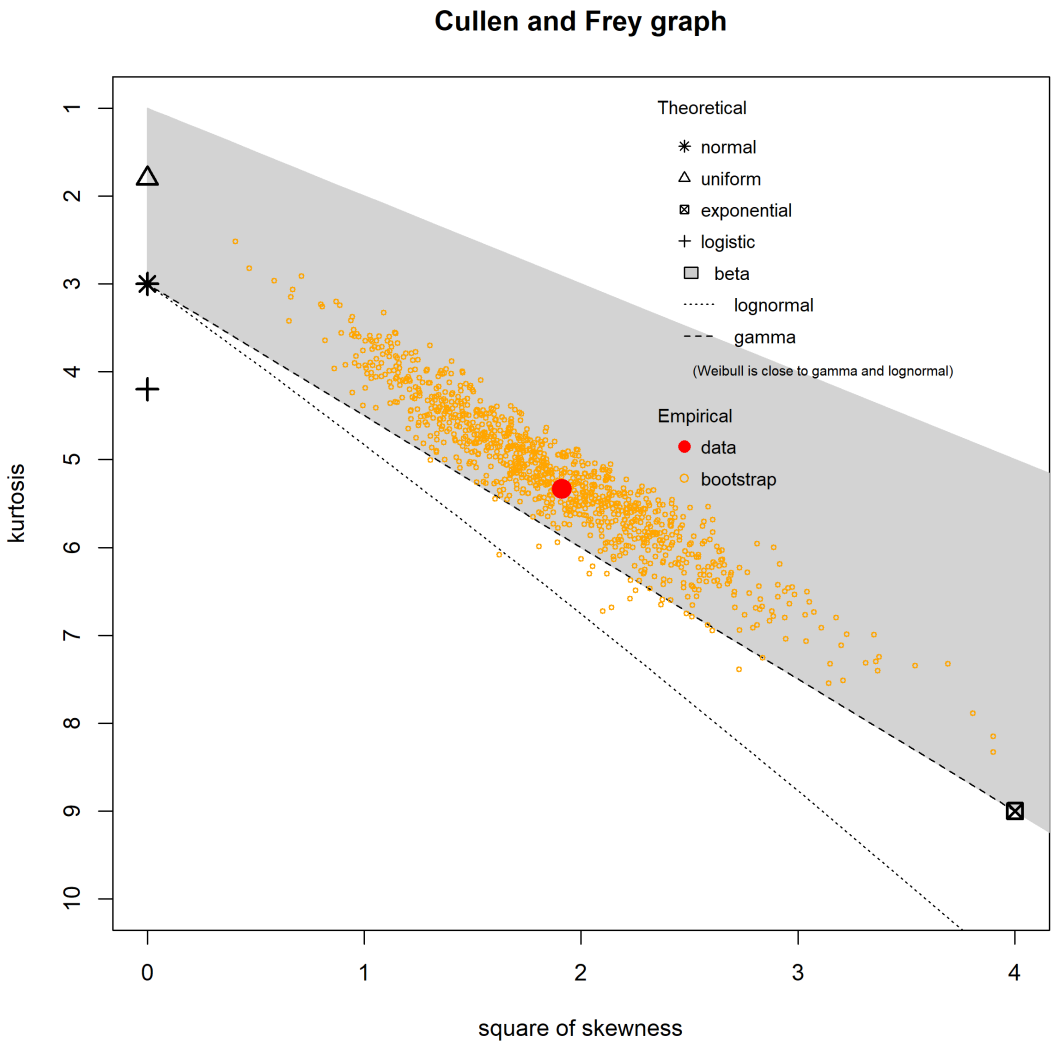


Figure B-36. A Cullen and Frey graph examining the distribution of the distance large wildfires (≥200 ha) burned from the wildland-urban interface (WUI) within the Southeastern USA Plains Level II ecoregion.

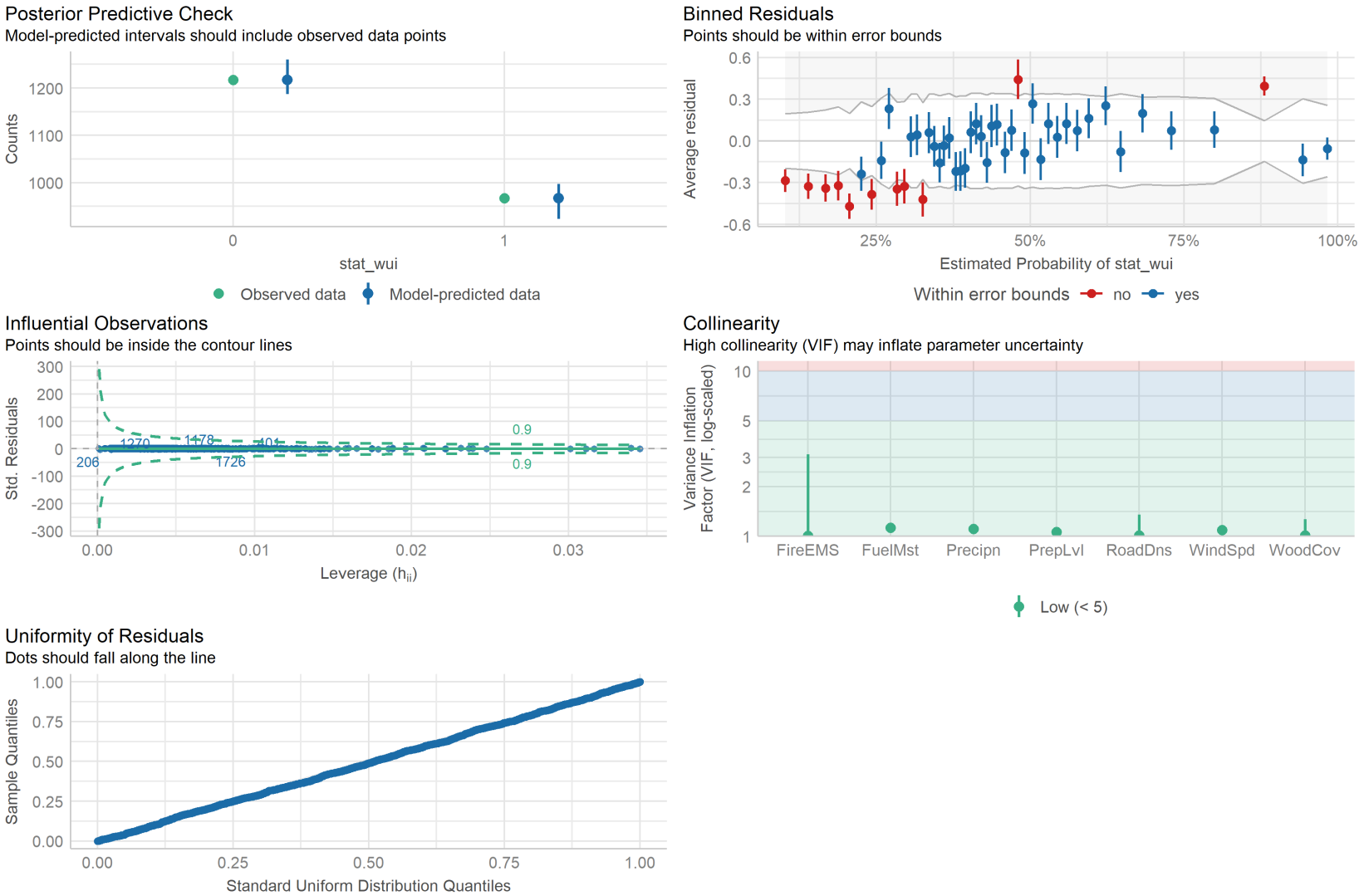


Figure B-37. Global model diagnostics for whether large wildfires (≥200 ha) burned in the wildland-urban interface (WUI) within the Eastern Temperate Forests Level I ecoregion.

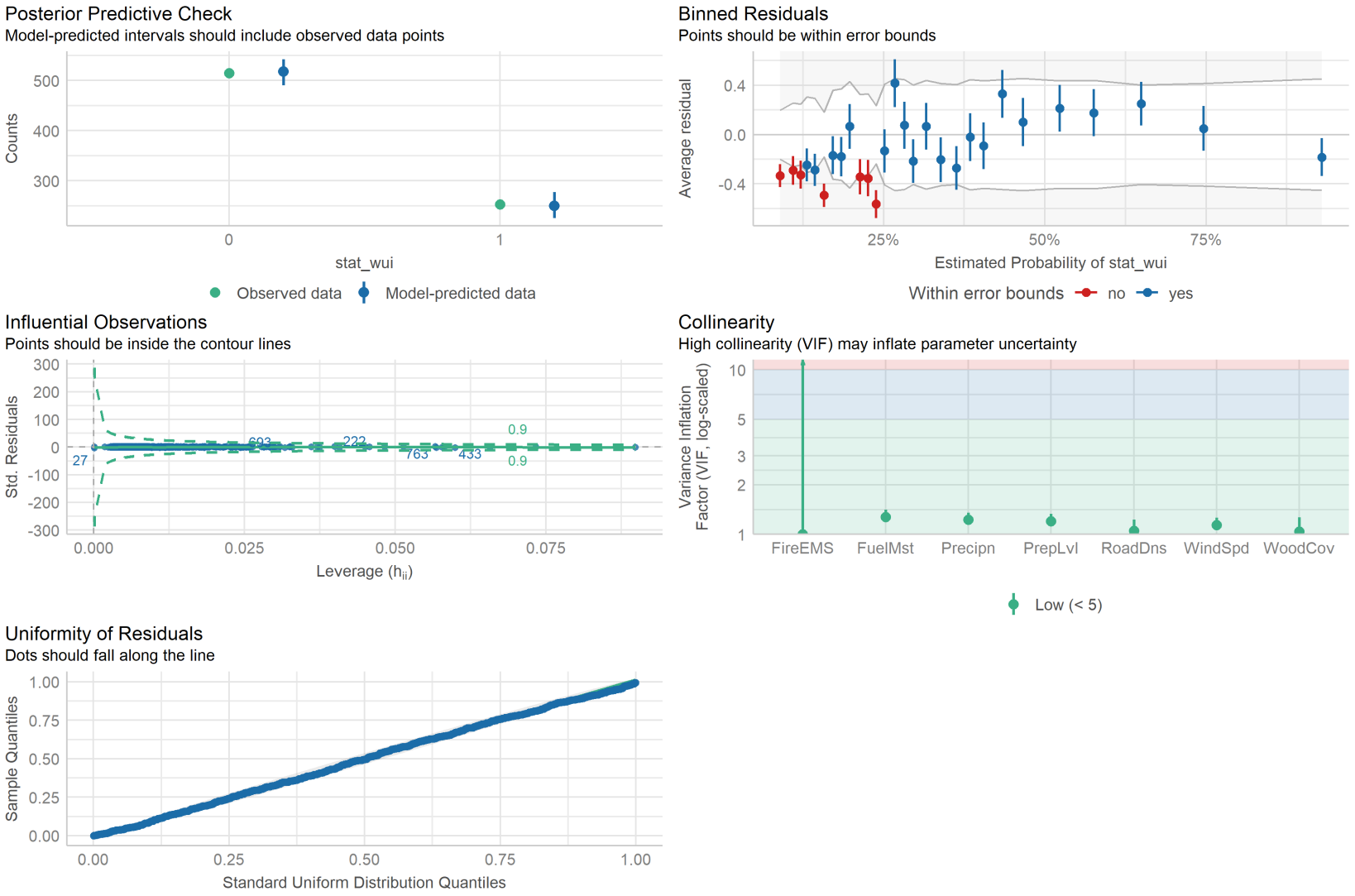


Figure B-38. Global model diagnostics for whether large wildfires (≥200 ha) burned in the wildland-urban interface (WUI) within the Mississippi Alluvial and Southeast USA Coastal Plains Level II ecoregion.

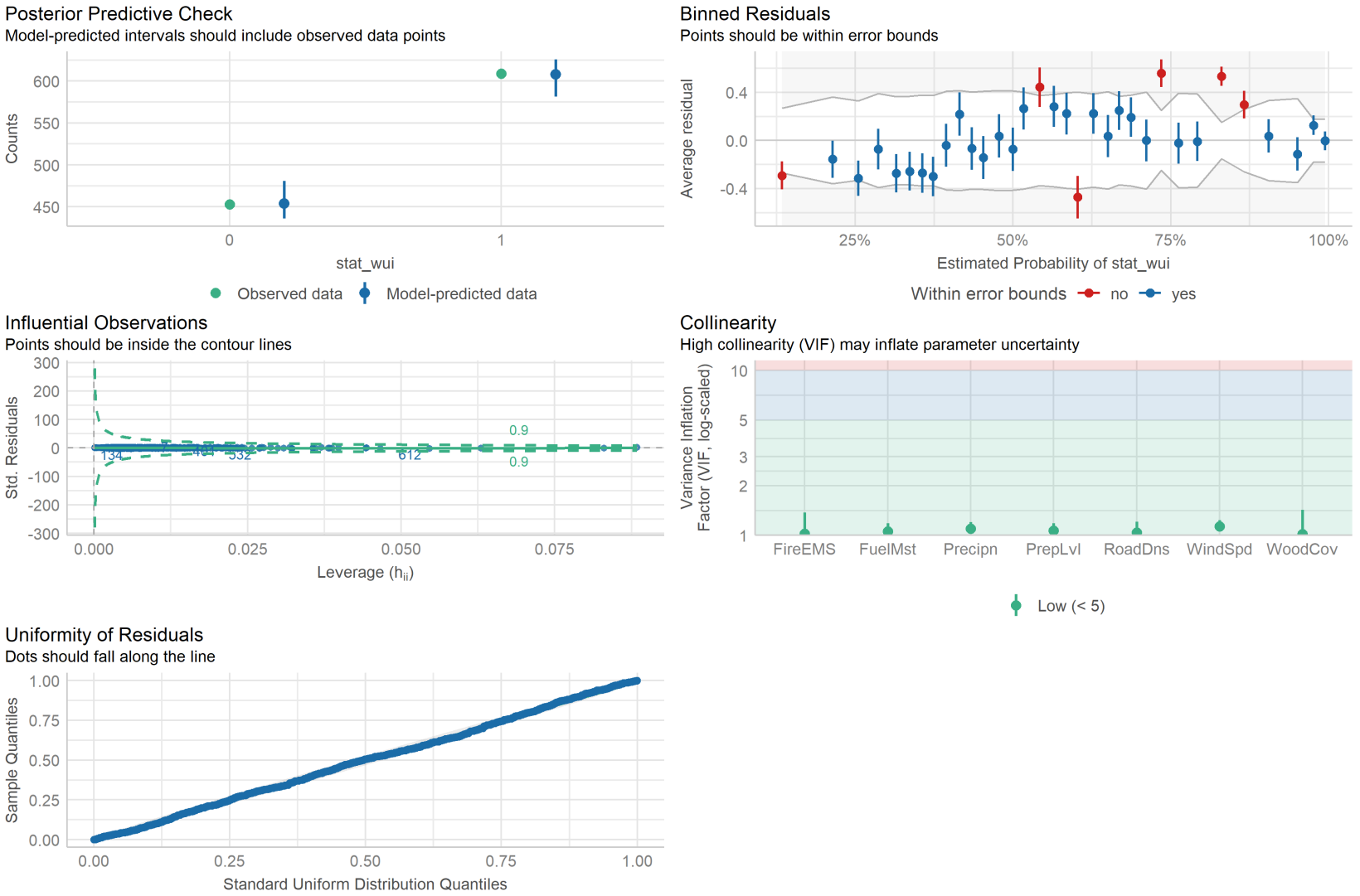


Figure B-39. Global model diagnostics for whether large wildfires (≥200 ha) burned in the wildland-urban interface (WUI) within the Ozark/Ouachita-Appalachian Forests Level II ecoregion.

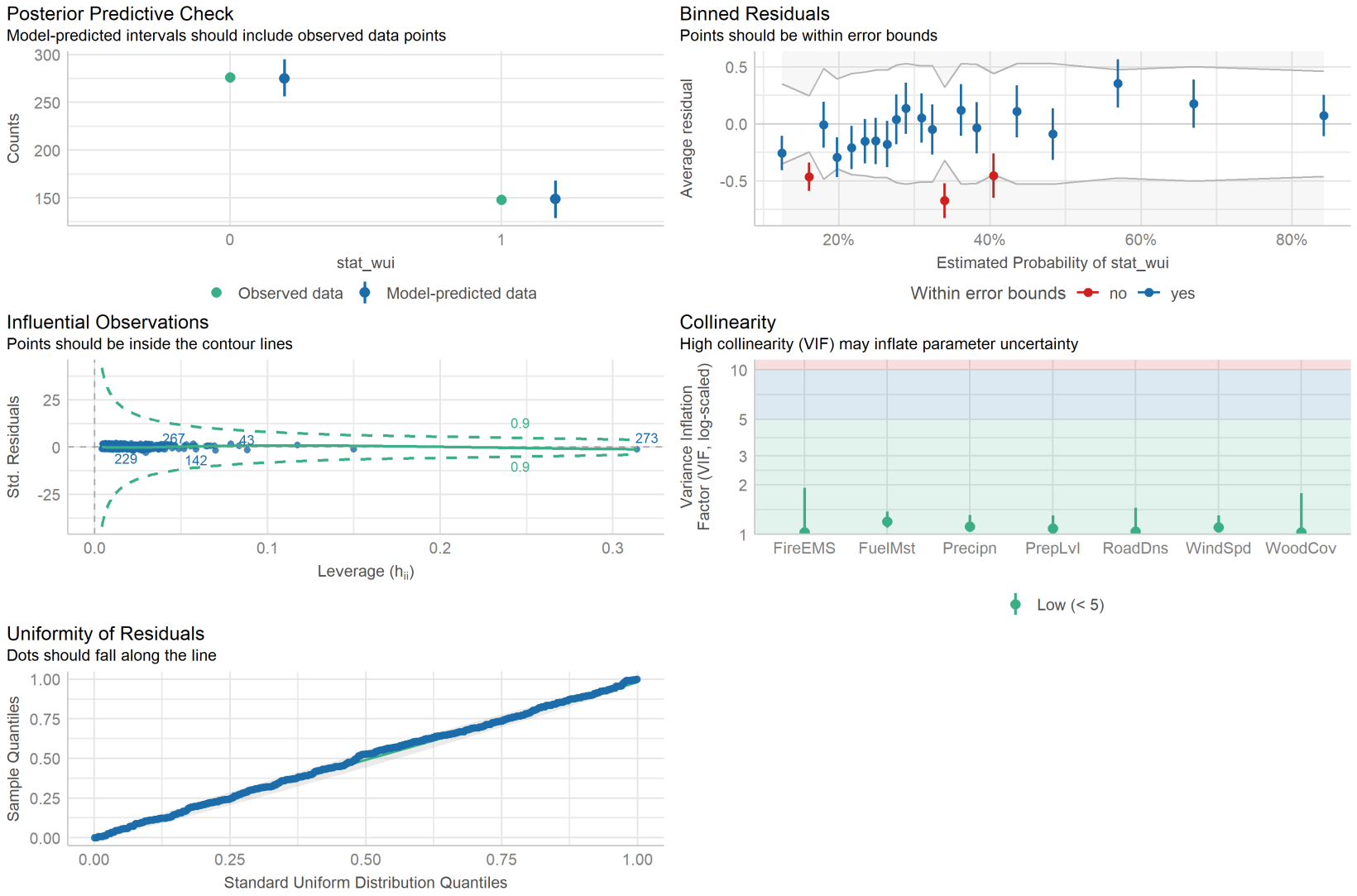


Figure B-40. Global model diagnostics for whether large wildfires (≥200 ha) burned in the wildland-urban interface (WUI) within the Southeastern USA Plains Level II ecoregion.

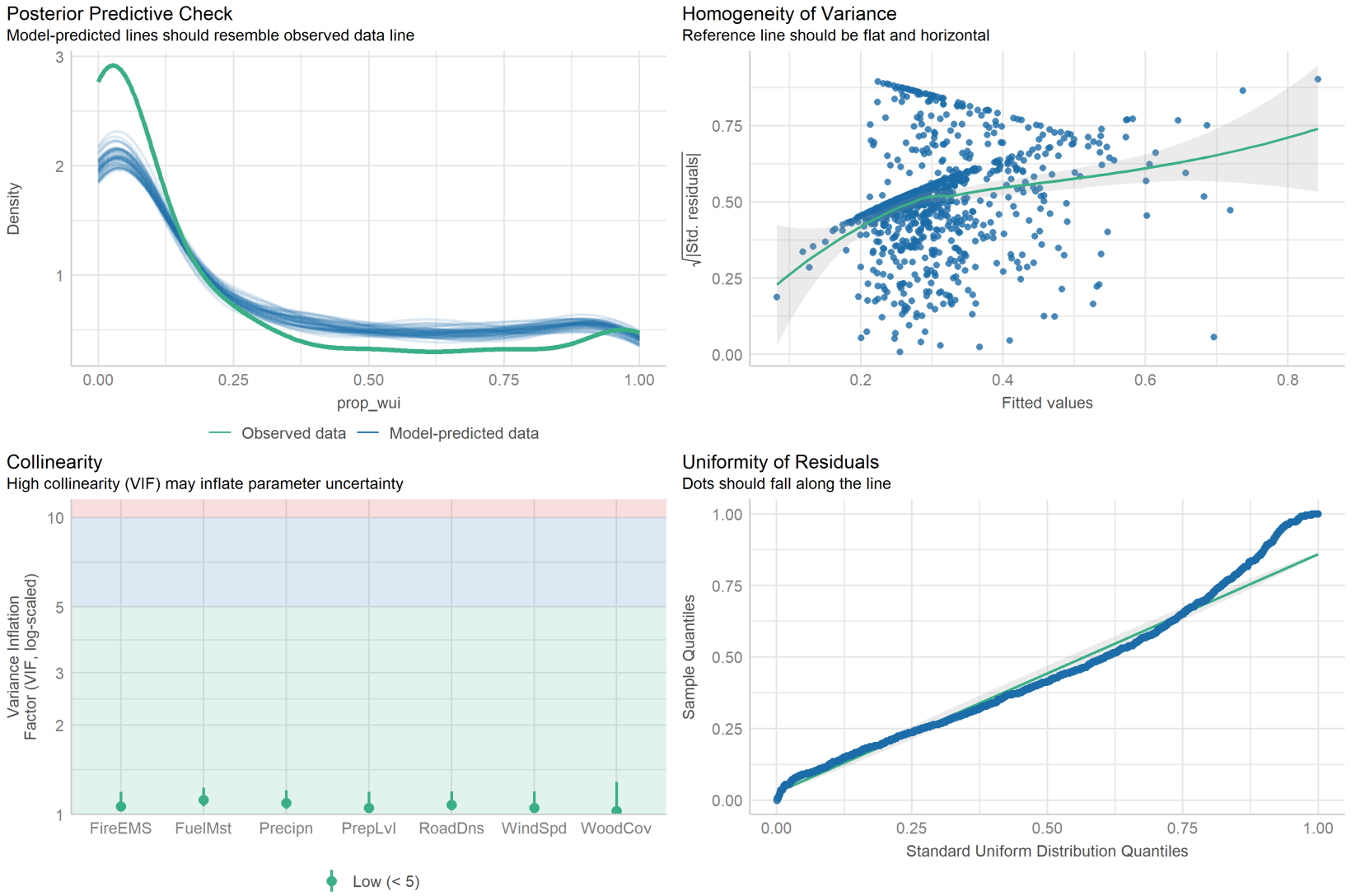


Figure B-41. Global model diagnostics for the proportion of a large wildfire's (≥200 ha) perimeter that burned in the wildland-urban interface (WUI) within the Eastern Temperate Forests Level I ecoregion.

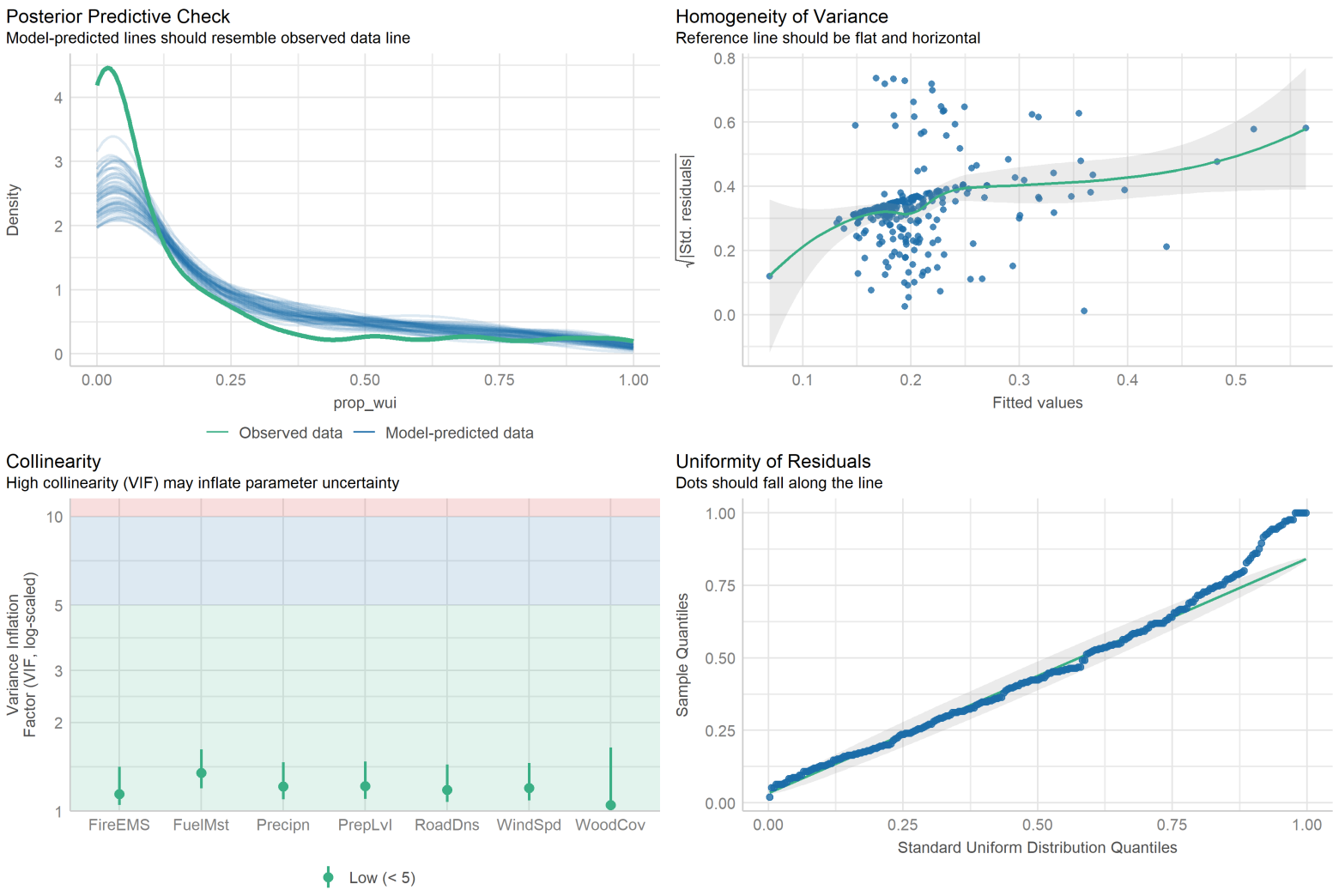


Figure B-42. Global model diagnostics for the proportion of a large wildfire's (≥200 ha) perimeter that burned in the wildland-urban interface (WUI) within the Mississippi Alluvial and Southeast USA Coastal Plains Level II ecoregion.

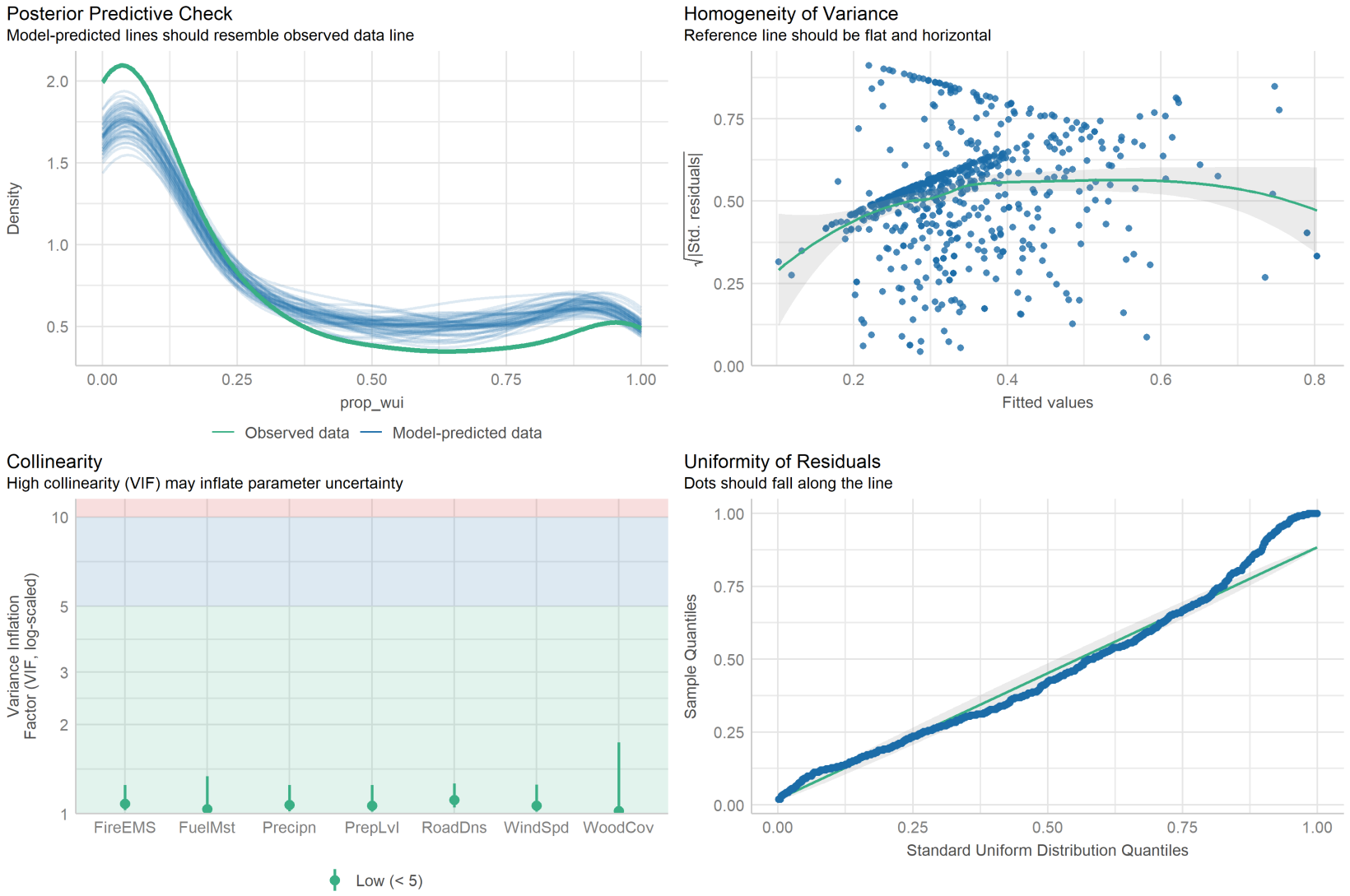


Figure B-43. Global model diagnostics for the proportion of a large wildfire's (≥200 ha) perimeter that burned in the wildland-urban interface (WUI) within the Ozark/Ouachita-Appalachian Forests Level II ecoregion.

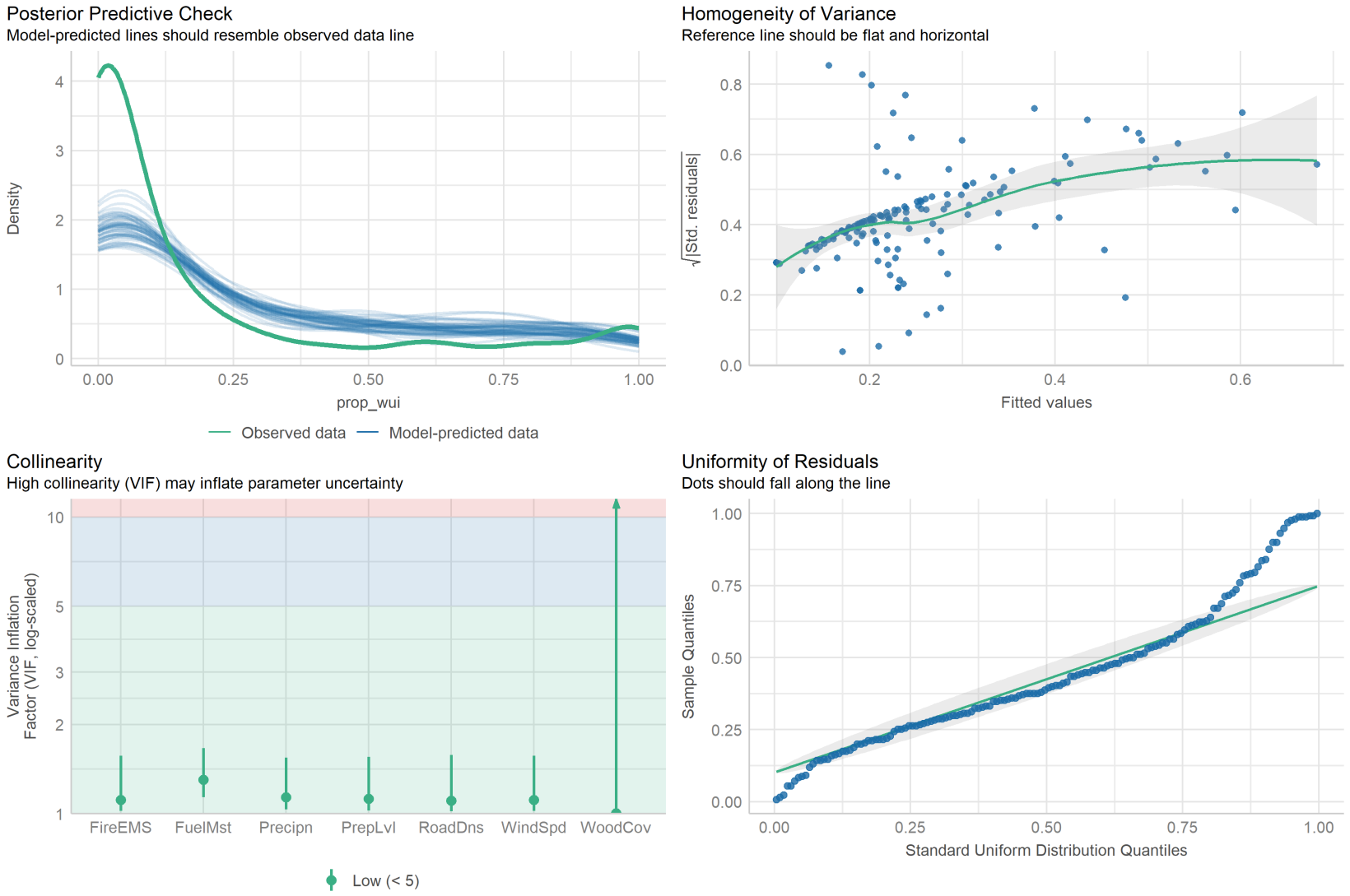


Figure B-44. Global model diagnostics for the proportion of a large wildfire's (≥200 ha) perimeter that burned in the wildland-urban interface (WUI) within the Southeastern USA Plains Level II ecoregion.

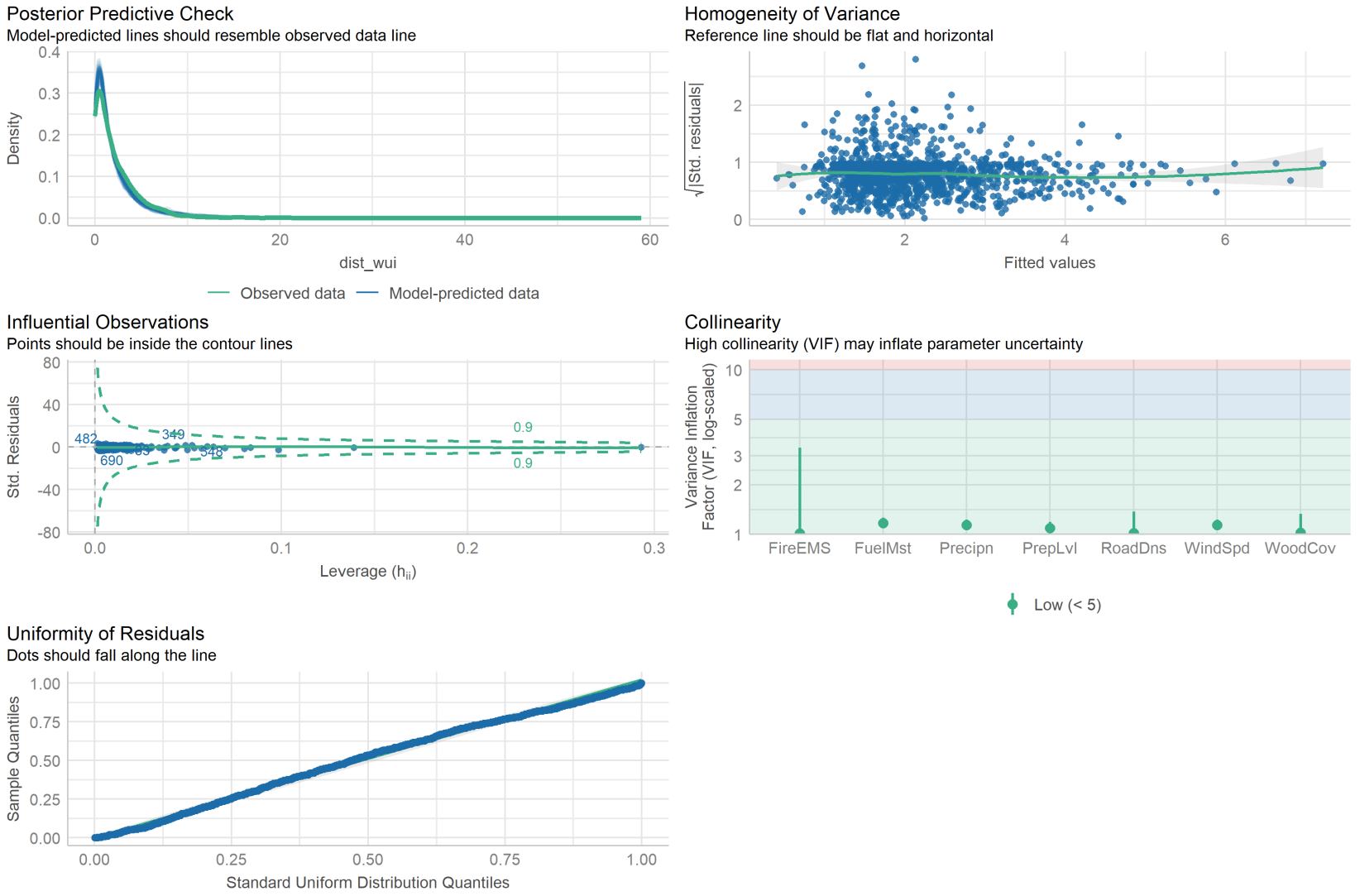


Figure B-45. Global model diagnostics for the distance large wildfires (≥200 ha) burned from the wildland-urban interface (WUI) within the Eastern Temperate Forests Level I ecoregion.

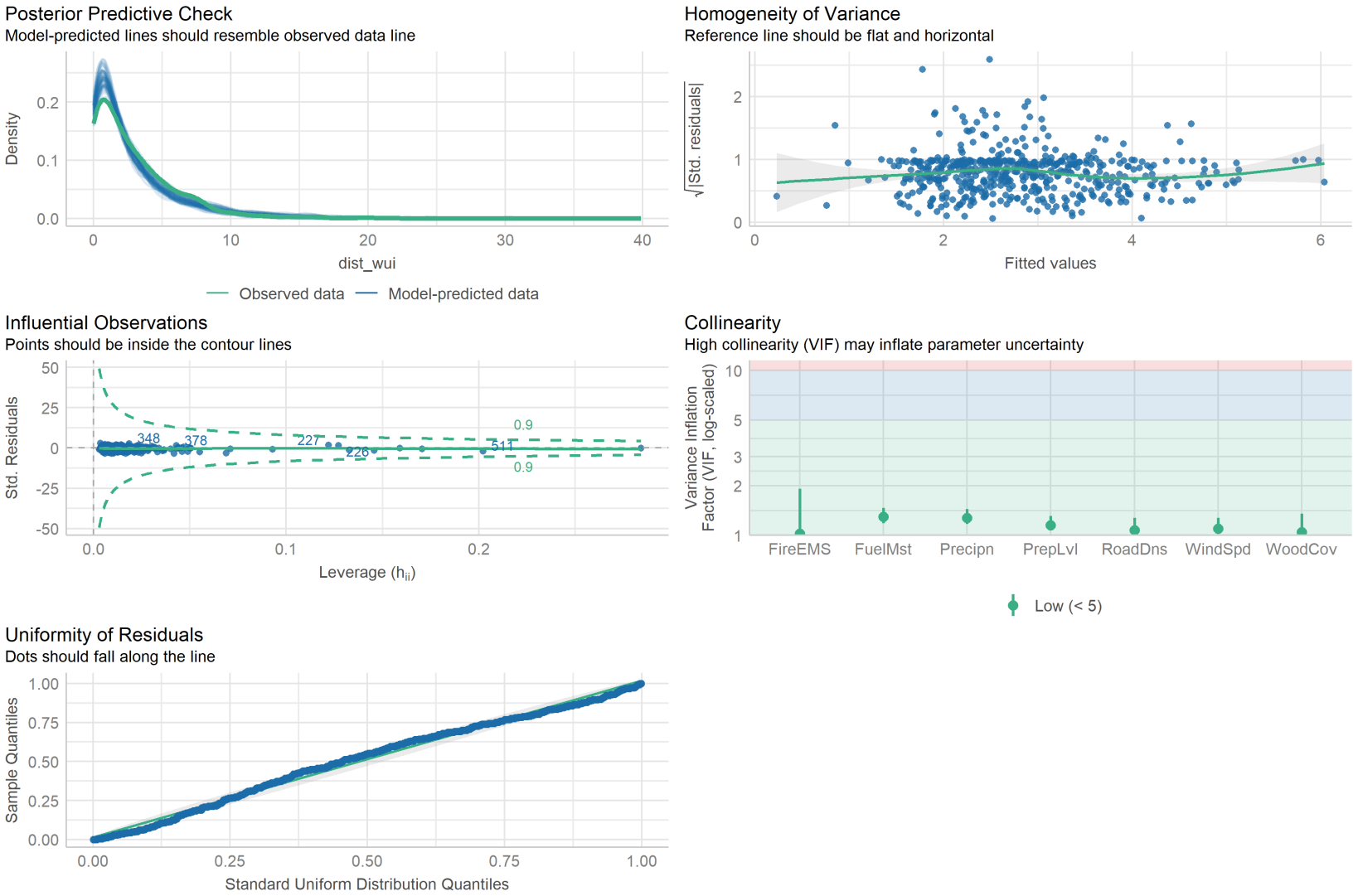


Figure B-46. Global model diagnostics for the distance large wildfires (≥200 ha) burned from the wildland-urban interface (WUI) within the Mississippi Alluvial and Southeast USA Coastal Plains Level II ecoregion.

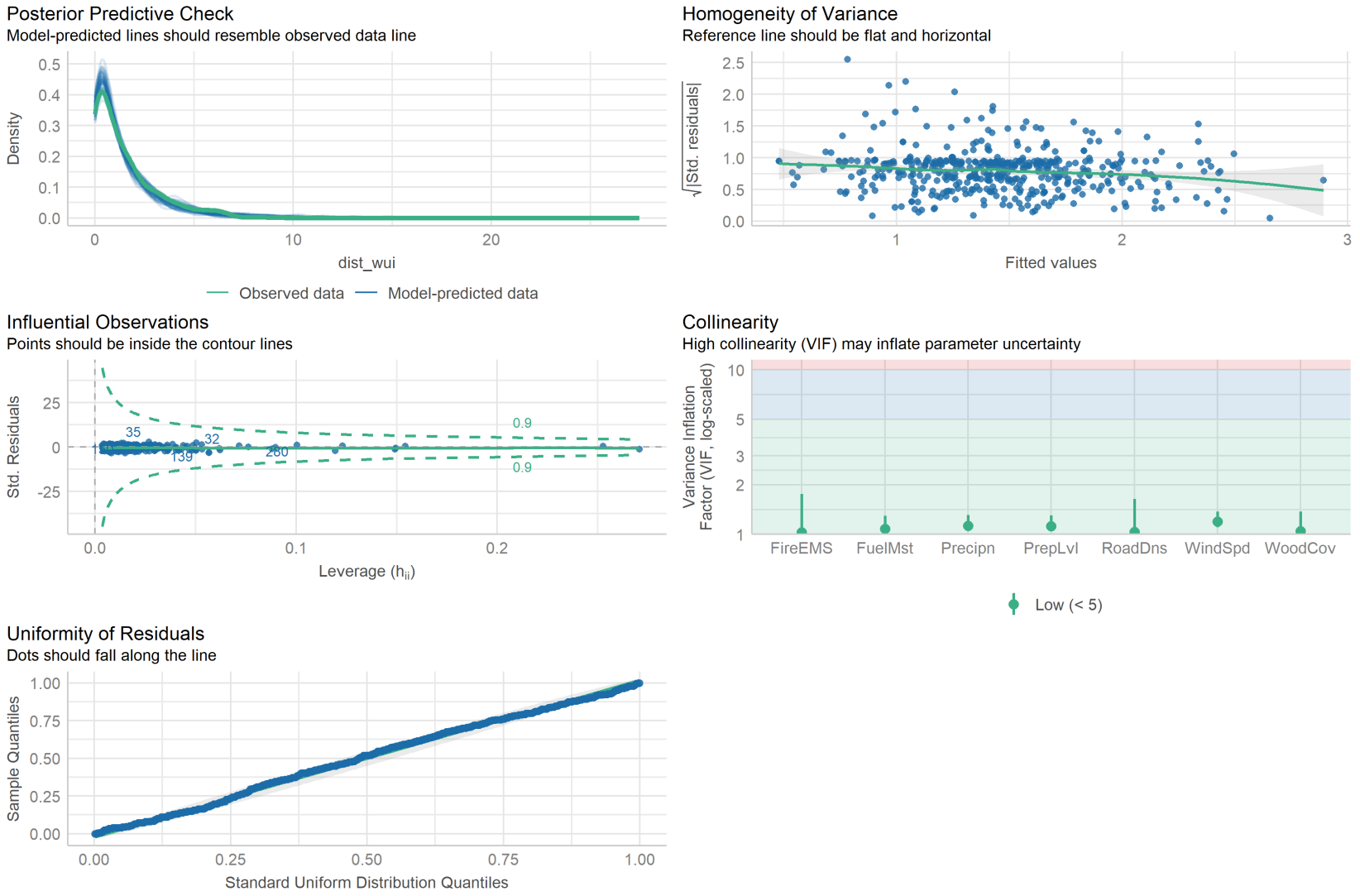


Figure B-47. Global model diagnostics for the distance large wildfires (≥200 ha) burned from the wildland-urban interface (WUI) within the Ozark/Ouachita-Appalachian Forests Level II ecoregion.

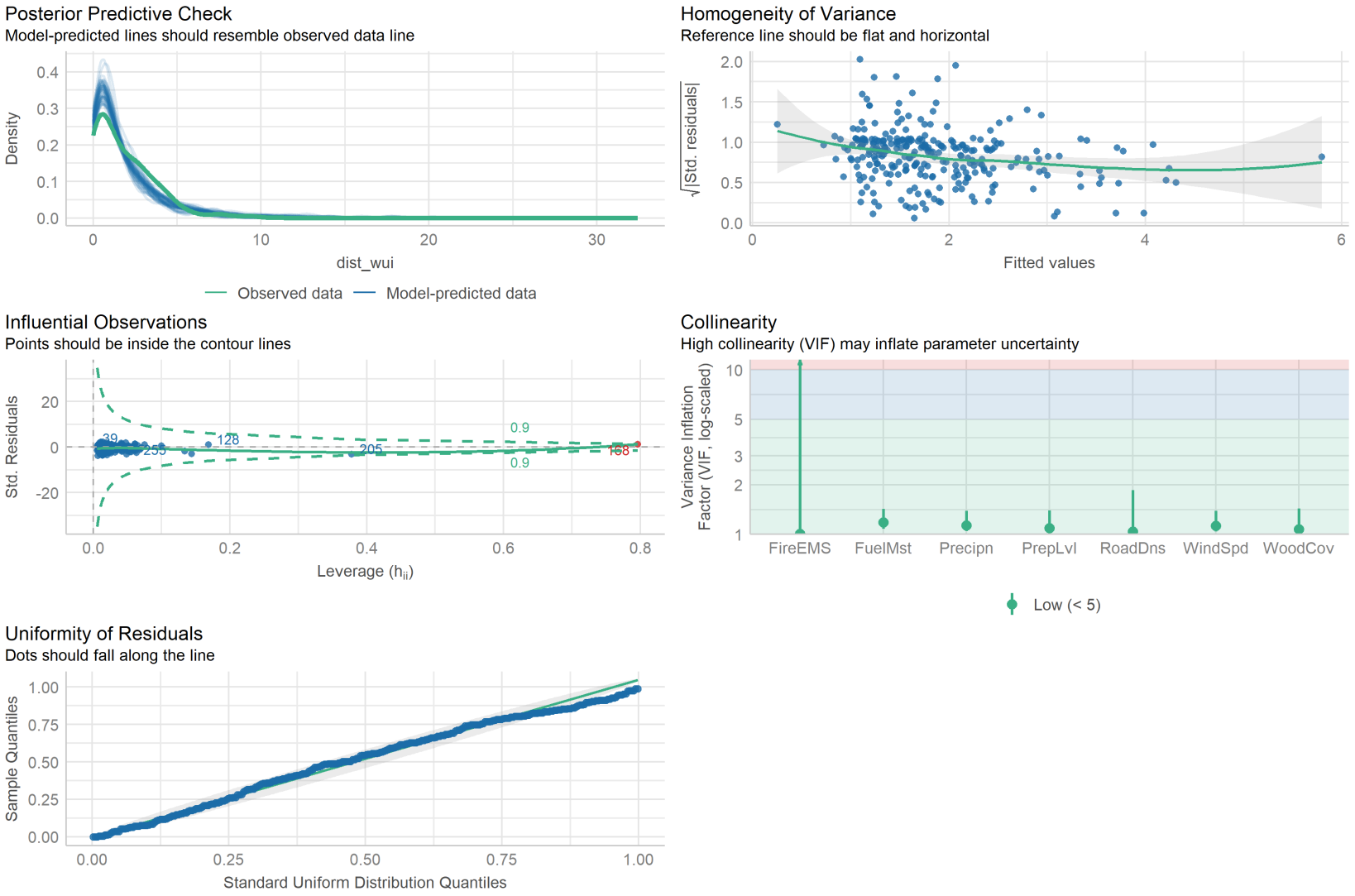


Figure B-48. Global model diagnostics for the distance large wildfires (≥200 ha) burned from the wildland-urban interface (WUI) within the Southeastern USA Plains Level II ecoregion.

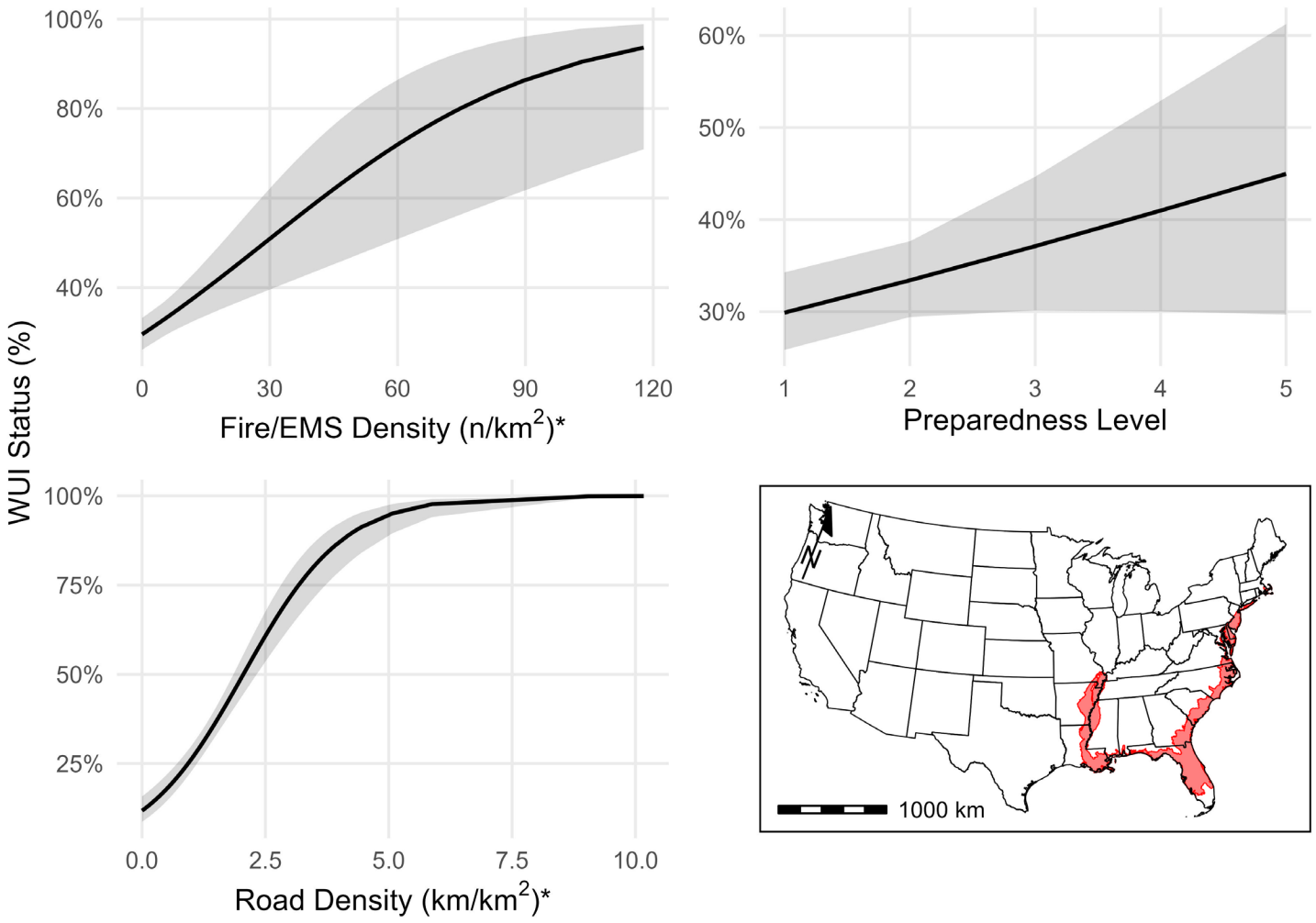


Figure B-49. Top model predictions for whether large wildfires (≥200 ha) burned in the wildland-urban interface (WUI) within the Mississippi Alluvial and Southeast USA Coastal Plains Level II ecoregion. The asterisk (*) indicates statistical significance (α = 0.05).

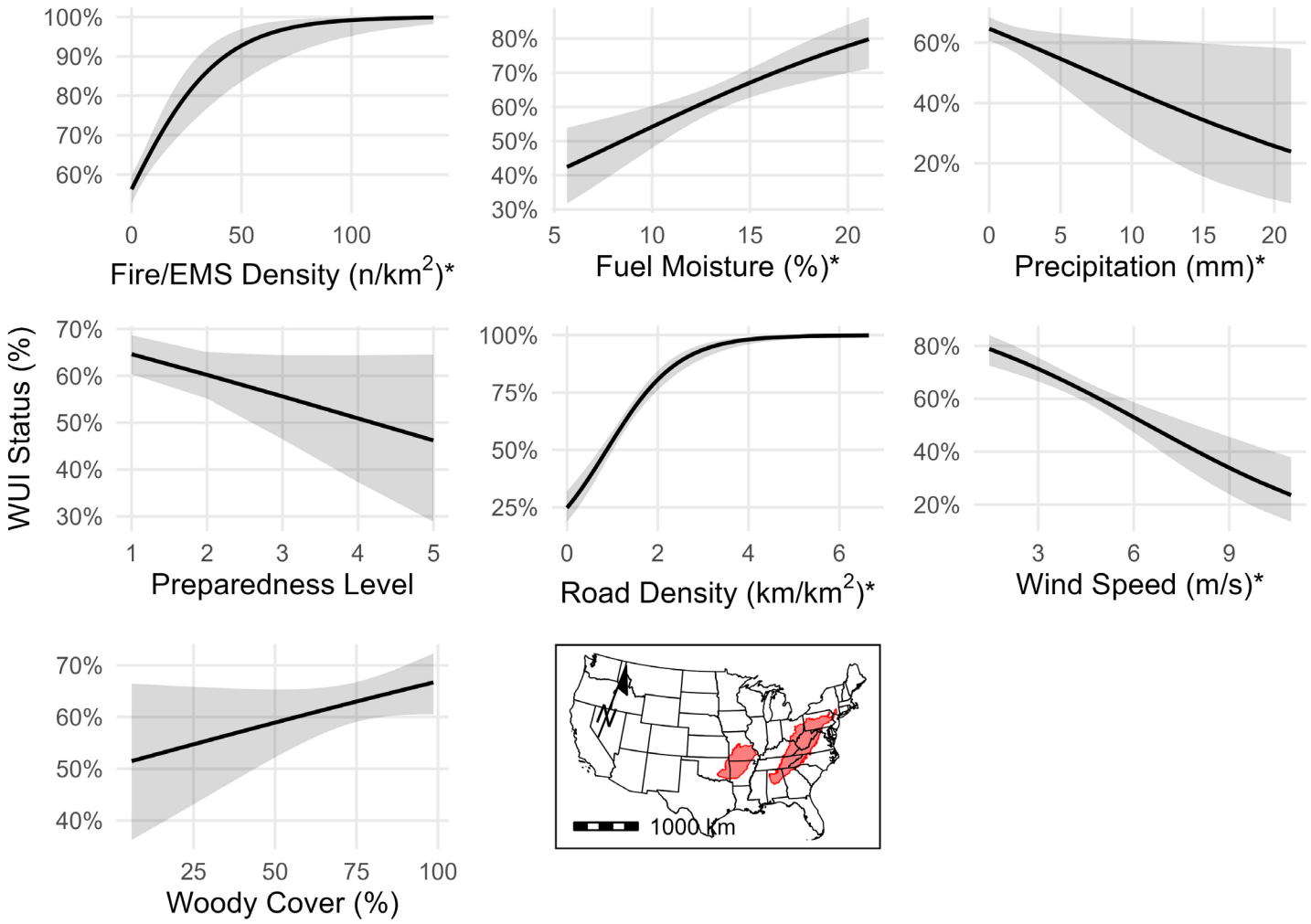


Figure B-50. Top model predictions for whether large wildfires (≥200 ha) burned in the wildland-urban interface (WUI) within the Ozark/Ouachita-Appalachian Forests Level II ecoregion. The asterisk (*) indicates statistical significance (α = 0.05).

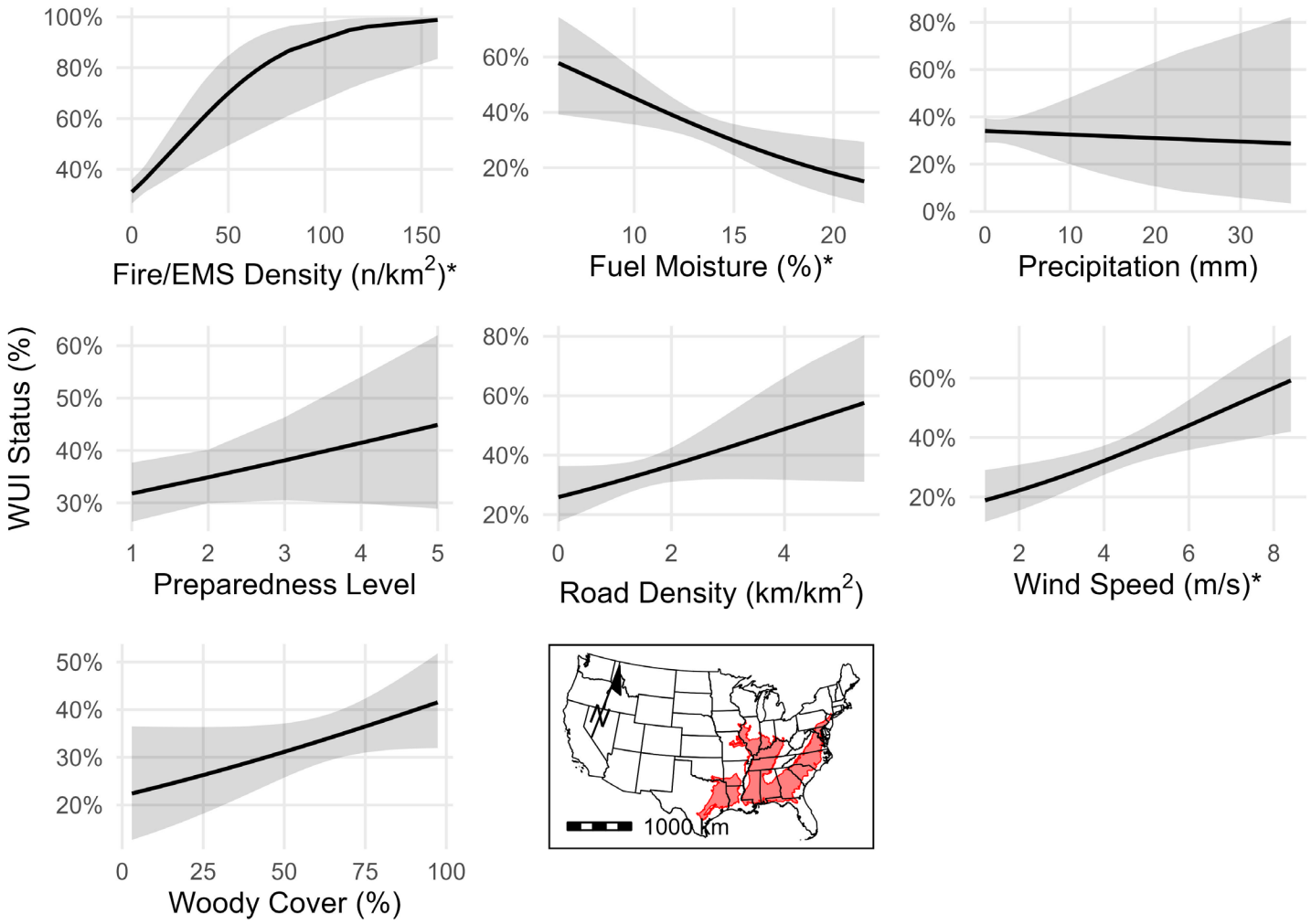


Figure B-51. Top model predictions for whether large wildfires (≥200 ha) burned in the wildland-urban interface (WUI) within the Southeastern USA Plains Level II ecoregion. The asterisk (*) indicates statistical significance (α = 0.05).

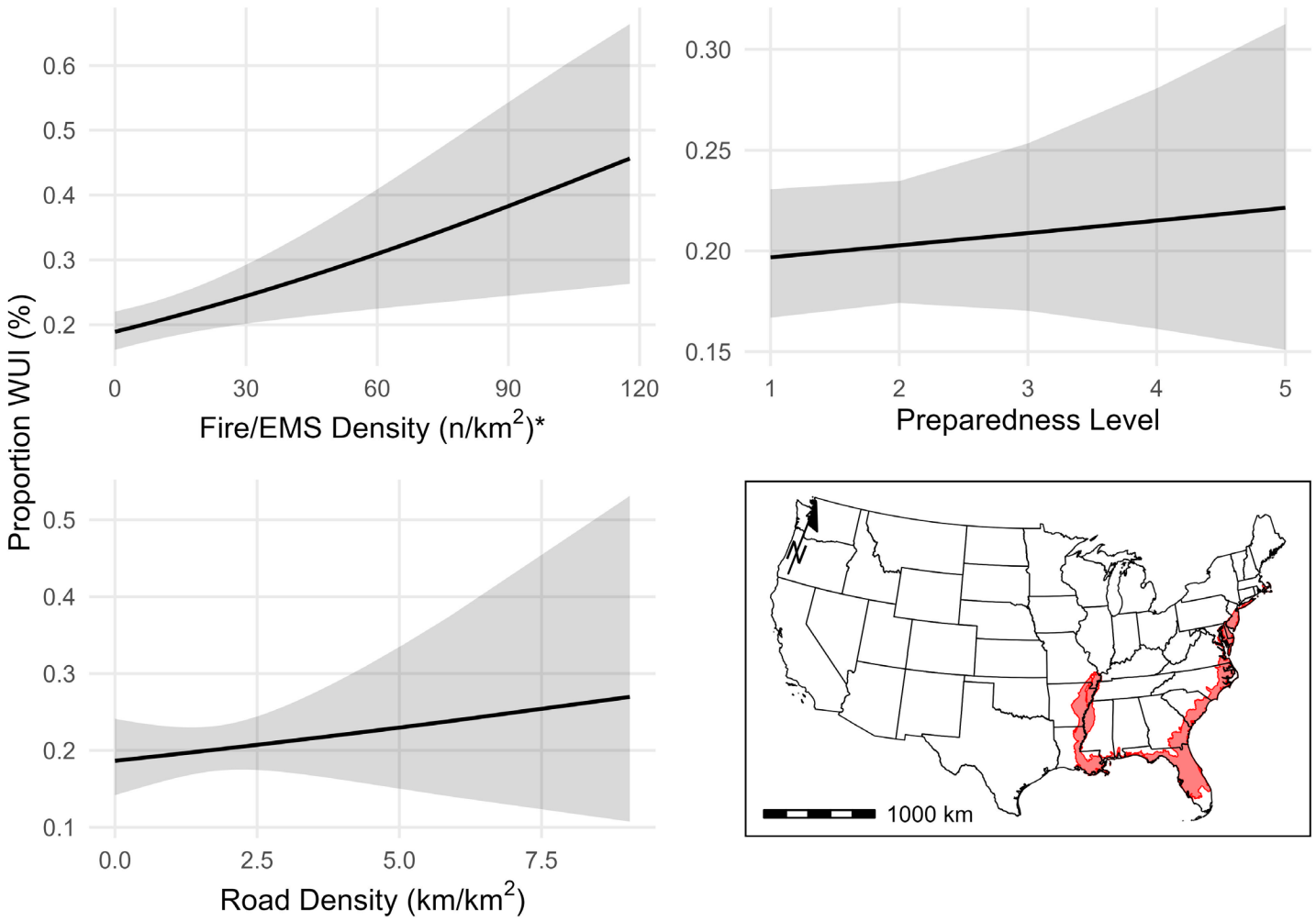


Figure B-52. Top model predictions for the proportion of a large wildfire's (≥200 ha) perimeter that burned in the wildland-urban interface (WUI) within the Mississippi Alluvial and Southeast USA Coastal Plains Level II ecoregion. The asterisk (*) indicates statistical significance (α = 0.05).

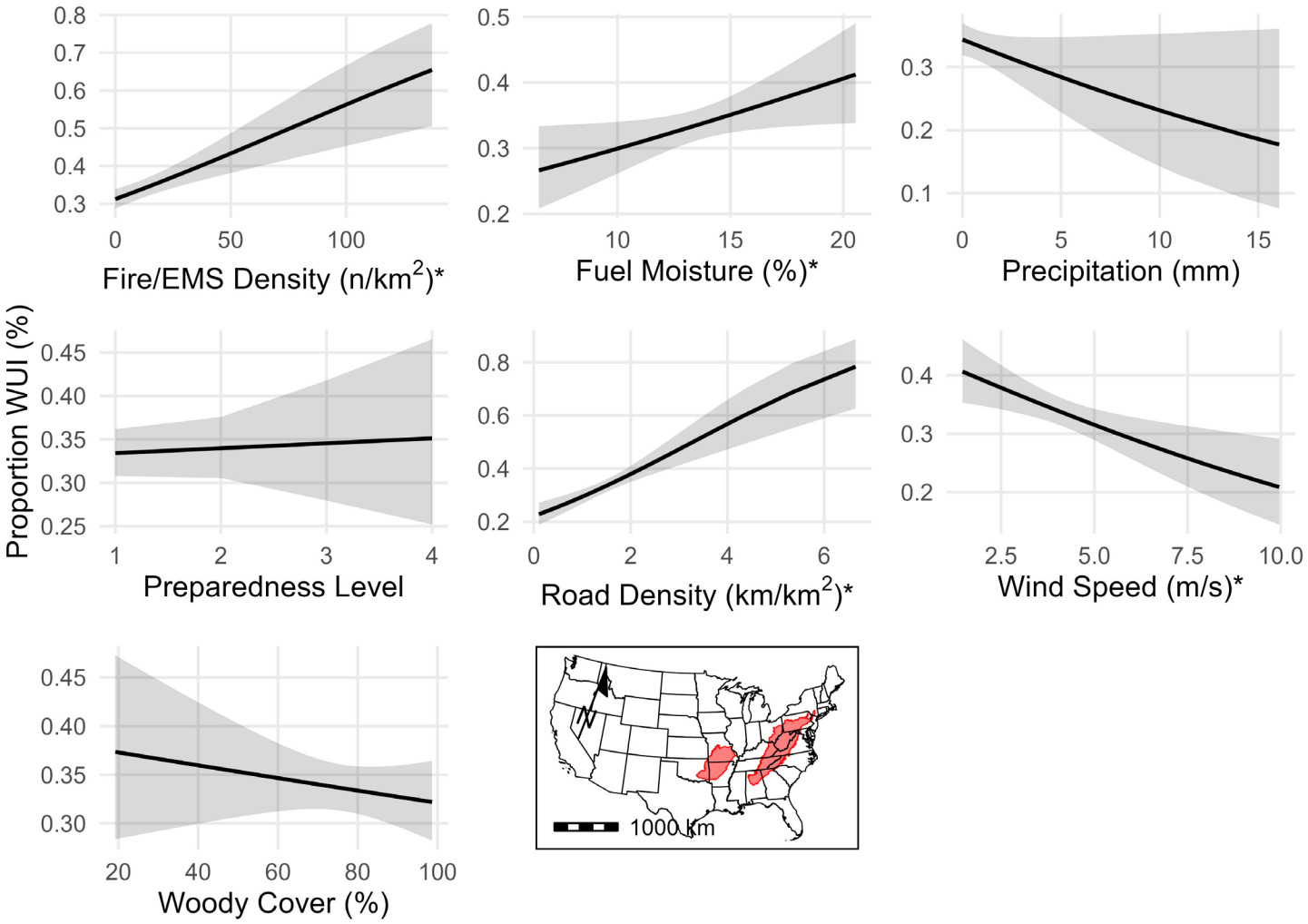


Figure B-53. Top model predictions for the proportion of a large wildfire's (≥200 ha) perimeter that burned in the wildland-urban interface (WUI) within the Ozark/Ouachita-Appalachian Forests Level II ecoregion. The asterisk (*) indicates statistical significance (α = 0.05).

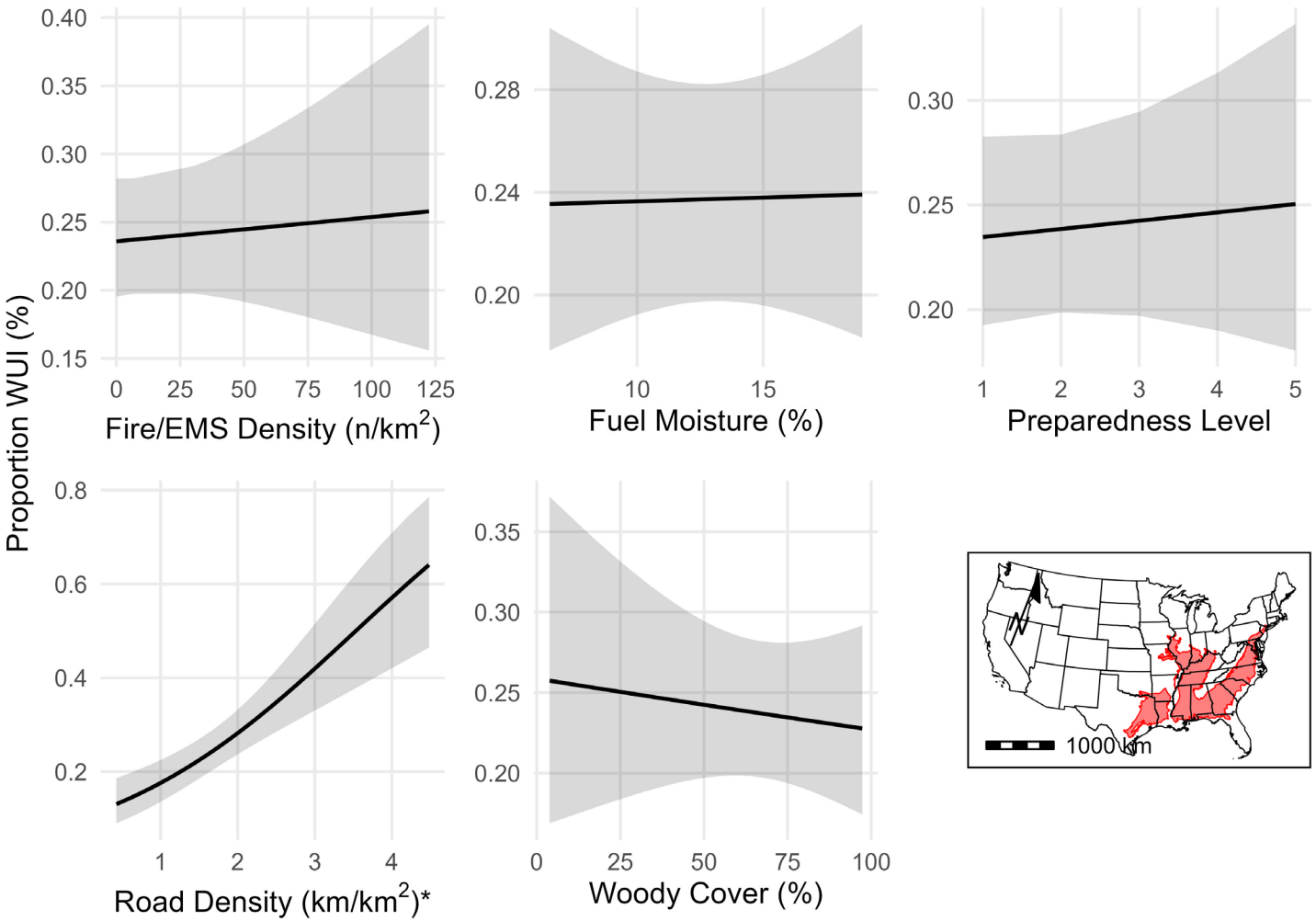


Figure B-54. Top model predictions for the proportion of a large wildfire's (≥200 ha) perimeter that burned in the wildland-urban interface (WUI) within the Southeastern USA Plains Level II ecoregion. The asterisk (*) indicates statistical significance (α = 0.05).

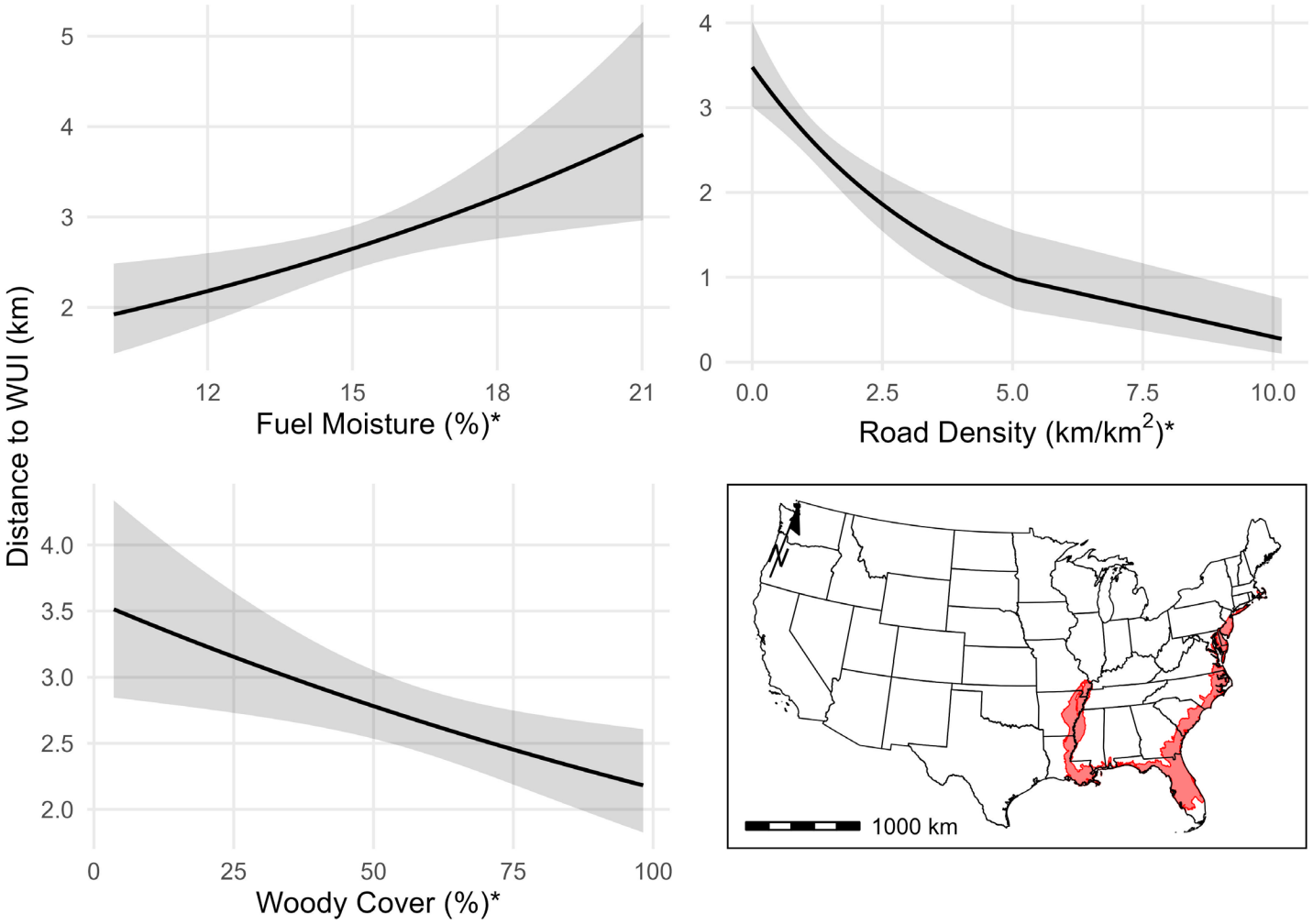


Figure B-55. Top model predictions for the distance large wildfires (≥200 ha) burned from the wildland-urban interface (WUI) within the Mississippi Alluvial and Southeast USA Coastal Plains Level II ecoregion. The asterisk (*) indicates statistical significance (α = 0.05).

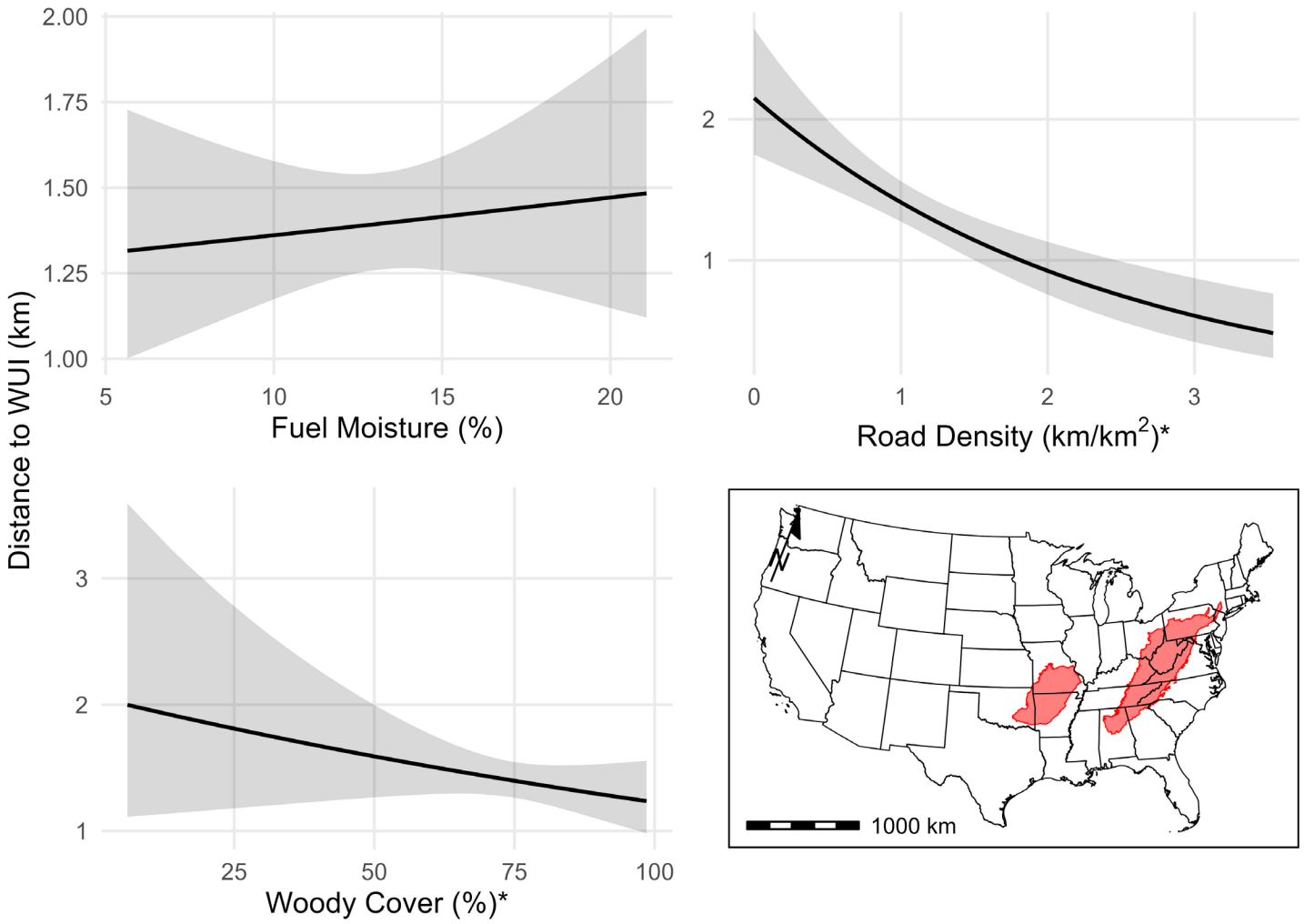


Figure B-56. Top model predictions for the distance large wildfires (≥200 ha) burned from the wildland-urban interface (WUI) within the Ozark/Ouachita-Appalachian Forests Level II ecoregion. The asterisk (*) indicates statistical significance (α = 0.05).

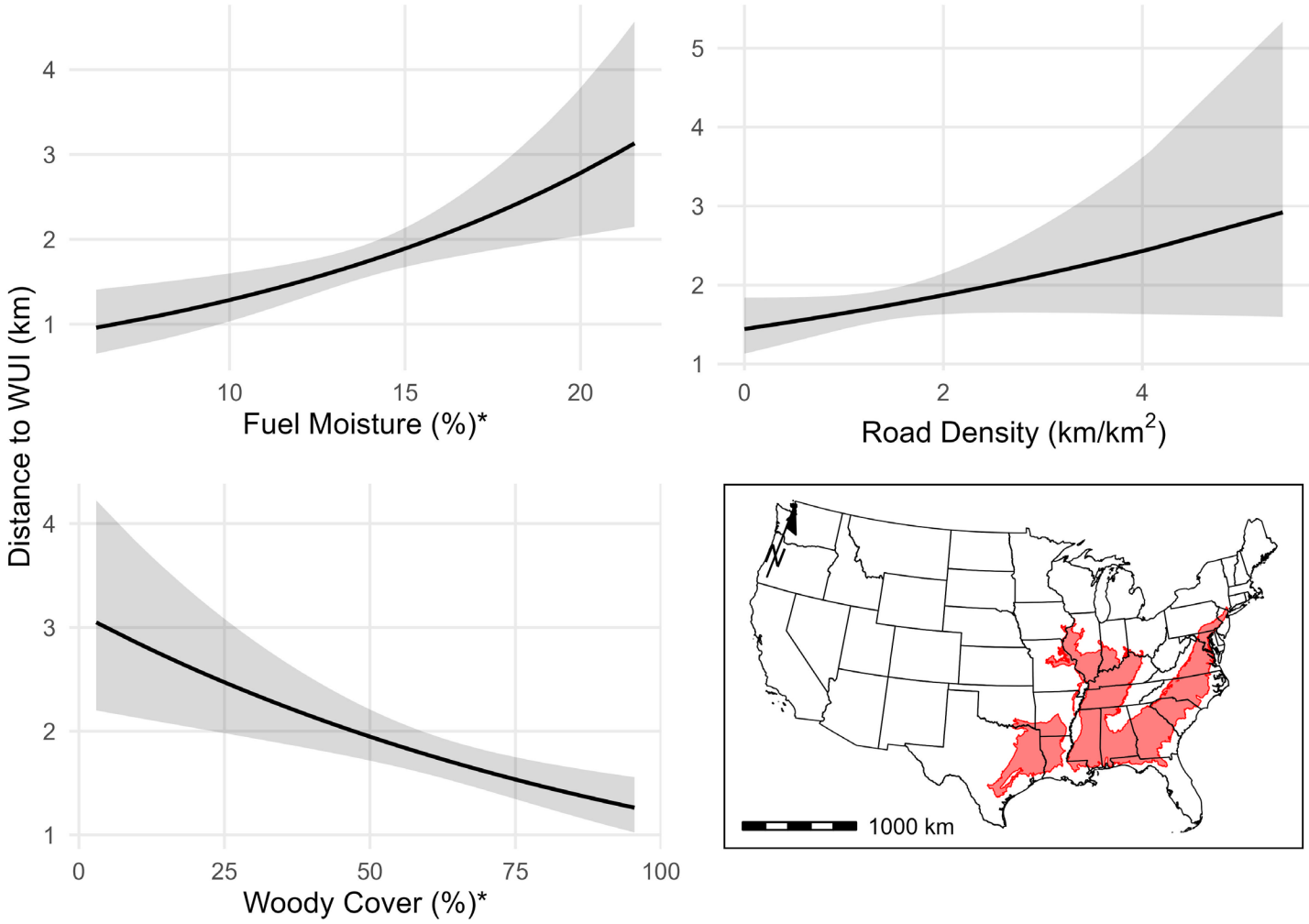


Figure B-57. Top model predictions for the distance large wildfires (≥200 ha) burned from the wildland-urban interface (WUI) within the Southeastern USA Plains Level II ecoregion. The asterisk (*) indicates statistical significance (α = 0.05).

LIST OF REFERENCES

Abatzoglou, J. T. (2013). Development of gridded surface meteorological data for ecological applications and modelling. *International Journal of Climatology*, *33*(1), 121–131. https://doi.org/10.1002/joc.3413

Abatzoglou, J. T., & Williams, A. P. (2016). Impact of anthropogenic climate change on wildfire across western US forests. *Proceedings of the National Academy of Sciences*, *113*(42), 11770–11775.

Abatzoglou, J. T., Williams, A. P., & Barbero, R. (2019). Global Emergence of Anthropogenic Climate Change in Fire Weather Indices. *Geophysical Research Letters*, *46*(1), 326–336. https://doi.org/10.1029/2018GL080959

Ahrens, M. (2013). *Brush, grass, and forest fires*. National Fire Protection Association, Fire Analysis and Research Division Quincy.

Akaike, H. (1973). Maximum likelihood identification of Gaussian autoregressive moving average models. *Biometrika*, *60*(2), 255–265. https://doi.org/10.1093/biomet/60.2.255

Alston, K. P., & Richardson, D. M. (2006). The roles of habitat features, disturbance, and distance from putative source populations in structuring alien plant invasions at the urban/wildland interface on the Cape Peninsula, South Africa. *Biological Conservation*, *132*(2), 183–198. https://doi.org/10.1016/j.biocon.2006.03.023

Andreu, A. G., Shea, D., Parresol, B. R., & Ottmar, R. D. (2012). Evaluating fuel complexes for fire hazard mitigation planning in the southeastern United States. *Forest Ecology and Management*, *273*, 4–16. https://doi.org/10.1016/j.foreco.2011.06.040

Balch, J. K., Bradley, B. A., Abatzoglou, J. T., Nagy, R. C., Fusco, E. J., & Mahood, A. L. (2017). Human-started wildfires expand the fire niche across the United States. *Proceedings of the National Academy of Sciences*, *114*(11), 2946–2951. https://doi.org/10.1073/pnas.1617394114

Balch, J. K., Iglesias, V., Mahood, A. L., Cook, M. C., Amaral, C., DeCastro, A., Leyk, S., McIntosh, T. L., Nagy, R. C., St. Denis, L., Tuff, T., Verleye, E., Williams, A. P., & Kolden, C. A. (2024). The fastest-growing and most destructive fires in the US (2001 to 2020). *Science*, *386*(6720), 425–431. https://doi.org/10.1126/science.adk5737

Barrett, K. (2020, November 16). *Wildfires destroy thousands of structures each year*. Headwaters Economics. https://headwaterseconomics.org/natural-hazards/structures-destroyed-by-wildfire/

Bartoń, K. (2024). *MuMIn: Multi-Model Inference* (Version 1.48.4) [Computer software]. https://cran.r-project.org/web/packages/MuMIn/index.html

Bedel, A. P., Mote, T. L., & Goodrick, S. L. (2013). Climate change and associated fire potential for the south-eastern United States in the 21st century. *International Journal of Wildland Fire*, *22*(8), 1034–1043. https://doi.org/10.1071/WF13018

Bowman, D. M. J. S., Kolden, C. A., Abatzoglou, J. T., Johnston, F. H., van der Werf, G. R., & Flannigan, M. (2020). Vegetation fires in the Anthropocene. *Nature Reviews Earth & Environment*, *1*(10), 500–515. https://doi.org/10.1038/s43017-020-0085-3

Bowman, D. M. J. S., Williamson, G. J., Abatzoglou, J. T., Kolden, C. A., Cochrane, M. A., & Smith, A. M. S. (2017). Human exposure and sensitivity to globally extreme wildfire events. *Nature Ecology & Evolution*, *1*(3), 1–6. https://doi.org/10.1038/s41559-016-0058

Bradley, B. A., Curtis, C. A., Fusco, E. J., Abatzoglou, J. T., Balch, J. K., Dadashi, S., & Tuanmu, M.-N. (2018). Cheatgrass (Bromus tectorum) distribution in the intermountain Western United States and its relationship to fire frequency, seasonality, and ignitions. *Biological Invasions*, *20*(6), 1493–1506. https://doi.org/10.1007/s10530-017-1641-8

Brewer, S. (2008). Declines in plant species richness and endemic plant species in longleaf pine savannas invaded by Imperata cylindrica. *Biological Invasions*, *10*(8), 1257–1264. https://doi.org/10.1007/s10530-007-9200-3

Brooks, M. E., Kristensen, K., Benthem, K. J. van, Magnusson, A., Berg, C. W., Nielsen, A., Skaug, H. J., Mächler, M., & Bolker, B. M. (2017). glmmTMB Balances Speed and Flexibility Among Packages for Zero-inflated Generalized Linear Mixed Modeling. *The R Journal*, *9*(2), 378–400.

Brooks, M. L., D'Antonio, C. M., Richardson, D. M., Grace, J. B., Keeley, J. E., DiTomaso, J. M., Hobbs, R. J., Pellant, M., & Pyke, D. (2004). Effects of Invasive Alien Plants on Fire Regimes. *BioScience*, *54*(7), 677–688. https://doi.org/10.1641/0006-3568(2004)054[0677:EOIAPO]2.0.CO;2

Brown, E. K., Wang, J., & Feng, Y. (2021). US wildfire potential: A historical view and future projection using high-resolution climate data. *Environmental Research Letters*, *16*(3), 034060. https://doi.org/10.1088/1748-9326/aba868

Bryce, S. A., Omernik, J. M., & Larsen, D. P. (1999). Environmental Review: Ecoregions: A Geographic Framework to Guide Risk Characterization and Ecosystem Management. *Environmental Practice*, *1*(3), 141–155. https://doi.org/10.1017/S1466046600000582

Burke, M., Driscoll, A., Heft-Neal, S., Xue, J., Burney, J., & Wara, M. (2021). The changing risk and burden of wildfire in the United States. *Proceedings of the National Academy of Sciences*, *118*(2), e2011048118. https://doi.org/10.1073/pnas.2011048118

Burnham, K. P., & Anderson, D. R. (2002). Model selection and multimodel inference: A practical-theoretical approach. *J. Wildl. Manag. Https://Doi. Org/10.1007/B97636*.

Burrell, A. M., Pepper, A. E., Hodnett, G., Goolsby, J. A., Overholt, W. A., Racelis, A. E., Diaz, R., & Klein, P. E. (2015). Exploring origins, invasion history and genetic diversity of Imperata cylindrica (L.) P. Beauv. (Cogongrass) in the United States using genotyping by sequencing. *Molecular Ecology*, *24*(9), 2177–2193. https://doi.org/10.1111/mec.13167

Butsic, V., Kelly, M., & Moritz, M. A. (2015). Land Use and Wildfire: A Review of Local Interactions and Teleconnections. *Land*, *4*(1), Article 1. https://doi.org/10.3390/land4010140

Calkin, D. E., Cohen, J. D., Finney, M. A., & Thompson, M. P. (2014). How risk management can prevent future wildfire disasters in the wildland-urban interface. *Proceedings of the National Academy of Sciences*, *111*(2), 746–751. https://doi.org/10.1073/pnas.1315088111

Calkin, D. E., Thompson, M. P., & Finney, M. A. (2015). Negative consequences of positive feedbacks in US wildfire management. *Forest Ecosystems*, *2*(1), 9. https://doi.org/10.1186/s40663-015-0033-8

Calviño-Cancela, M., Chas-Amil, M. L., García-Martínez, E. D., & Touza, J. (2016). Wildfire risk associated with different vegetation types within and outside wildland-urban interfaces. *Forest Ecology and Management*, *372*, 1–9. https://doi.org/10.1016/j.foreco.2016.04.002

Calviño-Cancela, M., Chas-Amil, M. L., García-Martínez, E. D., & Touza, J. (2017). Interacting effects of topography, vegetation, human activities and wildland-urban interfaces on wildfire ignition risk. *Forest Ecology and Management*, *397*, 10–17. https://doi.org/10.1016/j.foreco.2017.04.033

Carbaugh, L. W., & Marx, R. W. (1990). The TIGER system: A census bureau innovation serving data analysts. *Government Information Quarterly*, *7*(3), 285–306. https://doi.org/10.1016/0740-624X(90)90026-K

Carbone, L. M., Tavella, J., Marquez, V., Ashworth, L., Pausas, J. G., & Aguilar, R. (2025). Fire effects on pollination and plant reproduction: A quantitative review. *Annals of Botany*, *135*(1–2), 43–56. https://doi.org/10.1093/aob/mcae033

Carlson, A. R., Helmers, D. P., Hawbaker, T. J., Mockrin, M. H., & Radeloff, V. C. (2022). The wildland–urban interface in the United States based on 125 million building locations. *Ecological Applications*, *32*(5), e2597. https://doi.org/10.1002/eap.2597

Carlson, A. R., Radeloff, V. C., Helmers, D. P., Mockrin, M. H., Hawbaker, T. J., & Pidgeon, A. (2023). The extent of buildings in wildland vegetation of the conterminous U.S. and the potential for conservation in and near National Forest private inholdings. *Landscape and Urban Planning*, *237*, 104810. https://doi.org/10.1016/j.landurbplan.2023.104810

Carlson, A. R., Sebasky, M. E., Peters, M. P., Radeloff, V. C., Carlson, A. R., Sebasky, M. E., Peters, M. P., & Radeloff, V. C. (2021). The importance of small fires for wildfire hazard in urbanised landscapes of the northeastern US. *International Journal of Wildland Fire*, *30*(5), 307–321. https://doi.org/10.1071/WF20186

Chas-Amil, M. L., Touza, J., & García-Martínez, E. (2013). Forest fires in the wildland–urban interface: A spatial analysis of forest fragmentation and human impacts. *Applied Geography*, *43*, 127–137. https://doi.org/10.1016/j.apgeog.2013.06.010

Chen, B., Wu, S., Jin, Y., Song, Y., Wu, C., Venevsky, S., Xu, B., Webster, C., & Gong, P. (2024). Wildfire risk for global wildland–urban interface areas. *Nature Sustainability*. https://doi.org/10.1038/s41893-024-01291-0

Clements, C. B. (2011). Effects of complex terrain on extreme fire behavior. *Synthesis of Knowledge of Extreme Fire Behavior: Volume I for Fire Managers*, 5.

Coen, J. L., Cameron, M., Michalakes, J., Patton, E. G., Riggan, P. J., & Yedinak, K. M. (2013). *WRF-Fire: Coupled Weather–Wildland Fire Modeling with the Weather Research and Forecasting Model*. https://doi.org/10.1175/JAMC-D-12-023.1

Committee on the Chemistry of Urban Wildfires, Board on Chemical Sciences and Technology, Division on Earth and Life Studies, & National Academies of Sciences, Engineering, and Medicine. (2022). *The Chemistry of Fires at the Wildland-Urban Interface* (p. 26460). National Academies Press. https://doi.org/10.17226/26460

Cullen, A. C., Axe, T., & Podschwit, H. (2020). High-severity wildfire potential – associating meteorology, climate, resource demand and wildfire activity with preparedness levels. *International Journal of Wildland Fire*, *30*(1), 30–41. https://doi.org/10.1071/WF20066

Cunningham, C. X., Williamson, G. J., Nolan, R. H., Teckentrup, L., Boer, M. M., & Bowman, D. M. J. S. (2024). Pyrogeography in flux: Reorganization of Australian fire regimes in a hotter world. *Global Change Biology*, *30*(1), e17130. https://doi.org/10.1111/gcb.17130

Daniels, M. C., Braziunas, K. H., Turner, M. G., Ma, T.-F., Short, K. C., & Rissman, A. R. (2024). Multiple social and environmental factors affect wildland fire response of full or less-than-full suppression. *Journal of Environmental Management*, *351*, 119731. https://doi.org/10.1016/j.jenvman.2023.119731

Dennison, P. E., Brewer, S. C., Arnold, J. D., & Moritz, M. A. (2014). Large wildfire trends in the western United States, 1984–2011. *Geophysical Research Letters*, *41*(8), 2928–2933. https://doi.org/10.1002/2014GL059576

D'Evelyn, S. M., Jung, J., Alvarado, E., Baumgartner, J., Caligiuri, P., Hagmann, R. K., Henderson, S. B., Hessburg, P. F., Hopkins, S., Kasner, E. J., Krawchuk, M. A., Krenz, J. E., Lydersen, J. M., Marlier, M. E., Masuda, Y. J., Metlen, K., Mittelstaedt, G., Prichard, S. J., Schollaert, C. L., … Spector, J. T. (2022). Wildfire, Smoke Exposure, Human Health, and Environmental Justice Need to be Integrated into Forest Restoration and Management. *Current Environmental Health Reports*, *9*(3), 366–385. https://doi.org/10.1007/s40572-022-00355-7

Dobis, E. A., Cromartie, J., Williams, R., Reed, K., & United States. Department of Agriculture. Economic Research Service,. (2023). *Characterizing rugged terrain in the United States*. Economic Research Service, U.S. Department of Agriculture. https://doi.org/10.32747/2023.8134137.ers

Doherty, T. S., Geary, W. L., Jolly, C. J., Macdonald, K. J., Miritis, V., Watchorn, D. J., Cherry, M. J., Conner, L. M., González, T. M., Legge, S. M., Ritchie, E. G., Stawski, C., & Dickman, C. R. (2022). Fire as a driver and mediator of predator–prey interactions. *Biological Reviews*, *97*(4), 1539–1558. https://doi.org/10.1111/brv.12853

Donovan, V. M., Crandall, R. M., Fill, J. M., & Wonkka, C. L. (2023). Increasing Large Wildfire in the Eastern United States. *Geophysical Research Letters*, *50*(24), e2023GL107051. https://doi.org/10.1029/2023GL107051

Donovan, V. M., Fogarty, D. T., & Twidwell, D. (2023). Spot-fire distance increases disproportionately for wildfires compared to prescribed fires as grasslands transition to Juniperus woodlands. *PLOS ONE*, *18*(4), e0283816. https://doi.org/10.1371/journal.pone.0283816

Donovan, V. M., Roberts, C. P., Fogarty, D. T., Wedin, D. A., & Twidwell, D. (2022). Targeted grazing and mechanical thinning enhance forest stand resilience under a narrow range of wildfire scenarios. *Ecosphere*, *13*(5), e4061. https://doi.org/10.1002/ecs2.4061

Donovan, V. M., Wonkka, C. L., & Twidwell, D. (2017). Surging wildfire activity in a grassland biome. *Geophysical Research Letters*, *44*(12), 5986–5993. https://doi.org/10.1002/2017GL072901

Donovan, V. M., Wonkka, C. L., Wedin, D. A., & Twidwell, D. (2020). Land-Use Type as a Driver of Large Wildfire Occurrence in the U.S. Great Plains. *Remote Sensing*, *12*(11), Article 11. https://doi.org/10.3390/rs12111869

Drummond, M. A., Stier, M. P., McBeth, J. L., Auch, R. F., Taylor, J. L., & Riegle, J. L. (2020). Causes of land change in the U.S. Interior Highlands, 2001–2011. In *Data Series* (No. 1127). U.S. Geological Survey. https://doi.org/10.3133/ds1127

Eidenshink, J., Schwind, B., Brewer, K., Zhu, Z.-L., Quayle, B., & Howard, S. (2007). A Project for Monitoring Trends in Burn Severity. *Fire Ecology*, *3*(1), Article 1. https://doi.org/10.4996/fireecology.0301003

Ellis, T. M., Bowman, D. M. J. S., Jain, P., Flannigan, M. D., & Williamson, G. J. (2022). Global increase in wildfire risk due to climate-driven declines in fuel moisture. *Global Change Biology*, *28*(4), 1544–1559. https://doi.org/10.1111/gcb.16006

EPA. (2013). *Level III Ecoregions of the Conterminous United States* [Data and Tools]. U.S. EPA Office of Research and Development (ORD) - National Health and Environmental Effects Research Laboratory (NHEERL). https://www.epa.gov/eco-research/level-iii-and-iv-ecoregions-continental-united-states

Fairman, T. A., Nitschke, C. R., & Bennett, L. T. (2015). Too much, too soon? A review of the effects of increasing wildfire frequency on tree mortality and regeneration in temperate eucalypt forests. *International Journal of Wildland Fire*, *25*(8), 831–848. https://doi.org/10.1071/WF15010

FEMA. (2021). *Analysis of NFIRS Incidents in the Wildland Urban Interface*. https://www.usfa.fema.gov/wui/data/wildfire-report-series/nfirs-wui-incidents-california.html

Fernandez-Pello, A. C. (2017). Wildland fire spot ignition by sparks and firebrands. *Fire Safety Journal*, *91*, 2–10. https://doi.org/10.1016/j.firesaf.2017.04.040

Feron, S., Cordero, R. R., Damiani, A., MacDonell, S., Pizarro, J., Goubanova, K., Valenzuela, R., Wang, C., Rester, L., & Beaulieu, A. (2024). South America is becoming warmer, drier, and more flammable. *Communications Earth & Environment*, *5*(1), 1–10. https://doi.org/10.1038/s43247-024-01654-7

Fill, J. M., Davis, C. N., & Crandall, R. M. (2019). Climate change lengthens southeastern USA lightning-ignited fire seasons. *Global Change Biology*, *25*(10), 3562–3569. https://doi.org/10.1111/gcb.14727

Fisher, R. A. (1992). Statistical Methods for Research Workers. In S. Kotz & N. L. Johnson (Eds.), *Breakthroughs in Statistics: Methodology and Distribution* (pp. 66–70). Springer. https://doi.org/10.1007/978-1-4612-4380-9_6

FMB. (2019). *Federal Wildland Fire Policy Terms and Definitions*. https://www.nwcg.gov/sites/default/files/docs/eb-fmb-m-19-004a.pdf

Forbes, B., Reilly, S., Clark, M., Ferrell, R., Kelly, A., Krause, P., Matley, C., O'Neil, M., Villasenor, M., Disney, M., Wilkes, P., & Bentley, L. P. (2022). Comparing Remote Sensing and Field-Based Approaches to Estimate Ladder Fuels and Predict Wildfire Burn Severity. *Frontiers in Forests and Global Change*, *5*. https://doi.org/10.3389/ffgc.2022.818713

Fuentes-Ramirez, A., Veldman, J. W., Holzapfel, C., & Moloney, K. A. (2016). Spreaders, igniters, and burning shrubs: Plant flammability explains novel fire dynamics in grass-invaded deserts. *Ecological Applications*, *26*(7), 2311–2322. https://doi.org/10.1002/eap.1371

Gaither, C. J., Poudyal, N. C., Goodrick, S., Bowker, J. M., Malone, S., & Gan, J. (2011). Wildland fire risk and social vulnerability in the Southeastern United States: An exploratory spatial data analysis approach. *Forest Policy and Economics*, *13*(1), 24–36. https://doi.org/10.1016/j.forpol.2010.07.009

Ganteaume, A., Camia, A., Jappiot, M., San-Miguel-Ayanz, J., Long-Fournel, M., & Lampin, C. (2013). A Review of the Main Driving Factors of Forest Fire Ignition Over Europe. *Environmental Management*, *51*(3), 651–662. https://doi.org/10.1007/s00267-012-9961-z

Ganteaume, A., Jappiot, M., Lampin, C., Guijarro, M., & Hernando, C. (2013). Flammability of Some Ornamental Species in Wildland–Urban Interfaces in Southeastern France: Laboratory Assessment at Particle Level. *Environmental Management*, *52*(2), 467–480. https://doi.org/10.1007/s00267-013-0067-z

Ganteaume, A., & Syphard, A. D. (2018). Ignition sources. In *Encyclopedia of Wildfires and Wildland-Urban Interface (WUI) Fires* (pp. 1–17). Springer International Publishing Cham.

Gavier-Pizarro, G. I., Radeloff, V. C., Stewart, S. I., Huebner, C. D., & Keuler, N. S. (2010). Housing is positively associated with invasive exotic plant species richness in New England, USA. *Ecological Applications*, *20*(7), 1913–1925. https://doi.org/10.1890/09-2168.1

Gehlhausen, S. M., Schwartz, M. W., & Augspurger, C. K. (2000). Vegetation and microclimatic edge effects in two mixed-mesophytic forest fragments. *Plant Ecology*, *147*(1), 21–35. https://doi.org/10.1023/A:1009846507652

Gilliam, F. S. (2016). Forest ecosystems of temperate climatic regions: From ancient use to climate change. *New Phytologist*, *212*(4), 871–887. https://doi.org/10.1111/nph.14255

Gilliam, F. S., Goodale, C., Pardo, L., Geiser, L., & Lilleskov, E. (2011). Eastern Temperate Forests, Chapter 10. In L. Pardo, M. Robin-Abbott, & C. Driscoll (Eds.), *Assessment of Nitrogen deposition effects and empirical critical loads of Nitrogen for ecoregions of the United States* (pp. 99–116). U.S. Department of Agriculture, Forest Service, Northern Research Station. http://dx.doi.org/10.2737/NRS-GTR-80

Gong, D., Sun, L., & Hu, T. (2024). Characterizing the occurrence of wildland-urban interface fires and their important factors in China. *Ecological Indicators*, *165*, 112179. https://doi.org/10.1016/j.ecolind.2024.112179

González, T. M., González-Trujillo, J. D., Muñoz, A., & Armenteras, D. (2022). Effects of fire history on animal communities: A systematic review. *Ecological Processes*, *11*(1), 11. https://doi.org/10.1186/s13717-021-00357-7

Google Earth Engine. (2024). *IDAHO EPSCOR GRIDMET* [Dataset]. https://developers.google.com/earth-engine/datasets/catalog/IDAHO_EPSCOR_GRIDMET

Gorelick, N., Hancher, M., Dixon, M., Ilyushchenko, S., Thau, D., & Moore, R. (2017). Google Earth Engine: Planetary-scale geospatial analysis for everyone. *Remote Sensing of Environment*, *202*, 18–27. https://doi.org/10.1016/j.rse.2017.06.031

Guo, Y., Wang, J., Ge, Y., & Zhou, C. (2024). Global expansion of wildland-urban interface intensifies human exposure to wildfire risk in the 21st century. *Science Advances*, *10*(45), eado9587. https://doi.org/10.1126/sciadv.ado9587

Hanberry, B. B. (2020). Classifying Large Wildfires in the United States by Land Cover. *Remote Sensing*, *12*(18), Article 18. https://doi.org/10.3390/rs12182966

Hanes, C. C., Wang, X., Jain, P., Parisien, M.-A., Little, J. M., & Flannigan, M. D. (2019). Fire-regime changes in Canada over the last half century. *Canadian Journal of Forest Research*, *49*(3), 256–269. https://doi.org/10.1139/cjfr-2018-0293

Hartig, F., Lohse, L., & leite, M. de S. (2024). *DHARMa: Residual Diagnostics for Hierarchical (Multi-Level / Mixed) Regression Models* (Version 0.4.7) [Computer software]. https://cran.r-project.org/web/packages/DHARMa/index.html

Haynes, K., Short, K., Xanthopoulos, G., Viegas, D., Ribeiro, L. M., & Blanchi, R. (2020). Wildfires and WUI Fire Fatalities. In S. L. Manzello (Ed.), *Encyclopedia of Wildfires and Wildland-Urban Interface (WUI) Fires* (pp. 1–16). Springer International Publishing. https://doi.org/10.1007/978-3-319-51727-8_92-1

He, T., Lamont, B. B., & Pausas, J. G. (2019). Fire as a key driver of Earth's biodiversity. *Biological Reviews*, *94*(6), 1983–2010. https://doi.org/10.1111/brv.12544

Hessburg, P. F., Agee, J. K., & Franklin, J. F. (2005). Dry forests and wildland fires of the inland Northwest USA: Contrasting the landscape ecology of the pre-settlement and modern eras. *Forest Ecology and Management*, *211*(1), 117–139. https://doi.org/10.1016/j.foreco.2005.02.016

HIFLD. (2024). *Fire and Emergency Medical Service (EMS) Stations* [Dataset]. https://hifld-geoplatform.hub.arcgis.com/datasets/geoplatform::fire-and-emergency-medical-service-ems-stations

Hysa, A. (2021). Indexing the vegetated surfaces within WUI by their wildfire ignition and spreading capacity, a comparative case from developing metropolitan areas. *International Journal of Disaster Risk Reduction*, *63*, 102434. https://doi.org/10.1016/j.ijdrr.2021.102434

Iglesias, V., Balch, J. K., & Travis, W. R. (2022). U.S. fires became larger, more frequent, and more widespread in the 2000s. *Science Advances*, *8*(11), eabc0020. https://doi.org/10.1126/sciadv.abc0020

Ingalsbee, T. (2015). Ecological fire use for ecological fire management: Managing large wildfires by design. *In: Keane, Robert E.; Jolly, Matt; Parsons, Russell; Riley, Karin. Proceedings of the Large Wildland Fires Conference; May 19-23, 2014; Missoula, MT. Proc. RMRS-P-73. Fort Collins, CO: U.S. Department of Agriculture, Forest Service, Rocky Mountain Research Station. p. 120-127.*, *73*, 120–127.

Ivey, M., Wonkka, C. L., Weidig, N. C., & Donovan, V. M. (2024). Woody cover fuels large wildfire risk in the eastern US. *Geophysical Research Letters*, *51*(e2024GL110586). https://doi.org/10.1029/2024GL110586

Jaafari, A., Rahmati, O., Zenner, E. K., & Mafi-Gholami, D. (2022). Anthropogenic activities amplify wildfire occurrence in the Zagros eco-region of western Iran. *Natural Hazards*, *114*(1), 457–473. https://doi.org/10.1007/s11069-022-05397-6

Jain, P., Castellanos-Acuna, D., Coogan, S. C. P., Abatzoglou, J. T., & Flannigan, M. D. (2022). Observed increases in extreme fire weather driven by atmospheric humidity and temperature. *Nature Climate Change*, *12*(1), Article 1. https://doi.org/10.1038/s41558-021-01224-1

Jain, T. B., Abrahamson, I., Anderson, N., Hood, S., Hanberry, B., Kilkenny, F., McKinney, S., Ott, J., Urza, A., Chambers, J., Battaglia, M., Varner, J. M., & O'Brien, J. J. (2021). *Effectiveness of fuel treatments at the landscape scale: State of understanding and key research gaps* (JFSP Project Report Nos. 19-S-01–2; p. 65). Joint Fire Sciences Program.

Johnston, F. H., Henderson, S. B., Chen, Y., Randerson, J. T., Marlier, M., DeFries, R. S., Kinney, P., Bowman, D. M. J. S., & Brauer, M. (2012). Estimated Global Mortality Attributable to Smoke from Landscape Fires. *Environmental Health Perspectives*, *120*(5), 695–701. https://doi.org/10.1289/ehp.1104422

Johnston, L., Blanchi, R., & Jappiot, M. (2019). Wildland-Urban Interface. In S. L. Manzello (Ed.), *Encyclopedia of Wildfires and Wildland-Urban Interface (WUI) Fires* (pp. 1–13). Springer International Publishing. https://doi.org/10.1007/978-3-319-51727-8_130-1

Jones, M. O., Allred, B. W., Naugle, D. E., Maestas, J. D., Donnelly, P., Metz, L. J., Karl, J., Smith, R., Bestelmeyer, B., Boyd, C., Kerby, J. D., & McIver, J. D. (2018). Innovation in rangeland monitoring: Annual, 30 m, plant functional type percent cover maps for U.S. rangelands, 1984–2017. *Ecosphere*, *9*(9), e02430. https://doi.org/10.1002/ecs2.2430

Jones, M. W., Abatzoglou, J. T., Veraverbeke, S., Andela, N., Lasslop, G., Forkel, M., Smith, A. J. P., Burton, C., Betts, R. A., van der Werf, G. R., Sitch, S., Canadell, J. G., Santín, C., Kolden, C., Doerr, S. H., & Le Quéré, C. (2022). Global and Regional Trends and Drivers of Fire Under Climate Change. *Reviews of Geophysics*, *60*(3), e2020RG000726. https://doi.org/10.1029/2020RG000726

Kittel, T., Royle, J., Daly, C., Rosenbloom, N., Gibson, W., Fisher, H., Schimel, D., Berliner, L., & Participants, V. (1997). A gridded historical (1895-1993) bioclimate dataset for the conterminous United States. *Proceedings of the 10th Conference on Applied Climatology*, *20*(24), 20–24.

Knuckey, C. G., Van Etten, E. J. B., & Doherty, T. S. (2016). Effects of long-term fire exclusion and frequent fire on plant community composition: A case study from semi-arid shrublands. *Austral Ecology*, *41*(8), 964–975. https://doi.org/10.1111/aec.12388

Kramer, H. A., Mockrin, M. H., Alexandre, P. M., & Radeloff, V. C. (2019). High wildfire damage in interface communities in California. *International Journal of Wildland Fire*, *28*(9), 641. https://doi.org/10.1071/WF18108

Krannich, R. S., Luloff, A. E., & Field, D. R. (2011). Putting Rural Community Change in Perspective. In R. S. Krannich, A. E. Luloff, & D. R. Field (Eds.), *People, Places and Landscapes: Social Change in High Amenity Rural Areas* (pp. 9–25). Springer Netherlands. https://doi.org/10.1007/978-94-007-1263-8_2

Kreider, M. R., Higuera, P. E., Parks, S. A., Rice, W. L., White, N., & Larson, A. J. (2024). Fire suppression makes wildfires more severe and accentuates impacts of climate change and fuel accumulation. *Nature Communications*, *15*(1), 2412. https://doi.org/10.1038/s41467-024-46702-0

Kupfer, J. A., Terando, A. J., Gao, P., Teske, C., & Hiers, J. K. (2020). Climate change projected to reduce prescribed burning opportunities in the south-eastern United States. *International Journal of Wildland Fire*, *29*(9), 764–778. https://doi.org/10.1071/WF19198

Lee, R. J., & Chow, T. E. (2015). Post-wildfire assessment of vegetation regeneration in Bastrop, Texas, using Landsat imagery. *GIScience & Remote Sensing*, *52*(5), 609–626. https://doi.org/10.1080/15481603.2015.1055451

Liu, Z., Wimberly, M. C., Lamsal, A., Sohl, T. L., & Hawbaker, T. J. (2015). Climate change and wildfire risk in an expanding wildland–urban interface: A case study from the Colorado Front Range Corridor. *Landscape Ecology*, *30*(10), 1943–1957. https://doi.org/10.1007/s10980-015-0222-4

Lüdecke, D., Aust, F., Crawley, S., Ben-Shachar, M. S., & Anderson, S. C. (2024). *ggeffects: Create Tidy Data Frames of Marginal Effects for "ggplot" from Model Outputs* (Version 1.7.2) [Computer software]. https://cran.r-project.org/web/packages/ggeffects/index.html

Lüdecke, D., Makowski, D., Ben-Shachar, M. S., Patil, I., Højsgaard, S., Wiernik, B. M., Lau, Z. J., Arel-Bundock, V., Girard, J., Maimone, C., Ohlsen, N., Morrison, D. E., & Luchman, J. (2025). *parameters: Processing of Model Parameters* (Version 0.24.2) [Computer software]. https://cran.r-project.org/web/packages/parameters/index.html

Lüdecke, D., Makowski, D., Ben-Shachar, M. S., Patil, I., Waggoner, P., Wiernik, B. M., Thériault, R., Arel-Bundock, V., Jullum, M., gjo11, Bacher, E., & Luchman, J. (2024). *performance: Assessment of Regression Models Performance* (Version 0.12.4) [Computer software]. https://cran.r-project.org/web/packages/performance/index.html

Mandle, L., Bufford, J. L., Schmidt, I. B., & Daehler, C. C. (2011). Woody exotic plant invasions and fire: Reciprocal impacts and consequences for native ecosystems. *Biological Invasions*, *13*(8), 1815–1827. https://doi.org/10.1007/s10530-011-0001-3

Mani, Z. A., Khorram-Manesh, A., & Goniewicz, K. (2024). Global Health Impacts of Wildfire Disasters From 2000 to 2023: A Comprehensive Analysis of Mortality and Injuries. *Disaster Medicine and Public Health Preparedness*, *18*, e230. https://doi.org/10.1017/dmp.2024.150

Mann, H. B., & Whitney, D. R. (1947). On a Test of Whether one of Two Random Variables is Stochastically Larger than the Other. *The Annals of Mathematical Statistics*, *18*(1), 50–60. https://doi.org/10.1214/aoms/1177730491

Manzello, S. L., Hayashi, Y., Yoneki, T., & Yamamoto, Y. (2010). Quantifying the vulnerabilities of ceramic tile roofing assemblies to ignition during a firebrand attack. *Fire Safety Journal*, *45*(1), 35–43. https://doi.org/10.1016/j.firesaf.2009.09.002

Manzello, S. L., Park, S.-H., Suzuki, S., Shields, J. R., & Hayashi, Y. (2011). Experimental investigation of structure vulnerabilities to firebrand showers. *Fire Safety Journal*, *46*(8), 568–578. https://doi.org/10.1016/j.firesaf.2011.09.003

Maranghides, A., Link, E., Mell, W. “Ruddy,” Hawks, S., Wilson, M., Brewer, W., Brown, C., Vihnaneck, B., & Walton, W. D. (2021). *A Case Study of the Camp Fire – Fire Progression Timeline* (No. NIST TN 2135; p. NIST TN 2135). National Institute of Standards and Technology. https://doi.org/10.6028/NIST.TN.2135

Marques, S., Borges, J. G., Garcia-Gonzalo, J., Moreira, F., Carreiras, J. M. B., Oliveira, M. M., Cantarinha, A., Botequim, B., & Pereira, J. M. C. (2011). Characterization of wildfires in Portugal. *European Journal of Forest Research*, *130*(5), 775–784. https://doi.org/10.1007/s10342-010-0470-4

Matilainen, A., Pohja-Mykrä, M., Lähdesmäki, M., & Kurki, S. (2017). “I feel it is mine!” – Psychological ownership in relation to natural resources. *Journal of Environmental Psychology*, *51*, 31–45. https://doi.org/10.1016/j.jenvp.2017.03.002

McGranahan, D. A., & Wonkka, C. L. (2022). Fuel Properties of Effective Greenstrips in Simulated Cheatgrass Fires. *Environmental Management*, *70*(2), 319–328. https://doi.org/10.1007/s00267-022-01659-y

Mietkiewicz, N., Balch, J. K., Schoennagel, T., Leyk, S., St. Denis, L. A., & Bradley, B. A. (2020). In the Line of Fire: Consequences of Human-Ignited Wildfires to Homes in the U.S. (1992–2015). *Fire*, *3*(3), Article 3. https://doi.org/10.3390/fire3030050

Modaresi Rad, A., Abatzoglou, J. T., Kreitler, J., Alizadeh, M. R., AghaKouchak, A., Hudyma, N., Nauslar, N. J., & Sadegh, M. (2023). Human and infrastructure exposure to large wildfires in the United States. *Nature Sustainability*, *6*(11), Article 11. https://doi.org/10.1038/s41893-023-01163-z

Moritz, M. A., Morais, M. E., Summerell, L. A., Carlson, J. M., & Doyle, J. (2005). Wildfires, complexity, and highly optimized tolerance. *Proceedings of the National Academy of Sciences*, *102*(50), 17912–17917. https://doi.org/10.1073/pnas.0508985102

MTBS. (2023). *Burned Areas Boundaries Dataset* [Dataset]. https://www.mtbs.gov/direct-download

Murcia, C. (1995). Edge effects in fragmented forests: Implications for conservation. *Trends in Ecology & Evolution*, *10*(2), 58–62. https://doi.org/10.1016/S0169-5347(00)88977-6

Murphy, B. P., Bradstock, R. A., Boer, M. M., Carter, J., Cary, G. J., Cochrane, M. A., Fensham, R. J., Russell-Smith, J., Williamson, G. J., & Bowman, D. M. J. S. (2013). Fire regimes of Australia: A pyrogeographic model system. *Journal of Biogeography*, *40*(6), 1048–1058. https://doi.org/10.1111/jbi.12065

Nagy, R. C., Fusco, E., Bradley, B., Abatzoglou, J. T., & Balch, J. (2018). Human-Related Ignitions Increase the Number of Large Wildfires across U.S. Ecoregions. *Fire*, *1*(1), Article 1. https://doi.org/10.3390/fire1010004

Narayanaraj, G., & Wimberly, M. C. (2012). Influences of forest roads on the spatial patterns of human- and lightning-caused wildfire ignitions. *Applied Geography*, *32*(2), 878–888. https://doi.org/10.1016/j.apgeog.2011.09.004

Narayanaraj, G., & Wimberly, M. C. (2013). Influences of forest roads and their edge effects on the spatial pattern of burn severity. *International Journal of Applied Earth Observation and Geoinformation*, *23*, 62–70. https://doi.org/10.1016/j.jag.2012.12.006

Nelder, J. A., & Wedderburn, R. W. M. (1972). Generalized Linear Models. *Journal of the Royal Statistical Society. Series A (General)*, *135*(3), 370–384. https://doi.org/10.2307/2344614

Newcombe, R. G. (1998). Interval estimation for the difference between independent proportions: Comparison of eleven methods. *Statistics in Medicine*, *17*(8), 873–890. https://doi.org/10.1002/(SICI)1097-0258(19980430)17:8<873::AID-SIM779>3.0.CO;2-I

NIFC. (2024). *National Interagency Fire Center Preparedness Levels*. https://www.nifc.gov/fire-information/pl-month/01

Nowacki, G. J., & Abrams, M. D. (2008). The Demise of Fire and “Mesophication” of Forests in the Eastern United States. *BioScience*, *58*(2), 123–138. https://doi.org/10.1641/B580207

Omernik, J. M., & Griffith, G. E. (2014). Ecoregions of the Conterminous United States: Evolution of a Hierarchical Spatial Framework. *Environmental Management*, *54*(6), 1249–1266. https://doi.org/10.1007/s00267-014-0364-1

Ottmar, R. D. (2020). Ladder Fuels. In S. L. Manzello (Ed.), *Encyclopedia of Wildfires and Wildland-Urban Interface (WUI) Fires* (pp. 727–730). Springer International Publishing. https://doi.org/10.1007/978-3-319-52090-2

Palmero-Iniesta, M., Domènech, R., Molina-Terrén, D., & Espelta, J. M. (2017). Fire behavior in Pinus halepensis thickets: Effects of thinning and woody debris decomposition in two rainfall scenarios. *Forest Ecology and Management*, *404*, 230–240. https://doi.org/10.1016/j.foreco.2017.08.043

Parisien, M.-A., & Moritz, M. A. (2009). Environmental controls on the distribution of wildfire at multiple spatial scales. *Ecological Monographs*, *79*(1), 127–154. https://doi.org/10.1890/07-1289.1

Parks, S. A., Guiterman, C. H., Margolis, E. Q., Lonergan, M., Whitman, E., Abatzoglou, J. T., Falk, D. A., Johnston, J. D., Daniels, L. D., Lafon, C. W., Loehman, R. A., Kipfmueller, K. F., Naficy, C. E., Parisien, M.-A., Portier, J., Stambaugh, M. C., Williams, A. P., Wion, A. P., & Yocom, L. L. (2025). A fire deficit persists across diverse North American forests despite recent increases in area burned. *Nature Communications*, *16*(1), 1493. https://doi.org/10.1038/s41467-025-56333-8

Pausas, J. G., & Keeley, J. E. (2021). Wildfires and global change. *Frontiers in Ecology and the Environment*, *19*(7), 387–395. https://doi.org/10.1002/fee.2359

Pausas, J. G., Keeley, J. E., & Schwilk, D. W. (2017). Flammability as an ecological and evolutionary driver. *Journal of Ecology*, *105*(2), 289–297. https://doi.org/10.1111/1365-2745.12691

Pierce, G., Gabbe, C. J., & Rosser, A. (2022). Households Living in Manufactured Housing Face Outsized Exposure to Heat and Wildfire Hazards: Evidence from California. *Natural Hazards Review*, *23*(3), 04022009. https://doi.org/10.1061/(ASCE)NH.1527-6996.0000540

Potter, K. M., Riitters, K. H., Iannone, B. V., Guo, Q., & Fei, S. (2024). Forest plant invasions in the eastern United States: Evidence of invasion debt in the wildland-urban interface. *Landscape Ecology*, *39*(12), 207. https://doi.org/10.1007/s10980-024-01985-y

Pourmohamad, Y., Abatzoglou, J. T., Belval, E. J., Fleishman, E., Short, K., Reeves, M. C., Nauslar, N., Higuera, P. E., Henderson, E., Ball, S., AghaKouchak, A., Prestemon, J. P., Olszewski, J., & Sadegh, M. (2024). Physical, social, and biological attributes for improved understanding and prediction of wildfires: FPA FOD-Attributes dataset. *Earth System Science Data*, *16*(6), 3045–3060. https://doi.org/10.5194/essd-16-3045-2024

Povak, N. A., Hessburg, P. F., & Salter, R. B. (2018). Evidence for scale-dependent topographic controls on wildfire spread. *Ecosphere*, *9*(10), e02443. https://doi.org/10.1002/ecs2.2443

Pulver, S., Ulibarri, N., Sobocinski, K. L., Alexander, S. M., Johnson, M. L., McCord, P. F., & Dell'angelo, J. (2018). Frontiers in socio-environmental research: Components, connections, scale, and context. *Ecology and Society*, *23*(3). https://escholarship.org/uc/item/34b3h4h0

R Core Team. (2023). *R: A Language and Environment for Statistical Computing* (Version 4.3.2) [Computer software]. https://www.r-project.org/

Radeloff, V. C., Hammer, R. B., Stewart, S. I., Fried, J. S., Holcomb, S. S., & McKeefry, J. F. (2005). The Wildland–Urban Interface in the United States. *Ecological Applications*, *15*(3), 799–805. https://doi.org/10.1890/04-1413

Radeloff, V. C., Helmers, D. P., Kramer, H. A., Mockrin, M. H., Alexandre, P. M., Bar-Massada, A., Butsic, V., Hawbaker, T. J., Martinuzzi, S., Syphard, A. D., & Stewart, S. I. (2018). Rapid growth of the US wildland-urban interface raises wildfire risk. *Proceedings of the National Academy of Sciences*, *115*(13), 3314–3319. https://doi.org/10.1073/pnas.1718850115

Radeloff, V. C., Helmers, D. P., Mockrin, M. H., Carlson, A. R., Hawbaker, T. J., & Martinuzzi, S. (2023). *The 1990-2020 wildland-urban interface of the conterminous United States—Geospatial data (4th Edition)* [Dataset]. Fort Collins, CO: Forest Service Research Data Archive. https://doi.org/10.2737/RDS-2015-0012-4

Radeloff, V. C., Mockrin, M. H., Helmers, D., Carlson, A., Hawbaker, T. J., Martinuzzi, S., Schug, F., Alexandre, P. M., Kramer, H. A., & Pidgeon, A. M. (2023). Rising wildfire risk to houses in the United States, especially in grasslands and shrublands. *Science*, *382*(6671), 702–707. https://doi.org/10.1126/science.ade9223

Ranney, J. W. (1977). *Forest Island edges: Their structure, development, and importance to regional forest ecosystem dynamics* (No. EDFB/IBP-77/1). Oak Ridge National Lab. (ORNL), Oak Ridge, TN (United States). https://doi.org/10.2172/7278093

Rao, K., Williams, A. P., Diffenbaugh, N. S., Yebra, M., Bryant, C., & Konings, A. G. (2023). Dry Live Fuels Increase the Likelihood of Lightning-Caused Fires. *Geophysical Research Letters*, *50*(15), e2022GL100975. https://doi.org/10.1029/2022GL100975

Renkas, A., Popovych, V., & Rudenko, D. (2022). Optimization of Fire Station Locations to Increase the Efficiency of Firefighting in Natural Ecosystems. *Environmental Research, Engineering and Management*, *78*(1), 97–104. https://doi.org/10.5755/j01.erem.78.1.25581

Resco de Dios, V. (2020). Global Change, Pyrophysiology, and Wildfires. In V. Resco de Dios (Ed.), *Plant-Fire Interactions: Applying Ecophysiology to Wildfire Management* (pp. 177–197). Springer International Publishing. https://doi.org/10.1007/978-3-030-41192-3_10

Riitters, K. H., Coulston, J. W., & Wickham, J. D. (2012). Fragmentation of forest communities in the eastern United States. *Forest Ecology and Management*, *263*, 85–93. https://doi.org/10.1016/j.foreco.2011.09.022

Rogers, B. M., Balch, J. K., Goetz, S. J., Lehmann, C. E. R., & Turetsky, M. (2020). Focus on changing fire regimes: Interactions with climate, ecosystems, and society. *Environmental Research Letters*, *15*(3), 030201. https://doi.org/10.1088/1748-9326/ab6d3a

RStudio Team. (2023). *RStudio: Integrated Development Environment for R* [Computer software]. http://www.rstudio.com/

Rummer, B. (2008). Assessing the cost of fuel reduction treatments: A critical review. *Forest Policy and Economics*, *10*(6), 355–362. https://doi.org/10.1016/j.forpol.2008.01.001

Sanczuk, P., De Pauw, K., De Lombaerde, E., Luoto, M., Meeussen, C., Govaert, S., Vanneste, T., Depauw, L., Brunet, J., Cousins, S. A. O., Gasperini, C., Hedwall, P.-O., Iacopetti, G., Lenoir, J., Plue, J., Selvi, F., Spicher, F., Uria-Diez, J., Verheyen, K., … De Frenne, P. (2023). Microclimate and forest density drive plant population dynamics under climate change. *Nature Climate Change*, *13*(8), Article 8. https://doi.org/10.1038/s41558-023-01744-y

Schelhaas, M.-J., Nabuurs, G.-J., & Schuck, A. (2003). Natural disturbances in the European forests in the 19th and 20th centuries. *Global Change Biology*, *9*(11), 1620–1633. https://doi.org/10.1046/j.1365-2486.2003.00684.x

Schug, F., Bar-Massada, A., Carlson, A. R., Cox, H., Hawbaker, T. J., Helmers, D., Hostert, P., Kaim, D., Kasraee, N. K., Martinuzzi, S., Mockrin, M. H., Pfoch, K. A., & Radeloff, V. C. (2023). The global wildland–urban interface. *Nature*, *621*(7977), Article 7977. https://doi.org/10.1038/s41586-023-06320-0

Schultz, C. A., McCaffrey, S. M., & Huber-Stearns, H. R. (2019). Policy barriers and opportunities for prescribed fire application in the western United States. *International Journal of Wildland Fire*, *28*(11), 874–884. https://doi.org/10.1071/WF19040

Senande-Rivera, M., Insua-Costa, D., & Miguez-Macho, G. (2022). Spatial and temporal expansion of global wildland fire activity in response to climate change. *Nature Communications*, *13*(1), 1208. https://doi.org/10.1038/s41467-022-28835-2

Short, K. C. (2014). A spatial database of wildfires in the United States, 1992-2011. *Earth System Science Data*, *6*(1), 1–27. https://doi.org/10.5194/essd-6-1-2014

Short, K. C. (2022). *Spatial wildfire occurrence data for the United States, 1992-2020 [FPA_FOD_20221014]* (Version 6th Edition) [Dataset]. Fort Collins, CO: Forest Service Research Data Archive. https://doi.org/10.2737/RDS-2013-0009.6

Silverman, B. W. (1986). *Density Estimation for Statistics and Data Analysis*. Routledge. https://doi.org/10.1201/9781315140919

Sjöström, J., Plathner, F. V., & Granström, A. (2019). Wildfire ignition from forestry machines in boreal Sweden. *International Journal of Wildland Fire*, *28*(9), 666–677. https://doi.org/10.1071/WF18229

Sonti, N. F., Riemann, R., Mockrin, M. H., & Domke, G. M. (2022). Expanding wildland-urban interface alters forest structure and landscape context in the northern United States. *Environmental Research Letters*, *18*(1), 014010. https://doi.org/10.1088/1748-9326/aca77b

St. Denis, L. A., Short, K. C., McConnell, K., Cook, M. C., Mietkiewicz, N. P., Buckland, M., & Balch, J. K. (2023). All-hazards dataset mined from the US National Incident Management System 1999-2020. *Scientific Data*, *10*(1), 112. https://doi.org/10.1038/s41597-023-01955-0

Stasiewicz, A. M., & Paveglio, T. B. (2022). Exploring relationships between perceived suppression capabilities and resident performance of wildfire mitigations. *Journal of Environmental Management*, *316*, 115176. https://doi.org/10.1016/j.jenvman.2022.115176

Stefanidou, M., Athanaselis, S., & Spiliopoulou, C. (2008). Health Impacts of Fire Smoke Inhalation. *Inhalation Toxicology*, *20*(8), 761–766. https://doi.org/10.1080/08958370801975311

Stone, C., Hudak, A., & Morgan, P. (2004). Forest Harvest Can Increase Subsequent Forest Fire Severity. *USDA Forest Service / UNL Faculty Publications*. https://digitalcommons.unl.edu/usdafsfacpub/199

Swanston, C., Brandt, L. A., Janowiak, M. K., Handler, S. D., Butler-Leopold, P., Iverson, L., Thompson III, F. R., Ontl, T. A., & Shannon, P. D. (2018). Vulnerability of forests of the Midwest and Northeast United States to climate change. *Climatic Change*, *146*(1), 103–116. https://doi.org/10.1007/s10584-017-2065-2

Swimley, K. (2021). *The Influence of Wildland Urban Interface Areas on Resource Assignments to Large Wildland Fires*. https://scholarworks.umt.edu/etd/11802

Symonds, M. R. E., & Moussalli, A. (2011). A brief guide to model selection, multimodel inference and model averaging in behavioural ecology using Akaike's information criterion. *Behavioral Ecology and Sociobiology*, *65*(1), 13–21. https://doi.org/10.1007/s00265-010-1037-6

Syphard, A. D., Brennan, T. J., & Keeley, J. E. (2014). The role of defensible space for residential structure protection during wildfires. *International Journal of Wildland Fire*, *23*(8), 1165–1175.

Syphard, A. D., & Keeley, J. E. (2015). Location, timing and extent of wildfire vary by cause of ignition. *International Journal of Wildland Fire*, *24*(1), 37–47. https://doi.org/10.1071/WF14024

Syphard, A. D., Keeley, J. E., Gough, M., Lazarz, M., & Rogan, J. (2022). What Makes Wildfires Destructive in California? *Fire*, *5*(5), 133. https://doi.org/10.3390/fire5050133

Syphard, A. D., Keeley, J. E., Pfaff, A. H., & Ferschweiler, K. (2017). Human presence diminishes the importance of climate in driving fire activity across the United States. *Proceedings of the National Academy of Sciences*, *114*(52), 13750–13755. https://doi.org/10.1073/pnas.1713885114

Tang, W., Emmons, L. K., Wiedinmyer, C., Partha, D. B., Huang, Y., He, C., Zhang, J., Barsanti, K. C., Gaubert, B., Jo, D. S., Zhang, J., Buchholz, R., Tilmes, S., Vitt, F., Granier, C., Worden, H. M., & Levelt, P. F. (2025). Disproportionately large impacts of wildland-urban interface fire emissions on global air quality and human health. *Science Advances*, *11*(11), eadr2616. https://doi.org/10.1126/sciadv.adr2616

Tang, W., He, C., Emmons, L., & Zhang, J. (2024). Global expansion of wildland-urban interface (WUI) and WUI fires: Insights from a multiyear worldwide unified database (WUWUI). *Environmental Research Letters*, *19*(4), 044028. https://doi.org/10.1088/1748-9326/ad31da

Tepley, A. J., Thomann, E., Veblen, T. T., Perry, G. L. W., Holz, A., Paritsis, J., Kitzberger, T., & Anderson-Teixeira, K. J. (2018). Influences of fire–vegetation feedbacks and post-fire recovery rates on forest landscape vulnerability to altered fire regimes. *Journal of Ecology*, *106*(5), 1925–1940. https://doi.org/10.1111/1365-2745.12950

Theobald, D. M. (2005). Landscape Patterns of Exurban Growth in the USA from 1980 to 2020. *Ecology and Society*, *10*(1). https://www.jstor.org/stable/26267722

Theobald, D. M., & Romme, W. H. (2007). Expansion of the US wildland–urban interface. *Landscape and Urban Planning*, *83*(4), 340–354. https://doi.org/10.1016/j.landurbplan.2007.06.002

Thibeault, J. M., & Seth, A. (2014). Changing climate extremes in the Northeast United States: Observations and projections from CMIP5. *Climatic Change*, *127*(2), Article 2. https://doi.org/10.1007/s10584-014-1257-2

Thomas, D., Butry, D., Gilbert, S., Webb, D., & Fung, J. (2017). *The costs and losses of wildfires: A literature survey* (No. NIST SP 1215; p. NIST SP 1215). National Institute of Standards and Technology. https://doi.org/10.6028/NIST.SP.1215

Thompson, M. P., Gannon, B. M., & Caggiano, M. D. (2021). Forest Roads and Operational Wildfire Response Planning. *Forests*, *12*(2), 110. https://doi.org/10.3390/f12020110

Toman, E., Stidham, M., Shindler, B., McCaffrey, S., Toman, E., Stidham, M., Shindler, B., & McCaffrey, S. (2011). Reducing fuels in the wildland–urban interface: Community perceptions of agency fuels treatments. *International Journal of Wildland Fire*, *20*(3), 340–349. https://doi.org/10.1071/WF10042

Tomat-Kelly, G., Dillon, W. W., & Flory, S. L. (2021). Invasive grass fuel loads suppress native species by increasing fire intensity and soil heating. *Journal of Applied Ecology*, *58*(10), 2220–2230. https://doi.org/10.1111/1365-2664.13881

Trainor, T. F. (2005). The MAF/TIGER enhancement program: The mechanics and maintenance of a large-scale national spatial database. *Government Publications Review*, *13*, 181–201.

United States Fire Administration. (2021). *An Analysis of NFIRS Data for Selected Wildfires Including Impacts in Wildland Urban Interface Areas* [Wildfire Report Series]. United States Fire Administration. https://www.usfa.fema.gov/wui/data/wildfire-report-series/nfirs-data-for-selected-wildfires.html

U.S. Census Bureau. (1992). *TIGER/Line Shapefiles* [Dataset]. U.S. Department of Commerce; U.S. Department of Commerce. https://www2.census.gov/geo/tiger/

USDA Forest Service. (2021). *Forest Service Office Locations* [Dataset]. USFS Chief Information Office, Enterprise Data Warehouse. https://apps.fs.usda.gov/arcx/rest/services/EDW/EDW_FSOfficeLocations_01/MapServer/0

USDA & USDI. (2001). Urban Wildland Interface Communities Within the Vicinity of Federal Lands That Are at High Risk From Wildfire. Notices. *Federal Register*, *66*(3), 705–1011.

Vacca, P., Àgueda, A., Planas, E., Caballero, D., & Pastor, E. (2023). Methodology for the analysis of structural vulnerability of WUI settlements. *Fire Safety Journal*, *140*, 103853. https://doi.org/10.1016/j.firesaf.2023.103853

Vadrevu, K. P., Lasko, K., Giglio, L., Schroeder, W., Biswas, S., & Justice, C. (2019). Trends in Vegetation fires in South and Southeast Asian Countries. *Scientific Reports*, *9*(1), 7422. https://doi.org/10.1038/s41598-019-43940-x

Vaittinada Ayar, P., & Mailhot, A. (2021). Evolution of Dry and Wet Spells Under Climate Change Over North-Eastern North America. *Journal of Geophysical Research: Atmospheres*, *126*(5), e2020JD033740. https://doi.org/10.1029/2020JD033740

Wadhwani, R., Sullivan, C., Wickramasinghe, A., Kyng, M., Khan, N., & Moinuddin, K. (2022). A review of firebrand studies on generation and transport. *Fire Safety Journal*, *134*, 103674. https://doi.org/10.1016/j.firesaf.2022.103674

Wei, Y., Gannon, B., Young, J., Belval, E., Thompson, M., O'Connor, C., & Calkin, D. (2023). Estimating WUI exposure probability to a nearby wildfire. *Fire Ecology*, *19*(1), Article 1. https://doi.org/10.1186/s42408-023-00191-6

Weltzin, J. F., & McPherson, G. R. (2003). *Changing precipitation regimes and terrestrial ecosystems: A North American perspective*. University of Arizona Press.

Wickham, H. (2016). *ggplot2: Elegant Graphics for Data Analysis* (2nd ed.). Springer. https://link.springer.com/book/10.1007/978-3-319-24277-4

Wickham, J. D., Riitters, K. H., Wade, T. G., & Homer, C. (2008). Temporal change in fragmentation of continental US forests. *Landscape Ecology*, *23*(8), 891–898. https://doi.org/10.1007/s10980-008-9258-z

Wonkka, C. L., Rogers, W. E., & Kreuter, U. P. (2015). Legal barriers to effective ecosystem management: Exploring linkages between liability, regulations, and prescribed fire. *Ecological Applications*, *25*(8), 2382–2393. https://doi.org/10.1890/14-1791.1

Woodbridge, M., Keyser, T., & Oswalt, C. (2022). Stand and environmental conditions drive functional shifts associated with mesophication in eastern US forests. *Frontiers in Forests and Global Change*, *5*. https://www.frontiersin.org/articles/10.3389/ffgc.2022.991934

Zeileis, A., Cribari-Neto, F., Grün, B., Kosmidis, I., by), A. B. S. (earlier version, & by), A. V. R. (earlier version. (2024). *betareg: Beta Regression* (Version 3.2-1) [Computer software]. https://cran.r-project.org/web/packages/betareg/index.html

Zhai, J., Ning, Z., Dahal, R., & Yang, S. (2023). Wildfire Susceptibility of Land Use and Topographic Features in the Western United States: Implications for the Landscape Management. *Forests*, *14*(4), Article 4. https://doi.org/10.3390/f14040807

Zhu, Z. (Ed.). (2014). *Baseline and projected future carbon storage and greenhouse-gas fluxes in ecosystems of the eastern United States*. U.S. Department of the Interior, U.S. Geological Survey. https://doi.org/10.3133/pp1804

Zielstra, D., Hochmair, H. H., & Neis, P. (2013). Assessing the Effect of Data Imports on the Completeness of OpenStreetMap – A United States Case Study. *Transactions in GIS*, *17*(3), 315–334. https://doi.org/10.1111/tgis.12037

BIOGRAPHICAL SKETCH

Noah Weidig earned a Bachelor of Science in biological sciences from Northern Kentucky University in 2022, where he developed an interest in data science and landscape ecology. He went on to complete a Master of Science in forest resources and conservation from the University of Florida in 2025. His thesis focused on large wildfire patterns in the wildland-urban interface of the eastern United States. His personal website can be found at noahweidig.com.